



Nikolaj Nielsen

Function of Ion Transport Proteins in Pancreatic Stellate Cells (PSCs)

- 2015 -



- Biologie -

Function of Ion Transport Proteins in Pancreatic Stellate Cells (PSCs)

Inaugural-Dissertation

zur Erlangung des Doktorgrades
der Naturwissenschaften im Fachbereich Biologie
der Mathematisch-Naturwissenschaftlichen Fakultät
der Westfälischen Wilhelms-Universität Münster

Vorgelegt von
Nikolaj Nielsen
aus Værløse, Kopenhagen
Dänemark

- 2015 -

*I would like to dedicate this thesis to my family,
especially my parents and my girlfriend,
who continuously support me in everything I do.
I could not have made it without you!*

Dekan: Prof. Dr. phil. nat. Wolf-Michael Weber

Erster Gutachter: Prof. Dr. med. Albrecht Schwab

Zweiter Gutachter: Prof. Dr. phil. nat. Wolf-Michael Weber

Tag der mündlichen Prüfung: 28.05.2015

Tag der Promotion: 05.06.2015

Declaration and Certification of Originality

'I hereby declare that this submission is my own work and to the best of my knowledge contains no materials previously published or written by another person, nor material which to a substantial extent has been accepted for the award of any other degree or diploma at Westfälische Wilhelms-University of Münster or any other educational institution, except where due acknowledgement is made in the thesis. Any contribution made to the research by others, with whom I have worked with at University of Münster or elsewhere, is explicitly acknowledged in the thesis. I also declare that the intellectual content of this thesis is the product of my own work, except to the extent that assistance from others in the project's design and conception or in style, presentation and linguistic expression is acknowledged.'

Münster, _____

Nikolaj Nielsen

Preface

The thesis presented here, shows the work I have completed for obtaining a doctoral degree of Natural Science in Biology. The experimental work was carried out in the Laboratory of Cell Migration, Institute of Physiology II, Westfälische Wilhelms-University of Münster. The supervisor on my project was Prof. Dr. med. Albrecht Schwab and as a representative from the Faculty of Biology, Prof. Dr. phil. nat. Wolf-Michael Weber, Institute of Animal Physiology, Department of Biology, University of Münster.

The main focus of my thesis is the role of TRPC1 and TRPC6 channels in the response of pancreatic stellate cells (PSCs) to hypoxia and their importance for cell migration. The aim of Chapter 1 is to familiarize the reader with the role of PSCs in the development and progression of pancreatic cancer. The importance of cell migration is discussed in relation to PSC function, and the role of Ca^{2+} signalling for this process is highlighted. In the end of chapter 1, an introduction to TRP channels role as *sensors*, *modifiers* and *transduction/effectors* of the tumour microenvironment is outlined leading to the main aim and hypothesis of the thesis (described in Chapter 2). In Chapter 3, experimental materials and methods are outlined. This is followed by the major results discovered, described in Chapter 4. These findings are discussed in Chapter 5. Chapter 6 contains concluding remarks and perspectives of scientific findings presented in this study

Münster, March 30th 2015

Nikolaj Nielsen

University of Münster

Institute of Physiology II

Robert-Koch-Str. 27b

D-48149 Münster

Cell Migration Group:

<http://campus.uni-muenster.de/research1-physiologie2.html>

Acknowledgements

First and foremost I would like to thank my academic supervisor Prof. Albrecht Schwab for giving me the opportunity to carry out a PhD within his laboratory. You have been great at supporting me, and giving me scientific advice in time of need, but also letting me make my own decisions. You showed continued faith in me and my work and were genuinely interested in my project and its proceeding. For this I am very grateful.

Furthermore, I would like to thank Prof. Christian Stock, whose encouragement, guide and support has been a great help in times of need.

I would like to thank all the members of the Cell Migration Group and Endothelial Group, former and present, for being great company and for sharing some very enjoyable moments. I am really grateful for how you have welcomed me and made me feel accepted as a fellow scientist, despite my crazy Danish habits. Specially, Sandra, Jana and Sarah for help with analysing cell migration and other lab techniques.

Also thanks to all the members of the IonTraC consortium, PhD students as well as professors. It has indeed been an inspiring and instructive journey we had together, with many great experiences, scientific as well as personal. In connection to this I would like to give a special thanks to Katerina Kondratska from our cooperation partner in Lille, France. Thank you for welcoming me in my secondments and helping me in conducting experiments.

Thanks to Timothy Kelso for language corrections.

My parents deserve my gratefulness for their endless understanding, support and encouragement throughout my 3+ years abroad. Thank you for accepting and supporting my choices and for giving me strength to chase my dreams.

At last I dearly want to thank my girlfriend Stine for filling my heart with joy and love. Thank you for your patience and support. I know it has been a hard and challenging period testing our relationship and love to each other. I could not have completed it without your always kind and supporting attitude, especially over the last few months. I am deeply thankful for having you in my life. I Love you!

Financial support:

I would like to thank the European commission and Marie Curie Initial Training Network (ITN), Framework program 7 for financial support of my PhD.

Curriculum Vitae

Education:

Higher education:

PhD program:

Experience:

Beginning of the thesis:

Münster, _____

Nikolaj Nielsen

Contributions by the Author

Publications in peer reviewed journals:

Lindemann O, Strodthoff C, Horstmann M, **Nielsen N**, Jung F, Schimmelpfennig S, Heitzmann M, Schwab A. "TRPC1 regulates fMLP-stimulated migration and chemotaxis of neutrophil granulocytes". *Biochim Biophys Acta*. 2015, jan 14. pii: S0167-4889(15)00006-3. DOI: 10.1016/j.bbamcr2014.12.037.

Jabbari J, Olesen MS, Yuan L, Nielsen JB, Liang B, Macri V, Christoffersen IE, **Nielsen N**, Sajadieh A, Ellinor PT, Grunnet M, Haunsø S, Holst AG, Svendsen JH, Jespersen T. "Common and Rare Variants in *SCN10A* Modulate the Risk of Atrial Fibrillation". *Circ Cardiovasc Genet*. 2015, Feb;8(1):64-73. DOI: 10.1161/HCG.0000000000000022.

Nielsen N, Lindemann O, Schwab A. "TRP channels and STIM/ORAI proteins: sensors and effectors of cancer and stroma cell migration". *Br J Pharmacol*. 2014, July 2. 171, 5524-5540. DOI: 10.1111/bph.12721.

Winkel BG, Larsen MK, Berge KH, Leren TP, Nissen PH, Olesen MS, Hollegaard MV, Jespersen T, Yuan L, **Nielsen N**, Haunsø S, Svendsen JH, Wang Y, Kristensen IB, Jensen HK, Tfelt-Hansen J, Banner J. "The prevalence of mutations in *KCNQ1*, *KCNH2*, and *SCN5A* in an unselected national cohort of young sudden unexplained death cases". *Journal of Cardiovascular Electrophysiology*. 2012 Oct;23(10):1092-8. DOI: 10.1111/j.1540-8167.2012.02371.x.

Olesen MS, Yuan L, Lian B, Holst AG, **Nielsen N**, Nielsen JB, Hedley PL, Christiansen M, Olesen SP, Haunsø S, Schmitt N, Jespersen T and Svendsen JH "High Prevalence of Long QT Syndrome Associated *SCN5A* Variants in Patients with Early-Onset Lone Atrial Fibrillation". *Circulation Cardiovascular Genetics*. 2012 Aug 1;5(4):450-9. DOI:10.1161/CIRCGENETICS.111.962597.

Hannah Storck, Benedikt Hild, Sandra Schimmelpfennig, Sarah Sargin, **Nikolaj Nielsen**, Angela Zaccagnino, Thomas Budde, Ivana Novak, Holger Kalthoff, Albrecht Schwab. "Ion channels in control of pancreatic stellate cell migration". **Manuscript under revision.**

Conference talks:

Nielsen N, Kondratska K, Schimmelpfennig S, Welzig J, Prevarskaya N, Schwab A. "TRPC6 channels role in hypoxia-mediated activation of pancreatic stellate cells". *94nd Annual Meeting of the German Physiological Society*, Magdeburg, Germany, March 4-7, 2015. Abstract published in *Acta Physiologica*. 2015, March, vol. 213, suppl. 699: OS6-04.

Nielsen N, Schimmelpfennig S, Schwab A. "Characterization of TRPC1 and TRPC6 channels in Mouse Pancreatic Stellate Cells". *92nd Annual Meeting of the German Physiological Society*, Heidelberg, Germany, March 2-5, 2013. Abstract published in *Acta Physiologica*. 2013, March, vol. 207, suppl. 694: O59.

Conference Posters:

Nielsen N, Kondratska K, Prevarskaya N, Schwab A. "The Role of TRPC1 and TRPC6 Channels in Hypoxia-Mediated Activation of Pancreatic Stellate Cells". *PhD meeting of the Italian Society of Immunology Clinical Immunology and Allergology (SIICA)*, Bari, Italy, October 9-11, 2014

Nielsen N, Kondratska K, Prevarskaya N, Schwab A. "TRPC1 and TRPC6 Channels – Important Players in Hypoxia-Mediated Activation of Pancreatic Stellate Cells". *Marie Skłodowska-Curie Conference and the EuroScience Open Forum 2014*, Copenhagen, Denmark, June 19-20, 2014.

Nielsen N, Kondratska K, Prevarskaya N, Schwab A. "TRPC1 and TRPC6 Channels – Important Players in Hypoxia-Mediated Activation of Pancreatic Stellate Cells". *93rd Annual Meeting of the German Physiological Society*, Mainz, Germany, March 13-15, 2014. Abstract published in *Acta Physiologica*. 2014, March, vol. 210, suppl. 695: 136: 150. 82-228.

Nielsen N, Schimmelpfennig S, Kondratska K, Prevarskaya N, Schwab A. "Loss of TRPC1 or TRPC6 Channels Prevent Hypoxia-Mediated Activation of Pancreatic Stellate Cells". *Science Day University of Münster*, Münster, Germany, November 11, 2013.

Nielsen N, Schimmelpfennig S, Kondratska K, Prevarskaya N, Schwab A. "TRPC1 and TRPC6 channels – possible candidates for targeting stellate cells in pancreatic cancer?". *The Beatson International Cancer Conference*, Glasgow, Scotland, July 7-10, 2013.

Nielsen N, Schimmelpfennig S, Kondratska K, Prevarskaya N, Schwab A. "Role of TRPC1 and TRPC6 channels in murine pancreatic stellate cells". *The Sandbjerg meeting on Membrane Transport*, Sønderborg, Denmark, May 27-29, 2013.

Other activities:

- 04.2015 Drug development. IonTraC Summer School, Berlin.
- 07.2014 Team Management (German Workshop: Führungserfahrung entwickeln – Führungsgrundlagen), School of Life Sciences, University of Münster.
- 07.2014 Industrial Pharma Management, lecture series - Advanced level (2/2). School of Life Sciences, University of Münster.
- 06.2014 English for Academic Research. University of Münster.
- 05.2014 Writing Papers and Theses in Life Sciences. University of Münster.
- 03.2014 Leadership skills for scientist. University of Münster.
- 03.2014 Basic and translational oncology. IonTraC Summer School, Florence.
- 11.2013 Bioethics, scientific writing & grant application. IonTraC Workshop, University of Oxford.
- 11.2013 Industrial Pharma Management, lecture series - Basic level (1/2). School of Life Sciences, University of Münster.
- 05.2013 Membrane transport. IonTraC Summer School, Sandbjerg.
- 02.2013 Experimental methods in cancer research. IonTraC Winter School, Hamburg.
- 09.2012 Ion channels and transporters in cancer. IonTraC Summer School, Würzburg.
- 04.2012 German course level 3/6 (B1), 3+/6 (B1+), 5/6 (C1).

Overall Aim of The IonTraC Project

IonTraC, the acronym for “Ion Transport Proteins in Control of Cancer Cell Behaviour” is a Marie Curie Initial Training Network (ITN) on the role of Ion Transport Proteins in Pancreatic Cancer. The consortium consists of 10 academic and two industrial partners from five European countries with long-standing, complementary expertise in ion transport and carcinogenesis. It is funded by the European Commission and started its work on 1st October, 2011. FP7-PEOPLE-2011-ITN Grant Agreement No. 289648).

Homepage for IonTraC: <http://www.iontrac.uni-muenster.de/home.html>

(Short description adapted from the IonTraC homepage):

“Work carried out by us, our partners, other laboratories, and explorations of published gene arrays yield a strong expectation that ion transport proteins play a crucial role in pancreatic ductal adenocarcinoma progression.

*Thus, proteins involved in membrane transport have long been known as important drug targets in other pathologies (channelopathies). The IonTraC project builds upon mounting evidence that ion channels and transporters underlie many of the hallmarks of cancer as defined by Hanahan and Weinberg. Consequently, IonTraC was the first to propose a systematic analysis of the expression, function, as well as therapeutic and diagnostic potential of proteins involved in ion transport (the "**transportome**") in cancer.*

The overall aim of the IonTraC project is to comprehensively test the hypothesis that proteins involved in ion transport ("transportome") constitute novel diagnostic/therapeutic targets for Pancreatic Ductal Adenocarcinoma (PDAC).”

Summary

Pancreatic cancer is characterized by the presence of an excessive amount of connective tissue, primarily formed by pancreatic stellate cells (PSCs). This leads to a hypoxic tumour microenvironment that activates PSCs such that they secrete various growth factors, chemokines and matrix components. This stimulates PSC migration towards the tumour area as well as mutual growth factor/cytokine signalling with cancer cells. Thus, the ability of PSCs to migrate is recognized as a consequence of their activated state and as a requirement for efficient communication with cancer cells. Moreover, cell migration is a Ca^{2+} -dependent process that implicates the activity of transient receptor potential (TRP) channels. Many TRP channels are part of receptor signalling cascades, and are thereby essential components of the *transduction* and *effector* mechanisms underlying cellular responses to microenvironmental cues such as hypoxia. Furthermore, there is growing evidence supporting a role of TRP channels in *sensing* and *modifying* the (tumour) microenvironment. This is in particular evident for members of the TRPC family. However, the role of TRPC channels in the response of PSCs to hypoxia is unclear.

In the current study, the TRPC1 and TRPC6 channel showed the highest expression of all TRPC channels in murine PSCs. It was therefore postulated that these particular channels could play a role in regulating the responses of PSCs to hypoxia. Their role in PSC migration was investigated using primary cultured PSCs isolated from WT, TRPC1^{-/-} and TRPC6^{-/-} mice. Hypoxia was shown to increase WT mPSC motility, activate secretion of autocrine stimulants and enhance calcium signaling. In contrast, similar effects were not observed for TRPC1^{-/-} and TRPC6^{-/-} mPSCs. Hypoxia-mediated increase of TRPC1 expression in mPSCs was coupled to elevated cell motility, potentially via a *sensor* mechanism that is also important for correct cell size regulation. TRPC6 channels are part of a *modifier* mechanism due to their requirement for efficient autocrine stimulation under hypoxic conditions through growth factor/cytokine secretion. Moreover, by mediating increased calcium influx during hypoxia they activate Ca^{2+} sensitive effector proteins of the cellular migration machinery, evidencing a role in a *transduction/effector* pathway. Overall, these data show for the first time that the Ca^{2+} permeable TRPC1 and TRPC6 channels are important for the response of mPSCs to hypoxia by affecting their migratory behaviour.

German Resumé

Ein charakteristisches Merkmal des Pankreaskarzinoms ist die übermäßige Produktion von Bindegewebe, an der primär Pankreassternzellen (PSZ) beteiligt sind. Hierdurch entsteht ein hypoxisches Mikromilieu im Tumorgewebe, welches zu einer Aktivierung von PSZ und damit zu einer vermehrten Bildung von Wachstumsfaktoren, Chemokinen und Matrixkomponenten führt. Dies fördert die Migration von PSZ in das Tumorgewebe und ermöglicht eine Kommunikation mit den Karzinomzellen. Somit kann die Fähigkeit zur Migration als Folge der Aktivierung der PSZ und als eine Voraussetzung zur effizienten Kommunikation mit den Krebszellen angesehen werden. Zellmigration im allgemeinen ist ein Ca^{2+} -abhängiger Prozess, welcher TRP-Kanäle (transient receptor potential) impliziert. Viele Mitglieder der TRP-Kanal-Familie sind Teil von Rezeptor-Signalkaskaden, die die Antworten auf Stimuli aus der zellulären Umgebung vermitteln. Auch wenn es vereinzelte Hinweise für eine Beteiligung von TRP-Kanälen an der Detektion extrazellulärer Stimuli aus dem Tumor-Mikromilieu gibt, konnte ihre Rolle bei der Reaktion von PSZ auf hypoxische Bedingungen bisher nicht geklärt werden.

In der vorliegenden Arbeit konnte gezeigt werden, dass TRPC1 und TRPC6 die am stärksten exprimierten TRP-Kanäle in murinen PSZ (mPSZ) darstellen. Um ihre Rolle bei der Zellmigration zu klären, wurden mPSZ aus WT, TRPC1^{-/-} und TRPC6^{-/-} Mäusen isoliert. Hierbei konnte gezeigt werden, dass Hypoxie die Motilität, die Sekretion autokriner Stimuli und das Ca^{2+} -Signaling von WT mPSZ erhöht. Im Gegensatz hierzu konnten diese Effekte in TRPC1^{-/-} und TRPC6^{-/-} mPSZ nicht beobachtet werden. Die durch Hypoxie herbeigeführte Erhöhung der TRPC1 Expression in den WT Zellen wird dabei möglicherweise über einen Sensor-Mechanismus vermittelt, der ebenfalls an der Regulation der Zellgröße beteiligt ist. TRPC6-Kanäle scheinen dagegen an der effizienten autokrinen Stimulation durch Wachstumsfaktor- und der Zytokin-Sekretion unter hypoxischen Bedingungen beteiligt zu sein. Darüber hinaus führt die TRPC6-vermittelte Ca^{2+} -Mobilisierung unter Hypoxie zur Aktivierung von Effektor-Proteinen der Zellmigration. Zusammenfassend konnte in dieser Arbeit zum ersten Mal gezeigt werden, dass der Ca^{2+} -permeable TRPC1- und TRPC6-Kanal maßgeblich das Migrationsverhalten von mPSZ unter hypoxischen Bedingungen beeinflussen.

Table of Contents

DECLARATION AND CERTIFICATION OF ORIGINALITY	i
PREFACE.....	ii
ACKNOWLEDGEMENTS.....	iii
CURRICULUM VITAE	iv
CONTRIBUTIONS BY THE AUTHOR	vi
OVERALL AIM OF THE IONTRAC PROJECT.....	ix
SUMMARY	x
GERMAN RESÚME.....	xi
TABLE OF CONTENTS	I
ABBREVIATIONS	V

INTRODUCTION

1.1 Anatomy and Function of the Pancreas	1
1.2 Pancreatic Ductal Adenocarcinoma	3
1.2.1 Clinical Manifestation and Risk Factors.....	3
1.2.2 Characterisation and Molecular Pathogenesis of PDAC	4
1.3 Pancreatic Stellate Cells – Key Players in PDAC Progression and Metastasis	6
1.3.1 The History and Characterization of Pancreatic Stellate Cells	7
1.3.2 Pancreatic Stellate Cell Activation.....	8
1.3.3 Pancreatic Stellate Cells in the (PDAC) Microenvironment	10
1.3.3.1 Hypoxia – A Major Feature in PDAC and PSC Activation	11
1.3.3.2 PSCs Mutual Signalling with PDAC Cells	12
1.3.4 Autocrine Stimulation in PSCs.....	14
1.4 Cell Migration	15
1.4.1 Basic Principles of Cell Migration	15
1.4.2 Calcium-dependent Signalling in Cell Migration	17
1.5 TRP Channels in Migration and as Microenvironmental Sensors, Modifiers and Effectors	19
1.5.1 TRP Channel Family.....	19
1.5.1.1 TRP Channel Function	19

1.5.1.2 TRP Channels in Cell Migration and Interaction Partners	20
1.5.2 TRP Channels as Sensors and Effectors of the Tumour Microenvironment	23
1.5.2.1 TRP Channels as Mechanosensors and Modulators of the TME	23
1.5.2.2 TRP Channels in Hypoxia and Oxidative Stress	24

PROJECT AIM

2.1 Hypothesis, Objective and Strategy	29
---	-----------

MATERIALS AND METHODS

3.1 Materials	32
3.1.1 Media	32
3.1.2 Chemicals and Kits.....	32
3.1.3 Instruments	34
3.1.4 Oligonucleotides.....	35
3.2 Mouse Strains	36
3.2.1 Pancreatic Stellate Cells	36
3.3 Cell Biological Methods	37
3.3.1 Reactivating Frozen RLT-PSCs	37
3.3.2 Isolation of Mice Pancreatic Stellate Cells	37
3.3.2.1 Identification of mPSCs	38
3.3.3 Cell culture, Passaging and Cell Count	39
3.4 Molecular Biological Methods	39
3.4.1 Protein Biochemical Methods.....	39
3.4.1.1 Protein Isolation and Estimation.....	39
3.4.1.2 Protein Detection and Analysis	40
3.4.2 RNA Extraction and Purification from PSCs.....	43
3.4.3 Reverse Transcriptase PCR	43
3.4.4 Polymerase Chain Reaction (PCR)	44
3.4.5 DNA Electrophoresis	45
3.4.6 Quantitative Real-time PCR.....	46
3.5 In Vitro Migration Assays.....	48
3.5.1 Hypoxia treatment	48

3.5.2 Two-Dimensional Migration.....	49
3.5.3 Three-Dimensional Migration	50
3.5.4 Chemotaxis Assay.....	52
3.5.5 Autocrine Stimulation Assay	53
3.5.6 Analysis of Migration Data	53
3.6 Oxygen Consumption and Extracellular Acidification Measurements	55
3.6.1 Estimation of Oxygen consumption in 3D chamber.....	56
3.7 Manganese Quenching	58
3.8 Calcium Entry.....	60
3.9 Calpain Activity.....	60
3.10 Statistical Analysis	62

RESULTS

4.1 mPSC Identification.....	63
4.2 Quantitative Assessment of TRPC Channel Expression in mPSCs	64
4.3 mPSC Migration in Three Dimensional Space	65
4.3.1 Oxidative Cell Stress in Three Dimensional mPSC Migration.....	66
4.4 Hypoxia and mPSC Migration	68
4.4.1 Chemically Induced Hypoxia Stimulates mPSC Migration	68
4.4.1.1 DMOG Induces mPSC Migration in a Dose-Responsive Manner.....	68
4.4.1.2 Chronic Treatment with DMOG Induces an Anaerobic mPSC Phenotype.....	69
4.4.2 mPSCs Morphology Upon Hypoxia Stimulation.....	71
4.4.3 TRPC1 ^{-/-} and TRPC6 ^{-/-} mPSCs Display Diminished Motility Under Chemically Induced Hypoxia.....	72
4.4.4 Attenuated Autocrine Stimulation of TRPC1 ^{-/-} and TRPC6 ^{-/-} mPSCs Under Chemically Induced Hypoxia.....	74
4.4.5 TRPC1 ^{-/-} and TRPC6 ^{-/-} mPSCs Display Diminished Motility Under Hypoxia Stimulation	75
4.5 TRPC Channel Expression in mPSCs under Hypoxia	78
4.6 Assessment of Autocrine Stimulation of mPSCs under Hypoxia	80
4.7 Calcium Influx in Hypoxia Stimulated mPSCs.....	82
4.7.1 Calpain – a Downstream Effector in PSC Migration.....	83
4.8 PDGF Stimulation of mPSC Migration.....	84
4.8.1 PDGF Stimulates mPSC Migration in Three Dimensional Space	84
4.8.2 PDGF Chemotaxis	86

DISCUSSION

5.1 The “Ideal” Migration Setup	89
5.2 Hypoxia in PSC Activation	90
5.3 TRPC1 and TRPC6 Channels in the Hypoxia-Mediated Activation of mPSCs	91
5.3.1 TRPC1 Channel: Part of an Indirect Sensor Mechanism to Hypoxia in mPSCs.....	91
5.3.1.1 <i>The TRPC1 Channel is not Implicated in the Secretion of Autocrine Stimulants</i>	94
5.3.2 TRPC6 Channel: A Central Component in the Response of mPSCs to Hypoxia.....	94
5.3.2.1 <i>The TRPC6 Channel in a Modifier Mechanism</i>	95
5.3.2.2 <i>TRPC6 Channel: Important for Hypoxia-mediated Calcium Entry</i>	97
5.4 Future Objectives	99

CONCLUDING REMARKS AND PERSPECTIVES

6.1 Conclusions	102
6.2 Perspectives	104

REFERENCES

7. Reference List	107
--------------------------------	------------

Abbreviations

α -SMA	Alpha – smooth muscle actin
AP-1	Activator Protein-1
app.	approximately
a.u.	arbitrary unit
bp	Base pair
cAMP	Cyclic Adenosine Monophosphate
cDNA	Complementary Deoxyribonucleic Acid
Conc.	Concentration
COX2	Cyclooxygenase-2
CTGF	Connective Tissue Growth Factor
DAG	Diacylglycerol
DMEM	Dulbecco's Modified Eagle's Medium
DMOG	Dimethylxalglycine
DMSO	Dimethyl Sulfoxide
DNA	Deoxyribonucleic Acid
dNTP	Deoxyribonucleotid Triphosphate
ECAR	Extracellular Acidification rate
ECM	Extracellular Matrix
ER	Endoplasmatic Reticulum
EGF	Epidermal Growth Factor
ERK	Extracellular signal Regulated Kinase
FCS	Fetal Calf Serum
FGF	Fibroblast Growth Factor
GEMM	Genetically Engineered Mouse Models
GFAP	Glial fibrillary acidic protein
GPCR	G Protein-Coupled Receptor
HGF	Hepatocyte Growth factor
HSC	Hepatic Stellate Cell
HIF-1 α	Hypoxia Inducible Factor 1- α
IHH	Indian Hedgehog
IL	Interleukin

IP ₃	Inositol-1,4,5 triphosphate
IPMN	Intraductal Papillary Mucinous Neoplasm
JNK	c-jun amino terminal kinase
kb	Kilobase
kDa	Kilo-Dalton
KO	Knock out
Kv	Voltage Gated K ⁺ Channels
MAPK	Mitogen-Activated Protein Kinase
MCN	Mucinous cystic neoplasm
MCP-1	Monocyte Chemoattractant Protein 1
MMP	Matrix Metalloproteinase
mPSC	Mice Pancreatic Stellate Cells
mRNA	Messenger RNA
OCR	Oxygen Consumption rate
PanIN	pancreatic intraepithelial neoplasia
PBS	Phosphate Buffered Saline
PCR	Polymerase Chain Reaction
PDAC	Pancreatic Ductal Adenocarcinoma
PDGF	Plate-Derived Growth Factor
PI3K	Phosphatidylinositol-3-kinase
PKC	Protein Kinase C
PLC	Phospholipase C
PPAR- γ	Peroxisome Proliferator-Activated Receptor γ
PSC	Pancreatic Stellate Cells
RNA	Ribonucleic Acid
ROCE	Receptor-Operated Calcium Entry
ROCK	Rho-Rho Kinase
ROS	Reactive Oxygen Species
<i>rpm</i>	Rotations Per Minute
RTK	Receptor Tyrosine Kinase
RT-PCR	Reverse Transcriptase PCR
RT-qPCR	Real Time Quantitative Polymerase Chain Reaction
SDS	Sodium Dodecyl Sulfate

SDS-PAGE	SDS Polyacrylamide Gel Electrophoresis
si	Short Interfering
SOCE	Store Operated Calcium Entry
TIMP	Tissue Inhibitor of Metalloproteinase
TME	Tumour Microenvironment
TNF- α	Tumour Necrosis Factor- α
TGF- β 1	Transforming Growth Factor- β 1
TRP	Transient Receptor Potential
VEGF	Vascular Endothelial Growth Factor
WT	Wild type

Chapter 1

Introduction

Introduction

1.1 Anatomy and Function of the Pancreas

The primary function of the pancreas is to aid in the digestion of food through secretion of enzyme-rich pancreatic juice. Humans secrete approximately 1-2 l pancreatic juice per day. The pancreas is located in the upper abdomen, has a recognizable pinkish color and forms a lobular structure. It contacts the concave side of the duodenum and the spleen, thereby maintaining an intimate connection with vital blood vessels and organs. It is comprised four regions: head, neck, body and tail (*figure 1.1*) (Aumüller et al., 2014; Lee et al., 2012). The pancreas acts as both an exocrine and an endocrine gland. The endocrine glands, referred to as the islets of Langerhans, secrete hormones that regulate glucose metabolism. These include among others, Insulin, glucagon, somatostatin and pancreatic polypeptide, which are secreted from β -, α -, δ - and F-cells, respectively. A normal human pancreas contains between 500.000 to several millions islets, each measuring between 50 and 300 μm in diameter (Boron and Boulpaep, 2005). The exocrine pancreas is composed of lobules each made up of acini (clusters of acinar cells) surrounding a central lumen where to the acinar cells release their digestive enzymes via zymogen granules (*figure 1.1*). These enzymes include proteases, amylases, nucleases and lipases, which are mostly secreted as inactive precursor proteins. The acini lumen feeds into an intercalated duct and groups of acini are further drained by larger interlobular ducts that empty into a main duct connected to the lumen of the gastrointestinal tract (Boron and Boulpaep, 2005). Food digestion can stimulate digestive enzyme release through both neural (cholinergic) or hormonal (predominantly CCK, released from the duodenum) activity. In the duodenal lumen, enteropeptidase cleaves the pancreatic protease trypsinogen into active trypsin, which in turn catalyses the activation of all other pancreatic proteases.

The two primary functions of the pancreatic duct cells are to (a) secrete fluid that acts as a vehicle for the transport of secreted enzymes and (b) secrete HCO_3^- that is important for neutralizing gastric acid and provides the optimal pH environment for the digestive enzymes (Boron and Boulpaep, 2005; Lee et al., 2012). Pancreatic stellate cells (PSCs) are also residing in the exocrine pancreas (described in *section 1.3*). They are

mostly present in the periacinar space were they encircle the base of the acini, but they can also be found in perivascular and periductal regions of the pancreas (*figure 1.1*) (Apte

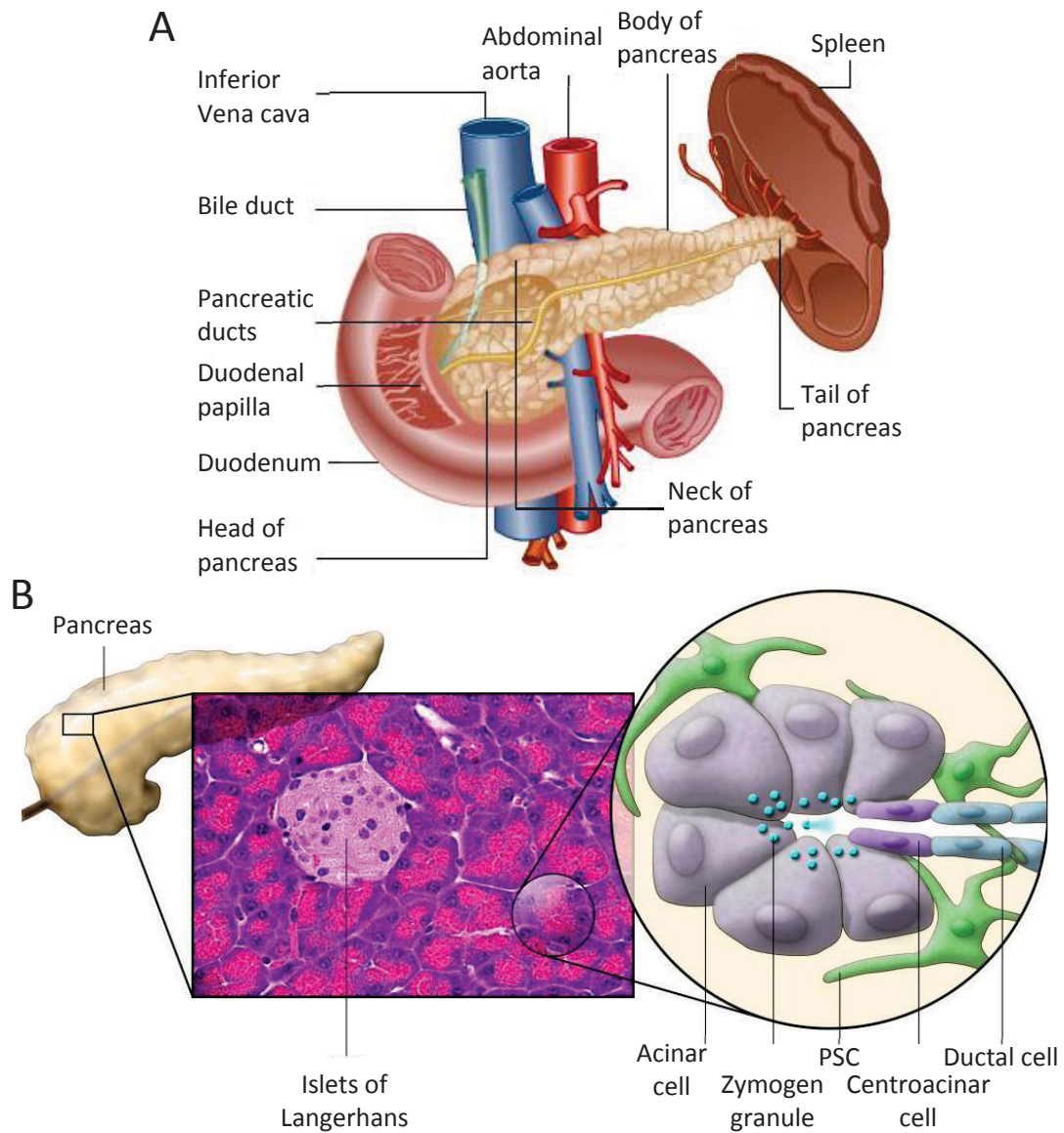


Figure 1.1. The Anatomy of Pancreas. (A) Placed deep in the abdominal cavity, the pancreas is situated close to many vital organs and blood vessels. It is anatomically divided into a head, neck, body and tail (adapted from <http://www.pancreaticcancerindia.com>). (B) The pancreas can be divided into an exocrine and endocrine component. The endocrine component, consisting of islets of Langerhans, functions to secrete hormones that regulate carbohydrate metabolism. The exocrine component consists of clusters of acinar cells (known as acini) that secrete numerous digestive enzymes into the acinar lumen that feeds into ductules. In the normal pancreas, quiescent PSCs are found in the periacinar and periductal space of exocrine areas, where their long cytoplasmic processes encircle the acinar and duct cells. PSCs participate in various physiological as well as pathophysiological processes in pancreas biology (Omary et al., 2007).

et al., 1998; Bachem et al., 1998; Omary et al., 2007). These cells play a role in regulating and controlling tissue homeostasis in both physiological as well as pathophysiological processes, including pancreatic cancer (Apte and Wilson, 2011; Bachem et al., 2008; Duner et al., 2011; Vonlaufen et al., 2008b).

1.2 Pancreatic Ductal Adenocarcinoma

Tumours arising from the epithelium of the exocrine pancreas are the most common type of pancreatic cancer and account for well over 95% of all pancreatic cancers. Of these, pancreatic ductal adenocarcinoma (PDAC) is the most common type, making up 90% of all exocrine tumours (Klimstra, 2007; Matthaios et al., 2011). PDAC tumours can be sub-grouped according to their localisation in the pancreas. 65% originate in the head of the pancreas, 30% in the body and tail and 5% can occur within the whole pancreas (Ryan et al., 2014). PDAC is not a common cancer type compared to that of lung, breast, prostate and colorectal cancer. In 2015, PDAC is projected to rank 10-12th in incidence rates worldwide (Ferlay et al., 2015; Siegel et al., 2015), which is lower than the previous years where it ranked 9-10th in 2009 in the United States (Jemal et al., 2009) and 7th in 2012 in European countries (Ferlay et al., 2010; Ferlay et al., 2013). Despite its low ranking in incidences, PDAC is the fourth most common cause of cancer related death in the world among men and women (Ferlay et al., 2015; Malvezzi et al., 2014; Siegel et al., 2015). Moreover, a recent projection of cancer incidence and death for 2020 and 2030 estimated that pancreatic cancer will surpass breast, prostate and colorectal cancers by 2030 to become the second leading causes of cancer-related deaths (Rahib et al., 2014). In total, PDAC has one of the worst prognoses of all cancers, with an overall 5-year survival rate of less than 5% and on average patients live for only 6 months after diagnosis. It therefore represents one of the most lethal cancers, where mortality is essentially equal to incidence (Hidalgo, 2010).

1.2.1 Clinical Manifestation and Risk Factors

The lethal nature of PDAC is due to its aggressive growth and the rapid development of distant metastasis. Moreover, symptoms of PDAC are mostly present at only an advanced stage, making diagnosis and treatment extremely difficult (Hidalgo,

2010; Maitra and Hruban, 2008; Oettle, 2014). The only potentially curative treatment so far is surgical resection followed by adjuvant chemotherapy, but less than 20% of patients are able to undergo surgery (Barugola et al., 2009; Jones et al., 2014). Additionally, surgical resection only prolongs the 5-year survival by 10% because of comorbidity or because the tumour has already become metastatic. 85% of these patients will therefore experience relapse and subsequent cancer-related death. Virtually all patients do not survive past 7-10 years of surgery (Alexakis et al., 2004; Carpelan-Holmstrom et al., 2005).

PDAC occurs primarily in elderly people and the aging European population means the incidence is very likely to increase (Malvezzi et al., 2014). Nevertheless, age is not the only risk factor for developing PDAC, as other factors include multiple genetic syndromes ([section 1.2.2](#)), a family history of cancer, as well as modifiable risk factors (reviewed in (Becker et al., 2014; Maisonneuve and Lowenfels, 2010)). Cigarette smoking represents the most prominent environmental risk factor of developing PDAC (Lowenfels and Maisonneuve, 2006), along with others such as diabetes, obesity, chronic pancreatitis and alcohol abuse (Fedeli et al., 2014; Maisonneuve and Lowenfels, 2010; Raimondi et al., 2009) as well as lack of sufficient physical activity (Eheman et al., 2012; Raimondi et al., 2009). Currently, no standards exists for screening and evaluating these high-risk patients (Bruenderman and Martin, 2014). To combat the mortality rates of PDAC, more effort is required to understand PDAC development and progression together with methods of early prevention, diagnosis and treatment of patients with advanced disease. Better screening and identification of early pancreatic cancer lesions can also improve the detection of patients suitable for surgical resection (Esposito et al., 2014; Haugk, 2010).

1.2.2 Characterisation and Molecular Pathogenesis of PDAC

Pancreatic intraepithelial neoplasia represents the best characterised histological indicator used to designate and identify proliferative duct lesions during progression of PDAC from normal duct epithelium to infiltrating cancer ([figure 1.2](#)) (PanIN) (Hruban et al., 2001; Hruban et al., 2000; Klimstra and Longnecker, 1994; Maitra et al., 2003). Intraductal papillary mucinous neoplasm (IPMN) and mucinous cystic neoplasm (MCN) are also associated with invasive PDACs (reviewed in (Hruban et al., 2007)). However, these lesions account for only ~5% of all primary pancreatic tumours (Visser et al., 2008).

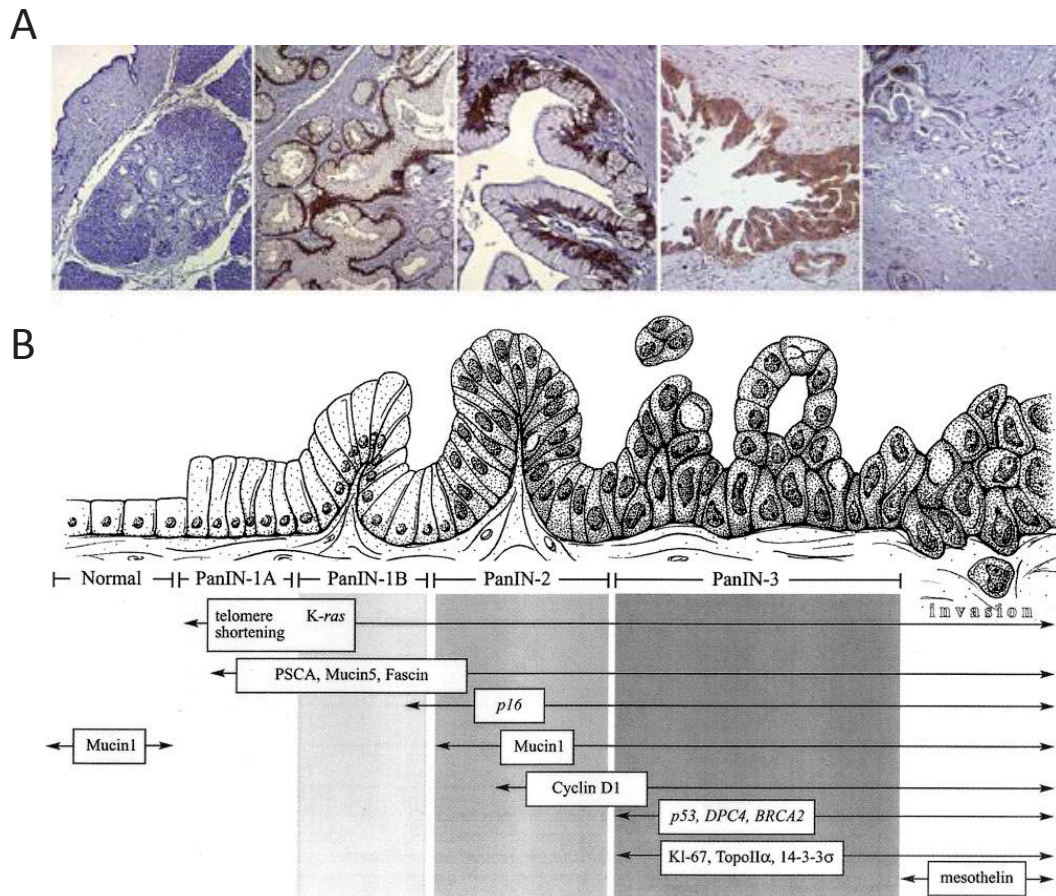


Figure 1.2. Progression Model of Pancreatic Ductal Adenocarcinoma. (A) Representative histopathological images illustrating the progressive abnormality changes from normal duct epithelium to PanIN-1 A/B, PanIN-2, PanIN-3 and to invasive PDAC (adapted from (Mihaljevic et al., 2010)). (B) A schematic drawing of the histopathological PanIN features of normal duct epithelium progression to infiltrating cancer (left to right). Underneath are given some of the main known mutagenic events occurring during PDAC progression together with novel tumor markers (see text). The length of the arrows indicates the occurrence of the events, some at early and some at later stages (adapted from (Duner et al., 2011; Maitra et al., 2003)).

All precursor lesions found for PDAC (PanIN, IPMN and MCN) are fundamental for early detection and treatment of patients (Becker et al., 2014; Haugk, 2010).

PDAC is a fundamentally genetic disease caused by alterations in cancer associated genes. In the past two decades we have witnessed an explosion in our understanding of PDAC, with a number somatic mutations being identified and mapped (Esposito et al., 2014; Maitra and Hruban, 2008; Maitra et al., 2006). These mutagenic abnormalities occur in parallel with PanIN lesions (*figure 1.2*) (Maitra et al., 2003). Overall, PanIN is driven by the expression of an oncogenic form of the *K-RAS* gene, which was the first genetic abnormality found in PDAC progression and is present in more than 90% of PDAC

tumours (Hruban et al., 1993). Telomere shortening is also one of the first events that occurs in PDAC development and is found in more than 95% of all PanIN lesions (van Heek et al., 2002). Other important tumour suppressor, oncogenes and maintenance genes implicated in PanIN progression include *P16/CDKN2A*, *Cyclin D1*, *SMAD4*, *P53*, *HER-2/neu* and *BRCA2* (some depicted in [figure 1.2 B](#)) (Reviewed in (Haugk, 2010; Mihaljevic et al., 2010; Ottenhof et al., 2011)). Each affects several central core signalling pathways important to fulfil the following hallmark criteria for tumour development defined by Hanahan and Weinberg (Hanahan and Coussens, 2012; Hanahan and Weinberg, 2011): (1) self-sufficiency in growth signals, (2) insensitivity to antigrowth signals, (3) evasion of apoptosis, (4) limitless replicative potential, (5) angiogenesis, and (6) invasion and metastasis (Hanahan and Weinberg, 2000; Mihaljevic et al., 2010). Several other genes have been found to be up- and down regulated (Biankin et al., 2012; Grutzmann et al., 2004; Jones et al., 2008). This has made it clear that PDAC is highly heterogeneous partially explaining the difficulties in treatment (Oettle, 2014; Ottenhof et al., 2011).

A representative group of novel PDAC tumour markers in different PanIN lesions are depicted in [figure 1.2 B](#) (PSCA, Mesothelin, Fascin, and 14-3-3). These genetic fingerprints or transcriptional profiles have allowed the identification of specific subtypes of PDAC (classical, quasimesenchymal (QM-PDA) and exocrine-like), which have different prognoses and distinct drug responses (Collisson et al., 2011)

1.3 Pancreatic Stellate Cells – Key Players in PDAC Progression and Metastasis

One of the most pronounced features compared to other cancers is the abundant deposition of connective tissue (fibrosis) surrounding the tumour also known as the desmoplastic reaction in PDAC (Apte et al., 2004; Vonlaufen et al., 2008b). This stroma content can form up to 90% of the total tumour mass in PDAC and correlate with its biological and clinical aggressiveness, chemo resistance and limited availability in drug delivery (Erkan et al., 2012; Mahadevan and Von Hoff, 2007; Schober et al., 2014). It is widely accepted that activated pancreatic stellate cells (PSC) are responsible for this reaction (Apte et al., 2004). This has increased the understanding of PDAC development and progression together with other general aspects of the tumour microenvironment

(TME) and its host cells in cancer progression (e.g. fibroblasts, macrophages and other immune cells or endothelial cells) (Brabek et al., 2010; Gupta and Massague, 2006; Hanahan and Weinberg, 2011; Joyce and Pollard, 2009). The tumour is now recognized as a continuously evolving organ and as the cancer progresses, the surrounding TME changes in parallel into an activated state (Gatenby and Gillies, 2008). This occurs mainly through continuous communication and mutual signalling between the cancer and stroma cells together with extracellular matrix (ECM) production and remodelling (Li et al., 2007b; Shimoda et al., 2010). This aspect in tumour progression is intimately related to the influence of PSCs in PDAC progression. Second, the physical and biochemical properties of the TME have an influence on PSC activation and PDAC progression (e.g. pressure, ECM components, stiffness, topography, acidity and hypoxia) together with oxidative stress and its metabolites including reactive oxygen species (ROS), ethanol, acetaldehyde and hydrogen peroxide (Feig et al., 2012; Kikuta et al., 2006; Masamune et al., 2002; Masamune et al., 2010). Overall, cancer progression can be viewed as an orchestra of multiple players.

1.3.1 The History and Characterization of Pancreatic Stellate Cells

The term “Stellate cell” was first used for isolated hepatic stellate cells (HSC) identified by Karl Wilhelm Kupffer although he classified these cells as phagocytes (Kupffer, 1876). In 1971, Wake identified these cells as HSC (Wake, 1971) and an agreement was made to use this as a standard name in 1996 (Ahern et al., 1996). PSC is the counterpart to HSC and was first reported in mice by Watari in 1982 (Watari et al., 1982) and later in human and rat (Ikejiri, 1990). However, the major impact in the understanding of fibrosis and desmoplasia in PDAC was first made after the development of the isolation and culture procedure for mammalian PSCs (Apte et al., 1998; Bachem et al., 1998) and the establishment of a human PSC line (RLT-PSC) (Jesnowski et al., 2005). This *in vitro* tool has provided valuable knowledge on PSC function and their pronounced influence on PDAC progression (Vonlaufen et al., 2010). A historical timeline with the most important milestones in the understanding of PDAC and PSC is shown in [figure 1.3](#).

In the normal pancreas, resident PSCs are located in the periacinal spaces adjacent to acinar cells and comprise 4-7% of all pancreatic cells. Here they maintain normal tissue integrity and homeostasis via tight regulation of extracellular matrix (ECM) turnover

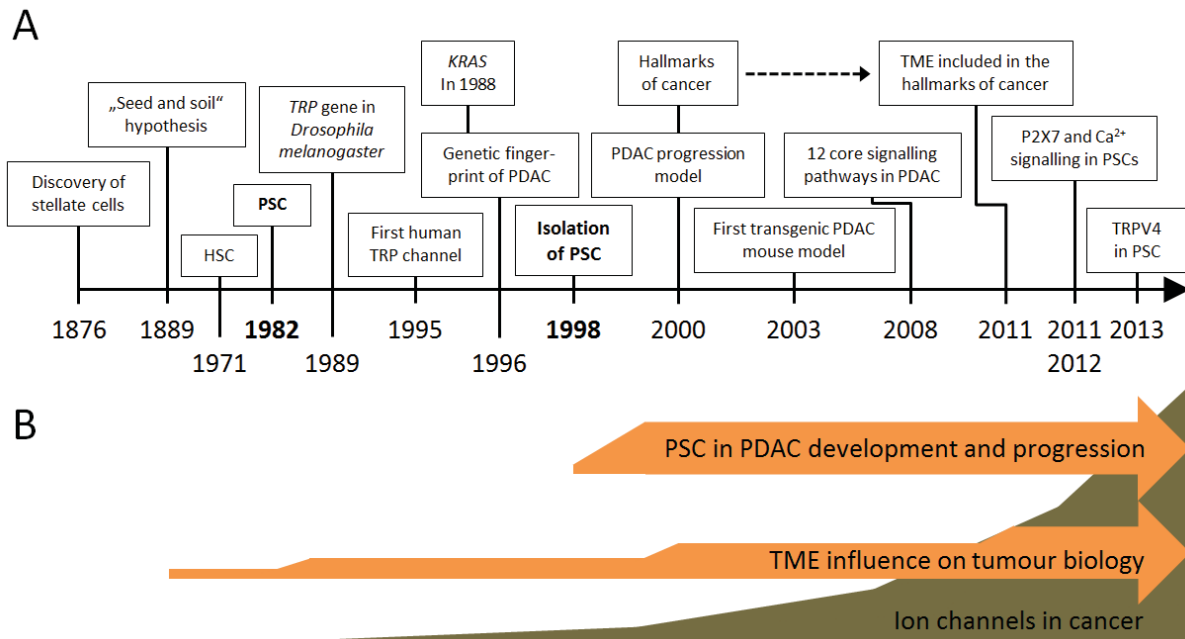


Figure 1.3. Major Milestones in Pancreatic Stellate Cell and PDAC Biology. (A) The key milestones in PSC and PDAC biology shown in a timeline with relation to following: (1) The implementation of the “seed and soil” hypothesis, (2) introduction of cancer hallmarks, (3) introduction of the TME to the cancer hallmarks, (4) discovery of TRP channels (5) to date only published papers on ion channels/receptors in PSCs (outlined in the text). (B) Illustration of the increasing research interest of the TME influence on tumour biology, PSCs role in PDAC development and progression, and ion channels related to cancer.

through the secretion of metalloproteinases (MMPs) and tissue inhibitors of MMPs (TIMPs) (Phillips et al., 2003a). Additionally, PSCs determine the proper formation and differentiation of acini during normal development through effective β 1-integrin cell adhesion to the basement membrane (Arcangeli et al., 2014; Riopel et al., 2013). In their quiescent stage PSCs can be characterised and identified by abundant Vitamin A droplets in their cytoplasm together with the expression of desmin and glial fibrillary acidic protein (GFAP). During pancreatic injury or PDAC, PSCs are activated, lose their lipid droplets and transform into an activated myofibroblast-like phenotype expressing α -smooth muscle actin (α -SMA). Of note, this transformation is also spontaneously induced by *in vitro* isolation and culturing of primary PSCs (Apte et al., 1998; Bachem et al., 1998).

1.3.2 Pancreatic Stellate Cell Activation

Upon activation, PSCs subsequently acquire the following functional capabilities: (1) increased proliferation rate, (2) higher migration activity, (3) excessive production of ECM

components as well as ECM modulators including MMP and TIMPs, and (4) secretion of proinflammatory growth factors and cytokines (Bachem et al., 2005; Phillips et al., 2003b).

Several *in vitro* and *in vivo* studies of mice, rat and human PSCs have identified a number of intra- and extracellular effector molecules that are secreted by PSCs. Many also originate from PDAC cells ([section 1.3.3.2](#)). These include numerous growth factors/cytokines, oxidative stress and ROS which exert both paracrine and autocrine effects ([figure 1.4](#)). Platelet-derived growth factor (PDGF) and transforming growth factor β 1 (TGF- β 1) are the two most established activators that lead to increased proliferation, ECM production, MMP secretion and cell migration of PSCs (Apte et al., 1999; Apte et al., 2012; Luttenberger et al., 2000; Masamune et al., 2009; Phillips et al., 2003b; Schneider et al., 2001; Tahara et al., 2013; Tang et al., 2012). PDGF is also a potent chemoattractant for PSCs (Hild, 2015; Phillips et al., 2003b). Other factors include hepatocyte growth factor (HGF), vascular endothelial growth factor (VEGF), connective tissue growth factor (CTGF), epidermal growth factor (EGF) fibroblast growth factor (FGF), interleukin (IL)-6, IL-8, IL-10, IL-15 and monocyte chemoattractant protein 1 (MCP-1) (Eguchi et al., 2013; Habisch et al., 2010; Masamune et al., 2009; Masamune et al., 2008a; Mews et al., 2002). PSCs also respond differently to a range of inflammatory cytokines. For example, tumour necrosis factor α (TNF- α) stimulates proliferation and collagen production, IL-10 stimulates collagen production, whereas IL-6 inhibits both functions (Mews et al., 2002).

In connection to this, the mitogen-activated protein kinase (MAPK) and the phosphatidylinositol-3-kinase (PI3K) pathway has been identified to be among the key signalling pathways of cytokine-related PSC activation (Jaster, 2004; Masamune and Shimosegawa, 2009). PDGF-induced PSC migration is regulated by the PI3K-Akt pathway (Masamune et al., 2003a; McCarroll et al., 2004), while PDGF-induced PSC proliferation is mediated via the extracellular signal regulated kinase (ERK1/2) pathway (Jaster et al., 2002; Masamune et al., 2003a). Oxidative stress and its metabolites including ROS, ethanol, acetaldehyde and hydrogen peroxide induce activation of the MAPK pathway in PSC through ERK1/2, p38 kinase and c-jun amino terminal kinase (JNK), transcription factor activator protein-1 (AP-1) as well as the two upstream signalling molecules PI3K and protein kinase C (PKC) (Kikuta et al., 2006; Masamune et al., 2002; Masamune et al., 2010). Additionally, the Rho-Rho kinase (ROCK) pathway is involved in the activation of

PSC through the reorganization of actin cytoskeleton (Masamune et al., 2003b) and activation of the Indian hedgehog (IHH) pathway, which promotes PSC migration (Shinozaki et al., 2008). In contrast, the nuclear hormone receptor peroxisome proliferator-activated receptor γ (PPAR- γ) pathway been implicated in PSC inhibition through a repression of PSC proliferation and α -SMA expression (Galli et al., 2000).

1.3.3 Pancreatic Stellate Cells in the (PDAC) Microenvironment

Sustained PSC activation leads to disturbance of the normal balance between ECM production and degradation promoting fibrogenesis. This occurs primarily through elevated expression of collagens (I, III, V), fibronectin and laminin in activated PSCs (Apte et al., 1999; Bachem et al., 1998; Wehr et al., 2011) (*figure 1.4*). Consequently, PSCs are present and activated within these hypoxic and fibrotic areas of PDAC as demonstrated by co-localisation studies with the hypoxia inducible factor 1- α (HIF-1 α) and carbonic anhydrase 9 (Couvelard et al., 2005; Eguchi et al., 2013). More, PSC-produced collagen I and V promote the malignant phenotype of PDAC (Apte et al., 2004; Armstrong et al., 2004; Berchtold et al., 2015; Vaquero et al., 2003; Wehr et al., 2011). In return ECM components influence PSC activity: fibrinogen, which is highly present in PDAC, induces collagen I, IL6, IL8, MCP-1, VEGF production in PSCs (Masamune et al., 2009). Additionally, the ECM can serve as a reservoir for numerous proteins and growth factors/cytokines, which are released during ECM turnover to promote PSC and PDAC cell activity. In connection to this, studies suggest that activated PSCs rather than PDAC cells are the main players in ECM turnover: PSCs are major sources of MMP and TIMP secretion (MMP-2, 9, 12 and 13) (Bachem et al., 2005; Erkan et al., 2009; Phillips et al., 2003a; Yoshida et al., 2004). For example, MMP-2 secretion exceeds by far that of cancer cells (Ellenrieder et al., 2000; Farrow et al., 2009; Schneiderhan et al., 2007). As general changes in ECM mechanics are related to promoting cancer progression (Werfel et al., 2013), this adds weight to the participation of PSCs in driving PDAC progression. Although targeting MMPs showed promising results only a few years ago (Alves et al., 2001), the inhibition of MMPs in cancer and stroma cells in later studies actually increased migration, questioning the potential of MMPs in cancer therapy (Friedl and Wolf, 2009a; Kessenbrock et al., 2010; Mierke, 2012).

1.3.3.1 Hypoxia – A Major Feature in PDAC and PSC Activation

Tumour compression, solid stress and high interstitial fluid pressure observed in PDAC promote intracellular oxidative stress pathways in PSCs (Asaumi et al., 2007; Kharraishvili et al., 2014), which leads to elevated secretion of TGF- β 1 and collagen I

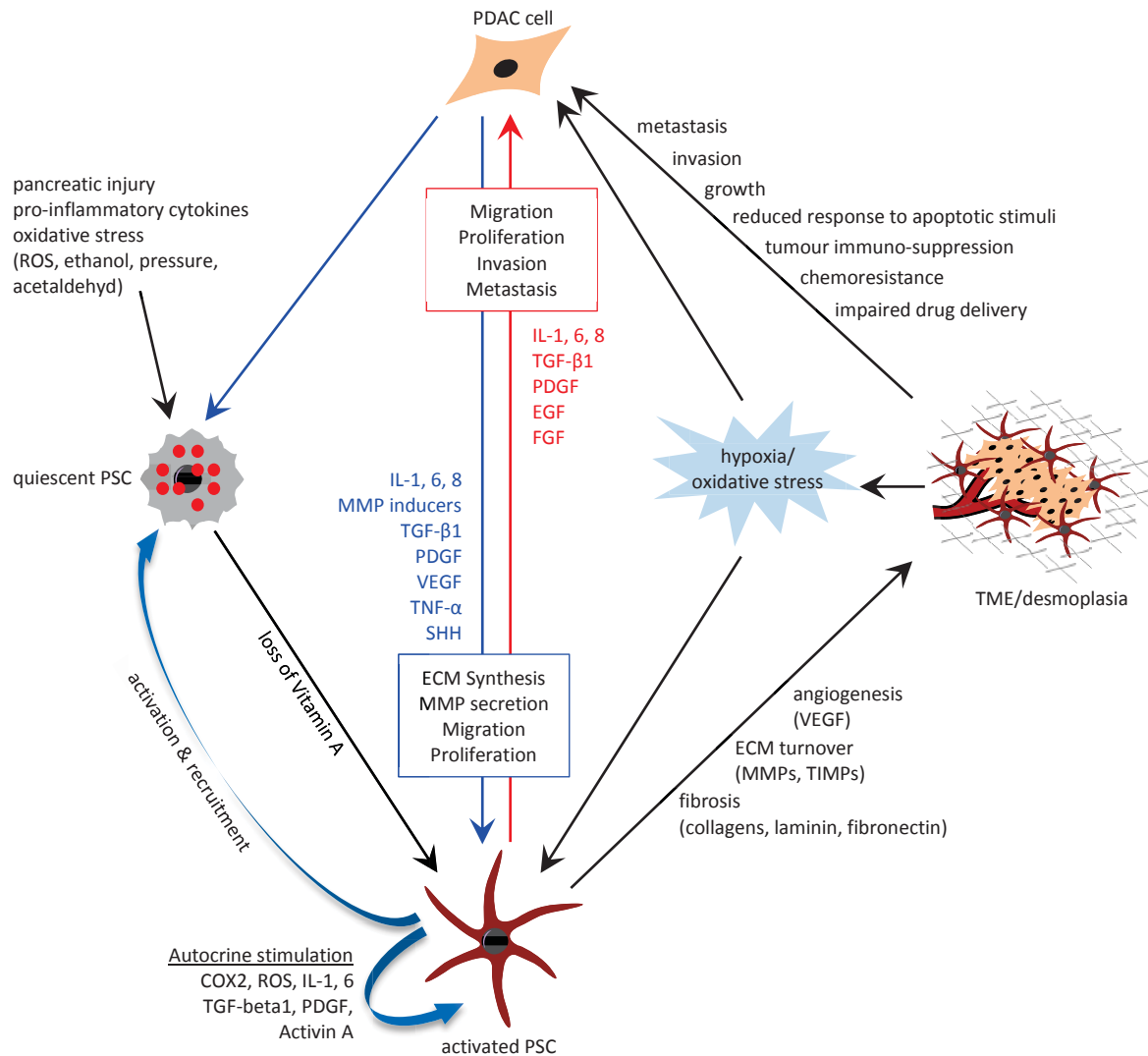


Figure 1.4. Pancreatic Stellate Cell Activation and Mutual Signalling with PDAC Cells. PSC can be activated or further stimulated by various paracrine stimulants released from PDAC cells (blue text), inflammatory immune cells or injured acinar/duct cells. Activated PSCs in turn secrete growth factors/cytokines (red text) and ECM components mediating stimulatory and survival effects on PDAC cells either directly or through a desmoplastic reaction. Activated PSCs can recruit/activate neighbouring PSCs and inflammatory immune cells. In this manner, a positive mutual stimulatory loop is maintained and an aggressive PDAC microenvironment formed. Additionally, PSCs can be activated by exogenous factors including oxidative stress or hypoxia caused by the desmoplastic reaction. Finally, PSCs are cable of autocrine stimulation perpetuating their own activity. Major PSC processes stimulated by PDAC cells and vice versa are given in blue and red boxes, respectively. Modified from (Tang et al., 2012) and (Duner et al., 2011).

(Watanabe et al., 2004). In addition, cell stress appears to participate in the early stages of fibrogenesis and oncogenesis by activating PSCs, with hypoxia playing a major role in this process (Erkan et al., 2009; Rebours et al., 2013). Hypoxia-mediated PSC activation involve elevated migratory activity together with expression and secretion of collagen I, fibronectin, CXCL12, TGF- β 1, FGF, CTGF, VEGF and MMPs expression. This facilitates a favourable TME for PDAC progression, migration and invasion (Eguchi et al., 2013; Erkan et al., 2009; Ide et al., 2006; Masamune et al., 2008a). Additionally, hypoxia-mediated secretion of VEGF by PSCs promotes angiogenesis in PDAC (Erkan et al., 2009; Masamune et al., 2008a) correlating with the degree of fibrosis (Kuehn et al., 1999) (*figure 1.4*). Hypoxia also favours the metabolic cooperation between stroma and cancer cells and the induction of chronic inflammation (Icard et al., 2014). Specifically, continuous secretion of proinflammatory cytokines (IL-1, 6, 8, 10 and MCP-1) in hypoxia-activated PSCs, together with that of PDAC cells, leads to recruitment and infiltration of immune cells. This gives rise to chronic tumour inflammation and an immune suppressive TME that accelerates tumour progression (Clark et al., 2007; Landskron et al., 2014; Lunardi et al., 2014; Wormann et al., 2014; Yang et al., 2013; Yu and Kim, 2014). For example, IL-8 and MCP-1 expression by PSCs may modulate the recruitment and accumulation of inflammatory cells in the pancreas and may play a role in perpetuating a state of inflammation in the TME (Andoh et al., 2000; Wehr et al., 2011). Even so, the molecular mechanisms behind the hypoxia-mediated stimulation of PSC are still yet to be elucidated. In summary, this supports the statement that PSCs establish a TME that favour PDAC progression and survival. Thus this is largely achieved through close mutual signalling between PSCs and PDAC cells (*figure 1.4*) (Apte and Wilson, 2011; Habisch et al., 2010; Tang et al., 2012; Vonlaufen et al., 2008b). This partnership was highlighted in a recent review, where a collection of all available *in vitro* and *in vivo* data demonstrated a close bi-directional interaction between PSCs and PDAC cells (Haqq et al., 2014)

1.3.3.2 PSCs Mutual Signalling with PDAC Cells

PDAC cells stimulate PSC proliferation, migration, matrix and MMP synthesis through secretion of PDGF, TGF- β 1 and FGF-2 (Apte et al., 2004; Bachem et al., 2005; Bachem et al., 2008; Vonlaufen et al., 2008a). In return, PSCs stimulate pancreatic cancer cell proliferation, migration, invasion/metastasis and decrease cancer cell apoptosis to

enhance cancer survival (Bachem et al., 2005; Bachem et al., 2008; Hwang et al., 2008). For instance, enhanced CTGF secretion from hypoxia-activated PSCs induces invasion of PDAC cells (Eguchi et al., 2013) and inhibition of CTGF improves chemotherapy responses without increasing drug delivery (Neesse et al., 2013). Hwang et al. found that conditioned media from PSCs induces PDAC resistance to gemcitabine and radiation (Hwang et al., 2008), although Mantoni et al. could not confirm these observations. Instead, they found that under both *in vitro* and *in vivo* settings PSCs radioprotect PDAC cells via a β 1-integrin-dependent signalling pathway (Mantoni et al., 2011). Further, PDAC cells stimulate PSCs to secrete VEGF promoting angiogenesis (Erkan et al., 2009; Masamune et al., 2008a) and the induction of COX-2 expression in PSC (Yoshida et al., 2005), which is coupled to autocrine stimulation in PSCs (Aoki et al., 2007). Also sphingosine-1-phosphate (S1P) activates PSCs to generate MMP-9, which increases PDAC cell migration and invasion *in vitro*. Following knock down of the S1P signalling pathway in PSCs, reduced pancreatic tumour growth and metastasis in an orthotopic PDAC model (Bi et al., 2014).

Moreover, a direct interaction between PSC and PDAC cells has been observed. Co-culture of PSC with PDAC cells significantly increased PDAC cell proliferation compared to regular co-culture systems using conditioned media. This activation was thought to be due to direct cell contact-activated notch signalling (Fujita et al., 2009). Overall, this supports the existence of an active and close cooperation between PSCs and PDAC cells in facilitating PDAC progression. *In vivo* studies in genetically engineered mouse models (GEMM) (12 in total, reviewed in (Hruban et al., 2006; Mazur and Siveke, 2012) have confirmed these observations.

GEMMs mimic the natural development and progression of PDAC more than standard xenograft and orthotopic PDAC models (Hruban et al., 2006; Mahadevan and Von Hoff, 2007; Mazur and Siveke, 2012). Co-injection of PSCs and PDAC cells into an orthotopic mice model developed larger tumours with extensive desmoplasia, elevated tumour progression and increased regional invasion and distant metastasis compared to PDAC cells injected alone (Bachem et al., 2008; Hwang et al., 2008; Vonlaufen et al., 2008a). Additionally, in a xenograft model PSCs accelerated tumour progression of PDAC through elevated secretion of MMP-2 (Schneiderhan et al., 2007). Sonic hedgehog (SHH) signalling is absent in the normal pancreas but upregulated in PDAC. In PDAC SHH elicits

paracrine effects on PSC differentiation and motility, contributing to the formation of desmoplasia by increased collagen I and fibronectin production (Bailey et al., 2008). Inhibition of SHH signalling in a GEMM reduced desmoplasia with subsequent increase in gemcitabine uptake due to improved vascularization of the tumour (Olive et al., 2009). Others found a prolonged survival in a GEMM through SHH inhibition (Feldmann et al., 2008). The contribution of PSCs in later stages of PDAC has been highlighted by their ability to co-metastasize to distant organs. Xu et al. showed in an orthotopic mouse model that PSCs were able to intravasate/extravasate to and from blood vessels and by that accompany PDAC cells to distant metastatic sites (Xu et al., 2010). This observation points to a possible role of stroma cells in guiding invasive cells through the ECM (Friedl and Alexander, 2011; Friedl and Wolf, 2009a) and in creating cell tracks for the cancer cells to follow (Gaggioli et al., 2007). Thus, all models have brought valuable knowledge to the understanding of PDAC and function of PSCs.

Consequently, the mutual interplay of PSCs with PDAC cells falls into the context of the long known “seed” and “soil” hypothesis in shaping the TME, with PDAC cells being the seed and PSCs shaping the soil for PDAC to progress (Gupta and Massague, 2006; Paget, 1889; Sleeman et al., 2012). PSCs are therefore acknowledged as a villain rather than as a friend in PDAC progression, and thus represent a potential therapeutic target together with PDAC cells in PDAC patients.

1.3.4 Autocrine Stimulation in PSCs

Notably, in addition to responding to paracrine exogenous stimulants in PDAC, several lines of evidence also point toward PSCs acting as mediators of autocrine stimulation that perpetuate their own activity. This leads to the hypothesis, that when activated by an exogenous factor, PSCs are capable of existing in a persistently activated state even in the absence of the initial trigger factors that drive pancreatic fibrogenesis (Apte et al., 2012; Bachem et al., 2006). This is observed in PSC secretion of TGF- β 1. PSCs express TGF- β 1 receptors and respond to TGF- β 1 by increased matrix synthesis and reduced proliferation (Bachem et al., 2006; Schneider et al., 2001; Shek et al., 2002). Additionally, autocrine stimulation loops have been identified in activated PSCs involving TGF- β 1, IL-1, IL-6 and cyclooxygenase-2 (COX2) through Smad3 and ERK(1/2) dependent pathways (Aoki et al., 2006a; Aoki et al., 2007; Aoki et al., 2006b; Kruse et al., 2000),

activin A, which is a member of the TGF- β superfamily (Ohnishi et al., 2003) and the peptide endothelin-1 (Klonowski-Stumpe et al., 2003) (*figure 1.4*). Furthermore, pro-oxidant compounds and ROS secreted from injured acinar/duct cells or inflammatory immune cells can stimulate PSCs to generate and secrete ROS as an auto- and paracrine stimulant (Apte et al., 2000; Masamune et al., 2008b). Thereby, production of ROS can perpetuate PSC activity. This is coupled to NADPH oxidase function. NADPH oxidase inhibition, in turn, was shown to decrease PSC proliferation and production of IL-1 and collagen. Moreover, NADPH oxidase inhibition abolished the transformation of isolated PSCs, supporting the hypothesis that oxidant production by PSCs might serve as a paracrine/autocrine stimulator during transformation (Asaumi et al., 2007; Masamune et al., 2008b). PDGF, TGF- β 1, IL-1 and angiogenesis II were also found to induce ROS production in PSCs (Cao et al., 2014; Masamune et al., 2008b).

1.4 Cell Migration

One common feature of stroma cells are their ability to migrate enabling them to reach the tumour site and recruit more cells to the tumour area (Hanahan and Coussens, 2012; Kalluri and Zeisberg, 2006). In the context of PDAC, the increased number of activated PSCs in fibrotic areas can be a result of: (i) stimulated attraction of PSCs by PDAC cells, (ii) stimulated attraction of PSCs by resident PSCs and (iii) stimulation of PSC proliferation. One major acquired capability in PSC transformation from quiescent to activated state is their elevated motility. It is now widely accepted that PSC migration is a consequence of their activated state and a requirement for their communication with PDAC cells (Phillips et al., 2003b).

1.4.1 Basic Principles of Cell Migration

Common for all mammalian cell migration modes is a polarized morphology along the axis of movement, which is a prerequisite for directed cell migration and makes it easy to distinguish between the front and rear end (*figure 1.5*). This polarization is particularly evident when cells are migrating on a two-dimensional (2D) surface (Keren et al., 2008; Nabi, 1999; Weihuang et al., 2015). The basic principle for polymerizing actin filaments at the front and contractile at the rear end has been defined for 2D migration

(Lauffenburger and Horwitz, 1996) however the majority of cells migrate in a three-dimensional (3D) environment (Friedl and Wolf, 2009b). Recently a 5-step migration process has been defined for this migration mode by Friedl and colleagues, for both single and collective migration (Friedl and Wolf, 2009b; Ilinca and Friedl, 2009; Lauffenburger and Horwitz, 1996; Schmidt and Friedl, 2010; Wolf and Friedl, 2011). Additionally, evidence suggests that cell migration is affected by ECM dimensionality by differences in structural organization including density, stiffness and orientation (Doyle et al., 2013; Grinnell, 2008; Keren et al., 2008). Although the basic principles are fulfilled (cells migrating along or through tissue structures), each cell type exerts migration in different contexts using distinct molecular repertoires and extracellular guidance (Friedl and Wolf, 2009a). Different components of the cellular migration machinery, including focal adhesions and receptors, are therefore active and expressed at either the cell front or rear end. This makes directed migration possible, as observed for neutrophils migrating towards a chemotactic gradient (Damann et al., 2009; Lindemann et al., 2013). Thus, coordinated cytoskeletal dynamics are fundamental and obligatory for any kind of cell motility (Anderson et al., 2008; Le Clairche and Carlier, 2008; Pollard and Borisy, 2003).

Studies from the last 15 years have shown increasing evidence that the plasma membrane itself and the ion transport across this structure play important roles in cell dynamics and migration including numerous of Na⁺, K⁺ and Ca²⁺ channels (Keren, 2011; Komuro and Rakic, 1998; Schwab et al., 2012; Schwab et al., 2007; Stock et al., 2013). This prediction is supported by the discussion of integrin-dependent and -independent migration that questions the importance of focal adhesions in cell migration (Friedl and Wolf, 2009a; Lammermann et al., 2008; Schmidt and Friedl, 2010). Ion channels are not only important for creating a correct intracellular milieu for cell polymerization, but they are also regulated by the cytoskeleton components (Dreval et al., 2005; Mazzochi et al., 2006; Nolz et al., 2006; Sasaki et al., 2014). Data concerning the role of ion channels in PSC function are currently virtually non-existent, emphasizing the need for further investigation.

1.4.2 Calcium-dependent Signalling in Cell Migration

Given that cell migration is a Ca^{2+} -dependent process (Komuro and Kumada, 2005; Pettit and Fay, 1998), the role of ion channels in setting and regulating the intracellular Ca^{2+} homeostasis is of critical importance, giving a higher intracellular $[\text{Ca}^{2+}]_i$ at the rear end than in the front of migrating cells (Brundage et al., 1991; Schwab et al., 1997). This in part mediates a polarization along the axis of movement, allowing different components of the cellular migration machinery to be expressed or to be functional at the cell front or rear end including focal adhesions, receptors and ion channels (Broussard et al., 2008; Eddy et al., 2000; Schwab et al., 2012; Stock et al., 2013). For instance, the increased Ca^{2+} concentration at the cell end is related to myosin II contraction and cleavage of focal adhesion, which subsequently causes retraction of the rear end (Eddy et al., 2000;

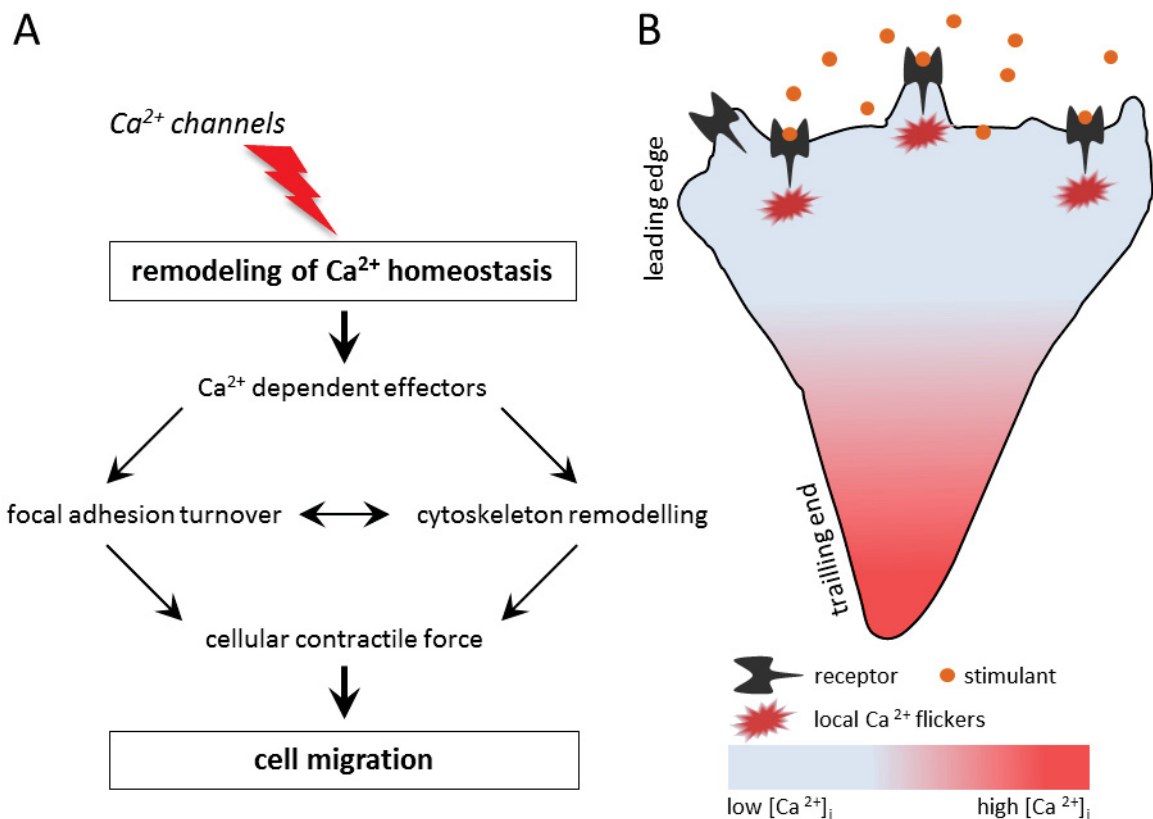


Figure 1.5. The Central Role of Ca^{2+} Signalling in Cell Migration. **(A)** Ca^{2+} channels play important roles in remodelling and setting Ca^{2+} homeostasis in migrating cells. Numerous effectors in the migration machinery are Ca^{2+} dependent regulating several downstream pathways implicated in cell migration e.g. focal adhesion turnover and cytoskeleton dynamics. **(B)** Ion channels set and regulate the intracellular front/rear Ca^{2+} gradient. The lower $[\text{Ca}^{2+}]_i$ at the front makes it possible for migrating cells to fine-tune their molecular repertoire and migration direction to extracellular guidance cues through locally elevated Ca^{2+} flickers.

Palecek et al., 1998). In addition, the front/rear Ca^{2+} gradient can be superimposed by locally elevated Ca^{2+} zones and short-lived Ca^{2+} flickers that play a role in regulating the directionality of migrating cells (*figure 1.5*) (Fabian et al., 2008; Tsai and Meyer, 2012; Wei et al., 2009). In this way, cells are able to fine-tune their molecular repertoire to extracellular guidance cues and the local microenvironment (Friedl and Wolf, 2009a). Numerous components of the cellular migration machinery and intracellular signalling pathways are Ca^{2+} sensitive. They can affect cytoskeletal remodelling, focal adhesion turnover, matrix degradation, leading edge guidance and localized cell volume changes (Falke and Ziemba, 2014; Schwab et al., 2012).

A rise of $[\text{Ca}^{2+}]_i$ can trigger the dynamic formation of lamellipodia through Rac1, thereby increasing migration or inducing stress fibres through RhoA activity, which in turn inhibits cell migration (Etienne-Manneville and Hall, 2002; Singh et al., 2007; Tian et al., 2010). Ca^{2+} signalling induces; (i) contraction of the actomyosin network (Yang and Huang, 2005); (ii) activation of calpain (Jang et al., 2010) required for ECM matrix modelling by regulating MMP2 and 9 activity (Monet et al., 2010; Sukumaran et al., 2013), and regulation of focal adhesion turnover (Giannone et al., 2004; Giannone et al., 2002; Lawson and Maxfield, 1995; Schafer et al., 2012; Svensson et al., 2010; Wells et al., 2005); and (iii) induction of localized changes of the cell volume of migrating cells (Happel et al., 2013; Schneider et al., 2000; Schwab et al., 1995; Watkins and Sontheimer, 2011). These examples demonstrate that cell migration is Ca^{2+} -dependent signalling process, which can be linked to both Ca^{2+} influxes through plasma membrane channels and/or Ca^{2+} release from internal Ca^{2+} stores. Thus far, data concerning Ca^{2+} signalling in PSCs are essentially lacking, counting to date only 4 published papers. Won et al. has shown that Ca^{2+} signalling is elevated in activated compared to quiescent PSCs together with increased expression of numerous surface receptors coupled to intracellular Ca^{2+} signalling (Won et al., 2010). Haanes et al. and Hennigs et al. have shown P2-receptor-mediated calcium signalling in activated PSCs (Haanes et al., 2012; Hennigs et al., 2011) and recently, the transient receptor potential (TRP) channel family member TRPV4 has been implicated in reactive calcium responses in high fat and alcohol activated PSCs (Zhang et al., 2013).

Evidence for the role of ion channels involved in the mechanisms underlying cancer development, progression and tumour-stroma interaction is accumulating (*figure 1.3 B*) (Arcangeli, 2011; Fraser and Pardo, 2008). Specifically TRP channels have increasing

interest during the last 15 years due to their role in setting Ca^{2+} homeostasis as discussed in my recently published review (Nielsen et al., 2014).

However, the molecular mechanisms by which they affect PSC migration as well as the mutual communication with PDAC cells are still elusive. TRP channels are interesting since they are able to sense and respond to microenvironmental changes occurring during cancer development and progression giving rise to increased migratory activity in stroma cells (Nielsen et al., 2014).

1.5 TRP Channels in Migration and as Microenvironmental Sensors, Modifiers and Effectors

1.5.1 TRP Channel Family

The first discovery of TRP channels was made in *Drosophila melanogaster* (Montell and Rubin, 1989) and 5 years later the first human homologue, TRPC1 followed (Wes et al., 1995; Zhu et al., 1995).

TRP channels are expressed ubiquitously in numerous excitable and non-excitable tissues (Kunert-Keil et al., 2006; Pedersen et al., 2005) implicating them in multiple hereditary, chronic and acquired diseases (Nilius and Szallasi, 2014). The TRP family can be classified and divided into seven main subfamilies based of amino acid sequence homology: the TRPC ('C_{anonical}') family, the TRPV ('V_{anilloid}') family the TRPM ('M_{elastatin}') family, the TRPP ('P_{olycystin}') family, the TRPML ('M_{ucolipin}') family, the TRPA ('A_{nkyrin}') family, and the TRPN ('N_{OMPC}') family. These can further be divided into subgroups based on the mode of activation and function (for review see (Nilius and Owsianik, 2011; Pedersen et al., 2005). Most TRP channels are non-selective cation channels that are permeable to Ca^{2+} and Na^{+} ($P_{\text{Ca}}/P_{\text{Na}} = 1-10$). Nonetheless, most studies dealing with TRP channels in cell migration related the functional impact of TRP channels to their Ca^{2+} permeability (Owsianik et al., 2006).

1.5.1.1 TRP Channel Function

TRPC, TRPM and TRPV channel families are attractive candidates for probing the TME because some of their members are exquisitely sensitive to components of the TME. For example, TRPC channels are part of G protein-coupled receptor (GPCR) and receptor

tyrosine kinase (RTK) signalling cascades mediating receptor-operated calcium entry (ROCE) (Ambudkar and Ong, 2007), and members of the TRPM family such as TRPM2 are activated by oxidative stress that is frequently encountered in tumours (Ray et al., 2012; Takahashi et al., 2012a; Tothhawng et al., 2013). GPCR activation leads to the activation of phospholipase C (PLC), which cleaves phosphatidylinositol 4,5-bisphosphate (PIP₂) into diacylglycerol (DAG) and inositol-1,4,5 triphosphate (IP₃). DAG induces ROCE by activating TRPC3/6/7 channels and IP₃ can give rise to Ca²⁺ release from intracellular stores into the cytosol. This elevation in cytosolic Ca²⁺ induces store-operated calcium entry (SOCE) (Clapham, 2003; Minke and Cook, 2002) through TRPC1/2/4/5 channels or the STIM/ORAI complex, with STIM being the endoplasmic reticulum (ER) Ca²⁺ sensor and ORAI the Ca²⁺-selective Ca²⁺ entry channel (Cahalan, 2009; Soboloff et al., 2012; Soboloff et al., 2006; Sours-Brothers et al., 2009).

TRP channels, besides forming homotetramers, can form heterotetramers with other subgroup members making their functional characterization even more complex (Pedersen et al., 2005). A dynamic assembly between TRPC1-STIM1-ORAI1 has been reported to be essential for SOCE and SOC function (Jardin et al., 2008; Ong et al., 2007; Rao et al., 2010; Sours-Brothers et al., 2009). However, a recent study shows evidence that TRPC1 and ORAI1 constitute distinct SOC and Ca²⁺ release-activated Ca²⁺ channels, both gated by STIM1 in response to store depletion (Cheng et al., 2011). This implies that the composition and expression of SOC channels is very complex and highly cell type and tissue specific (Ambudkar and Ong, 2007; Cahalan, 2009).

1.5.1.2 TRP Channels in Cell Migration and Interaction Partners

A substantial amount of data connects TRPC, TRPV and TRPM channels to cell migration of stroma and cancer cells, reviewed in Nielsen et al. Predominantly, it is assumed that the impact of most TRP channels on cell migration is due to their ability to mediate transduction/effector Ca²⁺ responses following the activation by growth factor or chemoattractant receptors (GPCR and RTK) (Nielsen et al., 2014).

Sustained growth factor signalling in PSCs and PDAC cells culminates in the activation of the TME with induction of tumour-promoting inflammation, ECM production/remodelling, sustained proliferation, angiogenesis and migration/invasion (Apte and Wilson, 2011; Tang et al., 2012; Vonlaufen et al., 2008b) (*figure 1.4*). These

processes have been linked to TRP channels as regulators of tumour and stroma cell migration in general, highlighting the huge diversity and contribution of TRP channels in the cancer–stroma interplay (*figure 1.6*) (Nielsen et al., 2014). TRP mediated Ca^{2+} entry further leads to the initiation of (local) intracellular Ca^{2+} signalling cascades important for cell migration. These include among others the PI3K pathway, ERK1/2, Akt/protein kinase B pathway, MAPK and the Ras-homologue-(Rho)-GTPases, which almost all depend on Ca^{2+} and affect cell migration (Falke and Ziemba, 2014). Importantly, these pathways are linked to PSC activation (described in *section 1.3.2*). Nonetheless, the connection of PSC activation and migration to TRP channel function is unknown.

TRP channels also interacts with the migration machinery by a reciprocal interplay with the cytoskeleton (Clark et al., 2008). TRPV1 and TRPV4 channels directly interact with actin and microtubules synergistically regulating cell migration in human hepatoblastoma and neuroblastoma cells (Goswami et al., 2006; Goswami et al., 2010). TRPM7 affects actomyosin contractility and cell adhesion in both human breast and neuroblastoma cells (Clark et al., 2006; Middelbeek et al., 2012) and TRPC6 is needed for actin polymerization in KC-stimulated neutrophils (Lindemann et al., 2013).

However, TRP channels themselves can also be regulated by the cytoskeleton. An intact actomyosin cytoskeleton are required for interaction of human endogenous expressed TRPC1 with the calcium sensor STIM1 (Lopez et al., 2006) and actin depolymerisation with calculin A induces the internalization of several TRPC channel members and blocks calcium entry in human neutrophils (Itagaki et al., 2004). Further, a disruption of the actin cytoskeleton in the neuroblastoma cells and in endothelial derived breast cancer cells are linked to impaired TRPV4-mediated currents and TRPV4 trafficking to the plasma membrane (Fiorio Pla et al., 2008; Fiorio Pla et al., 2012; Goswami et al., 2010). This reciprocal regulation mostly occurs through larger protein complexes where the TRP channels are linked to the actomyosin either directly or via scaffold proteins (Clark et al., 2006; Smani et al., 2013; Tang et al., 2000; Vandebrouck et al., 2007).

As stated in my review, TRP channels also functionally cooperate with other ion channels relevant for cell migration (Schwab et al., 2012). TRP-mediated calcium influx supply Ca^{2+} -sensitive channels such as $\text{K}_{\text{Ca}3.1}$, $\text{K}_{\text{Ca}2.3}$, CaCC (ANO/TMEM16) or CIC-3 with Ca^{2+} needed for their activation (Chantome et al., 2013; Cuddapah et al., 2013; Jacobsen et al., 2013; Turner and Sontheimer, 2013; Wanitchakool et al., 2014). In turn, TRP

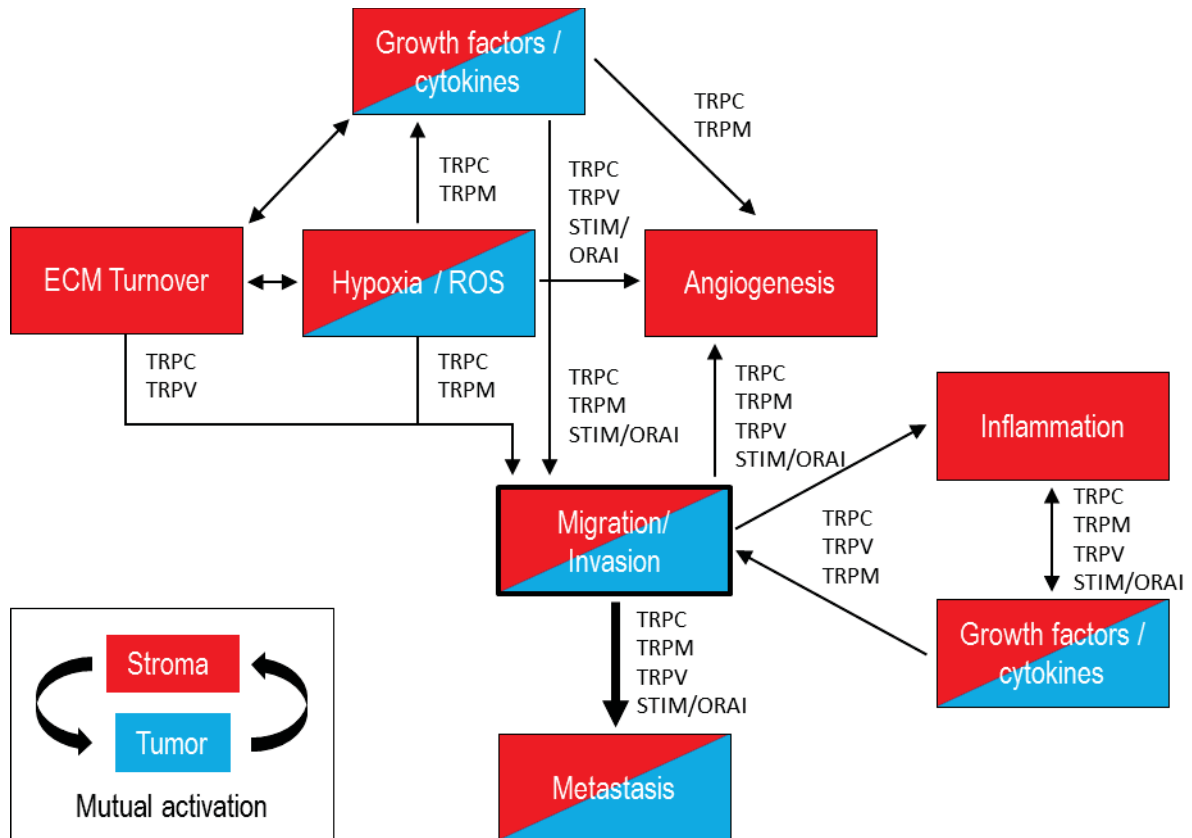


Figure 1.6. Major Mechanisms of the Tumour–Stroma Interplay in Cancer Progression. Illustration of major mechanisms underlying tumour invasion and metastasis involving cancer cells (blue), stroma cells (red) or both (red/blue). During tumour progression, cancer and stroma cells undergo a close mutual interaction with each other through continuous growth factor signalling, as observed between PSCs and PDAC cells. This shapes the TME and induces hypoxia, cellular oxidative stress, inflammatory responses, angiogenesis and ECM production/remodelling, all well-known characteristics of PDAC. At some point all these characteristics are connected to cell migration. Additionally, implicated TRP channel families and STIM/ORAI proteins are indicated. The contribution of TRP channels in PSC-PDAC interplay is unknown (modified from (Nielsen et al., 2014)).

channels rely on the activity of K^+ channels that hyperpolarize the cell membrane potential in order to maintain the electrochemical driving force for Ca^{2+} entry (Gao et al., 2010; Hammadi et al., 2012). Such cooperative mechanisms has been needed for efficient migration, invasion and metastases of different cell types (Chantome et al., 2013; Chimote et al., 2013; Cuddapah et al., 2013; Hammadi et al., 2012; Kuras et al., 2012; Siddiqui et al., 2012; Turner and Sontheimer, 2013).

Consequently, this enables regulation of TRP channels at multiple levels, as interference of these macromolecular complexes/transportomes can affect all its

members together with downstream effectors involved in cell migration (Nielsen et al., 2014).

1.5.2 TRP Channels as Sensors and Effectors of the Tumour Microenvironment

The membrane localization of TRP channels enables them to act as multifunctional cellular sensors to the dynamic changing TME during tumour progression in both stroma and cancer cells (reviewed by (Nielsen et al., 2014). TRP channel activation therefore spans between diverse intra- and extracellular stimuli that are either of physical (e.g. mechanical stress, osmotic pressure or temperature) or chemical nature (e.g. growth factors/cytokines, environmental irritants, pH, pO₂, ROS, hypoxia, ADP ribose (ADPr)). Further, these parameters can alter TRP channel expression and function in both stroma and cancer cells. For example, TRP channel expression is frequently dysregulated in both stroma and cancer cells during cancer progression strongly correlating with tumour aggressiveness, thus representing valuable diagnostic and/or prognostic markers (Bodding, 2007; Dhennin-Duthille et al., 2011; Nielsen et al., 2014; Ouadid-Ahidouch et al., 2013; Prevarskaya et al., 2007; Santoni and Farfariello, 2011). However, the implication of TRP channels in PSC activation and functions related to mechanisms in PDAC is completely unknown.

1.5.2.1 TRP Channels as Mechanosensors and Modulators of the TME

By being major modulators in PDAC, PSCs must respond to the dynamically changing TME. Stretch, stiffness, osmotic stress and high interstitial fluid pressure are some of the characteristic in the TME of PDAC known to activate PSCs (Asami et al., 2007; Kharraishvili et al., 2014), possibly through TRP channels via a mechanoregulatory sensor pathway (Kuipers et al., 2012). For example, in fibroblasts and smooth muscle cells TRPC1 and TRPC6 channels were activated by mechanically and osmotically induced membrane stretch, respectively (Fabian et al., 2012; Spassova et al., 2006), and in proportion to cell polarity, substrate stiffness mediate the activation of TRPC1 mediated SOCE in human bone osteosarcoma cells (Wei Huang et al., 2015). Moreover, hypoosmotic and pressure induced membrane stretch activates TRPC5 channels in neurons (Gomis et

al., 2008). Among the TRPV and TRPM family, TRPV2 is activated by stretch in aortic myocytes (Muraki et al., 2003) and TRPV4 is activated by osmotic cell swelling in several mammalian cells (Liedtke et al., 2000). TRPM3 show a putative role in kidney and brain cells and TRPM4 in smooth muscle cells, respectively (Dietrich et al., 2006; Earley et al., 2004; Grimm et al., 2003).

TRP channels also play a role in ECM modelling and migration. TRPC2 down-regulation attenuated migration and invasion of Rat thyroid cells through decreased secretion of MMP2 (Sukumaran et al., 2013). More importantly, *in vitro* and *in vivo* inhibition of TRPC3 in renal fibroblast decreased collagen production and MMP2/9 and TIMP1 secretion through ERK1/2 signalling preventing ECM modelling and fibrosis (Saliba et al., 2014). Further, siRNA-mediated TRPV2 silencing in prostate cancer cells down-regulates the expression of MMP2, MMP9 needed for migration and invasion (Monet et al., 2010). These findings point to the possible influence of TRP channels in PSCs bidirectional modelling of and adaptation to the changing TME.

1.5.2.2 TRP Channels in Hypoxia and Oxidative Stress

TRP channels can act as *sensors* and *effectors* of hypoxia- and oxidative stress-related stimuli by increasing their expression and/or activity (reviewed by (Numata et al., 2013; Shimizu et al., 2014; Takahashi et al., 2012b; Takahashi and Mori, 2011)). The ensuing cell responses often involve elevated migratory activity and/or production and secretion of growth factors/cytokines (*figure 1.7*) (Bauer et al., 2012; Chigurupati et al., 2010; Nielsen et al., 2014; Yamamoto et al., 2008) many of which are involved in the mutual signalling between PSCs and PDAC cells and in the autocrine stimulation of PSCs. Specifically, the functional expression of TRPC1, TRPC6 and TRPM2 channels have been coupled to hypoxia sensitivity and oxidative stress (reviewed in (Dietrich et al., 2014; Dietrich and Gudermann, 2014; Faouzi and Penner, 2014; Nesin and Tsiokas, 2014)). As described in *section 1.3.3.1*, PSCs are capable of responding to hypoxia and oxidative stress stimulation. Roles of TRP channels in these processes are therefore very likely. However, up to now there is only limited information about the influence of tumour hypoxia and oxidative stress on TRP channel function in general.

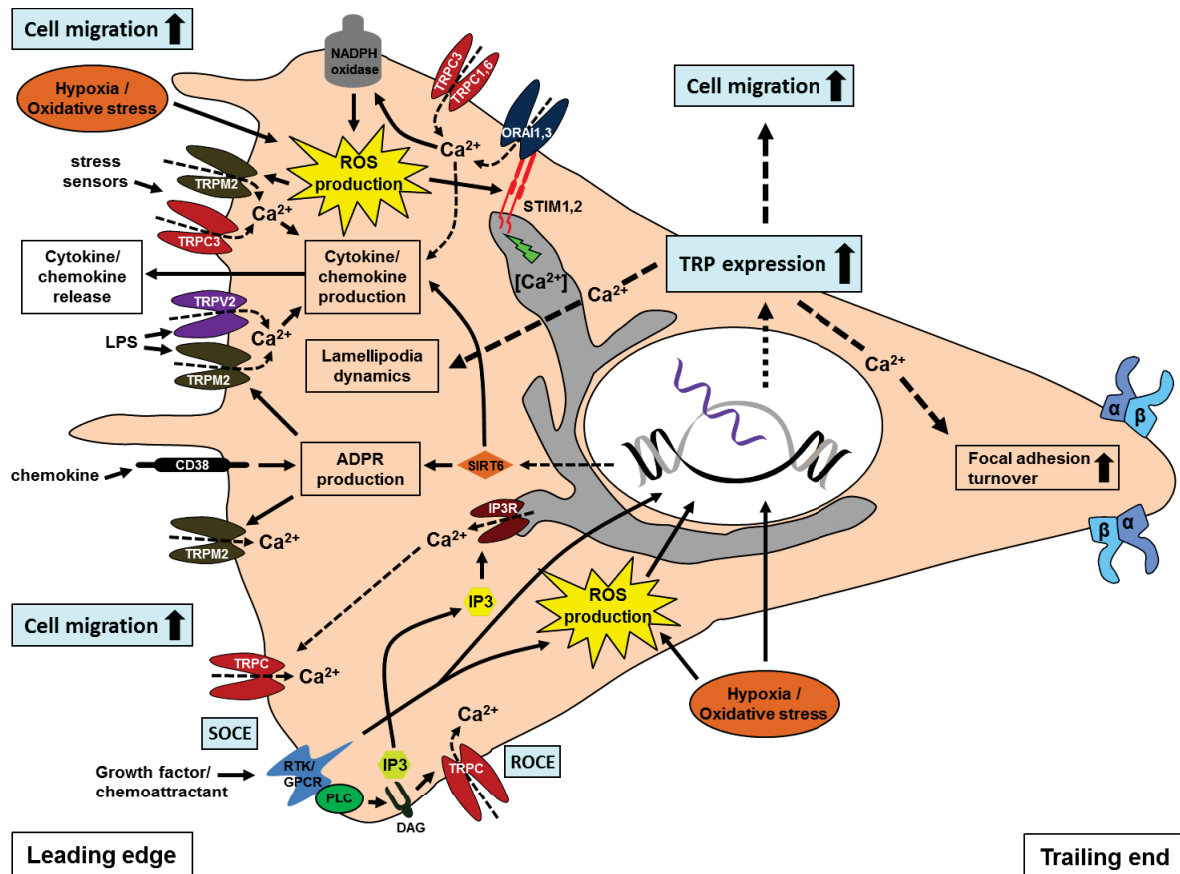


Figure 1.7. Multiple TRP Channel Sensor and Effector Functions in the Tumour Microenvironment. Illustration of major hypoxia and cellular oxidative stress-dependent mechanisms in cancer and stroma cells involving TRP channels. These mechanisms are connected to higher cell activity through elevated motility and/or cytokine/chemokine secretion. In cancer and stroma cells, TRP channels can have both a *sensor* function for extra-/intracellular stimuli mediating cellular responses and an *effector* function by increased expression and activation to induce cytokine/chemokine production in these cells. Further, hypoxia and oxidative stress can lead to up-regulation of TRP channels (e.g. TRPC1, TRPC3 and TRPC6) and mediate the production of ROS and ADPr. For the sake of clarity, this sketch does not include all signalling pathways mentioned in the text. Neither are all microenvironmental, growth factor- and chemokine-activated pathways involved in increased activation or expression of TRP channels included (modified from (Nielsen et al., 2014)).

So far, only the TRPA1 channel has been shown to sense pO_2 directly in murine and sensory neurons (Takahashi et al., 2011). Other TRP channels function indirectly as oxygen sensors through increased expression and/or activity (see (Numata et al., 2013) for a review). This is mostly under the control of hypoxia sensitive transcription factors such as HIF-1 α , which control the expression of various of hypoxia responsive genes such as growth factors/cytokines, enzymes, transporters and ion channels (Elvidge et al., 2006; Lum et al., 2007; Schofield and Ratcliffe, 2004; Tatum et al., 2006; Webb et al., 2009).

Concerning TRP channels, hypoxic pulmonary vasoconstriction involves the activation of TRPC1 and TRPC6 in mediating elevated $[Ca^{2+}]_i$ in both, human, rat and mice smooth muscle cells (Tang et al., 2010; Weissmann et al., 2006; Xu et al., 2014; Yang et al., 2015). Further, the TRPC1-STIM1-ORAI1 complex is needed for hypoxia-induced SOCE in pulmonary arterial smooth muscle cells of both rats and mice (Lu et al., 2008; Ng et al., 2012). In glioblastoma, an elevated expression of TRPC6 channels was found compared to normal brain tissue and demonstrated to be coupled to hypoxia through a notch signalling pathway. Furthermore, suppression of TRPC6 greatly inhibited hypoxia stimulated glioblastoma cell migration and invasion, possibly by inhibiting actin–myosin interactions (Chigurupati et al., 2010).

Notably, hypoxia facilitates the production of ROS in cancer, which leads to oxidative cellular stress and increased activity of present cells (Cook et al., 2004; Tothhawng et al., 2013; Yang et al., 2013). TRPM2 and TRPC3 channels serve as a sensor for oxidative stress in B-lymphoblasts helping the cells to reach or orient within the tumour (Roedding et al., 2012), and hypoxic stress induces the expression of TRPM2 channels in cardiac fibroblasts leading to increased proliferation and ECM production (Takahashi et al., 2012a). Furthermore, ROS can be generated as a result of growth factor stimulation of RTKs/GPCRs, thereby transmitting signals to induce cellular changes necessary for cell activity by affecting Ca^{2+} -sensitive effector molecules (Hurd et al., 2011; Ray et al., 2012; Tothhawng et al., 2013). Consequently, this suggests a role of TRP channels in the coupling between ROS and Ca^{2+} ions as stress-response messengers (*figure 1.7*) (Numata et al., 2013; Shimizu et al., 2014). In the pancreatic cancer cell line (BxPC-3), the stress responsive protein sirtuin 6 (SIRT6) promotes inflammation by enhancing the production of ADPr. In return, ADPr activates Ca^{2+} responses through TRPM2, promoting the secretion of the pro-inflammatory proteins IL-8 and TNF- α enhancing cell migration (Bauer et al., 2012). Moreover, the ectoenzyme CD38 mediates increased cADPr and ADPr generation from NAD (for a review, see (Malavasi et al., 2008)). ADPr binds to the TRPM2 channel leading to Ca^{2+} influx, which enhances the intracellular chemoattractant signal enabling chemotaxis of both tumour and stroma cells (Partida-Sanchez et al., 2007; Vaisitti et al., 2011). Another important factor in inflammatory cell responses is the NADPH oxidase-mediated generation of ROS. In granulocytes, the inflammatory process of NADPH oxidase-mediated superoxide production is related to

TRPC1, TRPC3, TRPC6 and ORAI1 channels (Brechard et al., 2008) and in lung endothelial cells to TRPC6 activity (*figure 1.7*) (Weissmann et al., 2011). NADPH oxidase activity in ROS production is relevant for PDAC and cancer in general (Cao et al., 2014; Yang et al., 2013). Moreover, its activity is regulated by growth factors in pancreatic cancer (Edderkaoui et al., 2011) and in the activation of PSCs (Asaumi et al., 2007; Masamune et al., 2008b). TRP channels could therefore indirectly play a role in PSC activation through NADPH oxidase activity regulation.

Similarly, ROS and stress promote TRP-dependent cytokine/chemokine production, emphasizing the role of TRP channels in modulatory mechanisms of the TME and cell activation. Activation of TRPM2 channels underlie enhanced cytokine/chemokine production in activated T-lymphocytes (Melzer et al., 2012), monocytes and neutrophils (Knowles et al., 2011; Wehrhahn et al., 2010; Yamamoto et al., 2008). The lipopolysaccharide-mediated Ca^{2+} entry via TRPV2 channels activates RAW264 macrophages to produce IL-6 and TNF- α (Yamashiro et al., 2010). In vascular endothelial cells the reactive nitrogen oxide, NO, activates TRPC5 channels inducing production of NO, resulting in a positive feedback cycle of receptor-activated Ca^{2+} and NO signalling (Takahashi et al., 2012b; Yoshida et al., 2006). In contrast to stimulatory effects, the overexpression of a dominant-negative mutant of TRPM4 or elimination of TRPM4 using RNAi in Jurkat T-cells induced elevated Ca^{2+} signalling with increased IL-2 production (Launay et al., 2004). Similar observations were found in mouse T-cells, affecting cell motility and IL-2 as well as IL-4 production (Weber et al., 2010). In turn, TRP channel activity itself can be regulated by cytokines. The transformation of fibroblasts into myofibroblast depends on TRPC6 channel expression (Davis et al., 2012). This process is similar to the TGF- β -mediated activation of PSCs (*section 1.3.2.1*). TGF- β stimulation induced elevated TRPC6 channel expression by p38/MAPK signalling leading to elevated Ca^{2+} signalling in WT fibroblast, whereas *Trpc6*^{-/-} fibroblasts showed no induction of α SMA positive stress fibers (activation marker) and reduced migration (Davis et al., 2012).

Thus, TRP channels modulation of secretion of growth factors/cytokines may constitute an important element in securing the following processes within the TME of PDAC: (i) regulation of mutual signalling between PSCs and PDAC cells, (ii) recruitment of additional stroma cells, (iii) regulation of (directed) cell migration and (iv) regulation of autocrine/paracrine stimulation pathways in PSCs.

In summary, the transmembrane localization of TRP channels puts them in an ideal position to function as multifunctional cellular sensors to the microenvironment strongly influencing both intracellular functions and modification of the microenvironment. TRP channels can thereby function as central intermediary regulators in transferring information in outside-in and inside-out directions. This can be divided into three major mechanisms implicating a (i) *sensor*-, (ii) *modifier*- and (iii) *transduction/effector* mechanism (see [figure 1.8](#)).

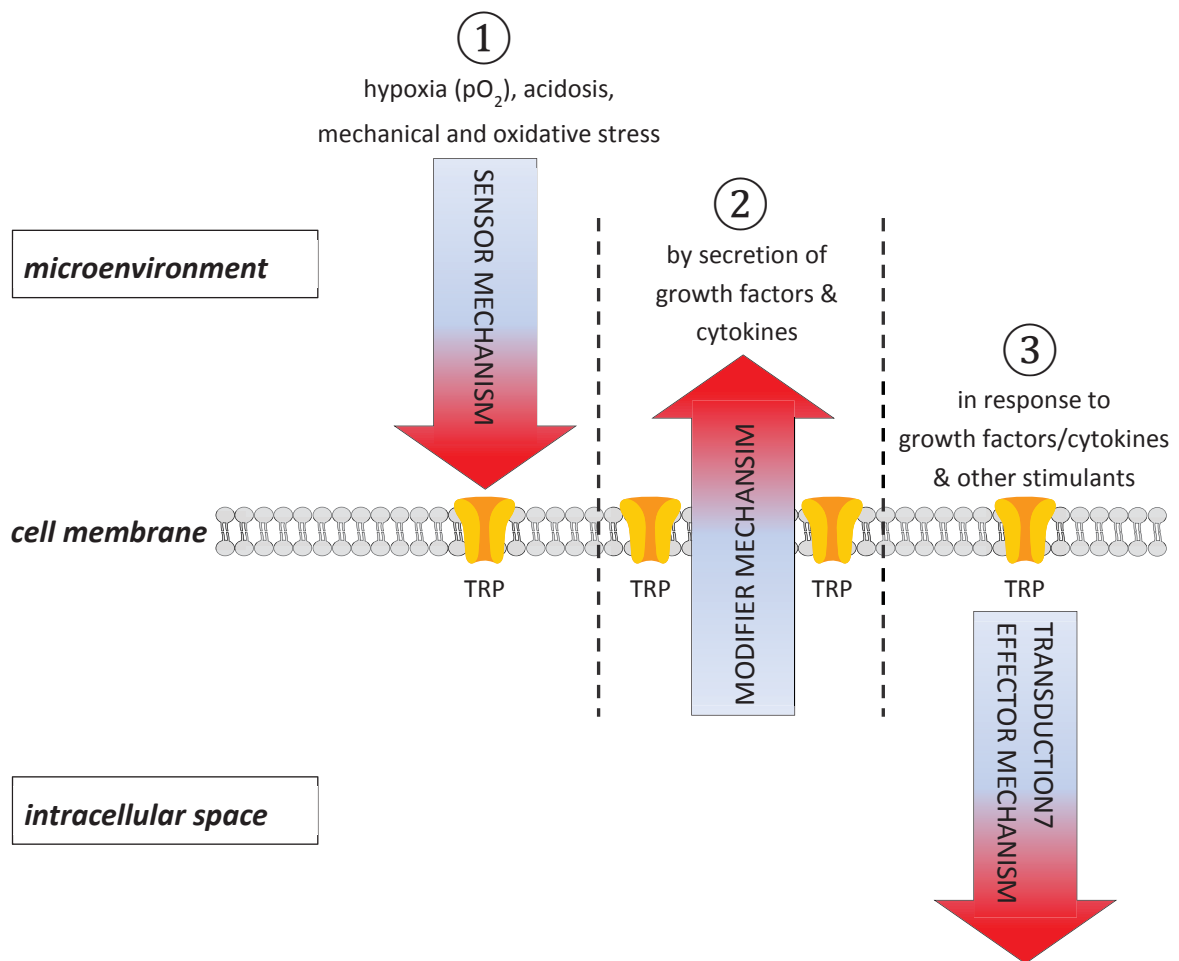


Figure 1.8. Major Mechanisms of TRP Channels in Cell Functions Coupled to the Microenvironment. TRP channels are important components of cellular responses to the microenvironment and vice versa. This interplay can be divided into three major mechanisms. **(1)** Direct/indirect *sensor* mechanism to extracellular stimuli such as hypoxia (pO_2), acidosis or cell stress. **(2)** *Modifier* mechanism of the microenvironment by being involved in secretion of growth factors/cytokines which can mediate both autocrine and paracrine stimulating effects. **(3)** Mediating cellular *transduction/effector* responses to stimulants.

Chapter 2

Project Aim

Project Aim

2.1 Hypothesis, Objective and Strategy

The close cooperation between PSCs and PDAC cells is a typical feature of PDAC, which depends on intense mutual growth factor/cytokine signalling to control activity of both cell types. This creates a TME with distinct physical and chemical properties that are permissive for tumour progression. Key properties include hypoxia, acidosis and an abundance of growth factors, all of which stimulate PDAC and PSC migration. It is widely accepted that PSC migration is a consequence for their activated phenotype.

Cell migration is a Ca^{2+} -dependent process that implicates the activity of TRP channels. There is growing evidence supporting a role of TRP channels in *sensing* and *modifying* the TME together with being essential cellular components of the transduction and effector cascades of cellular responses to the TME.

Owing to the hypoxic milieu of PDAC and the major contribution of this factor to malignancy and treatment resistance, the understanding of the responses of PSCs to hypoxia is of paramount significance. Mounting evidence supports direct or indirect participation of PSCs and correlates with their high occurrence in this context. Thus, it is very likely that TRP channels also play a critical role in the function of PSCs.

This led to the hypothesis that PSCs' response and adaptation to hypoxia can be regulated by TRPC1 and/or TRPC6 channels affecting the activated migratory phenotype of PSCs. One possibly mechanism is through altered TRPC1/6 mediated Ca^{2+} influx. A link between hypoxia and TRPC1/6 channels has already been found in various cell types. Furthermore, the TRPC1 and TRPC6 channel represent selective candidates of SOCE and ROCE, respectively. However, the exact mechanism how PSCs react to hypoxia together with the involvement of TRP channels in PSC activation and function remains elusive.

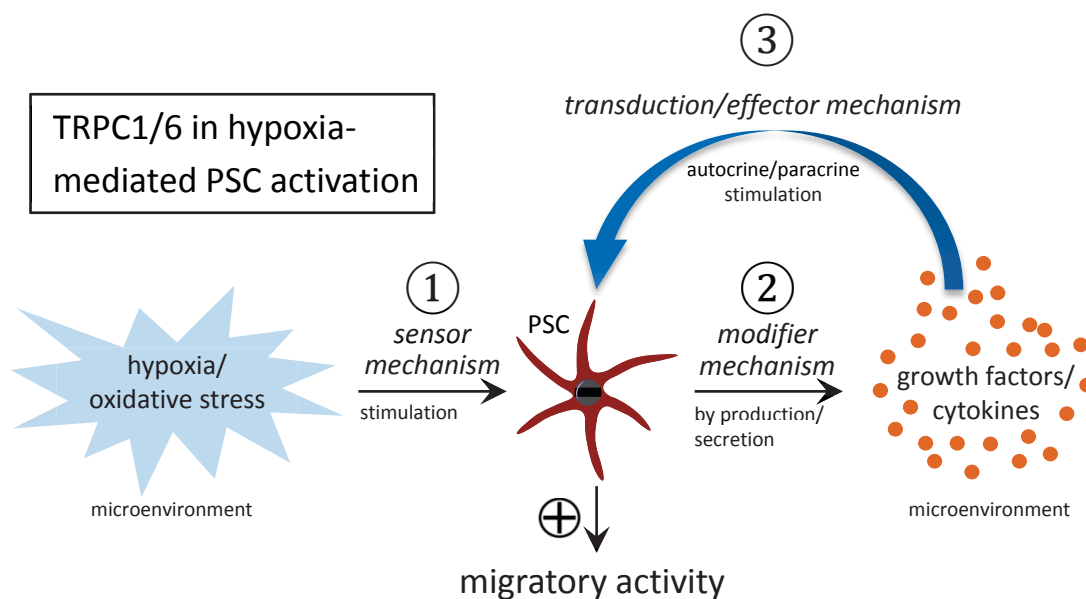


Figure 2.1. Possible Roles of TRPC1 and TRPC6 Channels in the Hypoxia-Mediated Activation of PSCs. TRPC1 and/or TRPC6 can influence PSCs activation by hypoxia in different ways. **(1)** A sensor mechanism leads to increased expression and/or activation upon hypoxic stimuli, **(2)** they modulate the microenvironment by being involved in production of growth factors/cytokines stimulating PSCs in autocrine ways, and **(3)** they mediate transduction/effector responses to stimulants secreted by PSCs and PDAC cells.

The current study was planned with aim to decipher the roles of TRPC1 and TRPC6 channels in regulating PSC responses and adaptations to hypoxia. Following hypothesis was predicted and set to be tested:

TRPC1 and/or TRPC6 channels are key components in sensing microenvironmental changes, thereby regulating PSC responses related to pancreatic cancer

In accordance with this hypothesis the following mechanisms were identified as potentially responsible for a role of TRPC1/6 channels in PSC activation (*figure 2.1*):

- TRPC1/6 channels can function as microenvironmental *effector-sensors* by their involvement in downstream sensory mechanisms of pO_2 (e.g. HIF-1 α) leading to elevated expression and/or activation (mechanism **(1)** in *figure 2.1*).

- TRPC1/6 channels are *modifiers* of the microenvironment by regulating hypoxia-triggered secretion of growth factors/cytokines that stimulate PSCs in an autocrine manner (mechanism ② [figure 2.1](#)).
- TRPC1/6 channels are *effectors* of intracellular *transduction* pathways triggered by growth factors/cytokines secreted by PSCs or PDAC cells (mechanism ③ [figure 2.1](#)).

All pathways (1-3), consequently lead to increased migratory activity

The ability of PSCs to migrate is a consequence of their activated state and could be used as a parameter for the experiments. In order to test the hypothesis and the potential involvement of the three underlying mechanisms, the migratory activity of primary cultured PSCs isolated from WT, TRPC1^{-/-} and TRPC6^{-/-} mice was characterised.

Chapter 3

Materials and Methods

Materials and Methods

3.1 Materials

3.1.1 Media

Table 3.1: Basic Media

Media	Producer/Manufacturer
DMEM/F12*	Sigma
DMEM*	Sigma
RPMI 1640	Sigma
GBSS	PAN Biotech
DPBS	PAN Biotech
FCS-Gold	GE Healthcare
Penicilin/Streptomycin	Biochrom

* When not stated otherwise, cell culture media includes 10% FCS-Gold and 1% Penicilin/Streptomycin.

3.1.2 Chemicals and Kits

Table 3.2: Chemicals and Kits

Chemical or Kit	Producer/Manufacturer
Agarose	SERVA
APS (Ammoniumpersulfate)	Sigma-Aldrich
BCA Pierce® Protein Assay Kit	Thermo Scientific
BCECF-AM	Life Technologies
Boric Acid	Merck
Bromophenolblue	Sigma
Chloroform	Sigma
(CMAC, t-BOC-Leu-Met)	Molecular Probes
Collagen I, Bovine	Biochrom AG
Collagen III, human	BD Biosciences
Collagen IV, mouse	BD Bioscience
Collagenase P	Roche

Complete mini	Roche
Dimethyloxalglycine (DMOG)	Frontier Scientific
Dimethyl Sulfoxide (DMSO)	Sigma
DTT (Dithiothreitol)	Boehringer
DNase	Ambion
dNTP-mix (10mM/dNTP)	VWR
EDTA	SERVA
Fibronectin	BD Biosciences
Fura-2-AM	Invitrogen
KC (murine), CXCL1	Biologend
Laminin	Sigma-Aldrich
Murine KC	Peppo tech
PDGF (recombinant human PDGF-BB)	Biologend
Phos-STOP	Roche
PVDF membrane	Millipore, Immobilon®-P
Reverse transcriptase (RT) Assay	Roche
SB 225002	Calbiochem
Super Signal West pico Luminol Kit	Thermo Scientific
Super Signal West Femto Luminol Kit	Thermo Scientific
SYBR® Gold nucleic acid gel stain	Invitrogen, Molecular Probes
Taq DNA Polymerase	Se genetic
Taq DNA Polymerase Buffers	Qiagen
TRAM-34	Sigma-Aldrich
Triton X-100	Roth
Trizol® Reagent	Invitrogen
TWEEN® 20	Roth
2xSsoFast™ EvaGreen® Super mix	Bio-Rad
6x Loading dye	New England BioLabs
1-Oleoyl-2-acetyl-sn-glycerol (OAG)	Sigma-Aldrich
100 bp DNA Ladder	New England BioLabs

3.1.3 Instruments

Table 3.3: Instruments

Instruments	Producer/Manufacturer
Axio Cam mRm	Zeiss
Axiovert 200	Zeiss
Bio photometer	Eppendorf
Bottle neck top filter, 0.22 µm, polystyrene	Corning
C1000 Thermal cycler, cFX 96™ Real-Time system	Bio-Rad
Camera XC-ST70CE	Hamatsu
Camera XC-77CE	Hamatsu
Cell culture dish, glasbottom, 35 mm, Cellview™	Greiner bio-one
Cell strainer	Corning
ChemiDoc™ XRS Gel documentation system	Bio-Rad
Electrophoresis Power PAC 3000	Bio-Rad
Fresco 21 centrifuge	Thermo Scientific
Galaxy 14S incubator (hypoxia)	New Brunswick
HERA Cell 150 incubator	Heraeus
Inkubator 1000	Heidolph
Master Cycler	Eppendorf
Microplate reader	Thermo Max
Microscope Axiovert 40C	Zeiss
Microscope Axiovert 25C	Zeiss
Microwave	Amica Internation GmbH, Germany
Milliex-GF Filter unit, 0.22 µm, PVDF membrane	Millipore
Multifuge 1 S-R	Heraeus
Polychromator System	Visichrome
Seahorse Extracellular Flux analyzer, XF96	Bioscience
Seahorse XF96 Prep station	Bioscience
SPOT camera	RT se Diagnostic
Thermo mixer	Eppendorf
Tissue culture dish, 100x20 mm	Corning

Tissue culture flask, T25, 12,5 cm²
 Trypsin
 Unimax 1010 shaker

Corning
 Biochrom
 Heidolph

3.1.4 Oligonucleotides

Table 3.4: Oligonucleotides for PCR and Quantitative Real-time PCR

Oligo Name	Sequence (5'-3')	Ref.
TRPC1_forward (1)	TGGGCCCACTGCAGATTTCAA	(Dietrich et al., 2005)
TRPC1_reverse (1)	AAGATGGCCACGTGCGCTAAGGAG	(Dietrich et al., 2005)
TRPC1_forward (2)	GCAACCTTTGCCCTCAAAGTG	(Liu et al., 2007)
TRPC1_forward (2)	GGAGGAACATTCCCAGAAATTTCC	(Liu et al., 2007)
TRPC1_forward (3)	CATGGAGCATCGTATTTAC	(Varga-Szabo et al., 2008)
TRPC1_reverse (3)	GAGTCGAAGGTAAGTCTAGAA	(Varga-Szabo et al., 2008)
TRPC2_forward	ACTTCACTACATATGATCTGGGTCAC	(Storch et al., 2012)
TRPC2_reverse	CACGTCCAGGAAGTCCAC	(Storch et al., 2012)
TRPC3_forward	AGCCGAGCCCCTGGAAAGACAC	(Dietrich et al., 2005; Weissmann et al., 2011)
TRPC3_reverse	CCGATGGCGAGGAATGGAAGAC	(Dietrich et al., 2005; Weissmann et al., 2011)
TRPC4_forward	GGGCGGCGTGCTGCTGAT	(Dietrich et al., 2005; Weissmann et al., 2011)
TRPC4_forward	CCGCGTTGGCTGACTGTATTGTAG	(Dietrich et al., 2005; Weissmann et al., 2011)
TRPC5_forward	GCTGAAGGTGGCAATCAAAT	(Storch et al., 2012)
TRPC5_forward	AAGCCATCGTACCACAAGGT	(Storch et al., 2012)
TRPC6_forward	GACCGTTCATGAAGTTGTAGCAC	(Dietrich et al., 2005; Weissmann et al., 2011)
TRPC6_forward	AGTATTCTTTGGGGCCTTGAGTCC	(Dietrich et al., 2005; Weissmann et al., 2011)
TRPC7_forward	CCCAAACAGATCTTCAGAGTGA	(Storch et al., 2012)
TRPC7_forward	TGCATTCGGACCAGATCAT	(Storch et al., 2012)
Hprt_forward	TCCTCCTCAGACCGCTTTT	(Storch et al., 2012)
Hprt_reverse	CCTGGTTCATCATCGCTAATC	(Storch et al., 2012)
β2M_forward	GCTATCCAGAAAACCCCTCAA	(Hill et al., 2013; Johnsen et al.,

β2M_reverse	CATGTCTCGATCCCAGTAGACGGT	2006) (Hill et al., 2013; Johnsen et al., 2006)

* All oligos were purchased from Metabion.

**Hprt1 (Hypoxanthin phosphoribosyltransferase 1) and β-2M (β-2 microglobulin)

3.2 Mouse Strains

mPSCs were isolated from 8-12 months old male/female 129Sv/C57BL/6J WT, *TRPC1*^{-/-} (Dietrich et al., 2007), and *TRPC6*^{-/-} mice (Dietrich et al., 2005). All animal experiments were approved from the State Agency for Nature, Environment and Consumer Protection NRW (from 2012: 84-02.05.2012.123) and were performed according to current animal welfare guidelines. All mice were genotyped by polymerase chain reaction (PCR) before the experiments to confirm KO and WT animals. Genotyping was performed by Jana Welzig or Dr. Otto Lindemann.

Notably, *TRPC1*^{-/-} and *TRPC6*^{-/-} mice are viable and fertile with a normal life expectancy and no phenotypic changes. Fertility and litter sizes were like those of WT mice (Dietrich et al., 2007; Dietrich et al., 2005). However, *TRPC1*^{-/-} mice have an increased body sizes and weights for unknown reasons (Dietrich et al., 2007).

3.2.1 Pancreatic Stellate Cells

Table 3.5: Primary Stellate Cells

Nomenclature	Description	Culture Media
mPSC	Isolated from mice (see section 3.3.2)	DMEM/F12
RLT-PSC	Immortalized human pancreatic stellate cell line (Jesnowski et al., 2005)	DMEM/F12

3.3 Cell Biological Methods

3.3.1 Reactivating Frozen RLT-PSCs

Freshly thawed RLT-PSC cells were re-suspended in 37°C DMEM/F12 and centrifuged at 1000 *rpm* for 5 min at RT. The supernatant was removed and the pellet was re-suspended in 10 ml preheated DMEM/F12. Culture media was changed daily the following 1-2 days. From then on cell culturing was performed as described ([section 3.3.3](#)).

3.3.2 Isolation of Mice Pancreatic Stellate Cells

The PSC isolation procedure was modified from Haanes *et al.* 2012. Mice were sacrificed by treating with Isoflurane followed by cervical dislocation. The pancreas was then removed and washed in cold GBSS before being cut into pieces with scissors and then transferred to a 15 ml Falcon-Tube containing 3 ml cold GBSS enzyme solution (2,5-3 mg Collagenase P (Roche) in 3 ml cold GBSS per pancreas). The falcon tube was then incubated at 37 degrees for 25 min on a shaker. After incubation, the suspension was mixed carefully by pipetting up and down 2-3 times with a 5 ml pipette. Thereafter, 5 ml warm GBSS was added to give a final volume of 8 ml before centrifuging the content at 1040 *rpm* for 8 min. During centrifugation a tissue culture dish (100 x 20 mm) was coated with 1 ml FCS Gold to make an adhesive surface for attachment of the PSCs (incubation time approx. 8-10 min). After centrifugation the supernatant was removed and the pellet re-suspended in 5 ml pre-warmed DMEM/F12 with a 5 ml pipette before an extra 5 ml DMEM/F12 were added to give a total volume of 10 ml. Then the mixture was transferred carefully to the pre-coated tissue culture dish and incubated for approx. 105 minutes. After incubation, the medium was removed and the bottom of the tissue culture dish forcefully washed 3-5 times with warm medium using a 10 ml pipette to remove other cells (e.g. duct cells) and cell debris. After each washing step cells were observed under the microscope to ensure optimal purity ([figure 3.1](#)). Next, the freshly isolated mPSCs were left in the incubator and media changed daily for 2 days. After 5-6 days cells were split out in 1-3 tissue culture dishes depending on the isolation efficiency. From then on cells could be used for experiments ([section 3.3.3](#)). This type of isolation procedure utilizes the different adhesion time of different cell types. Pancreatic stellate cells adhere

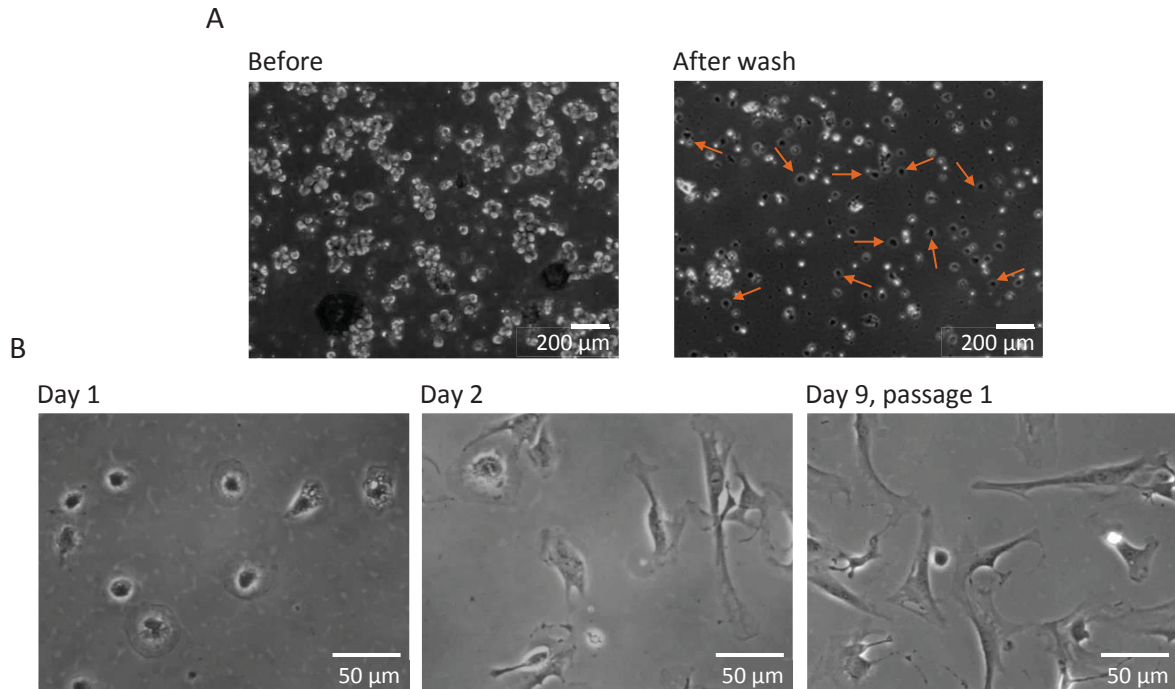


Figure 3.1. Mouse Pancreatic Stellate Cell Isolation. The upper panel (A) shows the washing step and the subsequent removal of cell debris and excessive cells (primarily acinar and duct cells) be observed. Attached mPSCs could be visualized by the appearance of small dark dots. For clarity, some mPSCs have been pointed out in the upper right figure. Cell growth and morphology changes of the mPSCs could the following days be observed (B). Examples are given 1 and 2 days post isolation and after being passaged one time (day 9 post isolation) (the two upper images (A) were kindly provided by Benedikt Hild).

earliest in this case, which allows the differentiation from other cells of the pancreas. After a few days in culture the contaminating cells detach, resulting in approx. 100% PSC population (Haanes et al., 2012).

3.3.2.1 Identification of mPSCs

Directly after isolation, mPSCs can be identified by the presence of Vitamin A droplets, indicating a state of quiescence (non-activated form). During culturing mPSCs gets activated, lose their Vitamin A droplets and can be stained for α -SMA and GFAP (Apte et al., 1998; Bachem et al., 1998). Validation of the isolation procedure of mPSCs was modified from Haanes et al. 2012 and further established in our laboratory prior to the start of this thesis by Benedikt Hild, a former medical student. I therefore refer to his dissertation for further reading regarding this subject (Hild, 2015).

3.3.3 Cell culture, Passaging and Cell Count

mPSCs were cultured in tissue culture dishes (100 x 20 mm) supplied with DMEM/F12 in a humidified atmosphere of 5% CO₂ and 95% air at 37°C. Under hypoxic conditions the O₂ level was lowered to approx. 1%. mPSCs were not allowed to reach more than 90% confluence and were not passaged below 30%. For experimental use, mPSCs were always used at passage 2-3. Before passaging, cells were washed twice with sterile PBS at 37°C. Cells were then incubated at 37°C with 1 mL 0.05% trypsin-0.1% EDTA per tissue culture dish for 2-4 minutes, until the cells detached from the culture surface. The reaction was terminated with the addition of 10 mL culture medium. Then cells were harvested and then centrifuged at 1000 *rpm* for 4 minutes at RT. The pellet was resuspended in 1 mL of culture medium and mixed well. For standardized cell density within each experiment, an aliquot of 10 µL was removed for cell counting using a haemocytometer and following equation:

$$\text{cell number (cells/ml)} = \frac{[(Q_1+Q_2+Q_3+Q_4)]*10^4}{4}$$

Q = Cell Number in a Large Quadrant

3.4 Molecular Biological Methods

3.4.1 Protein Biochemical Methods

3.4.1.1 Protein Isolation and Estimation

Protein isolation (*section 3.4.1.1 – 3.4.1.2*) was adapted and modified from Fabian et al. 2011. In brief, culture media was removed and cells were washed twice with cold PBS before 150-250 µl of freshly made lysis buffer were added (*table 3.6 & 3.7*). Lysis buffer was complemented with Complete mini (10x) and if required Phos-STOP (10x) (e.g. 450 µl lysis buffer + 87.5 µl Complete Mini + 50 µl Phos-STOP). Cells were loosened by tapping the dish and collected with a cell scraper. The cell/protein solution was then transferred to a 1.5 ml Eppendorf tube on ice and incubated on a rotating wheel for 30 min at 4°C. The solution was then centrifuged at 14.000 *g* for 15 min at 4°C and the supernatant transferred to a new 1.5 ml Eppendorf.

Table 3.6: RIPA Cell Lysis Buffer

Reagent	Volume (Total 500 ml)	Final conc.
1 M Tris-HCL pH 7.6	25 ml	25 mM
5M NaCl	15 ml	150 mM
NP-40	5 ml	1%
10% SDS	5 ml	0.1%
10% (240 mM) Sodium deoxycholate	50 ml	1%
ddH₂O	up to 500 ml	

Table 3.7: RIPA Cell Lysis Buffer for HIF1- α

Reagent	Volume (Total 100 ml)	Final conc.
1 M Tris-HCL pH 7.5	5 ml	50 mM
5M NaCl	3 ml	150 mM
NP-40	0.5 ml	0.5%
1% Triton X-100	1 ml	1%
1M NaF	5 ml	50 mM
ddH₂O	up to 100 ml	

An aliquot of the clear protein solution was used to measure protein concentration by the BCA Pierce® Protein Assay Kit (Thermo Scientific) according to the manufacturer's instructions and the remaining solution stored at -80°C. Briefly, a standard curve was established with the addition of 10 μ l BSA standard (25, 125, 250, 500, 750, 1000, 1500 and 2000 μ g/ml) into the wells of a 96 well plate to determine sample protein concentration. 10 μ l of sample were added into the appropriate well together with 200 μ l of the working reagent from the BCA kit. The plate was sealed and incubated at 37°C for 30 minutes. Absorbance was measured at 562nm using a microplate reader (THERMO max) and analyzed with the SoftMax pro 3.1.2 software. Samples and standard protein concentration measurements were performed in duplicates.

3.4.1.2 Protein Detection and Analysis

7.5% SDS polyacrylamide gel electrophoresis (SDS-PAGE) was used to separate sample proteins. The 7.5% SDS polyacrylamide gel was composed of two different gels (stacking and running gel) (see [table 3.8](#)). Protein standards of known molecular weight

were run alongside the samples including a visible (PageRuler™ Plus prestained Protein ladder) and an immunofluorescence detection ladder (MagicMark™ XP Western Standard).

Table 3.8: Composition of 7.5 % SDS Polyacrylamide Gel

5% Stacker Gel		7.5% Running Gel	
ddH ₂ O	1.3 ml	ddH ₂ O	1.3 ml
Rotiphorese® Gel A	357 µl	Rotiphorese® Gel A	357 µl
Rotiphorese® Gel B	150 µl	Rotiphorese® Gel B	150 µl
0.5 M Tris/SDS, pH 8.8	500 µl	1.5 M Tris/SDS, pH 6.8	500 µl
10% APS	25 µl	10% APS	25 µl
Temed	2.5 µl	Temed	2.5 µl

Before electrophoresis, the protein samples were first mixed in 1:5 with Blue SDS sample buffer (0.5 M Tris-HCL pH 7.6, 8.5% SDS, 27.5% Sucrose, 100 mM DTT, 0.003% Bromphenolblue) and preheated at 95°C for 5 min before loading to the gel. The amount of sample (µg protein) loaded per gel lane was dependent on the respective experiment. SDS-PAGE was performed in a gel chamber (BioRad) filled with running buffer (25 mM Tris, 200 mM Glycine, 1% SDS) and run for approximately 80-120 min at 100 V depending on the protein investigated. Thereafter, the proteins were transferred to a PVDF membrane using the Tank blotting method from Bio-Rad (Mini Trans-Blot® Cell). Prior to the transfer, the PVDF membrane was pre-activated in methanol for 5 min, before being put together in a sandwich like structure (composition from cathode: sponge – 2x filter paper – PVDF membrane – gel – 2x filter paper – sponge) and left to transfer overnight in a buffer tank at 4°C (transfer buffer: 10 mM Tris, 100 mM Glycine, 10% methanol). The PVDF membrane was then blocked in 5% milk PBS-tween (0.05%) for 2 h with rolling at RT to prevent non-specific binding of antibodies. Next, the membrane was incubated with the primary antibody of choice ([table 3.9](#)) diluted in 3-4 ml 5% milk PBS-tween (0.05%) overnight at 4°C on a tilting table. The following day the membrane was washed 4 times in PBS-tween (0.05%) for 10 min at RT and then incubated with the respective secondary antibody ([table 3.9](#)) diluted in approx. 10 ml 5% milk PBS-tween (0.05%) for 2 h at RT on a tilting table. This was followed by 4 washing steps again with PBS-tween (0.05%) as

described above. By using either the Super Signal West pico or West femto Luminol Kit (Thermo Scientific), depending on the protein analysed, relevant protein bands were detected in the gel documentations system (ChemiDoc™ XRS, Bio-Rad) with the Quantity One Software, version 4.6.6 (Bio-Rad).

Table 3.9: Antibodies and Ladders

Antibody/Ladder	Dilution	Protein size	Origin	Manufacturer	Cat. Nr.
Anti-β-Actin	1:15.000	45 kDa	Mouse	Sigma	A5441
Anti-CXCR2	1:300	55 kDa	Rabbit	Novus Biological	NB300-696
Anti-HIF1α	1:1000	120 kDa	Mouse	BD Transduction	610958
Anti-TRPC1	1:500	90 kDa	Mouse	Neuromab	clone 1F1
MagicMark™ XP Western Standard				Invitrogen	P/N LC5602
Anti-mouse POD	1:50.000		Goat	Dianova	115-035-003
Anti-rabbit POD	1:10.000		Goat	Sigma	A0545
PageRuler™ Plus Prestained Protein ladder				Thermo Scientific	#26619

When the same membrane was used to detect multiple proteins, the membrane was cut and antibody incubation performed in parallel, or the membrane stripped before incubation with the new antibody. This was performed by washing the membrane 3 times in ddH₂O for 5 min after development, incubating it for 5-10 min in 0.2 M NaOH and then washing the membrane again 3 times in ddH₂O for 5 min. The membrane was then ready for a new protein detection procedure starting from the blocking step with 5% milk PBS-tween (0.05%).

The program ImageJ was used to quantify the intensities protein bands in relation to that of the housekeeping gene (anti-β-Actin), thereby at the same time serving as a loading control. Secondly, background intensity was subtracted before band intensity was measured and calculated. For statistical reliability, Western Blots were performed at least 3 times with protein lysates from different experiments and animals.

3.4.2 RNA Extraction and Purification from PSCs

Total RNA was extracted from treated or non-treated mPSCs in passage 2. The supernatant was removed and cells were dissolved in 500 μ l Trizol[®] Reagent (Invitrogen) on ice. Cell suspension was collected with a cell scraper, transferred to a 1.5 ml Eppendorf tube and incubated for 5 min at RT. 100 μ l of chloroform were added and the suspension was vigorously shaken and further incubated for 2-3 min at RT. After incubation, the suspension was centrifuged at 12,000 g for 15 min at 4°C and the upper colourless liquid phase transferred to a new 1.5 ml Eppendorf tube. 250 μ l of isopropanol was added and suspension mixed by inverting the tube 10-15 times. The suspension was then incubated for 10 min again at RT and then centrifuged at 12,000 g for 10 min at 4°C. The supernatant was discarded and the RNA pellet then washed two times with 500 μ l of 70% ethanol by centrifugation at 7500 g for 5 min at 4°C. After the two washing steps the RNA pellet was air dried for 5-10 min before it was dissolved in 20 μ l RNase free water on ice. RNA concentration was measured using a Bio photometer (Eppendorf). The RNA sample was then stored at -80°C or used directly in the RT-PCR reaction to make cDNA ([section 3.4.3](#)).

3.4.3 Reverse Transcriptase PCR

Reverse transcriptase PCR was performed to synthesize cDNA from purified RNA ([section 3.4.2](#)), which was to be used in further mRNA quantification ([section 3.4.6](#)) and PCR experiments ([section 3.4.4](#)). The reverse transcriptase assay (Roche) was used according to the manufacturer's instructions and reactions were mixed as shown in [table 3.10](#). A RT-minus control sample with no RNA was always performed simultaneously. The volume of the reaction mixture varied between the experiments due to variations in RNA concentration between individual experiments. The reverse transcriptase mixture was first incubated at RT for 10 min, followed by incubation for 45 min at 55°C before incubation for 5 min at 85°C to inactivate the reverse transcriptase. The mixture was stored on ice and a further 50 μ l ddH₂O added. The cDNA sample was stored at -20°C for further use in PCR.

Table 3.10: RT-PCR Reaction Composition

Reagent	Volume
RNA Sample (~1 µg)*	1-2 µl
5x RT Buffer	4 µl
dNTP mix (10 mM)	2 µl
RT Random Oligo dt-primers (10 µM)*	2 µl
Reverse Transcriptase	0.5 µl
RNase out	0.5 µl
Nuclease Free Water	10 µl
Total Volume	20 µl

* To ensure denaturation of secondary structures, the RNA samples were first mixed with the oligo dt-primers and heated for 10 min at 60°C before being added to the RT-PCR reaction.

3.4.4 Polymerase Chain Reaction (PCR)

Primer pairs used for PCR and qPCR were selected from previously published data (primer pairs are shown in [table 3.4](#)) (Dietrich et al., 2005; Hill et al., 2013; Johnsen et al., 2006; Liu et al., 2007; Storch et al., 2012; Varga-Szabo et al., 2008; Weissmann et al., 2011). The specificity of primer pairs against target genes of interest in both WT and KO samples was tested and confirmed. For all PCR experiments the Taq DNA polymerase (Segetetic) was used. Taq DNA polymerase catalyses the polymerization of nucleotides into duplex DNA in the 5'-3' direction. The composition and conditions of the PCR are given in [table 3.11](#) and this reaction was performed in a Master Cycler (Eppendorf). After the PCR reaction had been completed the correct fragment size of amplified target genes was visualized by DNA electrophoresis ([section 3.4.5](#)).

Table 3.11: PCR Reaction Composition

Reagent	Volume	Reaction Step (35 cycles)	Temp.	Time
DNA Sample (~20 ng)	1 μ l	Initial Denaturation	94°C	5 min
10x DNA Polymerase Buffer	2 μ l	Denaturation	94°C	45 s
dNTP mix (10 mM)	1 μ l	Primer Annealing	50-55°C	15 s
Forward Primer (10 μ M)*	1 μ l	DNA Synthesis	72°C	30 s
Reverse Primer (10 μ M)*	1 μ l	Final Extension	72°C	10 min
Taq DNA Polymerase	0.3 μ l	Cooling	4°C	∞
5x Q Solution	4 μ l			
ddH ₂ O	9.7 μ l			
Total Volume	20 μl			

3.4.5 DNA Electrophoresis

DNA fragments were separated and visualized using agarose gel electrophoresis. The agarose concentration and DNA size markers were dependent on the predicted size of the DNA fragments under examination. For the preparation of 1% agarose gel, the appropriate amount of agarose (SERVA) was dissolved in 0.5x TBE buffer (45 mM Tris/HCL, 45 mM Boric acid, 1 mM EDTA) by heating the gel solution in a microwave (Amica International GmbH, Germany). After cooling to ~60°C, the gel solution was transferred to a gel chamber and a comb added to create evenly-sized wells. When the gel had completely polymerized, the comb was removed and the gel transferred to a gel electrophoresis chamber containing 0.5x TBE buffer. DNA samples were mixed with 6x loading dye (New England BioLabs), loaded into the gel and DNA fragments separated by electrophoresis (Electrophoresis Power PAC 3000, Bio-Rad) at 80 volts for approx. 60 minutes. After electrophoresis the gel was incubated with SYBR[®] Gold (Invitrogen) in 0.5x TBE buffer for 30 min with shaking. SYBR[®] Gold is a cyanine dye that stains nucleic acids and can therefore be used to visualize DNA fragments upon excitation with UV light in the agarose gel. The gel was visualized with the ChemiDoc[™] XRS Gel documentation system. A 100 bp DNA ladder (New England BioLabs) was run parallel to the samples for accurate prediction of the fragment sizes.

3.4.6 Quantitative Real-time PCR

Quantitative real-time PCR (qRT-PCR) was performed at the University of Lille, France under supervision from Kateryna Kondratska. The qPCR procedure was adapted from Kondratska et al. 2014, also described in Lindemann et al. 2015.

Total RNA was extracted as previously described ([section 3.4.2](#)). 5-10 µg RNA (total volume of 20 µl) was treated with DNase (Ambion) at 25°C for 30 min and purified using Phenol/Chloroform/Isoamyl (25:24:1), stabilized (Biosolve) with 5% 3 M Sodium Acetate (330 µl and 17.5 µl, respectively). Following centrifugation at 12.000g for 20 min the upper phase was collected and supplemented with 2.5x volume of ethanol and 10% 3 M Sodium Acetate. After overnight incubation at -20°C, the samples were washed with 70% ethanol, air dried and re-suspended in 15 µl ddH₂O. RNA concentration was measured and purity determined by gel electrophoresis ([section 3.4.5](#)) through the identification of two clear bands (18S and 28S ribosomal RNA). 2 µg of total RNA were reverse transcribed into cDNA using random hexamer primers (Roche) and MuLV reverse transcriptase (Roche) ([table 3.12](#)). The reverse transcriptase mixture was incubated at room temperature for 15 min followed by incubation for 30 min at 42°C before inactivating the reverse transcriptase for 10 min at 70°C. The mixture was first put on ice and then stored at -20°C for further use in qRT-PCR.

qRT-PCR is a method for DNA quantification where the amplification of a target sequence and its quantification are simultaneously performed. The reaction was carried out in a real-time thermal cycler Cfx C1000 (Bio-Rad). Quantification was performed by measuring fluorescence intensity after the extension step of each cycle using the cFX 96TM Real-Time system (Bio-Rad). The relative changes in gene expression were calculated by the $2^{-\Delta\Delta C_T}$ method (Livak and Schmittgen, 2001). This method relies on the following two assumptions. (1) The PCR reaction occurs with 100% efficiency, which means that the amount of product doubles in each PCR round. (2) There is a gene that is expressed at a constant level in each sample to correct for any difference in the amount of sample used for the reaction (Livak and Schmittgen, 2001). The rise of fluorescence is assumed to be proportional to the generated PCR product and thereby measures the amount of target DNA. The threshold cycle (C_T) was set to be automatically determined by the cFX 96TM Real-Time system. C_T indicates the fractional PCR cycle number at which the amount of amplified target gene reaches a fixed threshold.

Table 3.12: RT-PCR Reaction Composition for qPCR

Reagent	Volume	Total volume
RNA Sample (~2 µg)*	1-8.4 µl	9.6 µl
Random hexamer primers (2.5 mM)*	1.2 µl	
Nuclease Free Water*	Up to 9.6 µl	
10x RT Buffer (without Mg ²⁺)	2 µl	10.4 µl
MuLV Reverse Transcriptase	1 µl	
dNTP mix (10 mM)	4 µl	
RNase inhibitor	1 µl	
Total Volume		<u>20 µl</u>

* To ensure denaturation of secondary structures the RNA sample was first mixed with the hexamer primers and nuclease free water and then heated for 10 min at 70°C, before being added to the RT-PCR reaction mix.

Ten picomoles of each primer pair and 0.2 µl of the synthesized cDNA (first-strand synthesis) were mixed with 2xSsoFast™EvaGreen®Supermix (Bio-Rad) and qRT-PCR was carried out using following conditions: Initial denaturation activation step at 95°C for 30 s, followed by 41 cycles of 95°C for 5 s and 60°C for 30 s (for an overview, see [table 3.13](#)). To exclude fluorescence of primer dimers all primers were tested using diluted cDNA from the first-strand synthesis to confirm linearity of the reaction. Inclusion criteria for primers were an amplification efficiency of 90-110%, and an R2 value > 0.98 (parameter to evaluate PCR efficiency). A dissociation curve (melting curve analysis) was run for primers to exclude samples containing dimers using the following thermal profile: 95°C for 10 s, followed by a stepwise increase of temperature by 0.5°C every 5 s from 65°C to 95°C. Primer pairs that were used for the amplification of specific fragments from the first-strand synthesis are listed in [table 3.4](#). Note that primer set number 2 was used for amplification of TRPC1 in qRT-PCR. Both the Hypoxanthin phosphoribosyltransferase 1 (*hprt*) gene and β-2 microglobulin (β-2M) were used as endogenous controls to normalize variations in RNA extractions, the degree of RNA degradation, variability in reverse transcription and qRT-PCR efficiency. All experiments were performed in triplicates and repeated three times.

Table 3.13: Composition of the qRT-PCR and Protocol Steps

Reagent	Volume	Reaction Step	Temp.	Time
(41 cycles of step 2-3)				
2x SsoFast™ EvaGreen® Supermix	7.5 µl	1) Initiating Step	95°C	30 sec
Primer forward (10 µM)	0.45 µl	2) Denaturation	95°C	5 sec
Primer reverse (10 µM)	0.45 µl	3) Annealing/Synthesis	60°C	30 sec
ddH ₂ O	1.6 µl			
cDNA Sample*	5 µl	<u>Dissociation curve (melting curve analysis)</u>		
Total Volume	15 µl	Increment steps 65°C → 95°C	↑0.5°C	5 sec

* cDNA was taken from the dilution row 1/20 to 1/160 for the testing of primer efficiency. For quantification, the 1/40 dilution was found to be optimal.

3.5 In Vitro Migration Assays

To mimic tissue composition observed within the pancreas and in PDAC all migration experiments were performed with a matrix composed primarily of Collagen I (~90%) complemented with laminin, fibronectin, collagen III and IV, as observed in desmoplastic regions in PDAC. I will refer to this matrix as desmoplastic matrix. A detailed composition is given in [table 3.14](#).

3.5.1 Hypoxia treatment

mPSCs were exposed to a hypoxic environment within the hypoxic CO₂ incubator maintained at low oxygen tension (1% O₂, 5% CO₂ and 94% N₂). The treatment was initiated by replacing the culture medium in the culture with deoxygenated DMEM/F12 and incubating the mPSCs under hypoxic conditions. Deoxygenated medium was prepared prior to each experiment by equilibrating the medium within the hypoxic incubator for at least 5 h. The cell-permanent compound, dimethylalglycine (DMOG) (Frontier Scientific), was used to chemically induce hypoxia at a concentration of 0.5 mM with DMSO as control [1:10,000]. Different experiments were performed with DMOG: (1)

Evaluation of the optimal concentration and chronic effect of DMOG (tested in concentrations at: [0.25 mM] [0.50 mM], [0.75 mM], [1.0 mM] and [1.5 mM]) and (2) assessing the acute effect of DMOG ([0.50 mM]).

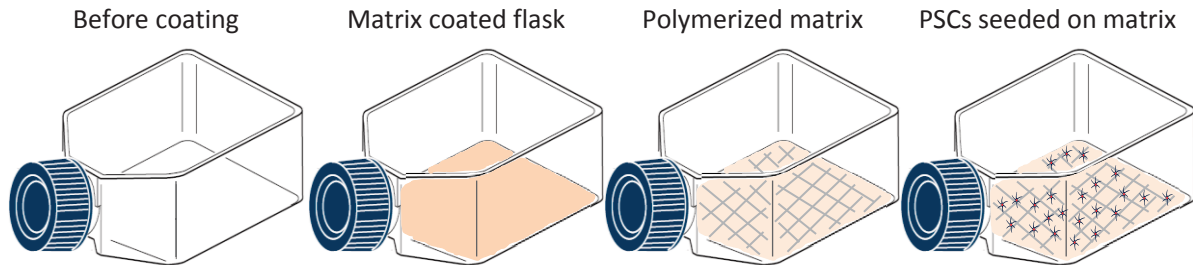


Figure 3.2. Schematic of the 2D Migration Setup. A 12.5 cm² culture flask with seal cap was coated with approx. 200 µl desmoplastic matrix (table 3.14) and left for polymerization overnight in a CO₂ incubator. The matrix should polymerize by the following day and be ready for experimental use. ~27,000 PSCs were then seeded out in 2.5 ml DMEM/F12 (plus FCS). After 6-7 h the cells should be firmly attached and ready for the experiment.

3.5.2 Two-Dimensional Migration

Culture flasks (12.5 cm²) were coated with 150 µl desmoplastic matrix (pH 7.4) (table 3.14) and left overnight to polymerize (~14-18 h) in the CO₂ incubator. mPSCs were seeded out (~27,000 mPSCs per flask) in 2.5 ml DMEM/F12 medium and left to attach for ~6 h. A schematic is shown in figure 3.2. Hereafter, the medium was changed and flask incubated overnight (~20-24 h) under the appropriate conditions. The following day the caps of the flasks were closed quickly inside the incubator and transferred to pre-heated chambers (37°C) on stages of inverted microscopes (10x and 20x objectives). Cell migration was recorded for varying time periods in 5 min intervals using time-lapse video microscopy (program HiPic and Wasabi) as described previously (Fabian et al., 2012; Fabian et al., 2008).

In the experiments with chemically-induced hypoxia the medium after PSC attachment was changed to fresh DMEM/F12 +/- DMOG or DMSO and incubated overnight (~20-22 h). Next day were the medium changed to RPMI/HEPES medium (minus FCS, pH 7.4, +/- DMSO or DMOG) and equilibrated in a heat closet for 30 min before transferring the closed flask to the microscope. This was performed to better mimic the conditions in the 3D migration experiment with the medium also being RPMI/HEPES minus FCS (see below).

Table 3.14: Composition of 2D Matrix

	Stock conc.	Volume	End Conc.	%
RPMI 5x	52 g/L	200 μ l	10.4 g/l	
HEPES 10x	100 mmol/L	100 μ l	10 mmol/l	
NaOH	1 M	4.8 μ l	pH = 7.4	
ddH₂O		397 μ l		
Laminin	1 mg/ml	40 μ l	40 μ g/ml	4.46%
Fibronectin	1 mg/ml	40 μ l	40 μ g/ml	4.46%
Collagen IV	0.9 mg/ml	6 μ l	5.4 μ g/ml	0.602%
Collagen III	1.0 mg/ml	12 μ l	12 μ g/ml	1.34%
Collagen I	4 mg/ml	200 μ l	800 μ g/ml	89.15%
Total		1 ml	897.4 μg/ml	100%

- Note: the given amounts in [table 3.14](#) are for coating of approx. 5 migration flasks.

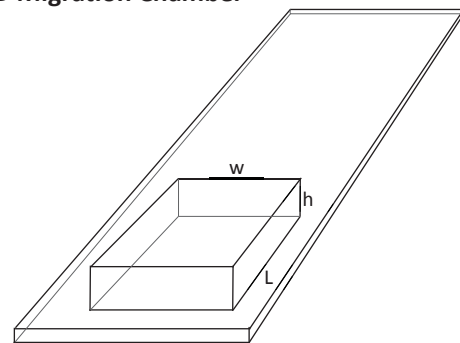
3.5.3 Three-Dimensional Migration

The 3D experimental migration setup is closely related to the one performed in 2D. The same matrix composition was used, but with an increased concentration of each individual component to achieve sufficient polymerization with embedded mPSCs.

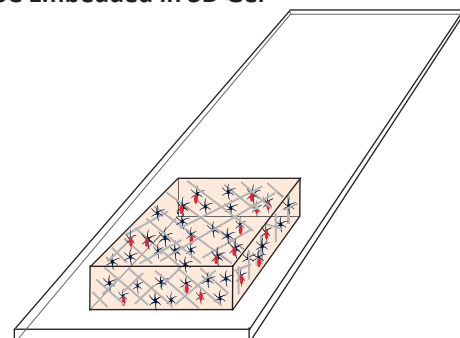
Initially, the migration chamber was built under semi-sterile conditions from a mixture of Paraffin and Vaseline (1:1) surrounding a spacer (l: 20 mm, w: 20 mm, h: 0.8 mm),

Figure 3.3. The 3D Migration Chamber. For clarity I omitted the Paraffin/Vaseline sealing of the chamber. **(Top)** A chamber was built onto a microscope slide out of paraffin/Vaseline (1:1) with a spacer (20 mm (L) x 20 mm (w) x 0.8 mm (h)). **(Bottom)** The matrix containing mPSCs was then loaded. After polymerization of the gel mPSC migration could be observed by means of time-lapse video microscopy.

3D Migration Chamber



PSC Embedded in 3D Gel



leaving one end open for loading (modified from (Stock et al., 2005)). Next, the 3D gel/+mPSCs mixture was made (~400 μ l matrix, pH \approx 7.35) ([table 3.15](#)), loaded and left upright for polymerization for 2.5 h at 37°C to prevent mPSCs from attaching to the side/bottom. An illustration of the 3D migration setup is shown in [figure 3.3](#). After polymerization the chamber was sealed with paraffin/Vaseline (1:1) and transferred to pre-heated chambers (37°C) on stages of inverted microscopes and cell migration recorded for varying time periods using time-lapse video microscopy. The focus was set on mPSCs localized in the middle plane of the chamber to ensure 3D migratory conditions. Only mPSCs showing migratory activity within the first hour of the time-lapse video recording were used for further analysis (see [section 3.5.6](#)). mPSCs in focus and not moving in the Z direction were fully analysed ([figure 4.3 D](#)). mPSCs which were out of focus, but observed to be active, were only analysed for migration velocity and translocation ([section 3.5.6](#)). For time-lapse video microscopy of 3D migration the program HiPic was used with the following settings: 10x microscope objective, 5 min intervals.

Table 3.15: Composition of 3D Matrix

	Stock conc.	Volume	End conc. (300 μ l matrix)	End conc. (400 μ l matrix)	%
RPMI 10x	104 g/L	30 μ l	10.4 g/l	10.4 g/l	
HEPES 20x	200 mmol/L	30 μ l	20 mmol/l	20 mmol/l	
NaOH	1 M	3.45 μ l		pH = 7.4	
Laminin	1 mg/ml	30 μ l	100 μ g/ml	75 μ g/ml	4.216%
Fibronectin	1 mg/ml	30 μ l	100 μ g/ml	75 μ g/ml	4.216%
Collagen IV	0.9 mg/ml	5.4 μ l	16.18 μ g/ml	12.135 μ g/ml	0.682%
Collagen III	1.0 mg/ml	10.8 μ l	36 μ g/ml	27 μ g/ml	1.516%
Collagen I	4 mg/ml	159 μ l	2120 μ g/ml	1590 μ g/ml	89.37%
PDGF	10 μ g/ml	2 μ l	66.66 ng/ml	50 ng/ml	
mPSC	In 1x RPMI/HEPES (20 mM, pH 7.4)	100 μ l		90-100,000 cells	
Total			2372.18 μg/ml	1779.13 μg/ml	100%

- Note that the given amounts in [table 3.15](#) are for one 3D migration experiment.

Notation to 2D and 3D matrices:

Bearing in mind that polymerization and self-assembly of collagen may be affected by free protons (Freire and Coelho-Sampaio, 2000; Williams et al., 1978), the pH values of the cell free 2D matrix composition (*table 3.14*) and the 3D matrix/+ mPSCs (*table 3.15*) were always adjusted to \approx pH 7.4. This ensured reproducible and consistently structured collagen polymerization, allowing for the exclusion of any effects based on pH-dependent differences in the matrix. The pH stability in the 3D chamber was in parallel to the time-lapse recording by measuring the pH at different time points in an eppendorf tube, including the same amount of matrix and PSCs.

3.5.4 Chemotaxis Assay

For 2D chemotaxis experiments the μ -Slide Chemotaxis^{2D} from Ibidi was used according to manufacturer's guidelines (Application Note 14, Ibidi protocol) (*figure 3.4*) and as described previously (Fabian et al., 2011). First, the observation area (*figure 3.4*) of the chemotaxis μ -Slide was coated for 1 hour with the same desmoplastic matrix as used in the 2D migration experiments (*table 3.14*). Hereafter, the remaining matrix solution was aspirated to remove excessive coating and filled with RPMI (10mM HEPES, no FCS) before seeding \sim 5,000-7,500 mPSCs into the channel. The mPSCs were allowed to attach for 5-7 h in a humid atmosphere at 37°C. Then the medium in the μ -Slide was replaced with fresh RPMI (10mM HEPES, no FCS) to get rid of non-attached mPSCs. The stimulant was then applied in one of the reservoirs to establish a gradient and mPSC chemotaxis/directionality was

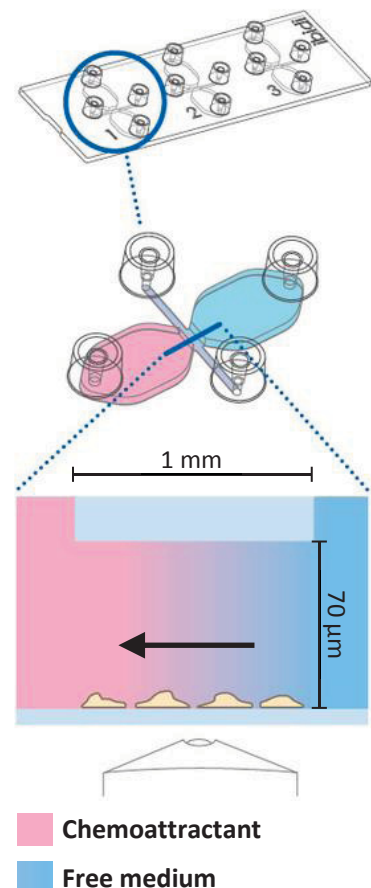


Figure 3.4. Ibidi 2D Chemotaxis μ -Slide. The μ -Slide Chemotaxis^{2D} from Ibidi consists of two large volume reservoirs (\sim 40 μ l) connected by a thin channel (1mm wide and 70 μ m high). mPSCs are seeded into this channel. The two reservoirs can then be filled individually with a chemoattractant (shown in red) and cell- and chemoattractant-free medium (shown in blue). There is a linear and stable concentration gradient of the chemoattractant inside the connecting channel generated by diffusion (modified from www.ibidi.com).

monitored by time-lapse video microscopy for 15 h using the program HiPic and Wasabi with following settings: 5x and 10x microscope objectives, 5 min intervals. The following stimulants were used (end concentration in the chemoattractant reservoir is shown): PDGF (800 ng/ml), VEGF (400 – 1600 ng/ml) and KC (10 – 10.000 ng/ml).

3.5.5 Autocrine Stimulation Assay

WT, TRPC1^{-/-} and TRPC6^{-/-} mPSCs (passage 2) were cultured under hypoxic conditions (1% O₂, 5% CO₂ and 94% N₂) in normal culture medium for 6 h before media was replaced with serum-free DMEM/F12 and further incubated for 18-24 h. The conditioned media were harvested, sterile filtered and applied to WT mPSCs pre-seeded on a desmoplastic matrix within 2D migration flasks (see [section 3.5.2](#)) for further evaluation of migration stimulation. Normoxically equilibrated culture media (DMEM/F12 minus FCS) were used as control.

3.5.6 Analysis of Migration Data

For quantification and tracking of 2D/3D mPSC migration and chemotaxis the Amira Imaging Software was used to label the circumferences of the cells as previously described (Fabian et al., 2012; Fabian et al., 2008). The individual cell contours or cell center were manually determined frame-by-frame over the entire migration movie, which then served as the basis for further analysis. Every other image of the time-lapse video was selected for analysis giving intervals of 10 min duration. The duration of the migration movie analyzed was between 4-18 h. Using a Java-based Plugin for ImageJ individual data files could be obtained for each segmented mPSC. This data file was then imported into Microsoft Excel and the following parameters were determined:

1) Migration velocity [$\mu\text{m}/\text{min}$]:

Calculated from the movement of the cell center per unit time.

2) Translocation [μm]:

Defined by the distance from start to end position.

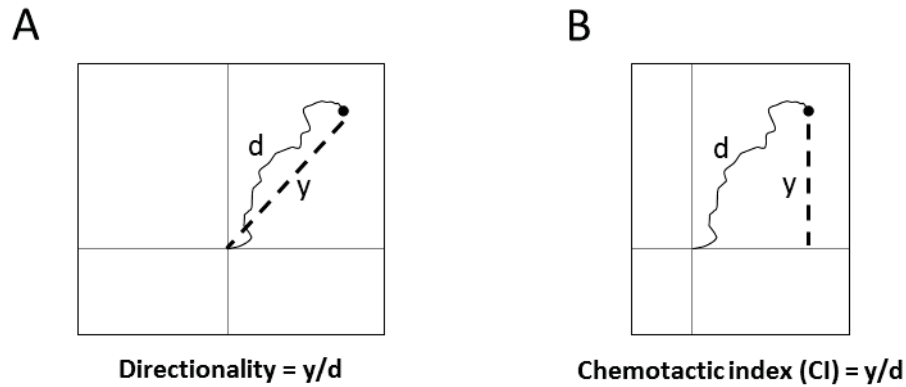


Figure 3.5. Definitions of Directionality and Chemotactic Index. (A) The directionality of migration is calculated by the translocation from start to end (y) divided by the total distance covered (d). Changes in the directionality can point toward difficulties in the cells steering capabilities. *(B)* The chemotactic index (CI) is calculated by the distance covered toward a gradient (y) divided by the total distance covered (d). The CI thereby provides information about cells' chemotaxis capabilities.

3) Total path length [μm]:

Defined by the total distance covered (from start to end position) during the migration movie. Calculated from mean velocity multiplied with the duration of the movie in minutes.

4) Chemotactic index (CI):

Indicates efficiency of cell chemotaxis toward a given stimulant. The chemotactic index (CI) is defined by the net distance covered towards the gradient in y -direction (y) divided by the total path length (d) (*figure 3.5*). Cells moving in a direct line towards the gradient will give the value "1", whereas cells changing direction often will give lower values, or even negative, when moving against the gradient.

5) Directionality:

The ability of the cell to move in a direct line from A to B. Calculated by the translocation (start to end point) (y) divided by the total path length (d) (*figure 3.5*). Cells moving in a direct line give values close to "1", whereas cells changing direction give lower values.

6) Cell Area [μm^2]:

Defined by the projected area covered by the cell. Not applicable to cells followed/marked only with a dot (cell center).

7) Structure Index [SI]:

The structure index defines cell morphology. Spherical cell shape structures give values close to “1”, whereas values closer to “0” indicate a more star-shape and extended structure/morphology. SI was calculated as follows:

$$SI = (4 * \pi * A) / p^2$$

- “A” is the area covered by the cell and p is the perimeter of A.

3.6 Oxygen Consumption and Extracellular Acidification Measurements

Oxygen consumption and extracellular acidification measurements of mPSCs were performed at Bayer A/G, Berlin, Germany under supervision from PhD student Ilya Kovalenko.

The Seahorse Extracellular Flux Analyser XF96 (Bioscience) was used to profile the metabolic activity of WT, TRPC1^{-/-} and TRPC6^{-/-} mPSCs under normoxia and chemically-induced hypoxia according to manufacturer’s guidelines (Installation and Operation Manual, Software Version 1.3, revision 12/21/10, www.seahorse.bio.com). This was performed by measuring O₂ concentration and pH, which are estimates of the two major energy producing pathways, mitochondrial respiration and glycolysis. The XF96 analyzer converts these measurements into oxygen consumption rate (OCR) in pmol/min, extracellular acidification rate (ECAR) in mpH/min and proton production rate (PPR) at intervals of approx. 2-5 minutes. OCR is an indicator of mitochondrial respiration, whereas both ECAR and PPR are measured from pH and are predominately the result of glycolysis. As cells change metabolic pathways e.g. under hypoxic conditions, the relationship between OCR and ECAR changes. This is also known as the Warburg effect (Asgari et al., 2015; Upadhyay et al., 2013). The OCR/ECAR (estimated metabolic index)

was also calculated. If this index changes from “high” to “low” e.g. normoxia vs. hypoxia, it indicates prevalence to glycolysis above oxygen and thereby a more anaerobic than aerobic metabolic phenotype. In this experiment we used DMOG [0.50 mM] to simulate and induce hypoxic conditions. Both the acute (1 hour) and chronic (18-22 h) effect of DMOG was measured.

The experiment was performed according to the manufacturer’s instructions. Briefly, on day one 25,000 mPSCs per well were seeded on a Seahorse 96-well cell culture plate and left to adhere for 3 h before DMOG or DMSO (control) were applied for the chronic experiments. Further, the Seahorse cartridge was equilibrated in Seahorse Bioscience XF96 Calibrant buffer overnight at 37°C in the Seahorse Prep station. In the acute DMOG experiment mPSCs were left in normal culture media overnight and DMOG/DMSO applied the next day to run the experiment simultaneously with the chronic DMOG treated mPSCs. At day 2 mPSC culture medium was replaced by XF Seahorse Assay medium (modified DMEM, pH 7.4, + 5 mM glucose, + 2 mM sodium pyruvate) +/- DMOG [0.50 mM] or DMSO and incubated for 60 min in a heating closet at 37°C prior to running the assay. The equilibrated Seahorse cartridge was placed together with a utility plate with calibration buffer in the XF96 Analyzer for calibration. After incubation the Seahorse 96-well cell culture plate with treated mPSCs was loaded into the XF96 Analyzer and the assay was performed. The measurements were performed in triplicates in 9 min steps. A baseline of 4 measurements was made and the mean of these then calculated. For further details about experimental instructions, I refer to the XF96 Extracellular Flux Analyzer and Prep Station, Installation and operation Manual (Seahorse Bioscience).

3.6.1 Estimation of Oxygen consumption in 3D chamber

Known volume in chamber:	350 μ l = 0.35 ml
Number of PSCs in chamber:	85.000 cells
Oxygen capacity at 37°C:	7 mg/l
1 mol oxygen:	32 g

Calculation of oxygen in chamber:

$$\frac{X}{7 \text{ mg}} = \frac{350 \mu\text{l}}{1 \text{ l}} \gg X = \frac{7 \cdot 350 \text{ mg}/\mu\text{l}}{1 \text{ l}} = \frac{7 \cdot 0.00035 \text{ mg/l}}{1 \text{ l}} = 0.00245 \text{ mg} = 2.45 \cdot 10^{-6} \text{ g}$$

$$\text{mol oxygen in chamber: } \frac{2.45 \cdot 10^{-6} \text{ g}}{32 \text{ g/mol}} = 7.656 \cdot 10^{-8} \text{ mol/ chamber}$$

OCR readout (Seahorse):

PSC WT readout:	(N = 3)	176.2 pmol/min	25,000 cells
KO TRPC1 readout:	(N = 3)	182.1 pmol/min	25,000 cells
KO TRPC6 readout:	(N = 3)	179.8 pmol/min	25,000 cells

PSC WT:

Oxygen consumption estimation in chamber

$$176.205 \text{ pmol/ min} \cdot 430 \text{ min} = 75.7875 \cdot 10^{-9} \text{ mol/ 430 min} \text{ for 25.000 cells}$$

$$= 10.575 \cdot 10^{-9} \text{ mol/hour} \text{ for 25.000 cells}$$

$$85.000 \text{ cells: } \frac{85000 \text{ cells}}{25000 \text{ cells}} \cdot 75.7875 \cdot 10^{-9} = 247.4775 \cdot 10^{-9} \text{ mol/ 430 min}$$

$$= 24.74775 \cdot 10^{-8} \text{ mol/ 430 min}$$

$$= 3.453 \cdot 10^{-8} \text{ mol/ hour}$$

$$\text{Estimated hypoxia after: } \frac{7.656 \cdot 10^{-8} \text{ mol/ chamber}}{3.453 \cdot 10^{-8} \text{ mol/hour}} \approx 2.217 \text{ hour} \approx 133 \text{ min}$$

PSC KO TRPC1:

Oxygen consumption estimation in chamber

$$182.133 \text{ pmol/ min} \cdot 430 \text{ min} = 78.317 \cdot 10^{-9} \text{ mol/ 430 min} \text{ for 25,000 cells}$$

$$= 10.928 \cdot 10^{-9} \text{ mol/hour} \text{ for 25,000 cells}$$

$$85.000 \text{ cells: } \frac{85000 \text{ cells}}{25000 \text{ cells}} \cdot 78.317 \cdot 10^{-9} = 266.2778 \cdot 10^{-9} \text{ mol/ 430 min}$$

$$= 26.62778 \cdot 10^{-8} \text{ mol/ 430 min}$$

$$= 3.7155 \cdot 10^{-8} \text{ mol/ hour}$$

$$\text{Estimated hypoxia after: } \frac{7.656 \cdot 10^{-8} \text{ mol/ chamber}}{3.7155 \cdot 10^{-8} \text{ mol/hour}} \approx 2.061 \text{ hour} \approx 124 \text{ min}$$

PSC KO TRPC6:

Oxygen consumption estimation in chamber

$$179.771 \text{ pmol/min} * 430 \text{ min} = 76.4415 * 10^{-9} \text{ mol/430 min} \text{ for 25,000 cells}$$

$$= 10.666 * 10^{-9} \text{ mol/hour} \text{ for 25,000 cells}$$

$$85.000 \text{ cells: } \frac{85000 \text{ cells}}{25000 \text{ cells}} * 76.4415 * 10^{-9} = 259.9011 * 10^{-9} \text{ mol/430 min}$$

$$= 25.99011 * 10^{-8} \text{ mol/430 min}$$

$$= 3.6265 * 10^{-8} \text{ mol/hour}$$

$$\text{Estimated hypoxia after: } \frac{7.656 * 10^{-8} \text{ mol/chamber}}{3.6265 * 10^{-8} \text{ mol/hour}} \approx 2.111 \text{ hour} \approx 126 \text{ min}$$

3.7 Manganese Quenching

The Manganese (Mn^{2+}) quenching method was used for indirectly measuring Ca^{2+} influx into Fura-2 (Calbiochem) loaded mPSCs (Fabian et al., 2011; Lindemann et al., 2013; Merritt et al., 1989). Mn^{2+} enters the cell via Ca^{2+} channels, binds with higher affinity than Ca^{2+} to the Ca^{2+} dye Fura-2 and thereby decreases the Ca^{2+} -induced fluorescence intensity. The decrease of Ca^{2+} -bound Fura-2 fluorescence intensity is thereby used as an indirect measure of Ca^{2+} influx. Fura-2 was excited at its isosbestic wavelength of 365 nm, where the emitted fluorescence at 500 nm is independent of changes in $[\text{Ca}^{2+}]_i$.

Glass bottom cell culture dishes (Cellview™, Greiner Bio-one) were coated with 0.8-1.0 ml desmoplastic matrix (1:10 diluted) ([table 3.14](#)) for 30-45 min at RT. Hereafter 20,00-25,000 mPSCs were seeded in a total volume of 2.5 ml and left to adhere for 4-6 h. mPSCs were then either incubated in 2.5 ml culture medium overnight (20-24 h) under hypoxic conditions (1% O_2) or in chemically-induced hypoxia with DMOG [0.50 mM] together with their respective controls (normoxia and DMSO). The next day, 1 ml medium was removed and the normoxia- and hypoxia-treated mPSCs loaded for 30 min with 5 μM Fura-2-AM (total volume of 1 ml) within the CO_2 incubator (no light). After incubation the cell dish was transferred to a 37°C heated inverted microscope (40x oil emission objective, Axiovert 200, Zeiss), and perfused for 5-10 min with Ringer's solution (pH 7.4) prior to the measurements. The experiment was performed with perfusion of 37°C pre-heated working solutions (given in [table 3.16](#)) and image sequences recorded in 5 s

intervals. The high speed poly chromator, camera and images were controlled by the Metaflour software (Visitron Systems). The experimental protocol was as follows: (1) Control period of 1.5-2.5 min in Ringer's-solution, (2) 2-3 min in Mn^{2+} containing Ringer's solution, (3) 2-3 min Ringer's solution. For data analysis the perinuclear fluorescence intensity was quantified and corrected for background fluorescence. Afterwards, regression analysis of fluorescence intensity over time was performed to determine the change in fluorescence quenching. Mean Fura-2 fluorescence intensity excited at its isobestic wavelength 365 nm (F_{365}) was normalized to the first stable values under control conditions. The corresponding mean change of the slope Δm ($m2 - m1$) was then calculated, with $m1$ equivalent to control conditions and $m2$ to Mn^{2+} . A more negative value for Δm in treated PSCs would then indicate a higher Ca^{2+} influx within these cells.

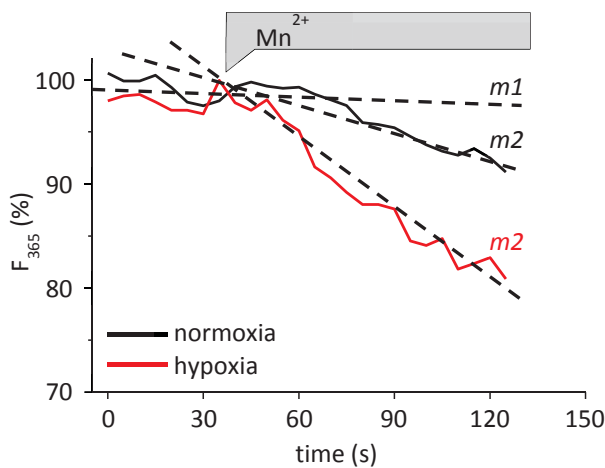


Figure 3.6. Principle of the Manganese Quenching Method. Representative graph showing an increased calcium influx in hypoxia stimulated mPSC (red slope, $m2$) compared to control (black slope, $m1$). Δm ($m2 - m1$) is giving a more negative value for hypoxia compared to normoxia treated mPSCs indicating a higher Ca^{2+} influx.

Table 3.16: Ringer's Solutions for $[Mn^{2+}]$ Measurements

Ringer-Solution, pH 7.4 at 37°C*		Stock
NaCl	122.5 mM	3M NaCl (157.32 g/l)
KCl	5.4 mM	1M KCl (74.55 g/l)
CaCl ₂	1.2 mM	0.1M (11.099 g/l)
MgCl ₂	0.8 mM	0,1M (20.33 g/l)
HEPES	10 mM	
Glucose	5.5 mM	

* For Mn^{2+} working solutions $MnCl_2$ (125.84 g/mol) was applied to give a final conc. of [200 μ M].

3.8 Calcium Entry

This experiment was performed in cooperation with Kateryna Kondratska, a PhD student from our cooperation partner from the University of Lille, France. Calcium imaging protocol was adapted and modified to our experimental setup from Kondratska et al. 2014.

Freshly isolated mPSCs (described in [section 3.3.2](#)) were directly seeded on glass bottom cell culture dishes (Cellview™, Greiner Bio-one) to carry out calcium imaging on non-culture-activated mPSCs, reflecting mPSCs in their quiescent state. We used mPSCs from passage 2 for calcium imaging on culture activated PSCs. The ratiometric dye Fura-2/AM (Calbiochem) was used as a Ca^{2+} indicator. Cells were loaded with 2 μM Fura-2/AM for 45 min at 37°C and 5% CO_2 in corresponding medium and subsequently washed three times with external solution containing: 140 mM NaCl, 5 mM KCl, 1mM MgCl_2 , 2 mM CaCl_2 , 5 mM glucose, 10 mM HEPES (pH 7.4). Experiments were carried out at room temperature. Excitation wavelength alternated between 340 and 380 nm, and the fluorescence emission was recorded at 500 nm. Images were acquired in 5-s intervals. High speed poly chromator, camera and images were controlled by the Metaflour software (Visitron Systems). Fluorescence intensity was measured over the whole cell area and was corrected for background fluorescence before $[\text{Ca}^{2+}]_i$ was calculated by the ratio of the wavelengths 340 nm / 380 nm (f/f_0) (Kondratska et al., 2014).

3.9 Calpain Activity

To determine calpain activity in single RLT-PSCs a so called Boc assay was modified and used according to previous published data (Glading et al., 2000; Rosser et al., 1993; Svensson et al., 2010). Glas bottom dishes (Greiner Bio-One, Frickenhausen, Germany) were coated for 30 min with 1:10 diluted basal lamina matrix ([table 3.17](#)), before $\sim 2.3 \cdot 10^4$ cells were plated in growth medium to attach for 3-4 h at 37°C and 5% CO_2 , 95% air. 5 min prior to the calpain experiment DMEM/F12 medium was replaced with HEPES-buffered Ringer solution. Cells were then either treated in the presence or absence of 50 ng/ml PDGF with DMSO (1:1000) or TRAM-34 (1-[(2-Chlorophenyl)diphenylmethyl]-1H-pyrazole, 10 $\mu\text{mol/l}$), an inhibitor of $\text{K}_{\text{Ca}3.1}$ channels for 30 min. Thereafter, cells were transferred to the microscope stage (Axiovert 200) and the calpain substrate 7-amino-4-

chloromethylcoumarin, t-BOC-L-leucyl-L-methionine amide (CMAC, t-BOC-Leu-Met; 10 μ M; Molecular Probes) was added. After 10 min at 37 °C fluorescence images were taken using a digital camera (model 9.0, RT-SE-Spot, Visitron Systems) and the MetaVue software (Visitron). At the end of the experiment cells were labelled with 2',7'-bis-(2-carboxyethyl)-5-(and-6)-carboxy-fluorescein (BCECF; 1.25 μ g/ml) for 2 min in order to obtain a uniform labeling of the cytosol. The following filter sets were used: excitation 365/12nm, beam splitter 395nm, emission 397nm (for CMAC, t-BOC-Leu-Met fluorescence) and excitation 470/40nm, beam splitter 510nm, emission 540/50nm (for BCECF-fluorescence). Image exposure settings were identical within each experiment: 100 ms for CMAC, t-BOC-Leu-Met and 500 ms for BCECF. Fluorescence intensity was measured over the whole cell area and corrected for background fluorescence in ImageJ. When local calpain activities were determined, CMAC, t-BOC-Leu-Met fluorescence were normalized to that of BCECF.

Table 3.17: Composition Basal Lamina Matrix

	Stock conc.	Volume	End Conc.	%
RPMI 5x	52 g/L	104 μ l	13.5 g/l	
HEPES 10x	100 mmol/L	52 μ l	12.99 mmol/l	
NaOH	1 M	7.5 μ l	pH = 7.4	
ddH₂O		52 μ l		
Laminin	1 mg/ml	12.5 μ l	31.2 μ g/ml	7.75%
Fibronectin	1 mg/ml	12.5 μ l	31.2 μ g/ml	7.75%
Collagen IV	0.9 mg/ml	160 μ l	339 μ g/ml	84.5%
Total		400 μ l	401.4 μg/ml	100%

- Note: 1:10 (400 + 3600 μ l ddH₂O) was used for coating.

3.10 Statistical Analysis

All experiments were repeated at least three times and tested for normal distribution by Shapiro-Wilk, Lilliefors and Kolmogorov Smirnov tests before performing any statistical analyses. For normally distributed data, statistical significance was determined using the Student t-test. Otherwise, the Mann-Whitney U test was used. Data are presented as means \pm standard error of mean (SEM). Differences between experimental groups reaching $p \leq 0.05$ were considered significantly different and presented as follows: (*) = $p \leq 0.05$. Non-significant data of interest were indicated as “n.s.” The number of experiments/replicates performed is given with by an “N” and number of data points with an “n”.

Chapter 4

Results

Results

4.1 mPSC Identification

Freshly isolated mPSCs could be identified by the presence of Vitamin A droplets, indicating a state of quiescence (non-activated form). During culturing mPSCs lose their Vitamin A droplets and change to their activated form that expresses α -SMA (*figure 4.1 A-B*). This transition can be observed after 2 days in culture. It is complete after approx. 5 days and the first cell passaging. Therefore, mPSCs were used in passage 2 for all experiments. The processes used for identification and confirmation of isolated mPSCs were established and performed in our laboratory by Benedikt Hild, a former medical student, prior to the start of this project. I will therefore refer to his dissertation for

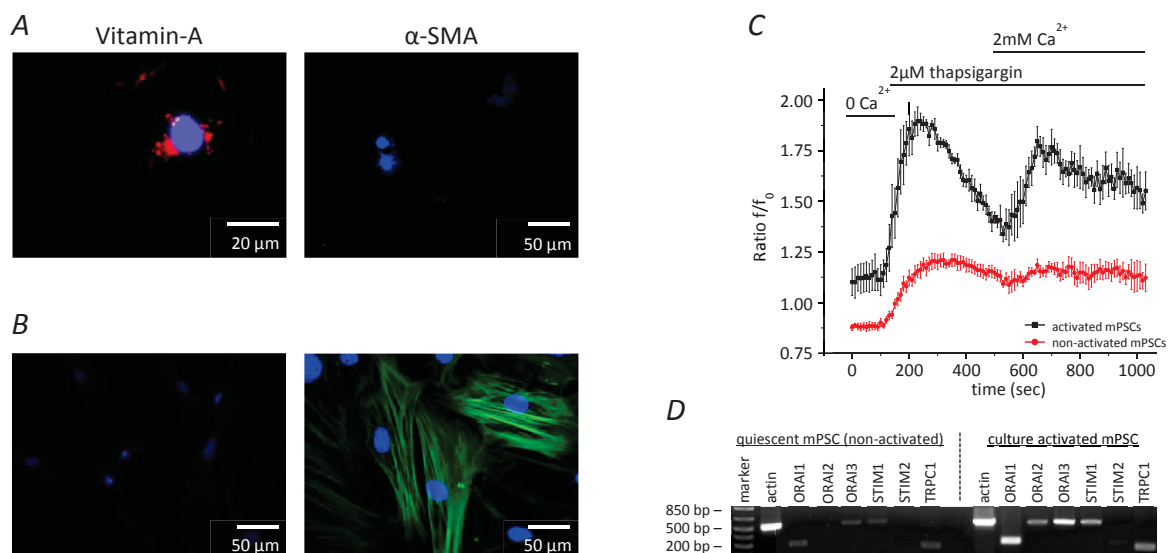


Figure 4.1. PSC Identification and Elevated Calcium Signalling in Activated mPSCs. **(A)** Mouse PSCs were identified directly after isolation through positive staining of Vitamin A, indicating a state of quiescence (non-activated form). **(B)** Upon culturing, mPSCs are activated, lose their vitamin A droplets and show positive staining for α -SMA (α -SMA staining after 5 days culturing is shown). **(C)** Store release and calcium influx were analysed by calcium imaging showing a higher calcium store release and influx in culture activated mPSCs compared to freshly isolated mPSCs. Data presented as means \pm S.D. N = 3. **(D)** Representative gel (N = 3) documenting the expression level of TRPC1, ORAI1-3 and STIM1-2 assessed by semi-quantitative PCR. All target genes show elevated expression level in culture-activated mPSCs when compared to freshly isolated mPSCs. (Figure A and B were with permission adapted from Hild B. 2015, and experiments C and D were performed in cooperation with Kateryna Kondratska).

further reading regarding this subject (Hild, 2015).

Calcium signalling is important for cell migration and for PSC activation. It was therefore determined whether calcium levels were altered upon culture activation of mPSCs. Calcium store release and SOCE were elevated in activated mPSCs compared to freshly isolated mPSCs (*figure 4.1 C*). The mRNA expression level of important SOCE members (ORAI1-3, STIM1-2 and TRPC1) was assessed by semi-quantitative PCR showing a higher expression of all the analysed candidates (*figure 4.1 D*). This correlates with the elevated calcium influx, which suggests that calcium plays an important role in the activation process of mPSCs. These findings also implicate Ca^{2+} regulatory ion channels, including TRPC family members, in the activation of PSCs.

4.2 Quantitative Assessment of TRPC Channel Expression in mPSCs

Quantitative Real-time PCR was used to identify which of the TRPC family members (TRPC1-7) were expressed at the highest level in mPSCs. This was done to determine, if the expression of the two candidate genes (*TRPC1* and *TRPC6*) were at a significant level. The level of expression was analysed in both WT, *TRPC1*^{-/-} and *TRPC6*^{-/-} mPSCs to determine if any compensatory differences were present. Both the hypoxanthin phosphoribosyltransferase 1 (*hprt*) and the β -2 microglobulin (β -2M) gene were used as

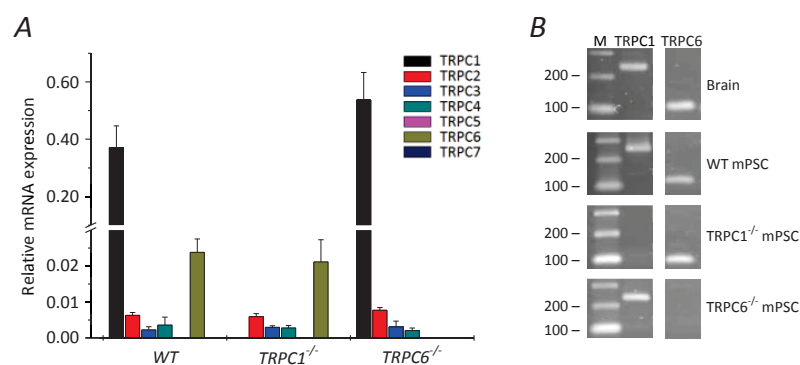


Figure 4.2. TRPC1-7 Expression in mPSCs. TRPC1 and TRPC6 channels are more abundantly expressed in mPSCs compared to other TRPC members. **(A)** qPCR detection of mRNA expression of TRPC1-7 in WT, *TRPC1*^{-/-} and *TRPC6*^{-/-} mPSCs relative to the internal control gene hypoxanthin phosphoribosyltransferase 1 (*hprt*). Data presented as means of triplicates \pm SEM, N = 3. **(B)** Representative gel showing primer specificity targeting TRPC1 and TRPC6 in mouse brain and WT, *TRPC1*^{-/-} and *TRPC6*^{-/-} mPSC. Band size depicted in base pairs.

endogenous controls and were unchanged for all samples tested. The data shown in [figure 4.2](#) uses *hprt* as the endogenous control. In mPSCs, TRPC1 and TRPC6 were the predominantly expressed members of the of TRPC channel family. Smaller levels of TRPC2, 3 and 4 expression were detected, but no expression of TRPC5 and TRPC7 was found. There was no compensatory increase in expression of other TRPC members in TRPC1^{-/-} and TRPC6^{-/-} mPSCs ([figure 4.2](#)). These findings, together with substantial data linking TRPC channels to regulation of migratory events (Nielsen et al., 2014) lead to the interpretation that TRPC1 and TRPC6 channels in mPSCs may be involved in regulating the migration of mPSCs. It was postulated that the loss of either of these two channels could give rise to cellular functional defects visualized through inhibited mPSC motility.

4.3 mPSC Migration in Three Dimensional Space

In order to mimic the tissue composition observed within the pancreas and in desmoplastic regions in PDAC, all migration experiments were performed with a desmoplastic matrix composed primarily of Collagen I (~90%) complemented with laminin, fibronectin, collagen III and IV (composition is given in [table 3.14 and 3.15](#)).

To confirm the physiological relevance of the loss of TRPC1 and TRPC6 channels, mPSCs were embedded in a desmoplastic matrix and loaded into a three dimensional migration chamber (modified from (Stock et al., 2005)). To visualize 3D migration focus was set on mPSCs surrounded by matrix and having a spindle-shaped cell morphology which is characteristic for such conditions ([figure 4.3, D](#)). Time lapse video recording of cell migration was monitored over a time period of approx. 7 h. TRPC6^{-/-} mPSCs showed a significant decrease of 14% in mean cell migration velocity (0.31 ± 0.01 to 0.26 ± 0.01 $\mu\text{m}/\text{min}$, $p = 0.00076$) and 30% in mean cell translocation (38.5 ± 3.9 to 26.9 ± 3.2 μm , $p = 0.041$) compared to corresponding WT values. In contrast, for TRPC1^{-/-} mPSCs no change in velocity was observed compared to WT, although a significant decrease of 29% in mean cell translocation was detected (38.5 ± 3.9 to 27.3 ± 2.8 μm , $p = 0.032$) ([figure 4.3 A-C](#)). The directionality of TRPC1^{-/-} mPSCs was therefore different from that of WT mPSCS (WT: 0.28 ± 0.03 , TRPC1^{-/-}: 0.21 ± 0.02 , $p = 0.03$). No differences in cell morphology and cell size were detected between the groups.

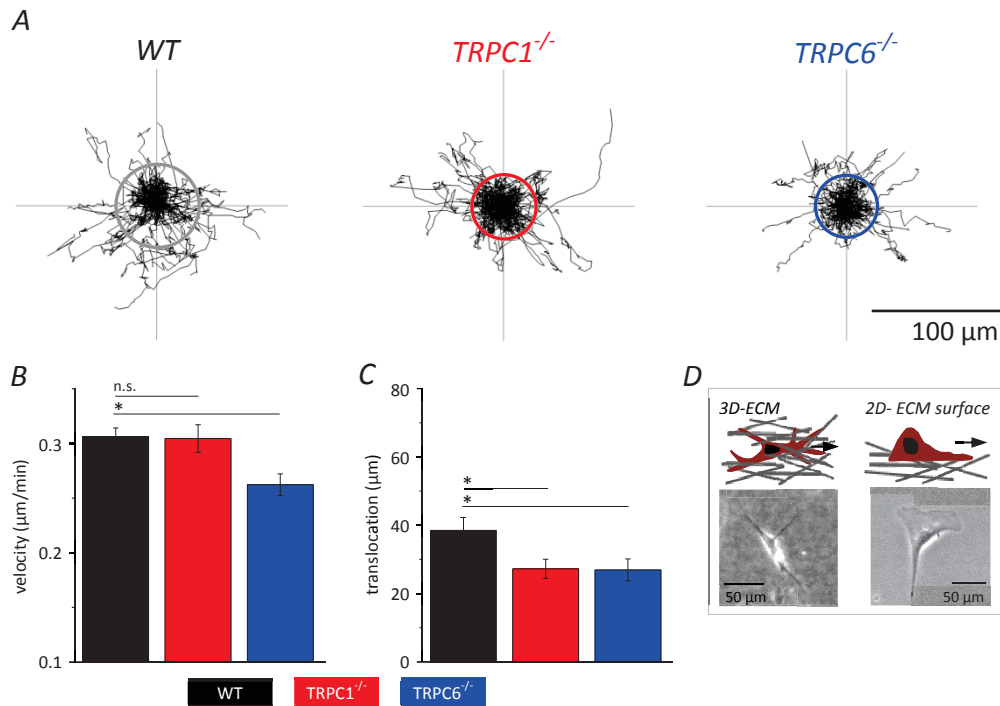


Figure 4.3. Three Dimensional Migration of mPSCs. mPSCs were embedded in a 3D migration chamber and cell migration was monitored with time-lapse video microscopy for 7 h. **(A)** Single cell trajectories were normalized to a common starting point and mean translocation determined from the radius of a circle. **(B)** Mean cell migration velocity was decreased in TRPC6^{-/-} mPSCs compared to WT, but not that of TRPC1^{-/-} mPSCs. **(C)** In contrast, both TRPC1^{-/-} and TRPC6^{-/-} mPSCs showed a decrease in mean translocation compared to that of WT mPSCs. **(D)** Representative phase contrast image of mPSC morphology in a 3D environment compared to that on a 2D surface. On a 2D surface one can clearly distinguish between cell front and trailing end. Values represent means \pm SEM. n.s. = $p > 0.05$, (*) = $p \leq 0.05$, Student t-test and Mann-Whitney U test. WT (N = 3, n = 52), TRPC1^{-/-} (N = 3, n = 59), TRPC6^{-/-} (N = 4, n=48).

4.3.1 Oxidative Cell Stress in Three Dimensional mPSC Migration

It was analysed whether additional factors have an impact on mPSC migration within the 3D migration setup. mPSC migration velocity and translocation were depicted over time and further divided into intervals of 2 h. As observed in [figure 4.4 D-E](#), WT mPSCs showed 55% higher migration velocity (0.23 ± 0.01 to 0.35 ± 0.01 $\mu\text{m}/\text{min}$, $p < 0.0005$) and translocation (13.6 ± 1.3 to 21.2 ± 2.1 μm , $p = 0.0027$) over the course of the experiment. This increase was absent in TRPC6^{-/-} mPSCs, with their final migration velocity and cell translocation being significantly lower than that of WT mPSCs (-35% in velocity ($p < 0.0005$) and -59% in cell translocation ($p = 0.0025$)). In TRPC1^{-/-} mPSCs, migration velocity increased by 27% (0.26 ± 0.01 to 0.33 ± 0.01 $\mu\text{m}/\text{min}$, $p < 0.0005$), but did not reach

the same level as that of WT mPSCs (-7%, $p = 0.042$). TRPC1^{-/-} cell translocation remained unchanged overtime, and was not significantly different from that of WT mPSCs.

The 3D migration chamber was assumed to be completely sealed from the outside, allowing for the point of “no” O₂ present within the chamber to be calculated (for calculation see [section 3.6.1](#) in materials and methods). In brief, this was estimated from oxygen consumption rate (OCR) (~180 pmol/min) and amount of O₂ present at the beginning of the experiment (~7.7*10⁻⁸ mol). In addition, parallel experiments determined

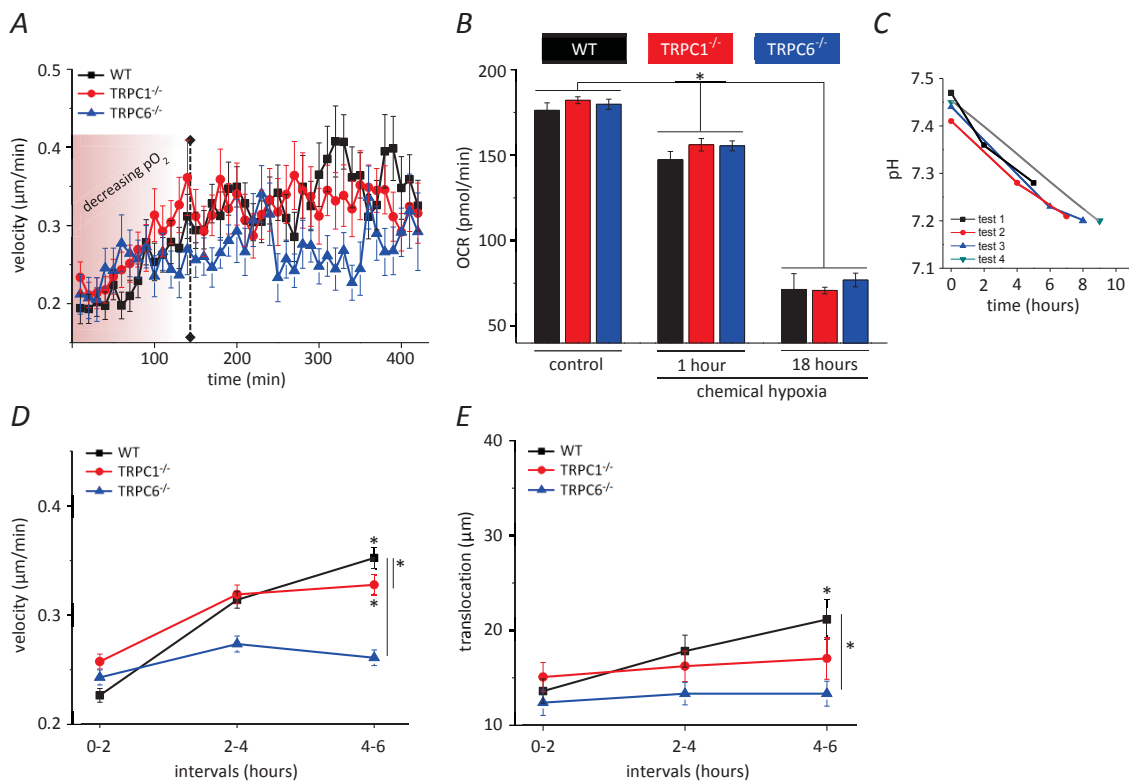


Figure 4.4. Decreasing pO₂ and pH Induce mPSC migration. WT mPSCs showed increased migration velocity and translocation to a higher level than both TRPC1^{-/-} and TRPC6^{-/-} mPSCs under decreasing pO₂ and pH. **(A)** Migration velocity over time for WT, TRPC1^{-/-} and TRPC6^{-/-} mPSCs under decreasing pO₂. The estimated time point at which all O₂ within the chamber is consumed is depicted with a line. For this calculation it was assumed that the chamber was sealed for O₂ from the environment. **(B)** Oxygen consumption rate (OCR) of WT, TRPC1^{-/-} and TRPC6^{-/-} mPSCs under normoxic conditions and after 1 and 18 h of chemically induced hypoxia with DMOG [0.50 mM], respectively. **(C)** Measurements of pH within the 3D cell-matrix mixture. **(D)** Migration velocity and **(E)** translocation over time in 2 h intervals. WT mPSCs showed an increase in migration velocity and translocation over the course of the experiment. This effect was completely absent in TRPC6^{-/-} mPSCs, whereas TRPC1^{-/-} mPSCs showed an increase in migration velocity, but not in translocation. Values represent means ± SEM. n.s. = $p > 0.05$, (*) = $p \leq 0.05$, Student t-test and Mann-Whitney U test. WT (N = 3, n = 52), TRPC1^{-/-} (N = 3, n = 59), TRPC6^{-/-} (N = 4, n = 48).

a concomitant drop in pH within the cell-matrix mixture (*figure 4.4, C*). Taken together, these data show that mPSCs demonstrate an increasing migratory activity under decreasing pO₂ and acidosis, with TRPC6^{-/-} mPSCs being unable to respond to these environmental cues.

4.4 Hypoxia and mPSC Migration

Hypoxia and oxidative stress are major stimulants of PSC activity, intensifying the mutual signalling between PSCs and PDAC cells, and consequently facilitating PDAC progression (*section 1.3.3*) (Eguchi et al., 2013; Erkan et al., 2009; Ide et al., 2006; Masamune et al., 2008a). Of note, the function of TRPC1 and TRPC6 channels is involved in the response of various cell types to hypoxia, giving rise to increased migratory activity (*section 1.5.2*). Therefore, as pointed out in the hypothesis (*section 2.1*), these two channels represent good candidates for mediating such cellular responses in PSCs.

Due to uncontrollable external parameters (including pO₂ and pH) in the 3D migration model, a simplified 2D model was introduced. This allowed more controlled investigation of the role of hypoxia as a major stimulating factor in mPSC migration.

4.4.1 Chemically Induced Hypoxia Stimulates mPSC Migration

4.4.1.1 DMOG Induces mPSC Migration in a Dose-Responsive Manner

DMOG acts to inhibit prolyl hydroxylases, preventing the degradation of HIF subunits to activate the HIF system and enhance transcription of target genes (Elvidge et al., 2006; Lum et al., 2007). In this way, it induces cell responses in high concordance to “real” hypoxic conditions (1% O₂, 5% CO₂ and 94% N₂). DMOG has not been tested on isolated primary mPSCs before and a dose response curve was therefore established with concentrations of DMOG ranging from 0.25 – 1.50 mM. The stimulating effect of DMOG was assessed by its ability to increase 2D mPSC migration on a desmoplastic matrix. Preliminary data (N = 1, n = 18, *data not shown*) showed that applying DMOG acutely stimulated mPSC migration approx. after 12 h incubation. To investigate the chronic effect of DMOG-induced hypoxia on mPSC migration, 20 h of incubation time was selected. It is worth noting, that after 20 h of treatment in normal culture medium (+DMOG), the medium was changed to serum free HEPES buffered RPMI media (+DMOG)

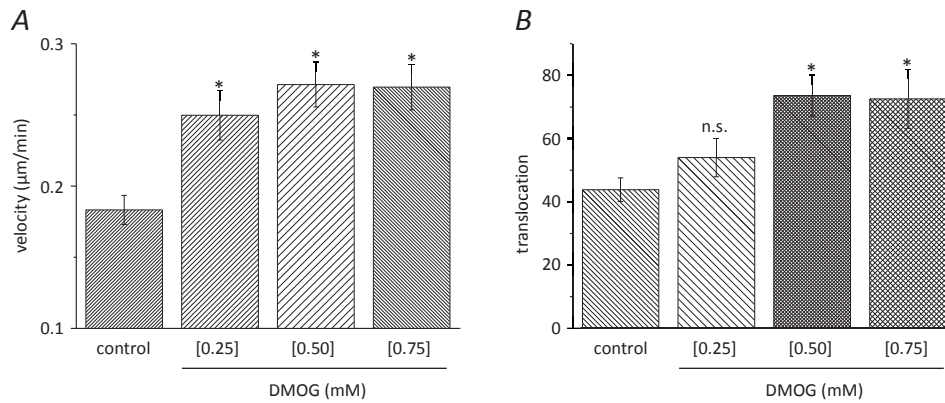


Figure 4.5. DMOG Induces Migration of mPSCs in a Dose-Responsive Manner. mPSCs were pre-activated with DMOG for 20 h before cell migration was monitored with time-lapse video microscopy for 8 h. DMOG increased mPSC migration velocity (**A**) and translocation (**B**) in a dose-responsive manner. The optimal level of activation was reached with 0.50 mM DMOG. Values represent means \pm SEM. n.s. = $p > 0.05$, (*) = $p \leq 0.05$, Student t-test. Control (N = 5, n = 49), [0.25 mM DMOG] (N = 3, n = 28), [0.50 mM DMOG] (N = 4, n = 46), [0.75 mM DMOG] (N = 3, n = 28).

prior to the start of the experiment, as this was the condition used in the 3D model. The first 8 h of the time lapse video microscopy were analyzed with DMOG at concentrations from 0.25 – 0.75 mM. Higher concentrations induced cell death (1.0 and 1.5 mM DMOG) (*data not shown*). [Figure 4.5](#) illustrates increased mPSC migration velocity and translocation at increasing concentrations of DMOG.

The optimal level of mPSC migration activation was reached with a concentration of 0.50 mM DMOG. mPSCs covered a mean distance of 73.6 ± 6.5 μm at a velocity of 0.27 ± 0.02 $\mu\text{m}/\text{min}$. Under control conditions, mPSCs only covered a mean translocation of 43.8 ± 3.7 μm with a velocity of 0.18 ± 0.02 $\mu\text{m}/\text{min}$. The increase in velocity and translocation was statistically significant ($p < 0.05$). All future experiments were conducted with 0.50 mM DMOG to investigate the hypoxic stimulation of mPSC migration.

4.4.1.2 Chronic Treatment with DMOG Induces an Anaerobic mPSC Phenotype

To verify that 0.50 mM DMOG induce an anaerobic phenotype with hypoxia characteristics, metabolic index was estimated for mPSCs treated under normoxic conditions and DMOG-induced hypoxia for 18-20 h. This was calculated by determining OCR and extracellular acidification rate (ECAR, pH related) of mPSCs. WT, TRPC1^{-/-} and TRPC6^{-/-} mPSCs showed significantly decreased OCR ($p < 0.0005$) and increased ECAR ($p < 0.005$) indicating a shift in the prevalence of glycolysis over oxygen, which is also known as the Warburg effect (Asgari et al., 2015; Upadhyay et al.,

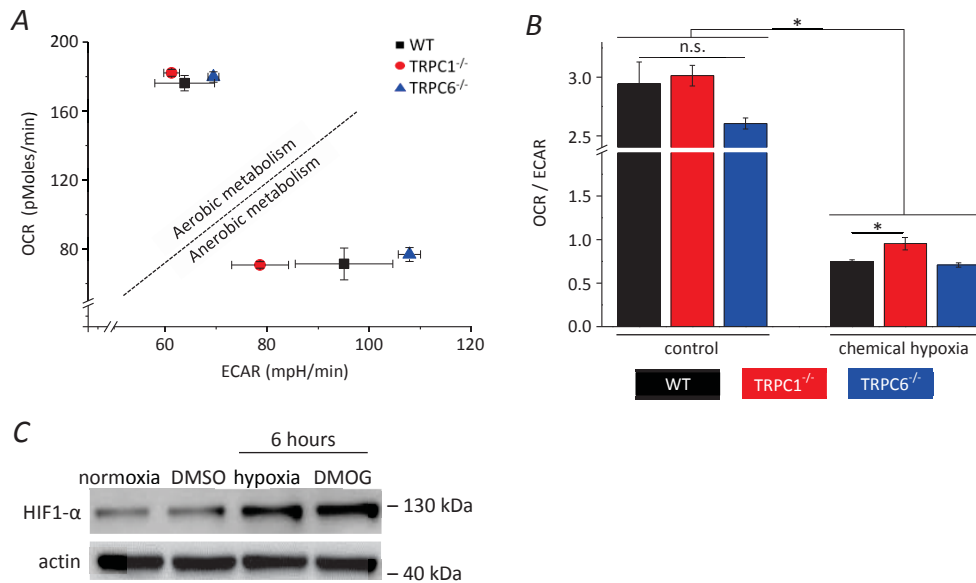


Figure 4.6. DMOG Induces an Anaerobic mPSC Phenotype Characteristic to Hypoxia. (A) mPSCs were pre-incubated for 1 or 18 hour(s) with DMOG to induce chemical hypoxia. OCR and ECAR show a well-known Warburg shift in the prevalence of glycolysis above oxygen ($p < 0.0005$). **(B)** An estimated metabolic index was calculated and represents a more anaerobic than aerobic metabolic phenotype ($p < 0.0005$). A difference in the metabolic index was found between WT and TRPC1^{-/-} mPSCs ($p = 0.011$). **(C)** Representative Western blot showing elevated HIF-1 α protein expression in mPSCs after 6 h of chemically induced hypoxia and hypoxia (1% pO₂) compared to controls. Values represent means \pm SEM. n.s. = $p > 0.05$, (*) = $p \leq 0.05$, Student t-test. All experiments were performed three times.

2013). The same effect was observed in the estimated metabolic index (OCR/ECAR) going from “high” to “low”, reflecting a more anaerobic than aerobic metabolic phenotype, when treated with DMOG (shown in [figure 4.6](#)). Surprisingly, a difference was detected between WT and TRPC1^{-/-} mPSCs ($p < 0.05$) indicative of a more anaerobic phenotype in WT than in TRPC1^{-/-} mPSCs following DMOG treatment ([figure 4.6, B](#)). Furthermore, DMOG caused acute effects after 1 hour of treatment, lowering the OCR significantly in all mPSC groups ($p < 0.05$) ([figure 4.4, B](#)) in addition to the ECAR and the metabolic index (*data not shown*). The increase in HIF-1 α protein expression served as further verification of hypoxic stress in mPSCs. As depicted in [figure 4.6 C](#), the expression of HIF-1 α increased in WT mPSCs after 6 h in both chemically induced hypoxia and in hypoxia treated (1% O₂, 5% CO₂ and 94% N₂) mPSCs compared to controls. Overall, these data suggest that DMOG induces practically the same metabolic response in mPSCs as hypoxia.

4.4.2 mPSCs Morphology Upon Hypoxia Stimulation

TRPC1^{-/-} mPSCs appear larger in cell size than WT mPSCs. Chemical induction of hypoxia caused a morphological change in WT mPSCs to a smaller cell type (*figure 4.7*). Projected cell area of WT mPSCs is reduced by 15% upon chemically induced hypoxia (5074±219 to 4301±225 μm^2 , $p = 0.016$). TRPC1^{-/-} mPSCs have a projected cell area of approx. 6000 μm^2 , which is significantly larger than that of WT mPSCs (+20% under control conditions ($p = 0.015$)). In contrast to WT mPSCs, projected cell area hardly decreased during hypoxia, such that the area of TRPC1^{-/-} mPSCs was 37% larger than that of WT mPSCs under hypoxic conditions ($p < 0.0005$). In comparison, TRPC6^{-/-} mPSCs have the same projected cell area as WT mPSCs (approx. 5100 μm^2). However, they do not change their projected area upon chemically induced hypoxia as observed for WT mPSCs ($p = 0.03$). These data were partly inconsistent with those observed under hypoxia conditions (*figure 4.7, B*). WT mPSCs had a tendency to have a smaller projected cell area under hypoxic conditions ($p = 0.08$), which was significantly smaller than that of TRPC1^{-/-} mPSCs ($p = 0.041$), but not than that of TRPC6^{-/-} mPSCs. No tendency or significant change

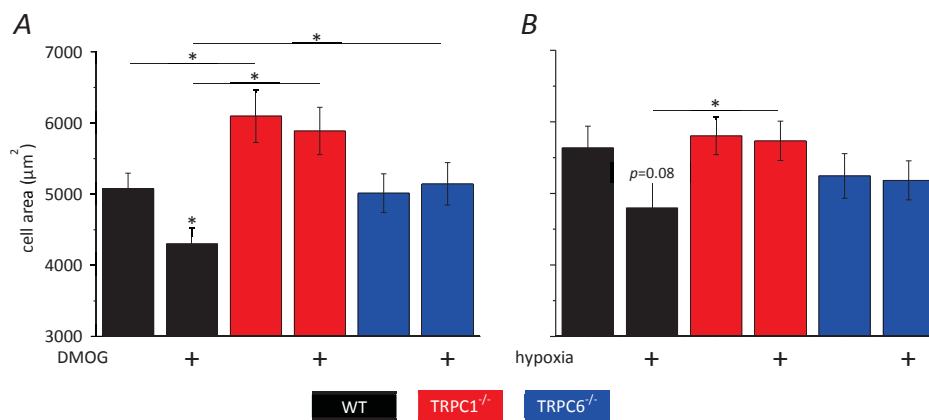


Figure 4.7. mPSCs Cell Size upon Hypoxic Stimulation. mPSCs were challenged with chemically induced hypoxia **(A)** or with hypoxic conditions **(B)** for 20 h before cell migration was monitored with time-lapse video microscopy for 8 h. The mean projected cell area was analyzed. WT mPSCs tend to display a smaller projected cell area upon hypoxic stimuli than TRPC1^{-/-} and TRPC6^{-/-} mPSCs. TRPC1^{-/-} mPSCs appear to have a larger projected cell area compared to WT mPSCs, although this is not consistent in both experiment. Values represent means \pm SEM. n.s. = $p > 0.05$, (*) = $p \leq 0.05$, Student t-test. WT (control: N = 5, n = 49 and DMOG: N = 4, n = 46), TRPC1^{-/-} (control: N = 3, n = 41 and DMOG: N = 4, n = 50) and TRPC6^{-/-} (control: N = 3, n = 35 and DMOG: N = 4, n = 53). WT (normoxia: N = 4, n = 51 and hypoxia: N = 4, n = 56), TRPC1^{-/-} (normoxia: N = 4, n = 49 and hypoxia: N = 4, n = 53) and TRPC6^{-/-} (normoxia: N = 4, n = 51 and hypoxia: N = 3, n = 53).

of projected cell area under hypoxia was observed for TRPC1^{-/-} and TRPC6^{-/-} mPSCs. This suggests that hypoxia induces morphological changes in mPSCs with TRPC1^{-/-} and TRPC6^{-/-} mPSCs responding differently, possibly with a different migratory behaviour as well.

4.4.3 TRPC1^{-/-} and TRPC6^{-/-} mPSCs Display Diminished Motility Under Chemically Induced Hypoxia

It was therefore next tested whether chemically induced hypoxia caused the same stimulatory effect of TRPC1^{-/-} and TRPC6^{-/-} mPSCs migration as observed for WT. mPSCs were incubated with DMOG for 20 h and cell migration was monitored with time-lapse video microscopy for 8 h. *Figure 4.8* depicts cell trajectories normalized to the same starting point from all mPSC groups. These data clearly show a significant increase by 48% in the migration velocity ($0.18 \pm 0.01 \mu\text{m}/\text{min}$ to $0.27 \pm 0.02 \mu\text{m}/\text{min}$, $p < 0.0005$) and 68% in translocation ($43.8 \pm 3.7 \mu\text{m}$ to $73.6 \pm 6.5 \mu\text{m}$, $p < 0.0005$) of WT mPSC under chemically induced hypoxia. TRPC1^{-/-} mPSCs also showed increased migration velocity, +25% ($0.16 \pm 0.01 \mu\text{m}/\text{min}$ to $0.20 \pm 0.01 \mu\text{m}/\text{min}$, $p = 0.009$) and translocation, +50% ($36.3 \pm 3.43 \mu\text{m}$ to $54.12 \pm 4.34 \mu\text{m}$, $p = 0.01$), but not to the same level as observed for WT mPSCs. In contrast, the stimulatory effect of chemically induced hypoxia was absent in TRPC6^{-/-} mPSCs. Their migration velocity ($0.16 \pm 0.01 \mu\text{m}/\text{min}$ to $0.19 \pm 0.08 \mu\text{m}/\text{min}$, n.s.) and translocation ($36.2 \pm 5.1 \mu\text{m}$ to $50.1 \pm 4.7 \mu\text{m}$, n.s.) did not increase. This suggests a dominance of TRPC6 over TRPC1 channels in the PSC response to hypoxia.

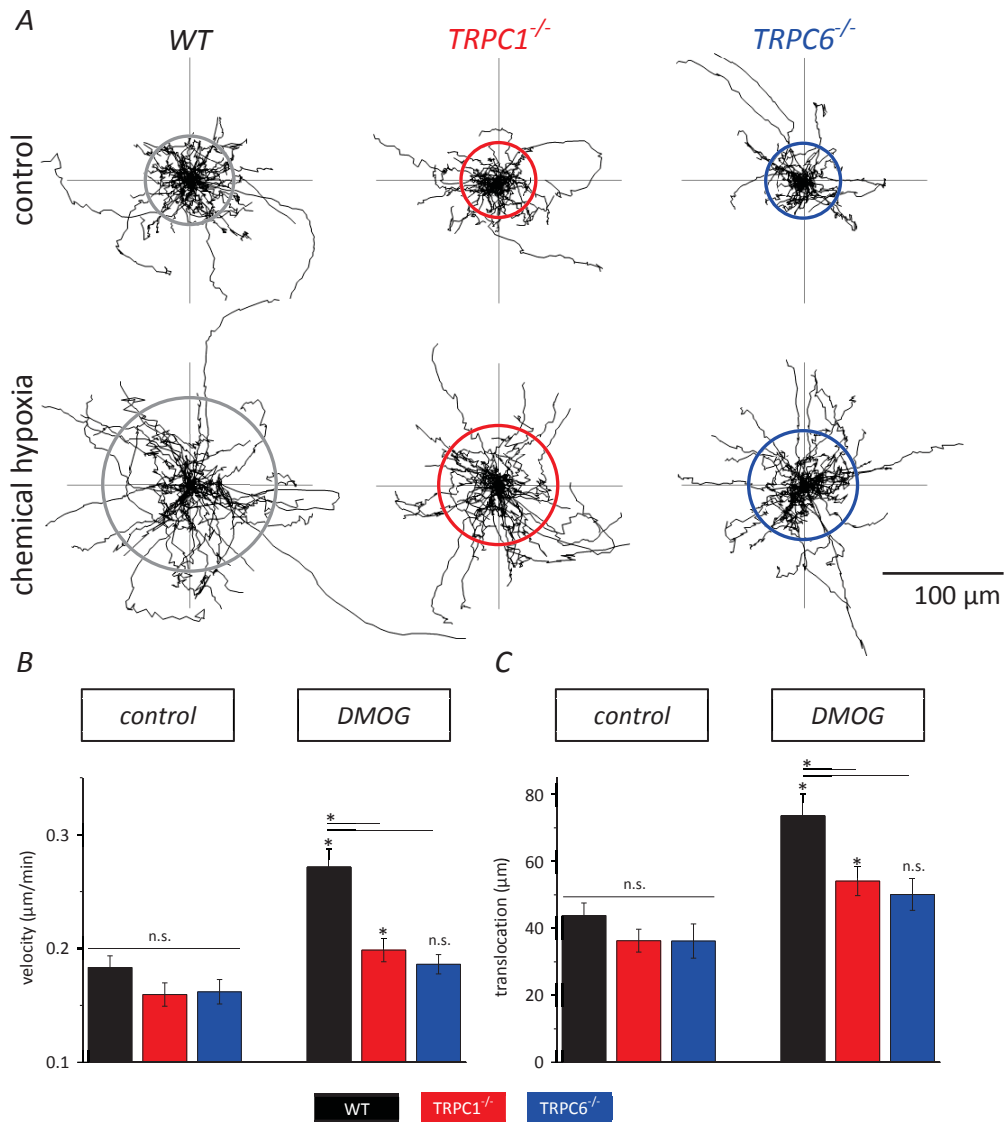


Figure 4.8. mPSCs Migration Under Chemically Induced Hypoxia. (A) Single cell trajectories were normalized to a common starting point and mean translocation determined from the radius of a circle. DMOG increased mPSC migration velocity (B) and translocation (C) of both WT and TRPC1^{-/-} but not that of TRPC6^{-/-} mPSCs. The increase in migration velocity and translocation of TRPC1^{-/-} mPSCs did not reach the level observed for WT. Values represent means \pm SEM. n.s. = $p > 0.05$, (*) = $p \leq 0.05$, Student t-test and Mann-Whitney U test. WT (control: N = 5, n = 49 and DMOG: N = 4, n = 46), TRPC1^{-/-} (control: N = 3, n = 41 and DMOG: N = 4, n = 50) and TRPC6^{-/-} (control: N = 3, n = 35 and DMOG: N = 4, n = 53).

4.4.4 Attenuated Autocrine Stimulation of TRPC1^{-/-} and TRPC6^{-/-} mPSCs Under Chemically Induced Hypoxia

Cell migration velocity and translocation were further plotted as a function of time and depicted in 2 h intervals (*figure 4.9*). This revealed an increasing migratory activity during the course of the experiment for the WT, but not for TRPC1^{-/-} and TRPC6^{-/-} mPSCs. Migration activity of WT mPSCs under chemically induced hypoxia increased to a final migration velocity of 0.30 ± 0.02 $\mu\text{m}/\text{min}$ and translocation of 26.5 ± 2.5 μm . Neither TRPC1^{-/-} (velocity: 0.20 ± 0.01 $\mu\text{m}/\text{min}$, translocation: 18.7 ± 1.7 μm) nor TRPC6^{-/-} mPSCs (velocity: 0.19 ± 0.01 $\mu\text{m}/\text{min}$, translocation: 16.3 ± 1.7 μm) showed this dynamic behaviour (*figure 4.9*). Significance between the last intervals for the three groups is indicated. Note that the media were changed before cell migration recording, suggesting that WT mPSC

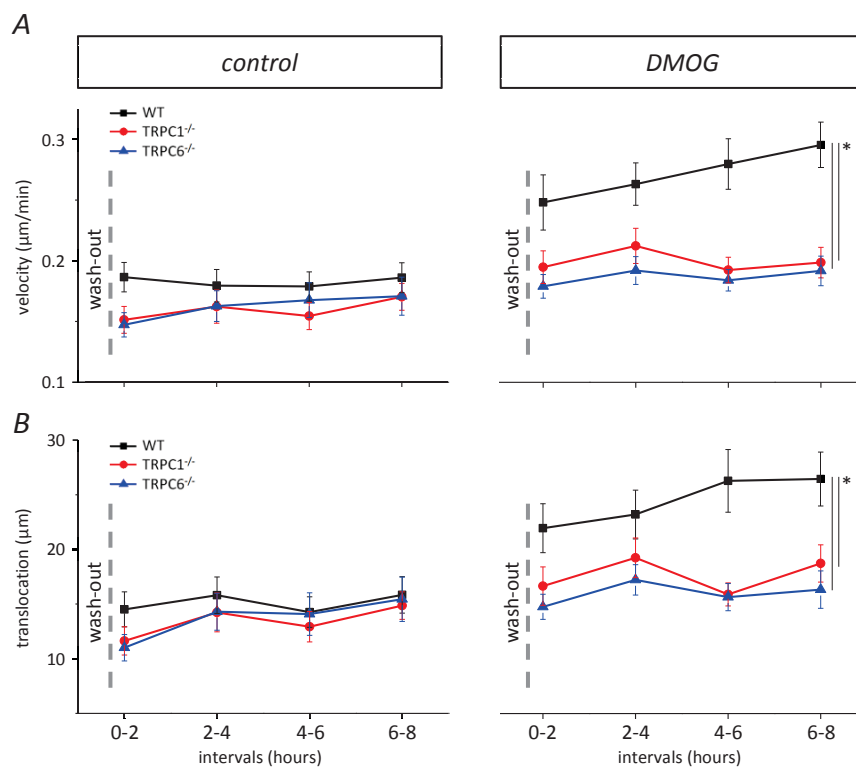


Figure 4.9. Indication of Autocrine Stimulation of mPSCs Under Chemically Induced Hypoxia.

Following media change (wash-out) WT mPSCs increased their migration velocity (**A**) and translocation (**B**) over time (2 h intervals) under chemically induced hypoxia. This was not observed in TRPC1^{-/-} and TRPC6^{-/-} mPSCs. Moreover, the final migration velocity and translocation were significantly higher in WT compared to TRPC1^{-/-} and TRPC6^{-/-} mPSCs. Values represent means \pm SEM. (*) = $p \leq 0.05$, Student t-test and Mann-Whitney U test. WT (control: N = 5, n = 49 and DMOG: N = 4, n = 46), TRPC1^{-/-} (control: N = 3, n = 41 and DMOG: N = 4, n = 50) and TRPC6^{-/-} (control: N = 3, n = 35 and DMOG: N = 4, n = 53).

under chemical hypoxia secrete certain factors that likely lead to autocrine stimulation. The response to this stimulation or the degree of stimulation may be affected by the loss of TRPC1 and/or TRPC6.

4.4.5 TRPC1^{-/-} and TRPC6^{-/-} mPSCs Display Diminished Motility Under Hypoxia Stimulation

DMOG is a chemical compound primarily inducing hypoxia effects by preventing the degradation of HIF subunits, thereby activating the HIF system. Other pathways regulated by hypoxia can be independent of the HIF pathway and hypoxia often also leads to cellular stress, induction of ROS etc. (Elvidge et al., 2006; Lum et al., 2007). It was therefore tested whether the observed stimulatory effect with chemically induced hypoxia is in concordance to “real” hypoxia ($pO_2 < 1\%$). mPSCs were incubated for 22-24 h under hypoxic conditions (1% O_2 , 5% CO_2 and 94% N_2) before cell migration was monitored for 8 h with time-lapse video microscopy.

In agreement with chemically induced hypoxia, incubation for 22-24 h under hypoxic conditions significantly increased WT mPSC migration velocity by 30% ($0.23 \pm 0.01 \mu\text{m}/\text{min}$ to $0.30 \pm 0.02 \mu\text{m}/\text{min}$, $p < 0.0005$) and translocation by 51% ($43.1 \pm 3.1 \mu\text{m}$ to $65.3 \pm 6.8 \mu\text{m}$, $p = 0.02$). TRPC1^{-/-} mPSCs slightly increased their migration velocity by 16% from $0.21 \pm 0.01 \mu\text{m}/\text{min}$ to $0.24 \pm 0.01 \mu\text{m}/\text{min}$ ($p = 0.04$), which was significantly lower than that of WT (-21%, $p = 0.002$). However, the translocation ($44.9 \pm 5.0 \mu\text{m}$ to $50.9 \pm 4.5 \mu\text{m}$, n.s.) was not statistically different from that of WT (-22%, $p = 0.2$, n.s.). Again the stimulating effect of hypoxia was absent in TRPC6^{-/-} mPSCs showing migration velocity and translocation values of $0.21 \pm 0.01 \mu\text{m}/\text{min}$ to $0.20 \pm 0.01 \mu\text{m}/\text{min}$ (n.s.) and $49.1 \pm 3.8 \mu\text{m}$ to $44.1 \pm 3.8 \mu\text{m}$ (n.s.), respectively (figure 4.10). This was in concordance with the observation detected under chemically induced hypoxia showing a more prominent effect on TRPC6^{-/-} than TRPC1^{-/-} mPSCs compared to corresponding WT values.

As before, cell migration velocity and translocation were plotted in 2 h intervals (figure 4.11). Of note, no media change (wash-out) was conducted as in the experiment with chemically induced hypoxia. Migration activity of WT mPSCs under hypoxia stimulation increased to a final migration velocity of $0.30 \pm 0.02 \mu\text{m}/\text{min}$ and translocation of $24.4 \pm 2.3 \mu\text{m}$ versus that of TRPC1^{-/-} (velocity: $0.26 \pm 0.02 \mu\text{m}/\text{min}$, translocation: $20.4 \pm 1.9 \mu\text{m}$) and TRPC6^{-/-} mPSCs (velocity: $0.19 \pm 0.01 \mu\text{m}/\text{min}$, translocation: 15.0 ± 1.4

μm) (figure 4.11). Significance between the last intervals for the three groups is indicated. Only TRPC6^{-/-} mPSCs showed statistically lower levels of activation at the final interval when compared to WT values. The velocity and translocation values for WT mPSCs under chemically induced hypoxia (from figure 4.9) are illustrated in grey. This demonstrates that the migratory activity, under chemically induced hypoxia, is increased to the same

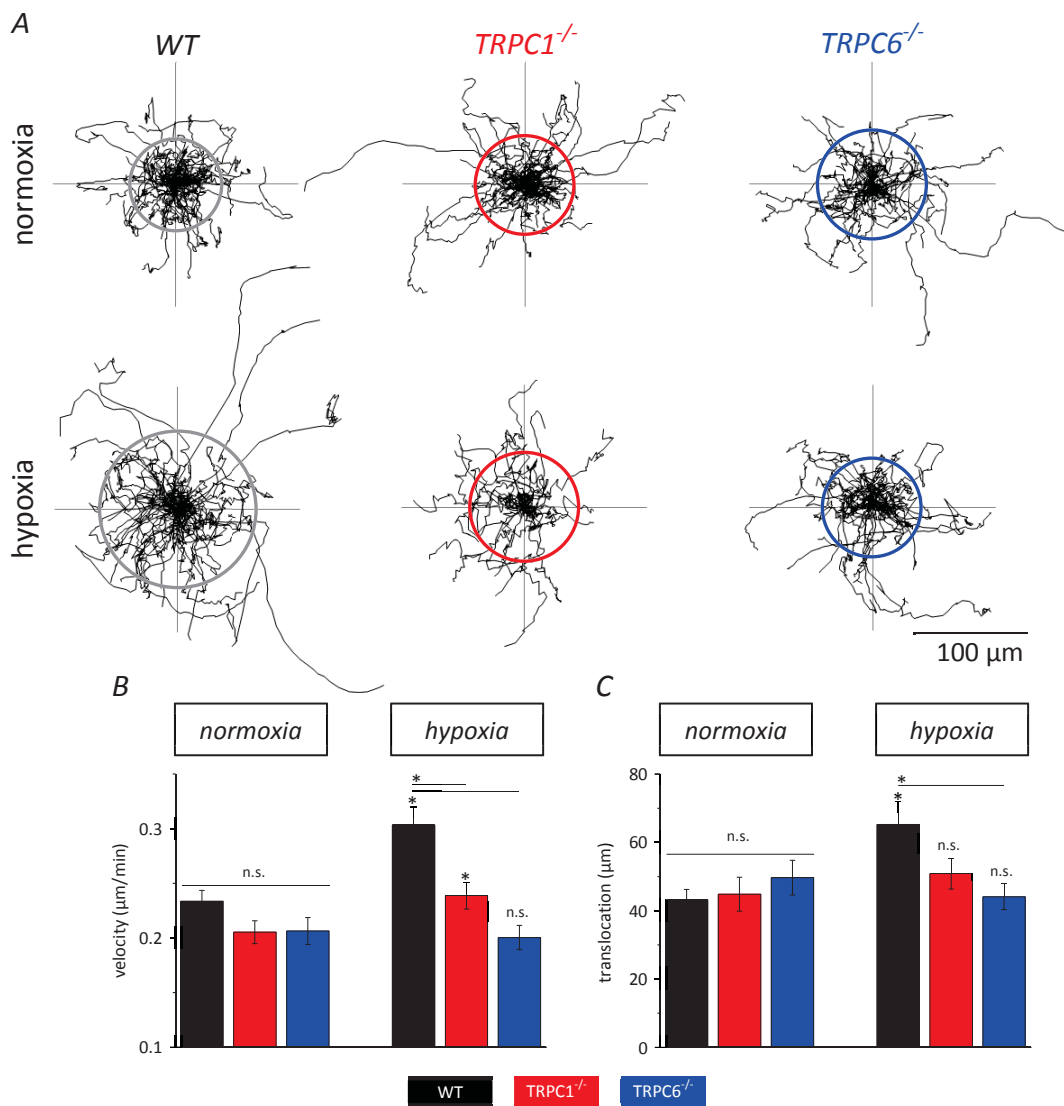


Figure 4.10. mPSCs Migration Under Hypoxia Stimulation. (A) Single cell trajectories were normalized to a common starting point. Mean translocation determined from the radius of a circle. (B) Mean cell migration velocity. (C) Mean cell translocation. Hypoxia increased WT mPSC migration velocity and translocation. Only translocation of TRPC1^{-/-} mPSCs was increased, but not to the same level as WT. Hypoxia stimulation was absent in TRPC6^{-/-} mPSCs. Values represent means \pm SEM. n.s. = $p > 0.05$, (*) = $p \leq 0.05$, Student t-test and Mann-Whitney U test. WT (normoxia: N = 4, n = 51 and hypoxia: N = 4, n = 56), TRPC1^{-/-} (normoxia: N = 4, n = 49 and hypoxia: N = 4, n = 53) and TRPC6^{-/-} (normoxia: N = 4, n = 51 and hypoxia: N = 3, n = 53).

level as observed for hypoxia via a possible autocrine stimulation mechanism (figure 4.11). Taken together, these data demonstrate that the TRPC1 and TRPC6 channel are important for mPSCs response to hypoxia stimulation by affecting cell motility. Thus the defect of TRPC6^{-/-} mPSCs is more pronounced than that of TRPC1^{-/-} mPSCs.

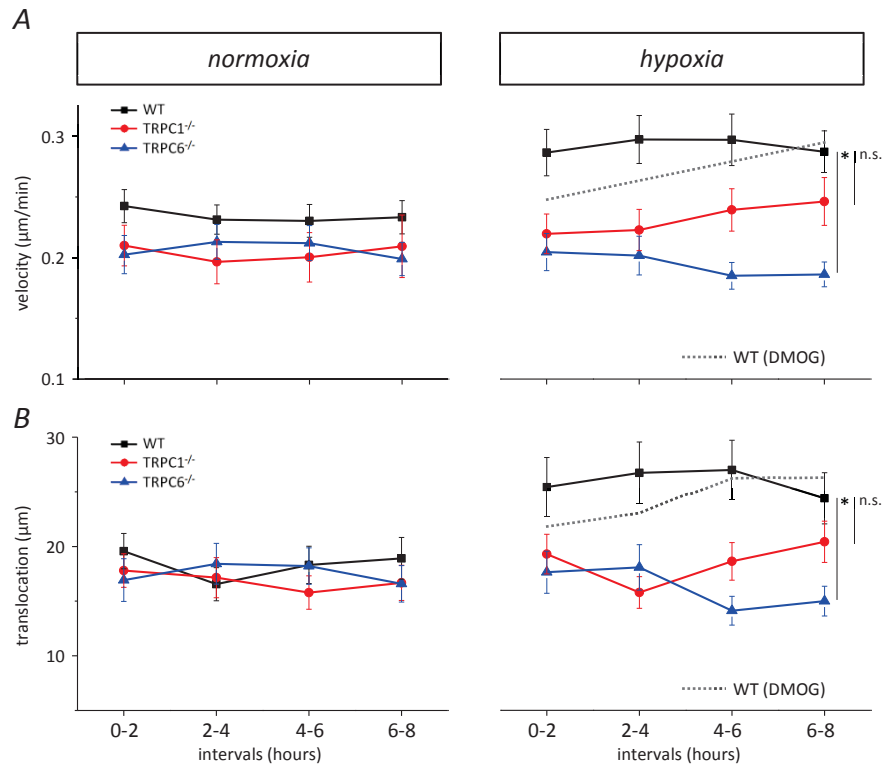
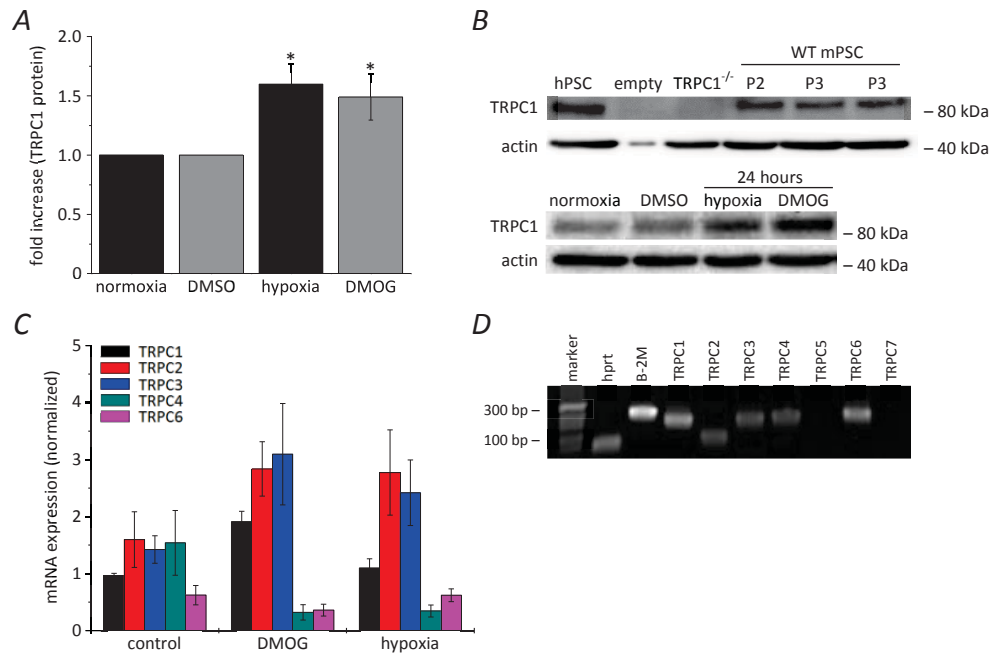


Figure 4.11. Chronic Hypoxia Stimulates the Migratory Activity of mPSCs. Following 22-24 h of hypoxia incubation WT mPSCs have reached a steady level of migratory activity. This could be observed by displaying cell migration velocity (A) and cell translocation (B) over time in 2 h intervals. The final migration velocity and translocation were significantly higher in WT compared to TRPC6^{-/-} mPSCs, but not that of TRPC1^{-/-} mPSCs. Values represent means \pm SEM. (*) = $p \leq 0.05$, Student t-test and Mann-Whitney U test. WT (normoxia: N = 4, n = 51 and hypoxia: N = 4, n = 56), TRPC1^{-/-} (normoxia: N = 4, n = 49 and hypoxia: N = 4, n = 53) and TRPC6^{-/-} (normoxia: N = 4, n = 51 and hypoxia: N = 3, n = 53).

4.5 TRPC Channel Expression in mPSCs under Hypoxia

TRPC1 and TRPC6 channel expression have previously been described to be elevated in various cell types in response to hypoxia and oxidative stress which demonstrated their role in regulatory mechanisms in *sensing* and/or responding to such changes (reviewed in (Dietrich et al., 2014; Dietrich and Gudermann, 2014; Faouzi and Penner, 2014; Nesin and Tsiokas, 2014)). It was therefore tested whether the lower migratory activity of TRPC1^{-/-} and TRPC6^{-/-} mPSCs under hypoxia stimulation correlated with the two channels being differently expressed. This would give further information about TRPC1 and TRPC6 being involved in downstream *sensing* mechanism to hypoxia in accordance to the postulated hypothesis ① ([section 2.1](#)).

WT mPSCs were incubated under hypoxic conditions (1% O₂, 5% CO₂ and 94% N₂), or chemically induced hypoxia (DMOG [0.50 mM]) for 24 h before protein lysates were harvested or RNA isolated and reverse transcribed. A 1.5 fold increase in TRPC1 protein expression could be confirmed by WB analysis. Specificity of antibody was proven by the use of protein lysates from TRPC1^{-/-} mPSCs and human PSCs ([figure 4.12 A-B](#)). mRNA quantification of all seven TRPC channel members (TRPC1-7) was performed. The level of mRNA expression from each TRPC channel member was normalized to that under control conditions. No expression of TRPC5 and TRPC7 could be detected. A tendency to hypoxia-induced up-regulation of TRPC1, TRPC2 and TRPC3 could be noticed together with a down-regulation of TRPC4 ([figure 4.12 C-D](#)). This points toward TRPC1-4, but not TRPC6 being part of a possible downstream *sensing* mechanism to hypoxia through regulated expression levels. This further suggests that the TRPC6 channel is implicated in a possible *modifier* mechanism or elicits important *transduction/effector* functions in mPSCs upon hypoxic stimulation in accordance to the postulated hypothesis ② and ③ ([section 2.1](#)).



		TRPC1		TRPC2		TRPC3		TRPC4		TRPC6	
		DMOG	hypoxia	DMOG	hypoxia	DMOG	hypoxia	DMOG	hypoxia	DMOG	hypoxia
<i>hprt</i>	fold change	1.98	1.14	1.78	1.74	2.18	1.70	0.21	0.22	0.58	1.00
	<i>p</i> value	0.0001(*)	0.44	0.04(*)	0.35	0.40	0.76	0.17	0.05(*)	0.49	0.51
β -2M	fold change	2.02	1.36	4.45	1.95	2.07	2.59	0.22	0.23	0.87	2.20
	<i>p</i> value	0.04(*)	0.29	0.005(*)	0.12	0.07	0.06	0.02(*)	0.02(*)	0.68	0.11

Figure 4.12. TRPC Channel Expression in mPSCs Under Hypoxia. (A) The protein expression of TRPC1 (~90 kDa) was increased 1.5 fold upon 24 h of hypoxic stimulation in mPSCs. Protein expression was normalized to the level of controls. Values represent means \pm SEM ($N \geq 3$). (B) Representative Western blot of TRPC1 protein expression and antibody specificity tested in human RLT-PSC cell line, TRPC1^{-/-} mPSCs, and WT mPSCs of passage 2 and 3. (C) qPCR detection of TRPC1-7 mRNA expression in WT mPSCs relative to the internal control gene *hprt*. Data presented as means of triplicates \pm SEM ($N = 3$), normalized to the expression level under control conditions. The relative fold change in relation to both internal control genes is depicted in the table underneath. (D) Representative gel of qPCR showing detectable bands of TRPC1-4 and TRPC6 but not of TRPC5 and TRPC7. (*) = $p \leq 0.05$, Student t-test.

4.6 Assessment of Autocrine Stimulation of mPSCs under Hypoxia

In relation to the lacking autocrine stimulation detected in [figure 4.9](#) and to the hypothesized *modifier* mechanism of TRPC1 and TRPC6 channels of the microenvironment ② ([section 2.1](#)), their role in the regulation of important hypoxia-mediated autocrine stimulants was tested. The stimulatory effect of hypoxia conditioned medium (18 h and no FCS added) from WT, TRPC1^{-/-} and TRPC6^{-/-} mPSCs on WT mPSC migration was investigated ([figure 4.13 F](#)). Normoxically equilibrated culture medium served as control (no FCS and no cell contact). Cell migration was monitored with time-lapse video microscopy for 4 h. As shown in [figure 4.13 A and B](#), WT and TRPC1^{-/-} mPSCs secrete autocrine stimulants upon hypoxia stimulation. The conditioned medium from both increased migration velocity by 34% and 33% (WT: 0.18±0.01 μm/min, $p = 0.0003$, TRPC1^{-/-}: 0.18±0.01 μm/min, $p = 0.0001$) as well as translocation by 40% and 32% (WT: 23.7±2.0, $p = 0.02$, TRPC1^{-/-}: 22.4±2.0 μm, $p = 0.05$), respectively. In contrast, the migration of WT mPSCs was significantly attenuated using conditioned medium from hypoxia treated TRPC6^{-/-} mPSCs. Migration velocity slightly increased by 7% (0.14±0.01 μm/min, n.s.) and translocation decreased by 6% (15.8±2.3, n.s.). Tendency to lower projected cell area was observed using conditioned medium from WT and TRPC1^{-/-} mPSCs, but not from TRPC6^{-/-} mPSCs ([figure 1.13, C](#)). The cell structure index (SI) was lowered ($p < 0.05$) with hypoxic conditioned medium from both WT, TRPC1^{-/-} and TRPC6^{-/-} mPSCs compared to the control value ([figure 1.13, D](#)). More, directional cell migration of WT mPSCs was lowered with conditioned medium from TRPC6^{-/-} mPSCs ([figure 1.13, E](#)). This suggests, that WT mPSCs respond to some secreted stimulants from TRPC6^{-/-} mPSCs by adapting a more elongated cell shape and/or having more cell protrusions, but the major stimulants for inducing mPSC migration together with a smaller projected cell area is lacking. From this the following can be concluded: (i) mPSCs secrete autocrine factors under hypoxia which stimulate mPSC migration, (ii) the TRPC1 channel is not implicated in the secretion of autocrine stimulants and (iii) the TRPC6 channel is implicated in the production and/or secretion of autocrine factors under hypoxia, thereby eliciting a *modifying* mechanism with respect to the microenvironment and PSC activation. Possibly, this is due to TRPC6^{-/-} mPSCs having a lower status of activation under hypoxia because of

attenuated growth factor/cytokine signaling via a TRPC6-mediated *transduction/effector* pathway. This can lead to lower levels of secreted autocrine stimulants important for further stimulation in a loop sequence.

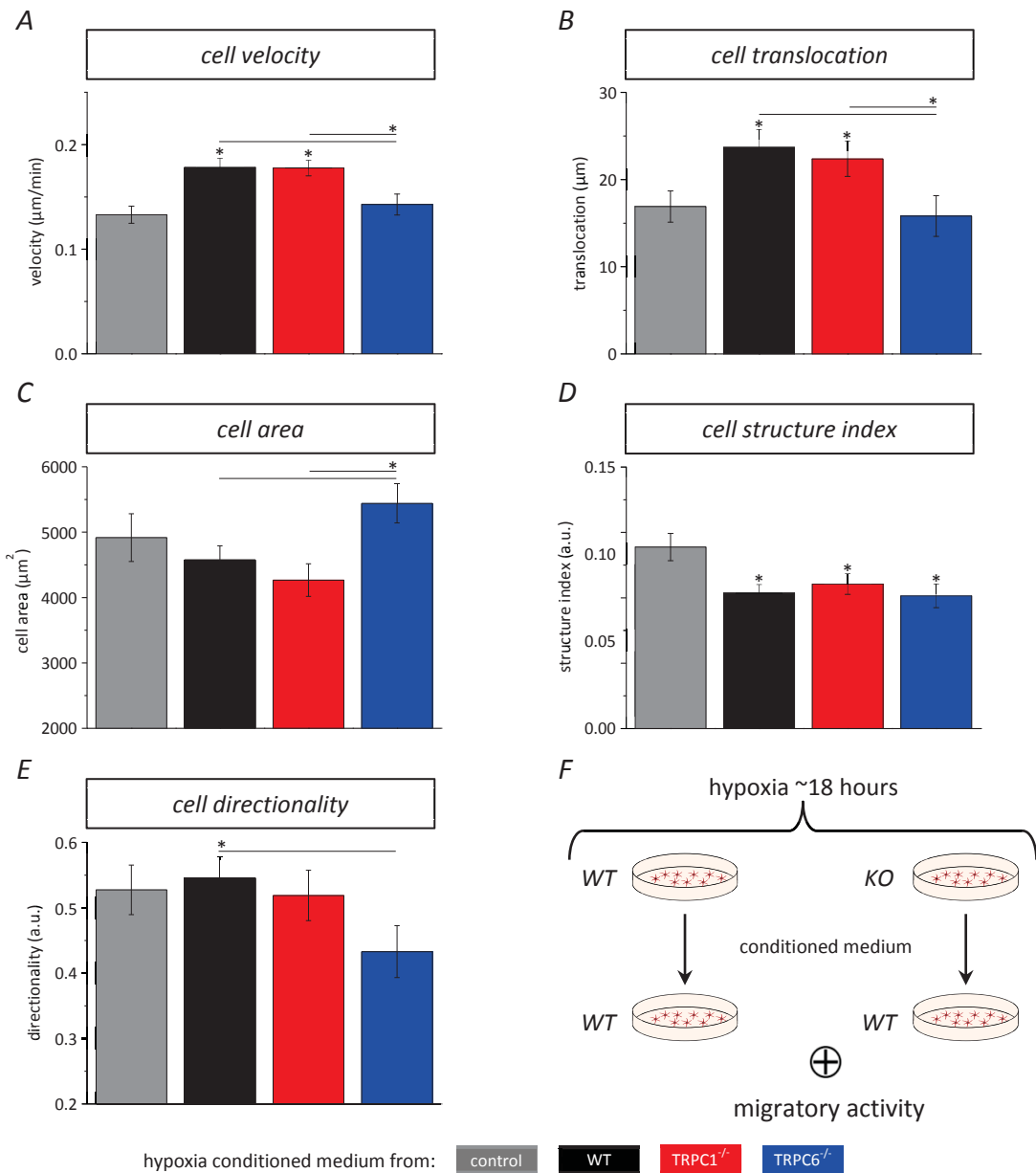


Figure 4.13. Autocrine Stimulation of mPSCs under Hypoxia. Hypoxically conditioned medium from WT, TRPC1^{-/-} and TRPC6^{-/-} mPSCs was used to stimulate WT mPSC migration and thereby determine any differences in secreted stimulants. Mean values of **(A)** cell migration velocity, **(B)** cell translocation, **(C)** cell area, **(D)** cell structure index and **(E)** directionality. **(F)** Experimental illustration. mPSCs secreted autocrine stimulants upon hypoxia stimulation. This response is attenuated in TRPC6^{-/-} mPSCs. Hypoxically conditioned medium mediated morphological changes in mPSCs by inducing a more elongated cell shape (lower SI value) and tendency to smaller cell size. Values represent means \pm SEM. (*) = $p \leq 0.05$. Student t-test and Mann-Whitney U test. (control media: N = 4, n = 51, WT hypoxia media: N = 3, n = 38, TRPC1^{-/-} hypoxia media: N = 3, n = 35, TRPC6^{-/-} hypoxia media: N = 3, n = 39).

4.7 Calcium Influx in Hypoxia Stimulated mPSCs

In order to test if TRPC6 channels are part of *transduction/effector* pathways in mPSCs upon hypoxic stimulation (hypothesis ③, [section 2.1](#)), the level of hypoxia-mediated calcium influx was investigated using the manganese quenching method. The decrease in Fura-2 fluorescence following the addition of Mn^{2+} is an indirect measure of calcium influx (Fabian et al., 2011; Lindemann et al., 2013; Merritt et al., 1989). [Figure 4.14 A](#) illustrates the mean decrease of intensity (F_{365}) in percentage in hypoxically activated WT and TRPC6^{-/-} mPSCs before and after addition of Mn^{2+} . In [figure 4.14 B](#) the mean delta slope (Δm) is depicted, which corresponds to the difference between the slopes before ($m1$) and after ($m2$) Mn^{2+} addition. Both hypoxia and chemically induced hypoxia elicited a higher quenching rate of the fluorescence compared to normoxic conditions in WT mPSCs of 43% (DMSO vs. DMOG, $p = 0.002$) and 39% (normoxia vs. hypoxia, $p = 0.0005$). This was not observed for TRPC6^{-/-} mPSCs being significantly different from that of WT mPSCs ($p < 0.05$). These results support the hypothesis of TRPC6 channels functioning in hypoxia-mediated *transduction/effector* mechanisms. Loss of TRPC6 leads to decreased calcium influx under hypoxic conditions, which may have profound effects on downstream signalling cascades important for mPSC migration.

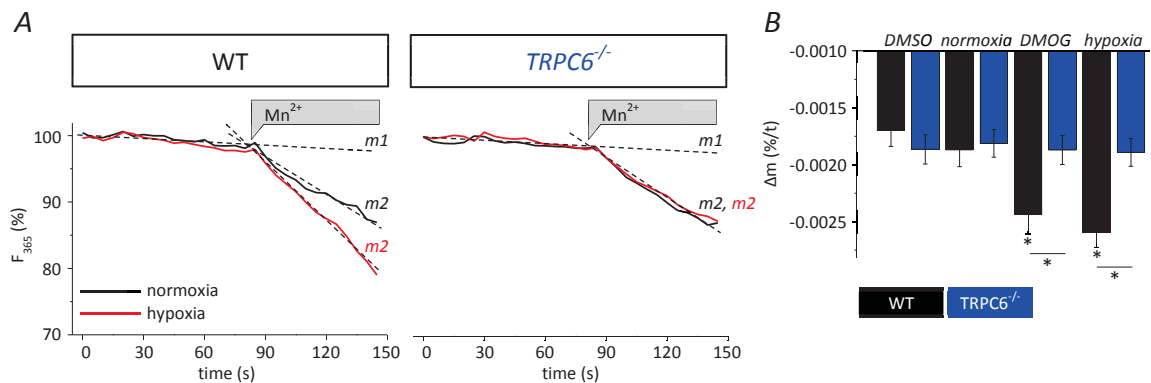


Figure 4.14. Hypoxia-Mediated Calcium Influx in mPSCs. Calcium influx is increased in WT mPSCs but not in TRPC6^{-/-} mPSCs when pre-activated by chronic hypoxia **(A)** Time course of mean Fura-2 fluorescence (F_{365}) when excited at its isosbestic wavelength of 365 nm for WT and TRPC6^{-/-} mPSCs. F_{365} is normalized to the first value under stable control conditions. **(B)** The corresponding mean change of the slope (Δm : $m2 - m1$). Values of graphs are represented as mean values and values of Δm as means \pm SEM. (*) = $p \leq 0.05$, Student t-test. WT mPSCs (normoxia: N = 4, n = 30, DMSO: N = 3, n = 28, hypoxia: N = 4, n = 35 and DMOG: N = 4, n = 35) and TRPC6^{-/-} mPSCs (normoxia: N = 3, n = 36, DMSO: N = 3, n = 26, hypoxia: N = 3, n = 29 and DMOG: N = 3, n = 29).

4.7.1 Calpain – a Downstream Effector in PSC Migration

Calpain is a calcium dependent proteolytic enzyme known to be active in processes related to cell migration in various cell types including integrin-mediated cell migration, cytoskeletal remodeling and cell adhesion (Glading et al., 2000; Saraiva et al., 2013; Svensson et al., 2010). It was therefore hypothesized that calpain could be a major effector downstream of hypoxia-mediated calcium signaling through TRPC channels.

This was addressed in an entirely different experimental setup. Unpublished data (*manuscript in revision*) have shown that TRPC3-mediated calcium influx, following PDGF stimulation (50 ng/ml) in the human established PSC line (RLT-PSC) is important for PSC migration, possibly via a mechanism involving calpain activity. Briefly, the calcium influx through TRPC3 channels was found to be coupled to the activity of the calcium-activated potassium channel ($K_{Ca}3.1$). Activation of $K_{Ca}3.1$ is followed by membrane hyperpolarization, which promotes calcium influx, in this context via TRPC3. Inhibition of $K_{Ca}3.1$ with TRAM-34 led to a decrease in TRPC3-mediated calcium entry and lower PSC migratory activity. Moreover, this was coupled to a lower activity of calpain. This suggests that calpain is a downstream effector of PDGF mediated PSC migration (*figure 4.15*). As illustrated in *figure 4.15 B*, the CMAC peptidase substrate, t-BOC-Leu-Met, was used to indirectly measure calpain activity in live RLT-PSCs stimulated with PDGF \pm TRAM-34.

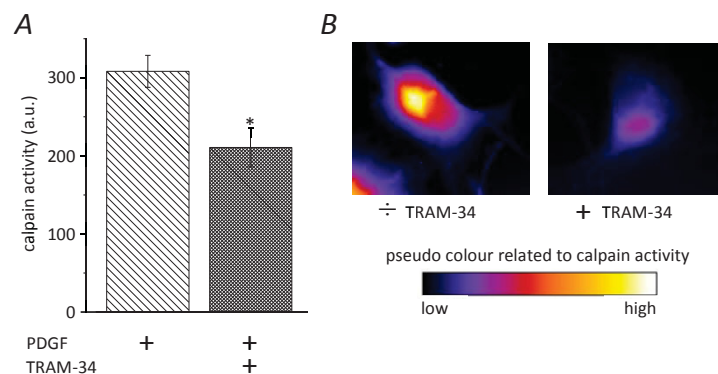


Figure 4.15. The Effect of $K_{Ca}3.1$ Inhibition on Calpain Activity. Inhibition of $K_{Ca}3.1$ activity with TRAM-34 decreased calpain activity in RLT-PSCs stimulated with PDGF (50 ng/ml). **(A)** Calpain activity was indirectly measured using the CMAC peptidase substrate, t-BOC-Leu-Met. Whole cell fluorescence intensity was measured, corrected for background fluorescence and depicted in arbitrary unit (a.u.). **(B)** Representative pseudo colour image of calpain activity under PDGF stimulation \pm TRAM-34. Values represent means \pm SEM. (*) = $p \leq 0.05$, Mann-Whitney U test. (PDGF: N = 3, n = 35 and PDGF + TRAM-34: N = 3, n = 31).

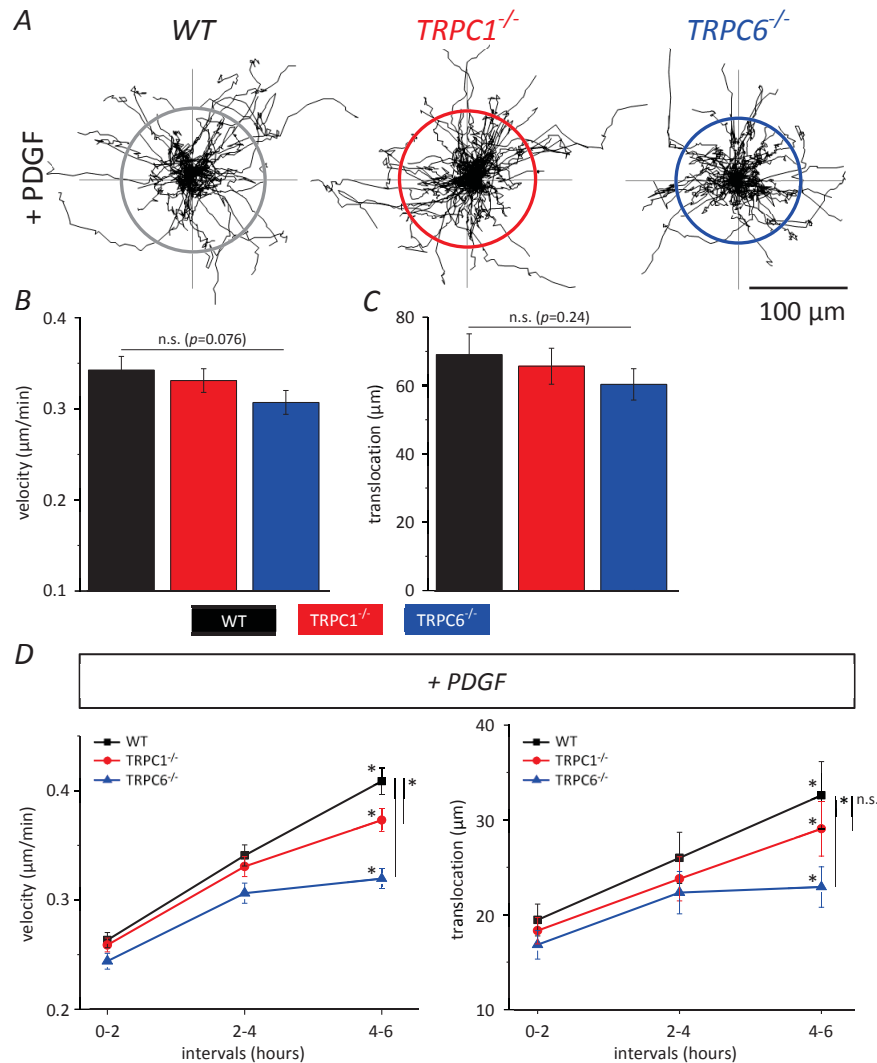
Whole cell fluorescence intensity was measured and corrected for background fluorescence. Addition of TRAM-34 decreased the calpain activity by 32% (308.1 ± 20.5 to 210.7 ± 24.9 a.u., $p < 0.0005$) demonstrating the mechanistic coupling of $K_{Ca}3.1$ mediated calcium influx through TRPC3 channels to calpain as regulator of PSC migration. Future experiments may elucidate whether calpain activity is decreased in hypoxia activated TRPC6^{-/-} mPSCs.

4.8 PDGF Stimulation of mPSC Migration

PDGF is known to be one of the main stimulants of PSC activity inducing both chemokinetic and chemotactic effects (Hild, 2015; Luttenberger et al., 2000; Phillips et al., 2003b). Furthermore, PDGF is secreted by PSCs upon activation and could thereby be one of the autocrine stimulants secreted by hypoxia-stimulated PSCs. Many downstream members of the PDGF receptor signaling pathway are Ca^{2+} dependent (see [section 1.3.2](#)). It was therefore tested whether TRPC1 and TRPC6 channels are involved in a downstream *effector* mechanism in the response of mPSCs to PDGF. In the human RLT-PSC line PDGF elicited a Ca^{2+} signaling cascade involving the activity of $K_{Ca}3.1$, TRPC3 channels and calpain ([section 4.7.1](#)).

4.8.1 PDGF Stimulates mPSC Migration in Three Dimensional Space

In a 3D model (described in [section 4.3](#)) the effect of PDGF was addressed in WT, TRPC1^{-/-} and TRPC6^{-/-} mPSCs. Time lapse video recording of cell migration was monitored over a time period of 7 h in the presence of PDGF (50 ng/ml) and mean migration velocity and cell translocation were calculated. PDGF significantly increased mean cell migration velocity and cell translocation compared to controls in all groups except the migration velocity of TRPC1^{-/-} mPSCs ([figure 4.16, table](#)). No significant difference between the groups was observed in the presence of PDGF, beside a tendency to lower migration velocity and translocation in TRPC6^{-/-} mPSCs ([figure 4.16 B-C](#)). Furthermore, the migration velocity and translocation were depicted over time in 2 h intervals ([figure 4.16 D](#)).



	PSC WT		PSC TRPC1 ^{-/-}		PSC TRPC6 ^{-/-}	
MEAN	<u>control</u>	<u>PDGF</u>	<u>control</u>	<u>PDGF</u>	<u>control</u>	<u>PDGF</u>
Translocation (µm)	38.5±3.9	69.1±6.1(*)	27.3±2.8	65.7±5.2(*)	26.9±3.2	60.3±4.6(*)
Velocity (µm/min)	0.31±0.01	0.34±0.02(*)	0.30±0.01	0.33±0.01(n.s.)	0.26±0.01	0.31±0.01(*)

Figure 4.16. PDGF Stimulation of mPSC in Three dimensional Space. The addition of PDGF (50 ng/ml) cannot overcome the loss of activation in TRPC6^{-/-} mPSCs. mPSCs were embedded in a 3D migration chamber and cell migration was monitored with time-lapse video microscopy for 7 h. **(A)** Single cell trajectories were normalized to a common starting point and mean translocation determined from the radius of a circle. **(B)** Mean cell migration velocity. **(C)** Mean cell translocation. **(D)** Cell migration and translocation in 2 h intervals in the presence of PDGF. All groups significantly increased their migration velocity and translocation from the first to the last interval. TRPC1^{-/-} and TRPC6^{-/-} mPSCs did not reach the same level of activation as observed for WT mPSCs with the defect being more pronounced for that of TRPC6^{-/-} mPSCs. Values represent means ± SEM. In the table the mean migration values under control conditions (from figure 4.3) and in the presence of PDGF are depicted. n.s. = $p > 0.05$, (*) = $p \leq 0.05$, Student t-test and Mann-Whitney U test. WT (N = 3, n = 53), TRPC1^{-/-} (N = 3, n = 72) and TRPC6^{-/-} (N = 4, n = 59).

All groups significantly increased their migration velocity and translocation from the first to the last interval. WT mPSCs increased their migration velocity by 55% (0.26 ± 0.01 to 0.41 ± 0.01 $\mu\text{m}/\text{min}$, $p < 0.0005$) and translocation by 67% (19.4 ± 1.7 to 32.6 ± 3.5 μm , $p = 0.001$), whereas TRPC1^{-/-} increased their migration velocity by 41% (0.26 ± 0.01 to 0.37 ± 0.01 $\mu\text{m}/\text{min}$, $p < 0.0005$) and translocation by 59% (18.3 ± 1.4 to 29.1 ± 2.9 μm , $p = 0.001$). Although not reaching the same level in migration velocity as WT mPSCs ($p = 0.0003$), TRPC6^{-/-} mPSCs increased their migration velocity by 31% (0.24 ± 0.01 to 0.32 ± 0.01 $\mu\text{m}/\text{min}$, $p < 0.0005$) and translocation by 36% (16.8 ± 1.5 to 22.9 ± 2.1 μm , $p = 0.02$). Both values are far from the corresponding WT values. Velocity was 22% lower ($p < 0.0005$) and translocation 30% lower ($p = 0.02$) (*figure 4.16 D*).

No other cell morphological changes were detected between and within individual groups. Therefore, it can be concluded, that TRPC1^{-/-} and TRPC6^{-/-} mPSCs have not lost their ability to respond to the chemokinetic stimulation by PDGF. However, keeping in mind the decreasing pO₂ and/or increasing cellular stress and acidosis throughout the experiment, the addition of PDGF could not overcome the loss of activation in TRPC6^{-/-} mPSCs.

4.8.2 PDGF Chemotaxis

PDGF is also known to elicit chemotaxis in PSCs through specific receptor binding (Hild, 2015; Phillips et al., 2003b) possibly leading to the activation of Ca²⁺ permeable channels involved in directed cell migration. The role of TRPC1 and TRPC6 channels in PDGF mediated chemotaxis of mPSCs was investigated using 2D ibidi chemotaxis slides coated with the same desmoplastic matrix used in previous migration experiments. Migrating in a PDGF gradient WT, TRPC1^{-/-} and TRPC6^{-/-} mPSCs significantly increased their migration velocity by 29%, 38% and 39% ($p < 0.0005$), respectively, and more than doubled their translocation rate ($p < 0.0005$) (*figure 4.17 A-B*). However, a 12-16% lower cell migration velocity ($p < 0.05$) was detected under control conditions in both TRPC1^{-/-} and TRPC6^{-/-} mPSCs versus that of WT. Additionally, TRPC6^{-/-} mPSCs showed a slightly diminished migration velocity of 11% ($p = 0.043$) during PDGF chemotaxis when compared to that of WT mPSCs. The chemotactic index of WT, TRPC1^{-/-} and TRPC6^{-/-} mPSCs was almost identical (0.44-0.49, $p > 0.05$, n.s.) (*figure 4.17 C*). These findings indicate that neither TRPC1 nor TRPC6 play a role in directed cell migration toward PDGF.

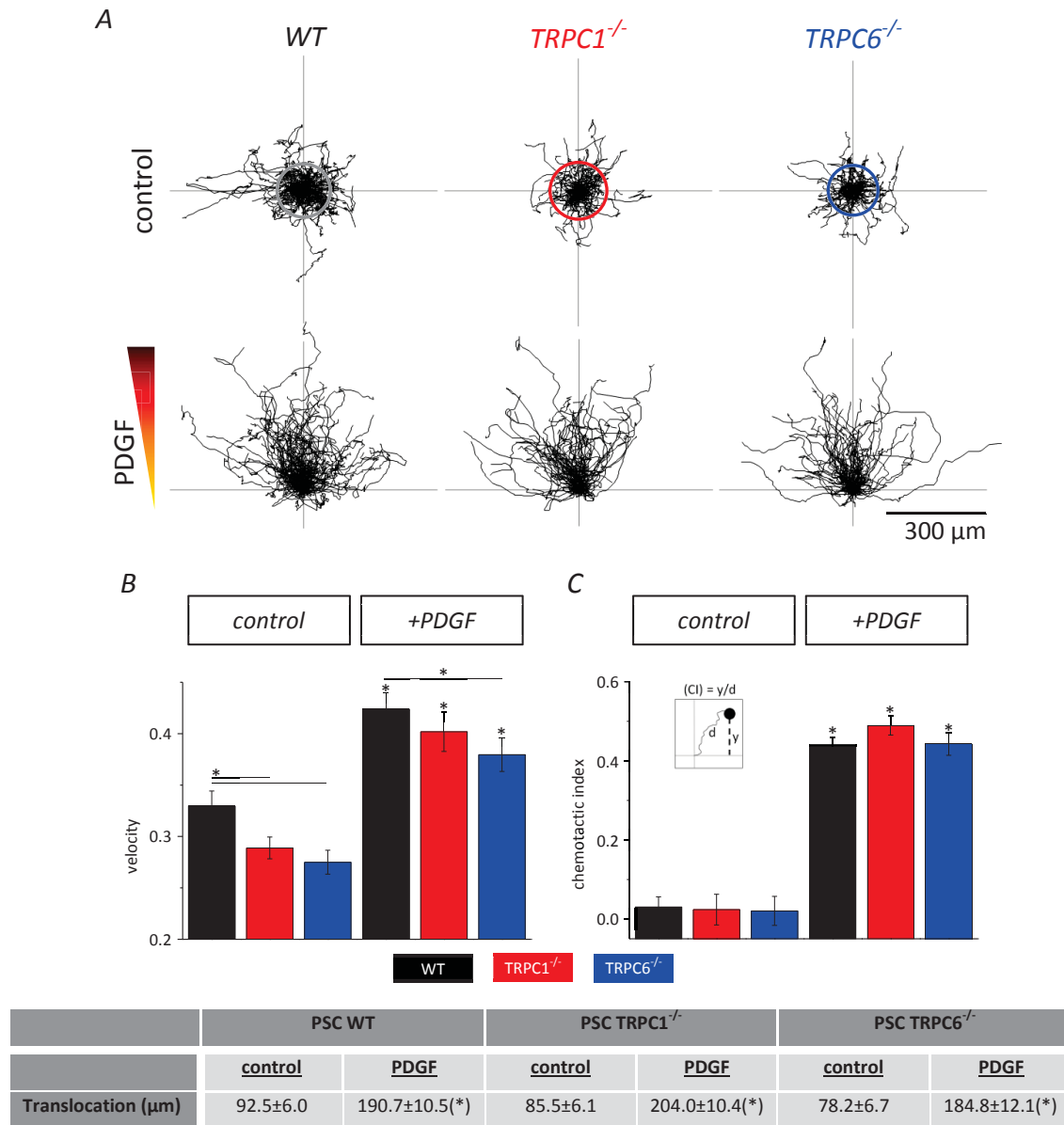


Figure 4.17. PDGF Chemotaxis. WT, TRPC1^{-/-} and TRPC6^{-/-} mPSCs efficiently chemotax in a gradient of PDGF. mPSCs were seeded into 2D Ibidi slides, PDGF was applied and chemotaxis monitored for 15 h using time-lapse video microscopy. **(A)** Single cell trajectories were normalized to a common starting point. Mean translocation values are given in the table. **(B)** Mean cell migration velocity was decreased in TRPC1^{-/-} and TRPC6^{-/-} mPSCs under control conditions and in TRPC6^{-/-} mPSCs upon PDGF stimuli. **(C)** Mean directed cell migration efficiency toward higher concentration of PDGF was increased in all groups, displayed by a chemotactic index (see [figure 3.5](#), materials and methods, [section 3.5.6](#)). Values represent means ± SEM. n.s. = $p > 0.05$, (*) = $p \leq 0.05$, Student t-test. WT (control: N = 3, n = 95, PDGF: N = 3, n = 98), TRPC1^{-/-} (control: N = 3, n = 64, PDGF: N = 3, n = 69) and TRPC6^{-/-} (control: N = 3, n = 60, PDGF: N = 3, n = 70).

Chapter 5

Discussion

Discussion

A link between TRP channel-mediated Ca^{2+} influx in cell migration is confirmed in various cell types (Fiorio Pla and Gkika, 2013; Nielsen et al., 2014; Schwab et al., 2012; Stock et al., 2013), however their role in PSC migration was completely unknown before the beginning of this thesis. Only the TRPV4 channel is demonstrated in PSC activation. This channel is implicated in reactive calcium responses in high fat and alcohol activated PSCs (Zhang et al., 2013). Similarly, not much is known about the role of TRP channel-mediated calcium signalling in the closely related HSCs. Only recently, the TRPM7 channel was reported to regulate PDGF-BB-induced HSC proliferation via PI3K and ERK signalling (Fang et al., 2013) and the TRPV4 channel to be involved in regulating TGF- β 1-induced HSC proliferation (Song et al., 2014).

The present study showed that SOC is transcriptionally and functionally upregulated in culture activated mPSCs compared to quiescent mPSCs (*figure 4.1*). This is in accordance to Won et al. who showed that Ca^{2+} signalling is elevated in activated compared to quiescent PSCs (Won et al., 2010). It demonstrates the importance of Ca^{2+} signalling in activated PSCs. In addition, the TRPC1 and TRPC6 channel are the predominantly expressed members of the of TRPC channel family in culture activated mPSCs (*figure 4.2*). Furthermore, TRPC1 and TRPC6 channels are recognized as *transducers* of chemically mediated Ca^{2+} signalling as well as *sensors* and *modifiers* of a wide variety of microenvironmental changes related to cell migration (Nielsen et al., 2014). However, their exact functional role in the response of PSCs to hypoxia remains elusive. The overall aim of this study was therefore to identify TRPC1 and TRPC6 channels as potential *sensors*, *modifiers* or *transducers/effectors* of hypoxia-mediated activation of PSCs (depicted in *figure 2.1*).

The key observations found in this study were as followed: (1) the mode of cell migration and involved proteins may diverge between 2D and 3D migration. (2) Hypoxia induces a migratory phenotype in mPSCs with smaller cell size. (3) Hypoxia-mediated increase of TRPC1 channel expression in mPSCs is coupled to elevated cell motility, potentially via a *sensor* mechanism that is also important for correct cell size regulation. (4) TRPC6 channels are part of a *modifier* mechanism in mPSC under hypoxic conditions through growth factor/cytokine secretion. (5) TRPC6 channels are part of a

transduction/effector pathway by mediating increased calcium influx during hypoxia required for stimulation of cell motility.

5.1 The “Ideal” Migration Setup

The ECM is a complex meshwork of fibrous proteins that provide a physical scaffold for cells to move. It provides guiding cues during development, wound repair together with support and maintenance of normal tissue architecture. Furthermore, the ECM is involved in coordinating cellular migratory functions by the activation of intracellular signalling pathways controlling cell motility (Doyle et al., 2013; Grinnell, 2008; Keren et al., 2008). Cells react to distinct physical and biochemical characteristics of the ECM (i.e. content and arrangement of the matrix). This highlights the importance of using experimental models mimicking 3D tissue networks and microenvironments observed both in healthy tissues and under pathological conditions (Doyle et al., 2013; Friedl and Wolf, 2009a; Petrie et al., 2009).

To investigate TRPC1 and TRPC6 channels' role in PSC migration, a 3D experimental model was modified and established from Stock et al. 2005. PSC migration could thereby be visualized in a microenvironment closely related to that observed within desmoplastic regions of pancreatic cancer. Accordingly, it has been observed that the overall mode of cell migration and signalling pathways involved may diverge between 2D and 3D migration. For example, a higher migration rate was detected for fibroblasts in a 3D environment compared to the corresponding 2D ECM. This further depended on ECM composition (Hakkinen et al., 2011). This is in agreement with data from this study, showing a higher final migration velocity for WT mPSCs migrating in a confined and dynamic 3D microenvironment with evolving increasing acidosis and hypoxia than for stimulated WT mPSCs migrating on a 2D ECM. However, the relative increase in mPSC migration activity upon stimulation (2D versus 3D) was more or less the same compared to their respective controls. Furthermore, consistent with previously published data, mPSCs spread to a flattened morphology when cultivated on 2D-surfaces (Apte et al., 1998; Bachem et al., 1998), whereas mPSCs surrounded by a 3D-fibrous matrix assumed an elongated cell shape that seemed to mimic that observed *in vivo* (Apte et al., 2004; Apte et al., 2012) (*figure 4.3 D*).

5.2 Hypoxia in mPSC Activation

As pointed out earlier, hypoxia is a potent stimulator of PSC activity, which also promotes inflammatory responses that lead to production and secretion of autocrine stimulants (see [section 1.3.3](#)). Moreover, it seems that hypoxia-mediated stimulation of PSC motility as present in this study and demonstrated previously by Erkan et al., 2009, Masamune et al., 2008a and Rebours et al., 2013, is not a universal cell response. In contrast to pancreatic and hepatic stellate cells (Novo et al., 2007; Novo et al., 2012; Wang et al., 2013), immune cells and (myo)fibroblast migration is inhibited by hypoxia (Qu et al., 2005; Riches et al., 2009; Turner et al., 1999; Vogler et al., 2013). The reasons for this discrepancy are not yet known. Despite the advantage of the 3D migration model to expose PSCs to conditions similar to that in PDAC, it has some disadvantages. While the initial physicochemical conditions can be controlled, this is not the case during the course of the experiment. A more simplified 2D model was therefore used to analyse the chronic effect of hypoxia on mPSC activation.

WT mPSCs decreased their projected cell area in response to hypoxia stimulation ([figure 4.7](#)). This is in contrast to that of mice L929 fibrosarcoma fibroblasts which increase their cell area and volume under hypoxia stimulation (Vogler et al., 2013). In a rat HSC line (HSC-T6) hypoxia induces an elongated cell structure through a HIF-1 α dependent pathway. Whether the rat HSCs also changed their cell size is unknown (Wang et al., 2013). This morphological response to hypoxia was not detected in TRPC1^{-/-} mPSCs, suggesting a role of TRPC1 in cell size regulation. This is further supported by the fact, that TRPC1^{-/-} mPSCs generally displayed a larger projected cell area than WT mPSCs ([figure 4.7](#)). More, previously published data from our group and by others have shown that functional expression of the TRPC1 channel is involved in cell size regulation. Chen et al. showed that a downregulation of TRPC1 in rat liver hepatoma cells (H4-IIIE cells) increased cell area and volume (Chen and Barritt, 2003). Fabian et al. could later support these findings by showing larger projected cell area and cell volume in murine TRPC1^{-/-} fibroblast and siTRPC1 treated Madin–Darby canine kidney focus cells (Fabian et al., 2012). Thus, the failure of TRPC1^{-/-} mPSCs to increase their activity under hypoxia stimulation could be due to a defect in cell size regulation.

5.3 TRPC1 and TRPC6 Channels in the Hypoxia-Mediated Activation of mPSCs

Generally, there are two major ways in which TRP channels can sense pO_2 : 1. through *direct* alteration of the redox status of the channel proteins themselves via modification of Cys residues. 2. through an indirect pathway via interaction with pO_2 sensitive complexes or the involvement in pathways of proteins carrying O_2 sensor domains (Numata et al., 2013). So far, however, only TRPA1 channels are known to sense pO_2 directly (Takahashi et al., 2011).

This study demonstrates for the first time, that TRPC1 and TRPC6 channels are important for mPSCs response to hypoxia stimulation by affecting cell motility. This is further suggested to be mediated by their contribution to distinct mechanisms underlying *sensor*, *modifier* and *transduction/effector* pathways of microenvironmental cues.

5.3.1 TRPC1 Channel: Part of an Indirect Sensor Mechanism to Hypoxia in mPSCs

The TRPC1 channel is predominantly viewed as a SOCE channel, although this property is still controversially discussed (Ambudkar, 2007; DeHaven et al., 2009; Dietrich et al., 2014; Nesin and Tsiokas, 2014). It is connected to the cytoskeleton in a bidirectional interplay, linking the channel directly to the migration machinery of the cell (Clark et al., 2008; Nielsen et al., 2014; Smani et al., 2013). An increase in TRPC1 function can lead to elevated Ca^{2+} influx important for the activation of Ca^{2+} -dependent signalling effectors coupled to cell migration. The understanding of the TRPC1 channel function in response to hypoxia, however, is only starting to emerge, mostly implicating the channel in an indirect *sensing* mechanism.

In this study it could be shown that TRPC1^{-/-} mPSCs have an attenuated migratory response to hypoxic stimulation when migrating on a 2D surface compared to WT mPSCs (*figure 4.8 and 4.10*). In contrast, under increasing acidosis and hypoxia, the loss of TRPC1 showed less pronounced effects when mPSCs were migrating in a 3D matrix (*figure 4.3 and 4.4*). This indicates that the impact of TRPC1 channels on mPSC depends on the used migration model, 2D versus 3D. There is limited information regarding TRPC1 channels as mechanosensors in 3D cell migration. In contrast, TRPC1 channels are linked to

mechanosignalling during 2D cell migration. In human bone osteosarcoma (Wei Huang et al., 2015) and primary cultures of synovial fibroblasts (Fabian et al., 2012) membrane stretch and substrate stiffness induced TRPC1-mediated SOCE, respectively. Hence, a loss of directionality in TRPC1^{-/-} mPSCs was found compared to that of WT mPSCs when migrating in a 3D environment (WT: 0.28±0.03, TRPC1^{-/-}: 0.21±0.02, $p = 0.03$) (*data not shown*). This is in accordance to Wei Huang et al. In a 2D migration model they found that TRPC1-mediated SOCE and cytoskeleton architecture plays a critical role in the formation of cell polarity during directional cell migration (Wei Huang et al., 2015). This indicates a dependence of the constitutive “steering” mechanism of mPSCs migrating in a 3D matrix. However, this effect could be rescued by the application of PDGF. Curiously, the difference in directionality was not observed when mPSCs were migrating on a 2D surface. TRPC1^{-/-} mPSCs were even capable of efficient chemotaxis in a PDGF gradient (*figure 4.17*). This differential response appears to be PSC specific since TRPC1 channels are implicated in the response to PDGF in rat hippocampal neuronal progenitor cells (Yao et al., 2012). Moreover, TRPC1 channels are involved in the response to other stimulants such as EGF, FGF-2, TGF- β and fMLP (Bomben et al., 2011; Dong et al., 2010; Fabian et al., 2011; Fiorio Pla et al., 2005; Lindemann et al., 2015; Tajeddine and Gailly, 2012).

Hypoxia increased the protein expression of TRPC1 by 1.5 fold, which could partly be confirmed by qPCR. This is in accordance to other published data. In smooth muscle cells, hypoxia increases TRPC1 channel expression in a HIF-1 α dependent manner, further leading to elevated SOCE (Jiang et al., 2014; Li et al., 2010; Wang et al., 2006; Yang et al., 2015). From this it can be suggested, that the hypoxia-mediated increase of TRPC1 channel expression is part of a *sensor* mechanism in mPSCs, possibly regulated by upstream hypoxia sensitive proteins such as HIF-1 α (*figure 5.1*). Surprisingly, hypoxia also regulated the mRNA expression of TRPC2, TRPC3 and TRPC4 channels in WT mPSCs (*figure 4.12*). Additional studies have to determine if this is also the case in TRPC1^{-/-} mPSCs and if any possible compensatory effects could be present.

In line with these observations it is tempting to speculate that the TRPC1 channel is an important contributor to hypoxia-mediated calcium influx in mPSCs needed for elevated cell motility in response to hypoxia. Furthermore, efficient TRPC1 channel interaction with STIM1 and ORAI1 is needed for SOCE in hypoxically stimulated pulmonary arterial smooth muscle cells of both rats and mice (Lu et al., 2008; Ng et al.,

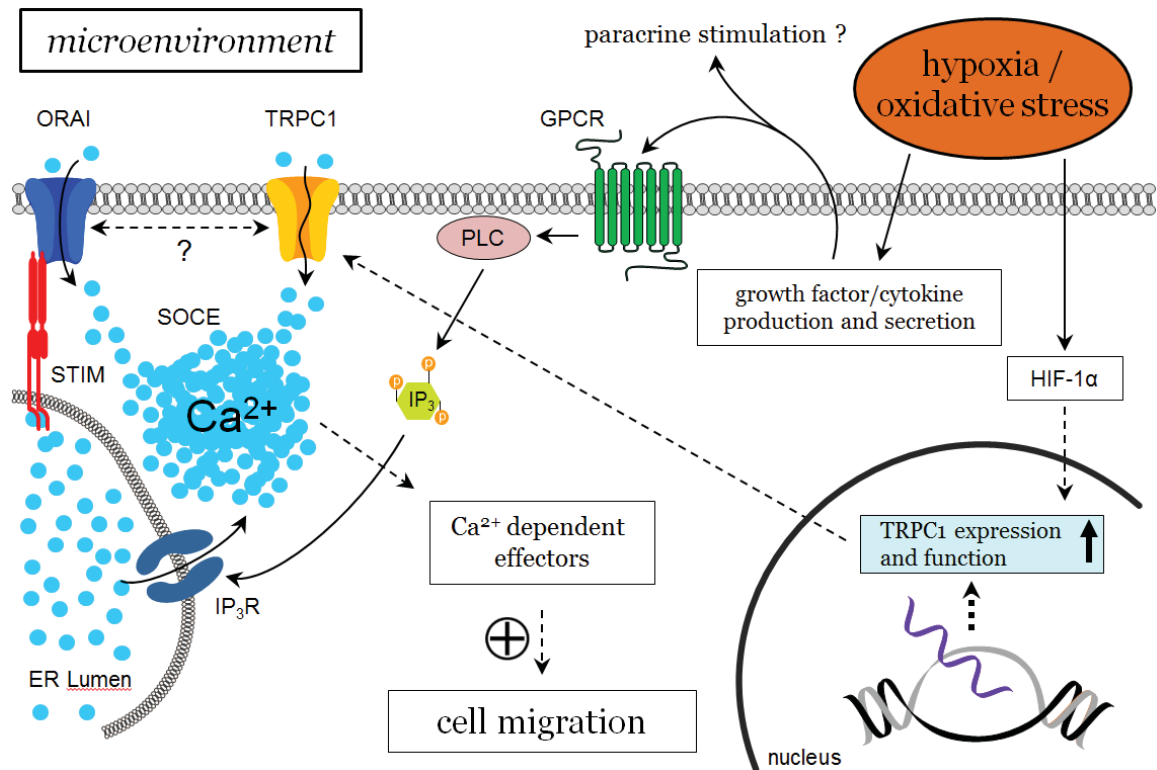


Figure 5.1. Illustration of the Role of TRPC1 Channels in mPSCs Under Hypoxic Stimulation. The TRPC1 channel is part of an indirect *sensor* mechanism to hypoxia in mPSCs by expression regulation. O₂ sensitive proteins such as HIF-1 α can increase the functional expression of TRPC1 leading to a possible elevation in Ca²⁺ influx. This mobilization of Ca²⁺ promotes the activation of other signaling proteins important for cell migration. Hypoxia and oxidative stress can also promote the secretion of autocrine stimulants binding to GPCRs leading to activation of PLC and formation of IP₃. IP₃ mediate Ca²⁺ efflux from the ER activating SOCE. TRPC1 channels can be part of the SOCE complex through interactions with STIM1 and ORAI.

2012). This is interesting as the response of TRPC1^{-/-} mPSCs to hypoxia is not completely absent, indicating that the TRPC1 channel is not the only regulator of this process. One possible explanation for this could be that hypoxia-mediated ROS production in mPSCs (see [section 1.3.3 -1.3.4](#)) modifies the Cys residue on either STIM1 or TRPC1, thereby altering their functional interaction in the TRPC1-STIM1-ORAI1 complex (Ng et al., 2012; Numata et al., 2013; Shimizu et al., 2014). Hence, the TRPC1 channel can function as part of a SOCE complex with STIM and ORAI in response to hypoxia (illustrated in [figure 5.1](#)). It would therefore be interesting to investigate SOCE in hypoxia-stimulated mPSCs and decipher the role of TRPC1 played therein. TRPC1 channels could also be part of GPCR-triggered pathways responding to autocrine stimulants. Frequently these signalling cascades also lead to SOCE activation (Clapham, 2003; Minke and Cook, 2002) ([figure 5.1](#)).

Along these lines the diminished migratory activity of TRPC1^{-/-} mPSCs could be explained by altered activity of Ca²⁺ dependent effectors needed for cell migration.

Additionally, TRPC1 channel function is related to inflammatory responses through its impact on NADPH oxidase mediated ROS production (Brechard et al., 2008). NADPH oxidase activity is known to be involved in PSC activation (Asaumi et al., 2007; Masamune et al., 2008b). This couples the TRPC1 channel to PSC activation under hypoxia by regulating such a process. The model in [figure 5.1](#), illustrates the signalling cascade, which link TRPC1 channels to the hypoxia-induced activation of PSCs. This model provides a framework to be further validated experimentally.

5.3.1.1 The TRPC1 Channel is not Implicated in the Secretion of Autocrine Stimulants

Indication of an autocrine stimulation defect in TRPC1^{-/-} mPSCs was detected under chemically induced hypoxia ([figure 4.9](#)). It was therefore tested whether the TRPC1 channel was implicated in a *modifying* mechanism by secretion of autocrine stimulants upon hypoxic stimulation. However, no difference in the secretion of autocrine stimulants was observed between WT and TRPC1^{-/-} mPSCs. Hypoxia conditioned media from WT and TRPC1^{-/-} mPSCs showed the same level of stimulation of WT mPSC migration ([figure 4.13](#)). Interestingly, the conditioned media induced a smaller and more elongated cell morphology ([figure 4.13, D](#)). Since this behaviour was detected with conditioned media from both genotypes it is proposed that TRPC1 channels are not part of a *modifier* mechanism of the microenvironment. However, at present moment the possibility that TRPC1 channels could be involved in the secretion of other stimulants having paracrine effects on cancer cells or other stroma host cells such as immune cells, epithelial cells and fibroblast cannot be excluded.

5.3.2 TRPC6 Channel: A Central Component in the Response of mPSCs to Hypoxia

The TRPC6 channel is viewed as a ROCE channel, thereby being part of a direct *transduction/effector* pathway downstream of the activation of growth factor or chemoattractant receptors (GPCR and RTK) (Dietrich and Gudermann, 2014). Hypoxia-induced Ca²⁺ signalling mediated by TRPC6 channels has been pointed out in [section](#)

1.5.2.2. It was therefore speculated whether TRPC6 channel activity is important for regulating responses to hypoxia leading to an elevated migratory activity.

This study shows convincing data that TRPC6 channels play an important role in the migratory response of mPSCs to hypoxia. Thus, in contrast to that of WT mPSCs, TRPC6^{-/-} mPSCs did not increase their level of motility under hypoxic stimulation. This was observed both when migrating on a 2D desmoplastic surface under hypoxia conditions (*figure 4.8-4.11*) and in a 3D matrix under increasing acidosis and hypoxia (*figure 4.3-4.4*). This is in concordance with other observations. For example, TRPC6 channel activity is important for migration of podocytes and fibroblasts (Tian et al., 2010), neutrophils (Damann et al., 2009; Lindemann et al., 2013; McMeekin et al., 2006), endothelial cells (Hamdollah Zadeh et al., 2008), head and neck squamous cell carcinomas (Bernaldo de Quiros et al., 2013) and glioblastoma (Chigurupati et al., 2010). Application of PDGF could not overcome the defect induced by the loss of TRPC6 in the 3D model (*figure 4.16*). More, TRPC6 is required for optimal PDGF induced migratory stimulation when migrating in a gradient of PDGF (*figure 4.17*). However, the ability to sense the directional cue imposed by a PDGF gradient was not affected suggesting a role of TRPC6 channels in regulation of the migration machinery and not a general defect in the steering mechanism, too.

Despite substantial data showing hypoxia-mediated up-regulation of TRPC6 channel expression in other cell types such as mesangial cells (Liao et al., 2012), venous smooth muscle cells (Li et al., 2010; Wang et al., 2006; Xu et al., 2014), arterial smooth muscle cells (Jiang et al., 2014; Yang et al., 2015) and in glioblastoma (Chigurupati et al., 2010), no such difference in TRPC6 channel mRNA expression was detected in mPSCs (*figure 4.12*). Different antibodies were tested to verify this on the protein level. However, unspecific binding of the antibody (WT versus KO) resulted in high uncertainty of the data. Protein analysis of TRPC6 channel expression is therefore not present in this study. Taken together, this finding excludes the TRPC6 channel to be part of a hypoxia-mediated *sensor* mechanism.

5.3.2.1 The TRPC6 Channel in a Modifier Mechanism

Not much is known about TRPC6-mediated production and secretion of stimulants under hypoxia. Such mechanisms have mostly been related to the activity of other TRP

channels, thus demonstrating the role of Ca^{2+} signalling in growth factor/cytokine secretion. TRPM2 channels underlie enhanced cytokine/chemokine production in activated T-lymphocytes (Melzer et al., 2012), monocytes and neutrophils (Knowles et al., 2011; Wehrhahn et al., 2010; Yamamoto et al., 2008) and pancreatic cancer cells (Bauer et al., 2012). TRPM4 channels regulate interleukin production in Jurkat T-cells (Launay et al., 2004) and mouse T-cells (Weber et al., 2010), TRPV2 channels that of macrophages (Yamashiro et al., 2010) and TRPC5 channel activation induces NO production in endothelial cells (Takahashi et al., 2012b; Yoshida et al., 2006). The inflammatory process of NADPH oxidase-mediated superoxide production is related to TRPC1, TRPC3, TRPC6 and ORAI1 channel activity in granulocytes (Brechard et al., 2008). More, NADPH oxidase-mediated generation of ROS is important for PSC activation (Asaumi et al., 2007; Masamune et al., 2008b). TRPC6 channels could therefore indirectly play a role in perpetuating PSC activation through NADPH oxidase activity regulation. Furthermore, the observation of TGF- β signalling in fibroblasts leading to elevated Ca^{2+} signalling through TRPC6 channels important for α SMA positive stress fibers (activation marker) is also of great interest (Davis et al., 2012). This is related to the activation of PSCs. First, α SMA is a marker of activation in PSCs and second, TGF- β is an important (autocrine) stimulant of PSC activity ([section 1.3.4](#)). TGF- β could be a TRPC6-dependent expressed stimulant under hypoxia in mPSCs and thereby explain the diminished autocrine effect observed in TRPC6^{-/-} mPSCs.

This study provides evidence for an autocrine stimulation defect in TRPC6^{-/-} mPSCs when hypoxia was induced chemically with DMOG ([figure 4.9](#)). This was confirmed by showing that conditioned medium from TRPC6^{-/-} mPSCs kept under hypoxic conditions was less potent in stimulating migration of WT mPSCs than that of WT cells ([figure 4.13 A-B](#)). More, it did not induce a smaller projected cell area as detected with conditioned medium from WT mPSCs and directional cell migration was diminished. However, it could induce the same elongated cell morphology ([figure 4.13, C-E](#)). This suggests, that some autocrine stimulants are secreted, but the major stimulants of mPSC migration are lacking. TRPC6 channels are therefore required for perpetuating mPSC activity under hypoxia by a *modifier* mechanism (illustrated in [figure 5.2](#)). This can either be elicited by: (i) a direct role of the TRPC6 channel in hypoxia-mediated growth factor/cytokine production and secretion or, (ii) loss of the TRPC6 channel leads to a lower activation

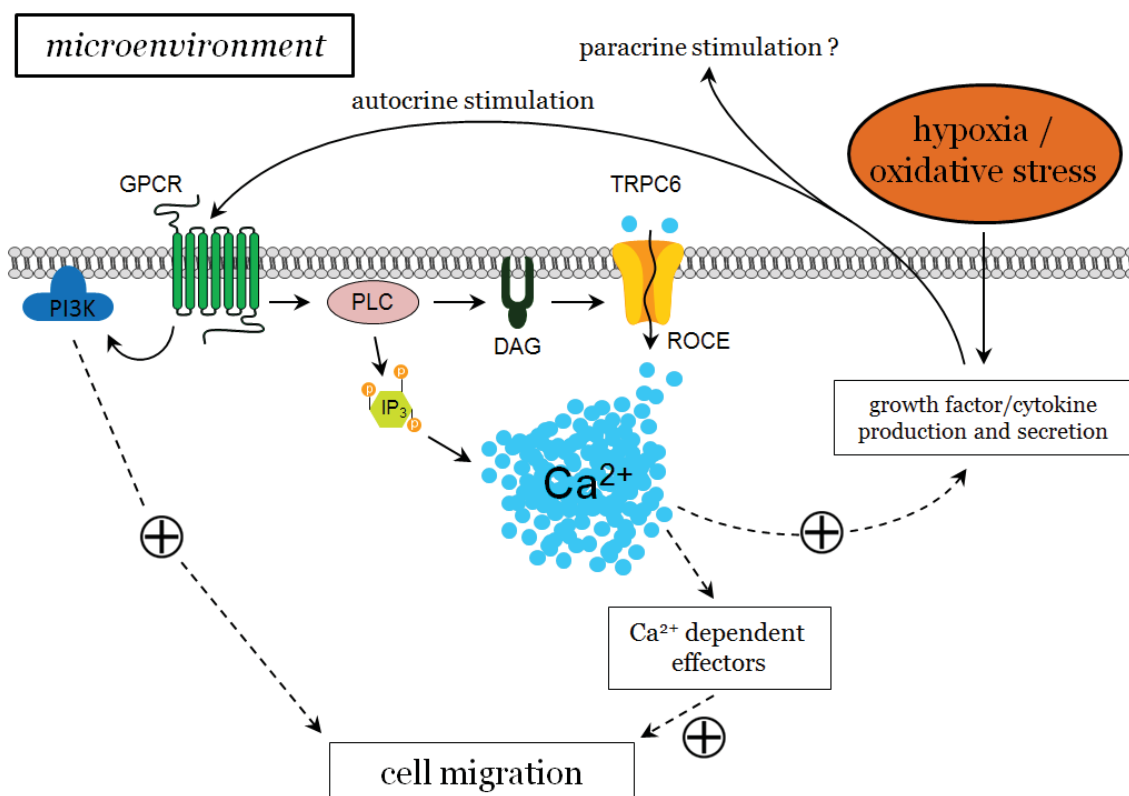


Figure 5.2. Illustration of the Role of TRPC6 Channels in mPSCs Under Hypoxic Stimulation. The TRPC6 channel is part of a possibly coupled *modifier* and *transduction/effector* mechanism activated in response to hypoxia in mPSCs. Hypoxia and oxidative stress can promote the secretion of autocrine stimulants binding to GPCR's leading to activation of PLC and formation of DAG and IP₃. IP₃ mediates Ca²⁺ efflux from the ER, whereas DAG directly binds to TRPC6 channels which promote Ca²⁺ influx (ROCE). The resulting increase of [Ca²⁺]_i induces the activation of signalling proteins important for cell migration. In addition, it drives the secretion of autocrine stimulants further stimulating PSC activity in a loop sequence. If these stimulants also elicit paracrine effects on PDAC cells remains elusive.

status under hypoxia, possibly by attenuated growth factor/cytokine signalling via a TRPC6 mediated *transduction/effector* pathway. This leads to lower levels of secreted autocrine stimulants important for stimulating PSC activation in a loop sequence. It could be interesting to determine if any paracrine signalling with PDAC cells is affected ([figure 5.2](#)). This would determine a role of TRPC6 channels in regulating the mutual signalling with PDAC cells, conclusively attenuating PDAC development and progression.

5.3.2.2 TRPC6 Channel: Important for Hypoxia-mediated Calcium Entry

It was investigated whether TRPC6 channels were required for mediating increased calcium influx during hypoxia in mPSCs. In hypoxically preconditioned WT mPSCs, the

level of calcium influx was increased (*figure 4.14*). This elevation in calcium influx, which was essentially absent in TRPC6^{-/-} mPSCs, may be important for the activation of Ca²⁺ sensitive effector proteins of the cellular migration machinery demonstrating a role of the TRPC6 channel in a *transduction/effector* pathway (illustrated in *figure 5.2*). For example, TRPC6-mediated reorganization of the cytoskeleton affecting cell migration is shown in neutrophils (Lindemann et al., 2013), glioblastoma (Chigurupati et al., 2010) and fibroblasts (Davis et al., 2012). This may also explain the attenuated morphological response to hypoxia, as WT mPSCs decreased their projected cell area under hypoxia stimulation, whereas TRPC6^{-/-} did not (*figure 4.7*).

It is not yet known, which mechanism lies behind the elevated TRPC6-dependent calcium influx under hypoxia in mPSCs. Since TRPC6 channel expression is unaffected, other mechanisms may be more relevant. SOCE members can interact and regulate TRPC6 function either directly or indirectly via the formation of heteromeric complexes including TRPC1 and STIM1 (Albarran et al., 2014; Yuan et al., 2007) and the STIM/ORAI complex (Jardin et al., 2009). Moreover, the functional expression of TRPC6 channels is coupled to SOCE (Chigurupati et al., 2010; Xu et al., 2014). Thus, additional studies measuring Ca²⁺ store-release and SOCE are needed to clarify whether TRPC6-mediated calcium influx is also a part of SOCE.

Accumulating evidence indicates that TRPC6 is involved in ROCE, and that it is activated directly by DAG via a PKC-independent mechanism (Dietrich and Gudermann, 2014; Hofmann et al., 1999). It has also been suggested that a stimulation of DAG production by GPCRs or RTKs is a prerequisite for oxygen sensing and signal transduction through TRPC6 channels in smooth muscle cells (Fuchs et al., 2011). Such a view supports the concept that hypoxia-induced TRPC6 activation is mediated by DAG accumulation, probably by activated phospholipases (Weissmann et al., 2006; Weissmann et al., 2011). However, Tang et al. could not verify such a role of DAG (Tang et al., 2010). They suggested instead, that the activation of TRPC6 is independent of PLC, but subsequent to an elevation in cellular AMP-activated kinase (AMPK) during hypoxia (Tang et al., 2010). The role of DAG in TRPC6 activation is therefore not definitive. Additional experiments with a DAG kinase inhibitor would clarify this mechanism in hypoxia activated mPSCs. Recent studies have also demonstrated that the TRPC6 channel represents a target of ROS (Graham et al., 2010; Wang et al., 2009; Wuensch et al., 2010), which is linked to PSC

activation ([section 1.3.4](#)). In all these scenarios the TRPC6 channel would function as *transducer/effector* and not as the primary hypoxia-sensor in mPSCs.

TRPC6 channels are non-selective cation channels that are also permeable for Na⁺. In rat aortic smooth muscle cells both global monotonic and localized transient [Na⁺]_i elevations were TRPC6-dependent (Poburko et al., 2007). The authors suggested, that Na⁺ entry via TRPC6-containing channels is a common response to a variety of phospholipase C-coupled receptors (Poburko et al., 2007). This can be a preserved mechanism in other cells such as PSCs. In this context it is interesting to note that Na⁺ is important for correct GPCR function. GPCRs contain a specific allosteric binding site for Na⁺, which can modulate agonist binding and thereby GPCR signal transduction (Katritch et al., 2014; Muller et al., 2012; Parker et al., 2008). From this it can be speculated that TRPC6-mediated Na⁺ entry could contribute to the correct function of GPCR receptors linked to autocrine stimulation pathways in PSC activation. In turn, GPCR induced DAG production activates TRPC6 channel activity. Loss of TRPC6 would therefore inhibit this loop of activation.

5.4 Future Objectives

The current study demonstrates that TRPC1 and TRPC6 channels are important for the response of mPSCs to hypoxia by contributing to distinct mechanisms underlying *sensor*, *modifier* and *transduction/effector* pathways regulating mPSC activation. However, some questions remain open. One of the future objectives is to further clarify the role of TRPC1 channels. This could be achieved by measuring SOCE in hypoxia-stimulated mPSCs in order to confirm a possible role of TRPC1 channels in this process. Moreover, it is not yet known which TRPC6-dependent autocrine stimulants are secreted by mPSCs and if these can also have paracrine effects on PDAC cells. Once the autocrine factors are identified, one could determine whether TRPC1 and TRPC6 channels are part of the intracellular *effector* pathways. These pieces of information are the final data sets needed for clarifying the role of the TRPC6 channel as *modifier* and/or *transducer* in hypoxia-stimulated migration of mPSCs.

The present study shows that TRPC1 and TRPC6 channels are not central components in the response of mPSCs to PDGF. Their involvement in the response to

other known stimulants of PSC activity such as EGF, FGF, TGF- β , VEGF, CTGF, ROS and several ILs is not yet known. However, many of these stimulants elicit their effects through GPCRs and RTKs leading to the activation of TRPC1 and TRPC6 channels (reviewed in (Dietrich and Gudermann, 2014; Nesin and Tsiokas, 2014)). For example, TRPC1 regulates cellular responses to EGF and fMLP (Bomben et al., 2011; Lindemann et al., 2015; Tajeddine and Gailly, 2012) and TRPC6 regulates responses to KC, VEGF and TGF- β (Davis et al., 2012; Hamdollah Zadeh et al., 2008; Lindemann et al., 2013). One way to identify TRPC6-dependent secreted growth factors and cytokines could be by comparing the supernatants from WT and TRPC6^{-/-} mPSCs. The most prominent candidate protein could then be tested in migration experiments. Comparing its stimulatory effect in WT and TRPC6^{-/-} mPSCs will show whether TRPC6 channels are – in addition to regulating growth factor/cytokine secretion – also play a role in its *transducer/effector* pathway.

The TRPC1- and TRPC6-mediated Ca²⁺ influx can regulate the reorganization of the cytoskeleton in cell movement and volume control. The identification of activated cytoskeletal effector proteins would thereby shed light upon the lacking morphological changes in TRPC1^{-/-} and TRPC6^{-/-} mPSCs under hypoxia stimulation. This regulation is primarily demonstrated by their effect on important signalling cascades including PI3K, MAPK and Rho, almost all of which depend on Ca²⁺ and affect cell migration (Falke and Ziemba, 2014). Activated PI3K generates PIP3 from PIP2. PIP3 activates the activity of Rac or Cdc42 via Guanine Nucleotide Exchange Factors (GEFs) such as Vav, Tiam1, PIX and p-REX (Benard et al., 1999; Fukata et al., 2003). The importance of GEF and Rho A signalling in actin dynamics and migration has been identified (Etienne-Manneville and Hall, 2002). MAPK signalling regulates the actomyosin network by activation of Rho and myosin-II (Li et al., 2013). In line with this, several studies showed that TRP channels elicit their effect on migration via these pathways. Examples include TRPM7-dependent polarization and migration of fibroblasts (Su et al., 2011) and TRPC1- and TRPC6-dependent chemotaxis of neutrophils (Damann et al., 2009; Lindemann et al., 2013). TRPC6 activity induces RhoA activation in smooth muscle cells (Jiang et al., 2014) and endothelial cells (Singh et al., 2007), which is important for cytoskeletal rearrangements. Moreover, TRPC6-mediated calcium influx increase RhoA activity which regulate fibroblast migration (Tian et al., 2010).

Many of these signalling cascades are implicated in PSC activation ([section 1.3.2](#)). Identification of a TRPC1- and/or TRPC6-dependent activation of such signalling cascades can improve the understanding of the mechanism by which these channels regulate mPSC migration under hypoxia. Preliminary studies have shown that WT mPSCs elicit elevated migratory activity in response to the GPCR CXCR2 ligand KC. A link is shown between KC, CXCR2 and TRPC6 activity in chemotaxis of murine neutrophils (Lindemann et al., 2013). Interestingly, KC (CXCL1) is upregulated in PDAC and mediates stimulating effects on pancreatic stromal fibroblasts leading to enhanced tumour growth. Inhibition of this KC-CXCR2 axis had a significant antitumor effect (Ijichi et al., 2011). These results suggest that inhibiting tumour-stromal interactions could be a promising therapeutic strategy for PDAC. This mechanism may be preserved in mPSCs as well. Moreover, in an entirely different experimental setup, inhibition of $K_{Ca}3.1$ led to a decrease in TRPC3-mediated calcium entry and lower PSC migratory activity. This TRPC3-mediated calcium influx was found to be required for calpain activity, thereby acting as the downstream Ca^{2+} effector in cell migration. Accordingly, calpain activity is also needed for efficient migration of fibroblasts (Glading et al., 2000), lymphocytes (Svensson et al., 2010), cervical cancer cells (Saraiva et al., 2013) and glioblastoma cells (Jang et al., 2010). This suggests that calpain may be a downstream effector of TRPC1- and/or TRPC6-mediated calcium entry in mPSCs migration under hypoxia stimulation.

Until now, most studies performed in other tumour stroma cells rely on 'proof of principle' experiments in 'normal' stroma cells showing that TRP channels are central for migration and/or growth factor secretion. Future experiments could therefore include *in vivo* experiments for further validation of the roles of TRPC1 and TRPC6 channels in PSC function in PDAC. Co-injection of TRPC1^{-/-} or TRPC6^{-/-} PSCs with PDAC cells into a murine PDAC model would clarify whether the two channels are required for PSCs to co-metastasise with PDAC cells. Furthermore, any signs of slower tumour progression, reduced tumour size or metastasis would indicate an important role of TRPC1 and/or TRPC6 channels in PSC function in PDAC. Such a finding would also argue for a protective role of inhibiting PSC function in PDAC.

Chapter 6

Concluding Remarks and Perspectives

Concluding Remarks and Perspectives

6.1 Conclusions

Cell migration is fundamental to cell and tissue homeostasis and therefore plays a vital role in many physiological and pathophysiological processes. On the other hand, uncontrolled migration or migration of an incorrect cell type can endanger the well-being of our body as observed in tumour metastasis and in the activation of stroma cells such as PSCs (Hanahan and Weinberg, 2011; Nielsen et al., 2014). Sustained PSC activation in PDAC leads to disturbance of the tissue architecture, primarily through increased deposition of connective tissue. This further leads to poor vascularization and thereby to the development of a progressively hypoxic and acidic TME (Apte et al., 2004; Vonlaufen et al., 2008b). In the view of PSCs, migration is a consequence of their activated state and a requirement for mutual signalling with cancer cells permissive for PDAC progression (Phillips et al., 2003b). Growing evidence supports a role of TRP channels in *sensing* and *modifying* the (tumour) microenvironment. More, by acting as Ca^{2+} permeable channels they are closely connected to cell migration as this is recognized as a Ca^{2+} dependent mechanism (Nielsen et al., 2014).

The overall aim for the studies described in this thesis was to decipher the role of TRPC1 and TRPC6 channels in regulating the responses of PSCs to hypoxia. This was postulated to occur through a *sensor*, *modifier* and/or *effector* mechanism mediated intracellular Ca^{2+} transients during hypoxic stimulation. This in turn could activate signalling pathways linked to cell migration and/or secretion of growth factors/cytokines that promote autocrine stimulation of PSCs. These data demonstrate for the first time that hypoxia-mediated increase of TRPC1 channel expression in mPSCs is coupled to elevated cell motility, possibly via a *sensor* mechanism. In addition, it seems TRPC1 is implicated in cell size regulation. Finally, TRPC6 channels are part of a *modifier* mechanism in mPSCs by being involved in efficient autocrine growth factor/cytokine secretion under hypoxia stimulation. More, TRPC6 channels are part of a *transduction/effector* pathway as they are required for increased calcium influx during hypoxia, which possibly activate Ca^{2+} sensitive effector proteins important for the cellular migration machinery.

In conclusion, the work described in this thesis supports the hypothesis TRPC1 and TRPC6 channels are important for the response of PSCs to hypoxia by contributing to distinct mechanisms underlying a *sensor*, *modifier* and *transduction/effector* pathways (illustrated in [figure 6.1](#)).

The results show a clear direction for future studies to further characterize the mechanistic role of TRPC1 and TRPC6 channels in mPSCs response to hypoxia. It is of great interest to: (i) determine which autocrine stimulants are secreted hypoxia- and TRPC6-dependently by mPSCs and whether TRPC6 channels are part of the intracellular effector

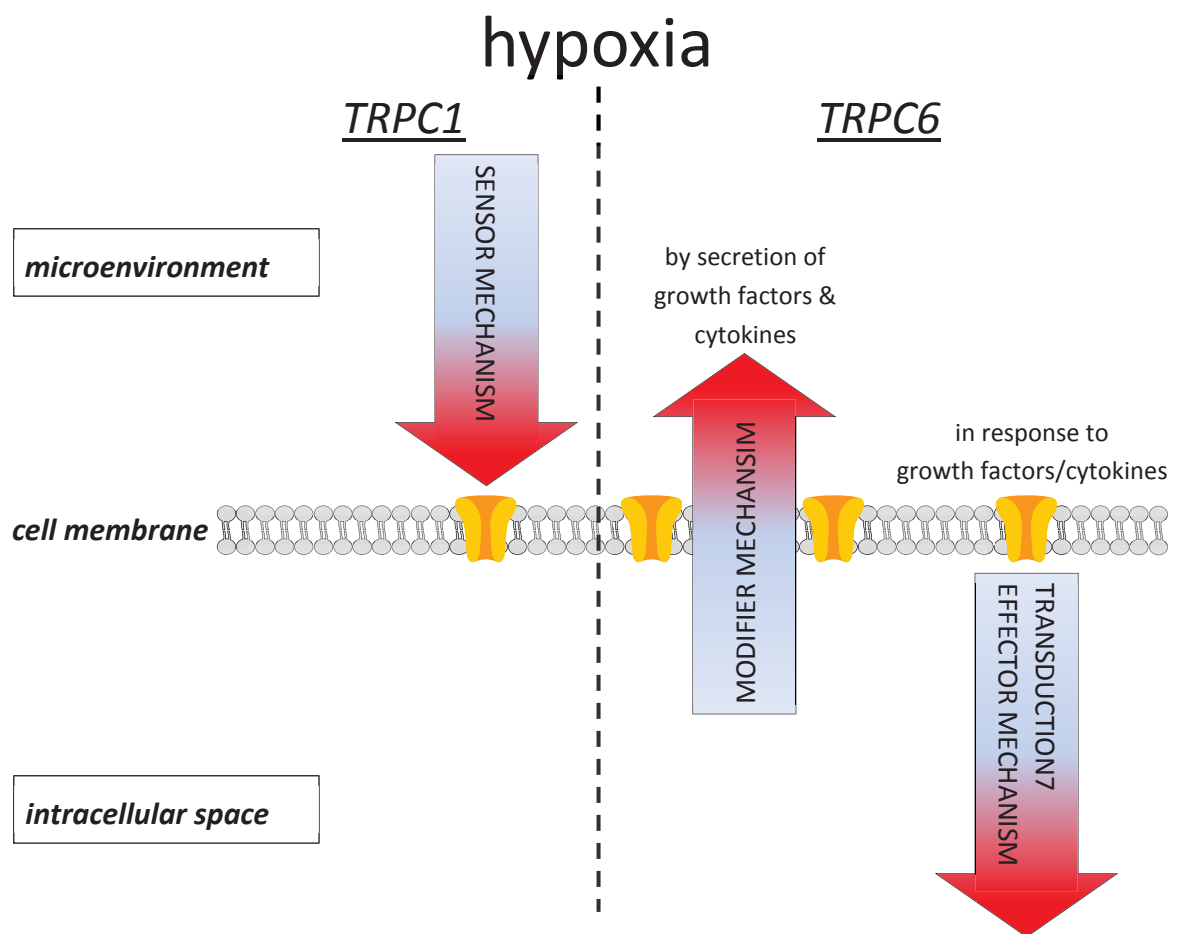


Figure 6.1. Overview of TRPC1 and TRPC6 Channels Functional Mechanism in mPSCs Under Hypoxic Stimulation. TRP channels are important components of cellular responses to the microenvironment and vice versa. Based on data in the present work the following mechanisms could be predicted for the role of TRPC1 and TRPC6 channels in the response of mPSCs to hypoxia: **(1)** The TRPC1 channel is part of an indirect *sensor* mechanism to hypoxia, **(2)** whereas the TRPC6 channels is part of a coupled *modifier* and *transduction/effector* mechanism by being involved in secretion of autocrine stimulants and mediating elevated calcium responses upon hypoxia stimulation (modified from [figure 1.8](#) in introduction).

pathways of these stimulants, (ii) identify TRPC1 channels contribution to calcium influx under hypoxia and (iii) determine TRPC1- and TRPC6-dependent downstream effector proteins important for cell migration.

6.2 Perspectives

It is logical that PSCs and the PDAC stroma are seen as important alternative therapeutic targets (Farrow et al., 2008; Feig et al., 2012). This is further highlighted by the observation that PSCs remain activated after *in vivo* chemoradiation (Cabrera et al., 2014) and perpetuate supporting microenvironments for PDAC stem cells survival (Lonardo et al., 2012). Thus, PDAC stem cells are shown to be major players in promoting PDAC formation and resistance (Hermann et al., 2007; Li et al., 2007a). Reprogramming PSCs and consequently the tumour stroma represents therefore a new paradigm that may be exploited to improve the outcome of PDAC therapy (Schober et al., 2014; Stromnes et al., 2014).

Promising results have been achieved in reprogramming PSCs to reprise their quiescent state, with increases in PDAC response to cancer therapy. Sherman et al. demonstrated that activation of the vitamin D receptor in PSCs acts as a genomic suppressor and inhibited PSC activation (Sherman et al., 2014). Retinoic acid induces quiescence and reduces PSC motility slowing tumour progression (Froeling et al., 2011). However, two recent publications question a tumour protective role of PSCs (Ozdemir et al., 2014; Rhim et al., 2014). Rhim et al. and Ozdemir et al. documented that removal of stroma promoting hedgehog signalling and depletion of PSCs, respectively, led to acceleration of PDAC progression in GEMMs. This was postulated to be caused by a decrease in desmoplasia subsequently leading to a more vascularized tumour, accelerated growth and metastasis, ultimately leading to poor survival (Coleman and Rhim, 2014; Ozdemir et al., 2014). These data underscore the complex role of PSCs in PDAC biology and demonstrate that their function is far from being completely understood. However, with the overall recognition of the tumour stroma role in PDAC progression, there has been a shift in the way treatment of advanced PDAC is viewed. For a long time gemcitabine has been the drug of choice (reviewed in (Jones et al., 2014; Oettle, 2014)). A recent phase III trial has shown convincing results that pave the way for

future treatment regimens that target not only the primary tumour but the surrounding stroma as well. A combination of Nab-paclitaxel (a stroma-targeted drug) plus gemcitabine (targeting PDAC cells) shows an increased survival rate ($p < 0.001$) compared to gemcitabine alone. The 1-year survival rate were 35% vs. 22%, and 9% vs. 4% at 2 years, respectively (Frese et al., 2012; Haqq et al., 2014; Oettle, 2014; Von Hoff et al., 2013; Von Hoff et al., 2011).

The prominent role of TRP channels in cancer can be related to the fact that the expression of TRP channels is frequently dysregulated in cancer in a stage and cancer type-dependent manner (Ouaïd-Ahidouch et al., 2013; Santoni and Farfariello, 2011; Van Haute et al., 2010). This property is shared with many other ion channels such as K^+ , Na^+ or Cl^- (Prevarskaya et al., 2010; Stock and Schwab, 2014). So far, there is relatively limited information about TRP channels in tumour stroma cells. Furthermore, as membrane proteins, TRPC channels are accessible from the extracellular side, which reduces the risk of multidrug resistance due to drug export from the cytoplasm. Targeting TRPC1 and TRPC6 channels expressed in both PDAC cells (unknown) and PSCs would offer the potential for a 'double hit' and break the vicious cycle of mutual PDAC and PSC cell stimulation. This is highlighted by the fact that these channels are not only involved in cell migration but also in other functions critical for cancer progression such as tumour cell proliferation. This has, among others, been observed for TRPC1 and TRPC6 in glioblastoma (Bomben and Sontheimer, 2010; Bomben et al., 2011; Chigurupati et al., 2010; Ding et al., 2010). Moreover, TRP channels are implicated in important functions of endothelial cells such as angiogenesis and vascularization of the tumour (Fiorio Pla et al., 2008; Fiorio Pla et al., 2012; Lodola et al., 2012) (reviewed in (Fiorio Pla and Gkika, 2013)).

Hypoxia and PSC activation are typical features of the PDAC stroma (Erkan et al., 2009; Fabian et al., 2012). The data present in this study identify a specific role of TRPC1 and/or TRPC6 channels in hypoxia-mediated activation of PSCs by distinct mechanisms. This brings new insights into several aspects of PSC biology and PDAC. Thus, further elucidation and identification of the functional role of TRP channels in hypoxia activated PSCs may lead to the development of new innovative tumour markers. Moreover, targeting PSCs and inhibiting their activity will indirectly also affect PDAC cells: (i) The mutual activation of PSCs and PDAC cells will be attenuated and (ii) inhibiting the PSC-mediated desmoplastic reaction will slow down tumour progression. Furthermore, it

highlights the importance of TRP channels in *sensing* (tumour) microenvironmental changes and in transducing the respective cellular responses in both tumour and stroma cells. This study therefore expands the knowledge and understanding of the functional diversity of TRP channels.

References

7. Reference List

- Ahern, M., P. Hall, and J. Halliday. 1996. Hepatic stellate cell nomenclature. *Hepatology*. 23:193.
- Albarran, L., N. Dionisio, E. Lopez, G.M. Salido, P.C. Redondo, and J.A. Rosado. 2014. STIM1 regulates TRPC6 heteromultimerization and subcellular location. *Biochem J*. 463:373-381.
- Alexakis, N., C. Halloran, M. Raraty, P. Ghaneh, R. Sutton, and J.P. Neoptolemos. 2004. Current standards of surgery for pancreatic cancer. *The British journal of surgery*. 91:1410-1427.
- Alves, F., U. Borchers, B. Padge, H. Augustin, K. Nebendahl, G. Kloppel, and L.F. Tietze. 2001. Inhibitory effect of a matrix metalloproteinase inhibitor on growth and spread of human pancreatic ductal adenocarcinoma evaluated in an orthotopic severe combined immunodeficient (SCID) mouse model. *Cancer Lett*. 165:161-170.
- Ambudkar, I.S. 2007. TRPC1: a core component of store-operated calcium channels. *Biochemical Society transactions*. 35:96-100.
- Ambudkar, I.S., and H.L. Ong. 2007. Organization and function of TRPC channelosomes. *Pflugers Arch*. 455:187-200.
- Anderson, T.W., A.N. Vaughan, and L.P. Cramer. 2008. Retrograde flow and myosin II activity within the leading cell edge deliver F-actin to the lamella to seed the formation of graded polarity actomyosin II filament bundles in migrating fibroblasts. *Mol Biol Cell*. 19:5006-5018.
- Andoh, A., H. Takaya, T. Saotome, M. Shimada, K. Hata, Y. Araki, F. Nakamura, Y. Shintani, Y. Fujiyama, and T. Bamba. 2000. Cytokine regulation of chemokine (IL-8, MCP-1, and RANTES) gene expression in human pancreatic periacinar myofibroblasts. *Gastroenterology*. 119:211-219.
- Aoki, H., H. Ohnishi, K. Hama, T. Ishijima, Y. Satoh, K. Hanatsuka, A. Ohashi, S. Wada, T. Miyata, H. Kita, H. Yamamoto, H. Osawa, K. Sato, K. Tamada, H. Yasuda, H. Mashima, and K. Sugano. 2006a. Autocrine loop between TGF-beta1 and IL-1beta through Smad3- and ERK-dependent pathways in rat pancreatic stellate cells. *Am J Physiol Cell Physiol*. 290:C1100-1108.
- Aoki, H., H. Ohnishi, K. Hama, S. Shinozaki, H. Kita, H. Osawa, H. Yamamoto, K. Sato, K. Tamada, and K. Sugano. 2007. Cyclooxygenase-2 is required for activated pancreatic stellate cells to respond to proinflammatory cytokines. *Am J Physiol Cell Physiol*. 292:C259-268.
- Aoki, H., H. Ohnishi, K. Hama, S. Shinozaki, H. Kita, H. Yamamoto, H. Osawa, K. Sato, K. Tamada, and K. Sugano. 2006b. Existence of autocrine loop between interleukin-6 and transforming growth factor-beta1 in activated rat pancreatic stellate cells. *Journal of cellular biochemistry*. 99:221-228.
- Apte, M.V., P.S. Haber, T.L. Applegate, I.D. Norton, G.W. McCaughan, M.A. Korsten, R.C. Pirola, and J.S. Wilson. 1998. Periacinar stellate shaped cells in rat pancreas: identification, isolation, and culture. *Gut*. 43:128-133.
- Apte, M.V., P.S. Haber, S.J. Darby, S.C. Rodgers, G.W. McCaughan, M.A. Korsten, R.C. Pirola, and J.S. Wilson. 1999. Pancreatic stellate cells are activated by proinflammatory cytokines: implications for pancreatic fibrogenesis. *Gut*. 44:534-541.
- Apte, M.V., S. Park, P.A. Phillips, N. Santucci, D. Goldstein, R.K. Kumar, G.A. Ramm, M. Buchler, H. Friess, J.A. McCarroll, G. Keogh, N. Merrett, R. Pirola, and J.S. Wilson. 2004. Desmoplastic reaction in pancreatic cancer: role of pancreatic stellate cells. *Pancreas*. 29:179-187.
- Apte, M.V., P.A. Phillips, R.G. Fahmy, S.J. Darby, S.C. Rodgers, G.W. McCaughan, M.A. Korsten, R.C. Pirola, D. Naidoo, and J.S. Wilson. 2000. Does alcohol directly stimulate pancreatic fibrogenesis? Studies with rat pancreatic stellate cells. *Gastroenterology*. 118:780-794.

- Apte, M.V., R.C. Pirola, and J.S. Wilson. 2012. Pancreatic stellate cells: a starring role in normal and diseased pancreas. *Front Physiol.* 3:344.
- Apte, M.V., and J.S. Wilson. 2011. Dangerous liaisons: pancreatic stellate cells and pancreatic cancer cells. *J Gastroenterol Hepatol.* 27 Suppl 2:69-74.
- Arcangeli, A. 2011. Ion channels and transporters in cancer. 3. Ion channels in the tumor cell-microenvironment cross talk. *Am J Physiol Cell Physiol.* 301:C762-771.
- Arcangeli, A., O. Crociani, and L. Bencini. 2014. Interaction of tumour cells with their microenvironment: ion channels and cell adhesion molecules. A focus on pancreatic cancer. *Philosophical transactions of the Royal Society of London. Series B, Biological sciences.* 369:20130101.
- Armstrong, T., G. Packham, L.B. Murphy, A.C. Bateman, J.A. Conti, D.R. Fine, C.D. Johnson, R.C. Benyon, and J.P. Iredale. 2004. Type I collagen promotes the malignant phenotype of pancreatic ductal adenocarcinoma. *Clin Cancer Res.* 10:7427-7437.
- Asaumi, H., S. Watanabe, M. Taguchi, M. Tashiro, and M. Otsuki. 2007. Externally applied pressure activates pancreatic stellate cells through the generation of intracellular reactive oxygen species. *Am J Physiol Gastrointest Liver Physiol.* 293:G972-978.
- Asgari, Y., Z. Zabihinpour, F. Schreiber, and A. Masoudi-Nejad. 2015. Alterations in cancer cell metabolism: The Warburg effect and metabolic adaptation. *Genomics.*
- Aumüller, G., G. Aust, J. Engele, J. Kirsch, G. Maio, A. Mayerhofer, S. Mense, D. Reißig, J. Salvetter, W. Schmidt, F. Schmitz, E. Schulte, K. Spanel-Borowski, G. Wennemuth, W. Wolff, L.J. Wurzinger, and H.-G. Zilch. 2014. Duale Reihe Anatomie. Thieme, Germany. 8 pp.
- Bachem, M.G., E. Schneider, H. Gross, H. Weidenbach, R.M. Schmid, A. Menke, M. Siech, H. Beger, A. Grunert, and G. Adler. 1998. Identification, culture, and characterization of pancreatic stellate cells in rats and humans. *Gastroenterology.* 115:421-432.
- Bachem, M.G., M. Schunemann, M. Ramadani, M. Siech, H. Beger, A. Buck, S. Zhou, A. Schmid-Kotsas, and G. Adler. 2005. Pancreatic carcinoma cells induce fibrosis by stimulating proliferation and matrix synthesis of stellate cells. *Gastroenterology.* 128:907-921.
- Bachem, M.G., S. Zhou, K. Buck, W. Schneiderhan, and M. Siech. 2008. Pancreatic stellate cells--role in pancreas cancer. *Langenbecks Arch Surg.* 393:891-900.
- Bachem, M.G., Z. Zhou, S. Zhou, and M. Siech. 2006. Role of stellate cells in pancreatic fibrogenesis associated with acute and chronic pancreatitis. *J Gastroenterol Hepatol.* 21 Suppl 3:S92-96.
- Bailey, J.M., B.J. Swanson, T. Hamada, J.P. Eggers, P.K. Singh, T. Caffery, M.M. Ouellette, and M.A. Hollingsworth. 2008. Sonic hedgehog promotes desmoplasia in pancreatic cancer. *Clin Cancer Res.* 14:5995-6004.
- Barugola, G., S. Partelli, S. Marcucci, N. Sartori, P. Capelli, C. Bassi, P. Pederzoli, and M. Falconi. 2009. Resectable pancreatic cancer: who really benefits from resection? *Annals of surgical oncology.* 16:3316-3322.
- Bauer, I., A. Grozio, D. Lasiglie, G. Basile, L. Sturla, M. Magnone, G. Sociali, D. Soncini, I. Caffa, A. Poggi, G. Zoppoli, M. Cea, G. Feldmann, R. Mostoslavsky, A. Ballestrero, F. Patrone, S. Bruzzone, and A. Nencioni. 2012. The NAD⁺-dependent histone deacetylase SIRT6 promotes cytokine production and migration in pancreatic cancer cells by regulating Ca²⁺ responses. *J Biol Chem.* 287:40924-40937.
- Becker, A.E., Y.G. Hernandez, H. Frucht, and A.L. Lucas. 2014. Pancreatic ductal adenocarcinoma: Risk factors, screening, and early detection. *World journal of gastroenterology : WJG.* 20:11182-11198.
- Benard, V., B.P. Bohl, and G.M. Bokoch. 1999. Characterization of rac and cdc42 activation in chemoattractant-stimulated human neutrophils using a novel assay for active GTPases. *J Biol Chem.* 274:13198-13204.
- Berchtold, S., B. Grunwald, A. Kruger, A. Reithmeier, T. Hahl, T. Cheng, A. Feuchtinger, D. Born, M. Erkan, J. Kleeff, and I. Esposito. 2015. Collagen type V promotes the malignant phenotype of pancreatic ductal adenocarcinoma. *Cancer Lett.* 356:721-732.

- Bernaldo de Quiros, S., A. Merlo, P. Secades, I. Zambrano, I.S. de Santa Maria, N. Ugidos, E. Jantus-Lewintre, R. Sirera, C. Suarez, and M.-D. Chiara. 2013. Identification of TRPC6 as a possible candidate target gene within an amplicon at 11q21-q22.2 for migratory capacity in head and neck squamous cell carcinomas. *BMC Cancer*. 13:116.
- Bi, Y., J. Li, B. Ji, N. Kang, L. Yang, D.A. Simonetto, J.H. Kwon, M. Kamath, S. Cao, and V. Shah. 2014. Sphingosine-1-phosphate mediates a reciprocal signaling pathway between stellate cells and cancer cells that promotes pancreatic cancer growth. *The American journal of pathology*. 184:2791-2802.
- Biankin, A.V., N. Waddell, K.S. Kassahn, M.C. Gingras, L.B. Muthuswamy, A.L. Johns, D.K. Miller, P.J. Wilson, A.M. Patch, J. Wu, D.K. Chang, M.J. Cowley, B.B. Gardiner, S. Song, I. Harliwong, S. Idrisoglu, C. Nourse, E. Nourbakhsh, S. Manning, S. Wani, M. Gongora, M. Pajic, C.J. Scarlett, A.J. Gill, A.V. Pinho, I. Rومان, M. Anderson, O. Holmes, C. Leonard, D. Taylor, S. Wood, Q. Xu, K. Nones, J.L. Fink, A. Christ, T. Bruxner, N. Cloonan, G. Kolle, F. Newell, M. Pinese, R.S. Mead, J.L. Humphris, W. Kaplan, M.D. Jones, E.K. Colvin, A.M. Nagrial, E.S. Humphrey, A. Chou, V.T. Chin, L.A. Chantrill, A. Mawson, J.S. Samra, J.G. Kench, J.A. Lovell, R.J. Daly, N.D. Merrett, C. Toon, K. Epari, N.Q. Nguyen, A. Barbour, N. Zeps, I. Australian Pancreatic Cancer Genome, N. Kakkar, F. Zhao, Y.Q. Wu, M. Wang, D.M. Muzny, W.E. Fisher, F.C. Brunicardi, S.E. Hodges, J.G. Reid, J. Drummond, K. Chang, Y. Han, L.R. Lewis, H. Dinh, C.J. Buhay, T. Beck, L. Timms, M. Sam, K. Begley, A. Brown, D. Pai, A. Panchal, N. Buchner, R. De Borja, R.E. Denroche, C.K. Yung, S. Serra, N. Onetto, D. Mukhopadhyay, M.S. Tsao, P.A. Shaw, G.M. Petersen, S. Gallinger, R.H. Hruban, A. Maitra, C.A. Iacobuzio-Donahue, R.D. Schulick, C.L. Wolfgang, et al. 2012. Pancreatic cancer genomes reveal aberrations in axon guidance pathway genes. *Nature*. 491:399-405.
- Bodding, M. 2007. TRP proteins and cancer. *Cell Signal*. 19:617-624.
- Bomben, V.C., and H. Sontheimer. 2010. Disruption of transient receptor potential canonical channel 1 causes incomplete cytokinesis and slows the growth of human malignant gliomas. *Glia*. 58:1145-1156.
- Bomben, V.C., K.L. Turner, T.T. Barclay, and H. Sontheimer. 2011. Transient receptor potential canonical channels are essential for chemotactic migration of human malignant gliomas. *J Cell Physiol*. 226:1879-1888.
- Boron, W.F., and E.L. Boulpaep. 2005. *Medical Physiology: A Cellular and Molecular Approach*. Elsevier Saunders, United States of America. 177 pp.
- Brabek, J., C.T. Mierke, D. Rosel, P. Vesely, and B. Fabry. 2010. The role of the tissue microenvironment in the regulation of cancer cell motility and invasion. *Cell Commun Signal*. 8:22.
- Brechard, S., C. Melchior, S. Plancon, V. Schenten, and E.J. Tschirhart. 2008. Store-operated Ca^{2+} channels formed by TRPC1, TRPC6 and Orai1 and non-store-operated channels formed by TRPC3 are involved in the regulation of NADPH oxidase in HL-60 granulocytes. *Cell Calcium*. 44:492-506.
- Broussard, J.A., D.J. Webb, and I. Kaverina. 2008. Asymmetric focal adhesion disassembly in motile cells. *Current opinion in cell biology*. 20:85-90.
- Bruenderman, E.H., and R.C. Martin, 2nd. 2014. High-risk population in sporadic pancreatic adenocarcinoma: guidelines for screening. *The Journal of surgical research*.
- Brundage, R.A., K.E. Fogarty, R.A. Tuft, and F.S. Fay. 1991. Calcium gradients underlying polarization and chemotaxis of eosinophils. *Science*. 254:703-706.
- Cabrera, M.C., E. Tilahun, R. Nakles, E.S. Diaz-Cruz, A. Charabaty, S. Suy, P. Jackson, L. Ley, R. Slack, R. Jha, S.P. Collins, N. Haddad, B.V. Kallakury, T. Schroeder, M.J. Pishvaian, and P.A. Furth. 2014. Human Pancreatic Cancer-Associated Stellate Cells Remain Activated after in vivo Chemoradiation. *Frontiers in oncology*. 4:102.
- Cahalan, M.D. 2009. STIMulating store-operated Ca^{2+} entry. *Nat Cell Biol*. 11:669-677.

- Cao, W.L., X.H. Xiang, K. Chen, W. Xu, and S.H. Xia. 2014. Potential role of NADPH oxidase in pathogenesis of pancreatitis. *World journal of gastrointestinal pathophysiology*. 5:169-177.
- Carpelan-Holmstrom, M., S. Nordling, E. Pukkala, R. Sankila, J. Luttges, G. Kloppel, and C. Haglund. 2005. Does anyone survive pancreatic ductal adenocarcinoma? A nationwide study re-evaluating the data of the Finnish Cancer Registry. *Gut*. 54:385-387.
- Chantome, A., M. Potier-Cartereau, L. Clarysse, G. Fromont, S. Marionneau-Lambot, M. Gueguinou, J.C. Pages, C. Collin, T. Oullier, A. Girault, F. Arbion, J.P. Haelters, P.A. Jaffres, M. Pinault, P. Besson, V. Joulin, P. Bougnoux, and C. Vandier. 2013. Pivotal role of the lipid Raft SK3-Orai1 complex in human cancer cell migration and bone metastases. *Cancer Res*. 73:4852-4861.
- Chen, J., and G.J. Barritt. 2003. Evidence that TRPC1 (transient receptor potential canonical 1) forms a Ca^{2+} -permeable channel linked to the regulation of cell volume in liver cells obtained using small interfering RNA targeted against TRPC1. *Biochem J*. 373:327-336.
- Cheng, K.T., X. Liu, H.L. Ong, W. Swaim, and I.S. Ambudkar. 2011. Local Ca^{2+} entry via Orai1 regulates plasma membrane recruitment of TRPC1 and controls cytosolic Ca^{2+} signals required for specific cell functions. *PLoS Biol*. 9:e1001025.
- Chigurupati, S., R. Venkataraman, D. Barrera, A. Naganathan, M. Madan, L. Paul, J.V. Pattisapu, G.A. Kyriazis, K. Sugaya, S. Bushnev, J.D. Lathia, J.N. Rich, and S.L. Chan. 2010. Receptor channel TRPC6 is a key mediator of Notch-driven glioblastoma growth and invasiveness. *Cancer Res*. 70:418-427.
- Chimote, A.A., P. Hajdu, V. Kucher, N. Boiko, Z. Kuras, O. Szilagyi, Y.H. Yun, and L. Conforti. 2013. Selective inhibition of KCa3.1 channels mediates adenosine regulation of the motility of human T cells. *J Immunol*. 191:6273-6280.
- Clapham, D.E. 2003. TRP channels as cellular sensors. *Nature*. 426:517-524.
- Clark, C.E., S.R. Hingorani, R. Mick, C. Combs, D.A. Tuveson, and R.H. Vonderheide. 2007. Dynamics of the immune reaction to pancreatic cancer from inception to invasion. *Cancer Res*. 67:9518-9527.
- Clark, K., M. Langeslag, B. van Leeuwen, L. Ran, A.G. Ryazanov, C.G. Figdor, W.H. Moolenaar, K. Jalink, and F.N. van Leeuwen. 2006. TRPM7, a novel regulator of actomyosin contractility and cell adhesion. *Embo J*. 25:290-301.
- Clark, K., J. Middelbeek, and F.N. van Leeuwen. 2008. Interplay between TRP channels and the cytoskeleton in health and disease. *Eur J Cell Biol*. 87:631-640.
- Coleman, S.J., and A.D. Rhim. 2014. Molecular biology of pancreatic ductal adenocarcinoma. *Current opinion in gastroenterology*. 30:506-510.
- Collisson, E.A., A. Sadanandam, P. Olson, W.J. Gibb, M. Truitt, S. Gu, J. Cooc, J. Weinkle, G.E. Kim, L. Jakkula, H.S. Feiler, A.H. Ko, A.B. Olshen, K.L. Danenberg, M.A. Tempero, P.T. Spellman, D. Hanahan, and J.W. Gray. 2011. Subtypes of pancreatic ductal adenocarcinoma and their differing responses to therapy. *Nature medicine*. 17:500-503.
- Cook, J.A., D. Gius, D.A. Wink, M.C. Krishna, A. Russo, and J.B. Mitchell. 2004. Oxidative stress, redox, and the tumor microenvironment. *Semin Radiat Oncol*. 14:259-266.
- Couvelard, A., D. O'Toole, R. Leek, H. Turley, A. Sauvanet, C. Degott, P. Ruzsiewicz, J. Belghiti, A.L. Harris, K. Gatter, and F. Pezzella. 2005. Expression of hypoxia-inducible factors is correlated with the presence of a fibrotic focus and angiogenesis in pancreatic ductal adenocarcinomas. *Histopathology*. 46:668-676.
- Cuddapah, V.A., K.L. Turner, and H. Sontheimer. 2013. Calcium entry via TRPC1 channels activates chloride currents in human glioma cells. *Cell Calcium*. 53:187-194.
- Damann, N., G. Owsianik, S. Li, C. Poll, and B. Nilius. 2009. The calcium-conducting ion channel transient receptor potential canonical 6 is involved in macrophage inflammatory protein-2-induced migration of mouse neutrophils. *Acta Physiol (Oxf)*. 195:3-11.

- Davis, J., A.R. Burr, G.F. Davis, L. Birnbaumer, and J.D. Molkenin. 2012. A TRPC6-dependent pathway for myofibroblast transdifferentiation and wound healing in vivo. *Dev Cell*. 23:705-715.
- DeHaven, W.I., B.F. Jones, J.G. Petranka, J.T. Smyth, T. Tomita, G.S. Bird, and J.W. Putney, Jr. 2009. TRPC channels function independently of STIM1 and Orai1. *The Journal of physiology*. 587:2275-2298.
- Dhennin-Duthille, I., M. Gautier, M. Faouzi, A. Guilbert, M. Brevet, D. Vaudry, A. Ahidouch, H. Sevestre, and H. Ouadid-Ahidouch. 2011. High expression of transient receptor potential channels in human breast cancer epithelial cells and tissues: correlation with pathological parameters. *Cell Physiol Biochem*. 28:813-822.
- Dietrich, A., V. Chubanov, H. Kalwa, B.R. Rost, and T. Gudermann. 2006. Cation channels of the transient receptor potential superfamily: their role in physiological and pathophysiological processes of smooth muscle cells. *Pharmacology & therapeutics*. 112:744-760.
- Dietrich, A., M. Fahlbusch, and T. Gudermann. 2014. Classical Transient Receptor Potential 1 (TRPC1): Channel or Channel Regulator? *Cells*. 3:939-962.
- Dietrich, A., and T. Gudermann. 2014. TRPC6: physiological function and pathophysiological relevance. *Handbook of experimental pharmacology*. 222:157-188.
- Dietrich, A., H. Kalwa, U. Storch, M. Mederos y Schnitzler, B. Salanova, O. Pinkenburg, G. Dubrovskaja, K. Essin, M. Gollasch, L. Birnbaumer, and T. Gudermann. 2007. Pressure-induced and store-operated cation influx in vascular smooth muscle cells is independent of TRPC1. *Pflugers Arch*. 455:465-477.
- Dietrich, A., Y.S.M. Mederos, M. Gollasch, V. Gross, U. Storch, G. Dubrovskaja, M. Obst, E. Yildirim, B. Salanova, H. Kalwa, K. Essin, O. Pinkenburg, F.C. Luft, T. Gudermann, and L. Birnbaumer. 2005. Increased vascular smooth muscle contractility in TRPC6^{-/-} mice. *Mol Cell Biol*. 25:6980-6989.
- Ding, X., Z. He, K. Zhou, J. Cheng, H. Yao, D. Lu, R. Cai, Y. Jin, B. Dong, Y. Xu, and Y. Wang. 2010. Essential role of TRPC6 channels in G2/M phase transition and development of human glioma. *J Natl Cancer Inst*. 102:1052-1068.
- Dong, H., K.N. Shim, J.M. Li, C. Estrema, T.A. Ornelas, F. Nguyen, S. Liu, S.L. Ramamoorthy, S. Ho, J.M. Carethers, and J.Y. Chow. 2010. Molecular mechanisms underlying Ca²⁺-mediated motility of human pancreatic duct cells. *Am J Physiol Cell Physiol*. 299:C1493-1503.
- Doyle, A.D., R.J. Petrie, M.L. Kutys, and K.M. Yamada. 2013. Dimensions in cell migration. *Current opinion in cell biology*. 25:642-649.
- Dreval, V., P. Dieterich, C. Stock, and A. Schwab. 2005. The role of Ca²⁺ transport across the plasma membrane for cell migration. *Cell Physiol Biochem*. 16:119-126.
- Duner, S., J. Lopatko Lindman, D. Ansari, C. Gundewar, and R. Andersson. 2011. Pancreatic cancer: the role of pancreatic stellate cells in tumor progression. *Pancreatology*. 10:673-681.
- Earley, S., B.J. Waldron, and J.E. Brayden. 2004. Critical role for transient receptor potential channel TRPM4 in myogenic constriction of cerebral arteries. *Circ Res*. 95:922-929.
- Edderkaoui, M., C. Nitsche, L. Zheng, S.J. Pandol, I. Gukovsky, and A.S. Gukovskaya. 2011. NADPH oxidase activation in pancreatic cancer cells is mediated through Akt-dependent up-regulation of p22phox. *J Biol Chem*. 286:7779-7787.
- Eddy, R.J., L.M. Pierini, F. Matsumura, and F.R. Maxfield. 2000. Ca²⁺-dependent myosin II activation is required for uropod retraction during neutrophil migration. *Journal of cell science*. 113 (Pt 7):1287-1298.
- Eguchi, D., N. Ikenaga, K. Ohuchida, S. Kozono, L. Cui, K. Fujiwara, M. Fujino, T. Ohtsuka, K. Mizumoto, and M. Tanaka. 2013. Hypoxia enhances the interaction between pancreatic stellate cells and cancer cells via increased secretion of connective tissue growth factor. *The Journal of surgical research*. 181:225-233.
- Eheman, C., S.J. Henley, R. Ballard-Barbash, E.J. Jacobs, M.J. Schymura, A.M. Noone, L. Pan, R.N. Anderson, J.E. Fulton, B.A. Kohler, A. Jemal, E. Ward, M. Plescia, L.A. Ries, and B.K. Edwards. 2012. Annual Report to the Nation on the status of cancer, 1975-2008, featuring

- cancers associated with excess weight and lack of sufficient physical activity. *Cancer*. 118:2338-2366.
- Ellenrieder, V., B. Alber, U. Lacher, S.F. Hendler, A. Menke, W. Boeck, M. Wagner, M. Wilda, H. Friess, M. Buchler, G. Adler, and T.M. Gress. 2000. Role of MT-MMPs and MMP-2 in pancreatic cancer progression. *International journal of cancer. Journal international du cancer*. 85:14-20.
- Elvidge, G.P., L. Glenny, R.J. Appelhoff, P.J. Ratcliffe, J. Ragoussis, and J.M. Gleadle. 2006. Concordant regulation of gene expression by hypoxia and 2-oxoglutarate-dependent dioxygenase inhibition: the role of HIF-1alpha, HIF-2alpha, and other pathways. *J Biol Chem*. 281:15215-15226.
- Erkan, M., C. Reiser-Erkan, C.W. Michalski, S. Deucker, D. Sauliunaite, S. Streit, I. Esposito, H. Friess, and J. Kleeff. 2009. Cancer-stellate cell interactions perpetuate the hypoxia-fibrosis cycle in pancreatic ductal adenocarcinoma. *Neoplasia*. 11:497-508.
- Erkan, M., C. Reiser-Erkan, C.W. Michalski, B. Kong, I. Esposito, H. Friess, and J. Kleeff. 2012. The impact of the activated stroma on pancreatic ductal adenocarcinoma biology and therapy resistance. *Current molecular medicine*. 12:288-303.
- Esposito, I., B. Konukiewitz, A.M. Schlitter, and G. Kloppel. 2014. Pathology of pancreatic ductal adenocarcinoma: Facts, challenges and future developments. *World journal of gastroenterology : WJG*. 20:13833-13841.
- Etienne-Manneville, S., and A. Hall. 2002. Rho GTPases in cell biology. *Nature*. 420:629-635.
- Fabian, A., J. Bertrand, O. Lindemann, T. Pap, and A. Schwab. 2012. Transient receptor potential canonical channel 1 impacts on mechanosignaling during cell migration. *Pflugers Arch*. 464:623-630.
- Fabian, A., T. Fortmann, E. Bulk, V.C. Bomben, H. Sontheimer, and A. Schwab. 2011. Chemotaxis of MDCK-F cells toward fibroblast growth factor-2 depends on transient receptor potential canonical channel 1. *Pflugers Arch*. 461:295-306.
- Fabian, A., T. Fortmann, P. Dieterich, C. Riethmuller, P. Schon, S. Mally, B. Nilius, and A. Schwab. 2008. TRPC1 channels regulate directionality of migrating cells. *Pflugers Arch*. 457:475-484.
- Falke, J.J., and B.P. Ziemba. 2014. Interplay between phosphoinositide lipids and calcium signals at the leading edge of chemotaxing ameboid cells. *Chem Phys Lipids*.
- Fang, L., S. Zhan, C. Huang, X. Cheng, X. Lv, H. Si, and J. Li. 2013. TRPM7 channel regulates PDGF-BB-induced proliferation of hepatic stellate cells via PI3K and ERK pathways. *Toxicology and applied pharmacology*. 272:713-725.
- Faouzi, M., and R. Penner. 2014. Trpm2. *Handbook of experimental pharmacology*. 222:403-426.
- Farrow, B., D. Albo, and D.H. Berger. 2008. The role of the tumor microenvironment in the progression of pancreatic cancer. *The Journal of surgical research*. 149:319-328.
- Farrow, B., D. Rowley, T. Dang, and D.H. Berger. 2009. Characterization of tumor-derived pancreatic stellate cells. *The Journal of surgical research*. 157:96-102.
- Fedeli, U., G. Zoppini, N. Gennaro, and M. Saugo. 2014. Diabetes and cancer mortality: A multifaceted association. *Diabetes research and clinical practice*. 106:e86-89.
- Feig, C., A. Gopinathan, A. Neesse, D.S. Chan, N. Cook, and D.A. Tuveson. 2012. The pancreas cancer microenvironment. *Clin Cancer Res*. 18:4266-4276.
- Feldmann, G., N. Habbe, S. Dhara, S. Bisht, H. Alvarez, V. Fendrich, R. Beaty, M. Mullendore, C. Karikari, N. Bardeesy, M.M. Ouellette, W. Yu, and A. Maitra. 2008. Hedgehog inhibition prolongs survival in a genetically engineered mouse model of pancreatic cancer. *Gut*. 57:1420-1430.
- Ferlay, J., D.M. Parkin, and E. Steliarova-Foucher. 2010. Estimates of cancer incidence and mortality in Europe in 2008. *European journal of cancer*. 46:765-781.
- Ferlay, J., I. Soerjomataram, R. Dikshit, S. Eser, C. Mathers, M. Rebelo, D.M. Parkin, D. Forman, and F. Bray. 2015. Cancer incidence and mortality worldwide: Sources, methods and

- major patterns in GLOBOCAN 2012. *International journal of cancer. Journal international du cancer*. 136:E359-386.
- Ferlay, J., E. Steliarova-Foucher, J. Lortet-Tieulent, S. Rosso, J.W. Coebergh, H. Comber, D. Forman, and F. Bray. 2013. Cancer incidence and mortality patterns in Europe: estimates for 40 countries in 2012. *European journal of cancer*. 49:1374-1403.
- Fiorio Pla, A., and D. Gkika. 2013. Emerging role of TRP channels in cell migration: from tumor vascularization to metastasis. *Front Physiol*. 4:311.
- Fiorio Pla, A., C. Grange, S. Antoniotti, C. Tomatis, A. Merlini, B. Bussolati, and L. Munaron. 2008. Arachidonic acid-induced Ca²⁺ entry is involved in early steps of tumor angiogenesis. *Mol Cancer Res*. 6:535-545.
- Fiorio Pla, A., D. Maric, S.C. Brazer, P. Giacobini, X. Liu, Y.H. Chang, I.S. Ambudkar, and J.L. Barker. 2005. Canonical transient receptor potential 1 plays a role in basic fibroblast growth factor (bFGF)/FGF receptor-1-induced Ca²⁺ entry and embryonic rat neural stem cell proliferation. *J Neurosci*. 25:2687-2701.
- Fiorio Pla, A., H.L. Ong, K.T. Cheng, A. Brossa, B. Bussolati, T. Lockwich, B. Paria, L. Munaron, and I.S. Ambudkar. 2012. TRPV4 mediates tumor-derived endothelial cell migration via arachidonic acid-activated actin remodeling. *Oncogene*. 31:200-212.
- Fiorio Pla, A., and D. Gkika. 2013. Emerging role of TRP channels in cell migration: from tumor vascularization to metastasis. *Frontiers in Physiology*. 4.
- Fraser, S.P., and L.A. Pardo. 2008. Ion channels: functional expression and therapeutic potential in cancer. Colloquium on Ion Channels and Cancer. *EMBO Rep*. 9:512-515.
- Freire, E., and T. Coelho-Sampaio. 2000. Self-assembly of laminin induced by acidic pH. *J Biol Chem*. 275:817-822.
- Frese, K.K., A. Neesse, N. Cook, T.E. Bapiro, M.P. Lolkema, D.I. Jodrell, and D.A. Tuveson. 2012. nab-Paclitaxel potentiates gemcitabine activity by reducing cytidine deaminase levels in a mouse model of pancreatic cancer. *Cancer discovery*. 2:260-269.
- Friedl, P., and S. Alexander. 2011. Cancer invasion and the microenvironment: plasticity and reciprocity. *Cell*. 147:992-1009.
- Friedl, P., and K. Wolf. 2009a. Plasticity of cell migration: a multiscale tuning model. *J Cell Biol*. 188:11-19.
- Friedl, P., and K. Wolf. 2009b. Proteolytic interstitial cell migration: a five-step process. *Cancer Metastasis Rev*. 28:129-135.
- Froeling, F.E., C. Feig, C. Chelala, R. Dobson, C.E. Mein, D.A. Tuveson, H. Clevers, I.R. Hart, and H.M. Kocher. 2011. Retinoic acid-induced pancreatic stellate cell quiescence reduces paracrine Wnt-beta-catenin signaling to slow tumor progression. *Gastroenterology*. 141:1486-1497, 1497 e1481-1414.
- Fuchs, B., M. Rupp, H.A. Ghofrani, R.T. Schermuly, W. Seeger, F. Grimminger, T. Gudermann, A. Dietrich, and N. Weissmann. 2011. Diacylglycerol regulates acute hypoxic pulmonary vasoconstriction via TRPC6. *Respiratory research*. 12:20.
- Fujita, H., K. Ohuchida, K. Mizumoto, T. Egami, K. Miyoshi, T. Moriyama, L. Cui, J. Yu, M. Zhao, T. Manabe, and M. Tanaka. 2009. Tumor-stromal interactions with direct cell contacts enhance proliferation of human pancreatic carcinoma cells. *Cancer science*. 100:2309-2317.
- Fukata, M., M. Nakagawa, and K. Kaibuchi. 2003. Roles of Rho-family GTPases in cell polarisation and directional migration. *Current opinion in cell biology*. 15:590-597.
- Gaggioli, C., S. Hooper, C. Hidalgo-Carcedo, R. Grosse, J.F. Marshall, K. Harrington, and E. Sahai. 2007. Fibroblast-led collective invasion of carcinoma cells with differing roles for RhoGTPases in leading and following cells. *Nat Cell Biol*. 9:1392-1400.
- Galli, A., D. Crabb, D. Price, E. Ceni, R. Salzano, C. Surrenti, and A. Casini. 2000. Peroxisome proliferator-activated receptor gamma transcriptional regulation is involved in platelet-derived growth factor-induced proliferation of human hepatic stellate cells. *Hepatology*. 31:101-108.

- Gao, Y.D., P.J. Hanley, S. Rinne, M. Zuzarte, and J. Daut. 2010. Calcium-activated K^+ channel $K_{Ca3.1}$ activity during Ca^{2+} store depletion and store-operated Ca^{2+} entry in human macrophages. *Cell Calcium*. 48:19-27.
- Gatenby, R.A., and R.J. Gillies. 2008. A microenvironmental model of carcinogenesis. *Nature reviews. Cancer*. 8:56-61.
- Giannone, G., P. Ronde, M. Gaire, J. Beaudouin, J. Haiech, J. Ellenberg, and K. Takeda. 2004. Calcium rises locally trigger focal adhesion disassembly and enhance residency of focal adhesion kinase at focal adhesions. *J Biol Chem*. 279:28715-28723.
- Giannone, G., P. Ronde, M. Gaire, J. Haiech, and K. Takeda. 2002. Calcium oscillations trigger focal adhesion disassembly in human U87 astrocytoma cells. *J Biol Chem*. 277:26364-26371.
- Glading, A., P. Chang, D.A. Lauffenburger, and A. Wells. 2000. Epidermal growth factor receptor activation of calpain is required for fibroblast motility and occurs via an ERK/MAP kinase signaling pathway. *J Biol Chem*. 275:2390-2398.
- Gomis, A., S. Soriano, C. Belmonte, and F. Viana. 2008. Hypoosmotic- and pressure-induced membrane stretch activate TRPC5 channels. *J Physiol*. 586:5633-5649.
- Goswami, C., M. Dreger, H. Otto, B. Schwappach, and F. Hucho. 2006. Rapid disassembly of dynamic microtubules upon activation of the capsaicin receptor TRPV1. *J Neurochem*. 96:254-266.
- Goswami, C., J. Kuhn, P.A. Heppenstall, and T. Hucho. 2010. Importance of non-selective cation channel TRPV4 interaction with cytoskeleton and their reciprocal regulations in cultured cells. *PLoS One*. 5:e11654.
- Graham, S., M. Ding, Y. Ding, S. Sours-Brothers, R. Luchowski, Z. Gryczynski, T. Yorio, H. Ma, and R. Ma. 2010. Canonical transient receptor potential 6 (TRPC6), a redox-regulated cation channel. *J Biol Chem*. 285:23466-23476.
- Grimm, C., R. Kraft, S. Sauerbruch, G. Schultz, and C. Harteneck. 2003. Molecular and functional characterization of the melastatin-related cation channel TRPM3. *J Biol Chem*. 278:21493-21501.
- Grinnell, F. 2008. Fibroblast mechanics in three-dimensional collagen matrices. *J Bodyw Mov Ther*. 12:191-193.
- Grutzmann, R., C. Pilarsky, O. Ammerpohl, J. Luttgies, A. Bohme, B. Sipos, M. Foerder, I. Alldinger, B. Jahnke, H.K. Schackert, H. Kalthoff, B. Kremer, G. Kloppel, and H.D. Saeger. 2004. Gene expression profiling of microdissected pancreatic ductal carcinomas using high-density DNA microarrays. *Neoplasia*. 6:611-622.
- Gupta, G.P., and J. Massague. 2006. Cancer metastasis: building a framework. *Cell*. 127:679-695.
- Haanes, K.A., A. Schwab, and I. Novak. 2012. The P2X7 receptor supports both life and death in fibrogenic pancreatic stellate cells. *PLoS one*. 7:e51164.
- Habisch, H., S. Zhou, M. Siech, and M.G. Bachem. 2010. Interaction of Stellate Cells with Pancreatic Carcinoma Cells. *cancers*. 2:1661-1682.
- Hakkinen, K.M., J.S. Harunaga, A.D. Doyle, and K.M. Yamada. 2011. Direct comparisons of the morphology, migration, cell adhesions, and actin cytoskeleton of fibroblasts in four different three-dimensional extracellular matrices. *Tissue engineering. Part A*. 17:713-724.
- Hamdollah Zadeh, M.A., C.A. Glass, A. Magnussen, J.C. Hancox, and D.O. Bates. 2008. VEGF-mediated elevated intracellular calcium and angiogenesis in human microvascular endothelial cells in vitro are inhibited by dominant negative TRPC6. *Microcirculation*. 15:605-614.
- Hammadi, M., V. Chopin, F. Matifat, I. Dhennin-Duthille, M. Chasseraud, H. Sevestre, and H. Ouadid-Ahidouch. 2012. Human ether à-gogo K^+ channel 1 (hEag1) regulates MDA-MB-231 breast cancer cell migration through Orai1-dependent calcium entry. *J Cell Physiol*. 227:3837-3846.
- Hanahan, D., and L.M. Coussens. 2012. Accessories to the crime: functions of cells recruited to the tumor microenvironment. *Cancer cell*. 21:309-322.
- Hanahan, D., and R.A. Weinberg. 2000. The hallmarks of cancer. *Cell*. 100:57-70.

- Hanahan, D., and R.A. Weinberg. 2011. Hallmarks of cancer: the next generation. *Cell*. 144:646-674.
- Happel, P., K. Moller, N.K. Schwering, and I.D. Dietzel. 2013. Migrating oligodendrocyte progenitor cells swell prior to soma dislocation. *Sci Rep*. 3:1806.
- Haqq, J., L.M. Howells, G. Garcea, M.S. Metcalfe, W.P. Steward, and A.R. Dennison. 2014. Pancreatic stellate cells and pancreas cancer: Current perspectives and future strategies. *European journal of cancer*.
- Haugk, B. 2010. Pancreatic intraepithelial neoplasia-can we detect early pancreatic cancer? *Histopathology*. 57:503-514.
- Hennigs, J.K., O. Seiz, J. Spiro, M.J. Berna, H.J. Baumann, H. Klose, and A. Pace. 2011. Molecular basis of P2-receptor-mediated calcium signaling in activated pancreatic stellate cells. *Pancreas*. 40:740-746.
- Hermann, P.C., S.L. Huber, T. Herrler, A. Aicher, J.W. Ellwart, M. Guba, C.J. Bruns, and C. Heeschen. 2007. Distinct populations of cancer stem cells determine tumor growth and metastatic activity in human pancreatic cancer. *Cell stem cell*. 1:313-323.
- Hidalgo, M. 2010. Pancreatic cancer. *The New England journal of medicine*. 362:1605-1617.
- Hild, B. 2015. Migration und Chemotaxis von Pankreatische Sternzellen, Medical Faculty of Münster. 1-58.
- Hill, C., A. Wurfel, J. Heger, B. Meyering, K.D. Schluter, M. Weber, P. Ferdinandy, A. Aronheim, R. Schulz, and G. Euler. 2013. Inhibition of AP-1 signaling by JDP2 overexpression protects cardiomyocytes against hypertrophy and apoptosis induction. *Cardiovascular research*. 99:121-128.
- Hofmann, T., A.G. Obukhov, M. Schaefer, C. Harteneck, T. Gudermann, and G. Schultz. 1999. Direct activation of human TRPC6 and TRPC3 channels by diacylglycerol. *Nature*. 397:259-263.
- Hruban, R.H., N.V. Adsay, J. Albores-Saavedra, M.R. Anver, A.V. Biankin, G.P. Boivin, E.E. Furth, T. Furukawa, A. Klein, D.S. Klimstra, G. Kloppel, G.Y. Lauwers, D.S. Longnecker, J. Luttges, A. Maitra, G.J. Offerhaus, L. Perez-Gallego, M. Redston, and D.A. Tuveson. 2006. Pathology of genetically engineered mouse models of pancreatic exocrine cancer: consensus report and recommendations. *Cancer Res*. 66:95-106.
- Hruban, R.H., N.V. Adsay, J. Albores-Saavedra, C. Compton, E.S. Garrett, S.N. Goodman, S.E. Kern, D.S. Klimstra, G. Kloppel, D.S. Longnecker, J. Luttges, and G.J. Offerhaus. 2001. Pancreatic intraepithelial neoplasia: a new nomenclature and classification system for pancreatic duct lesions. *The American journal of surgical pathology*. 25:579-586.
- Hruban, R.H., M. Goggins, J. Parsons, and S.E. Kern. 2000. Progression model for pancreatic cancer. *Clin Cancer Res*. 6:2969-2972.
- Hruban, R.H., A. Maitra, S.E. Kern, and M. Goggins. 2007. Precursors to pancreatic cancer. *Gastroenterology clinics of North America*. 36:831-849, vi.
- Hruban, R.H., A.D. van Mansfeld, G.J. Offerhaus, D.H. van Weering, D.C. Allison, S.N. Goodman, T.W. Kensler, K.K. Bose, J.L. Cameron, and J.L. Bos. 1993. K-ras oncogene activation in adenocarcinoma of the human pancreas. A study of 82 carcinomas using a combination of mutant-enriched polymerase chain reaction analysis and allele-specific oligonucleotide hybridization. *The American journal of pathology*. 143:545-554.
- Hurd, T.R., M. DeGennaro, and R. Lehmann. 2011. Redox regulation of cell migration and adhesion. *Trends Cell Biol*. 22:107-115.
- Hwang, R.F., T. Moore, T. Arumugam, V. Ramachandran, K.D. Amos, A. Rivera, B. Ji, D.B. Evans, and C.D. Logsdon. 2008. Cancer-associated stromal fibroblasts promote pancreatic tumor progression. *Cancer Res*. 68:918-926.
- Icard, P., P. Kafara, J.M. Steyaert, L. Schwartz, and H. Lincet. 2014. The metabolic cooperation between cells in solid cancer tumors. *Biochimica et biophysica acta*. 1846:216-225.
- Ide, T., Y. Kitajima, A. Miyoshi, T. Ohtsuka, M. Mitsuno, K. Ohtaka, Y. Koga, and K. Miyazaki. 2006. Tumor-stromal cell interaction under hypoxia increases the invasiveness of pancreatic

- cancer cells through the hepatocyte growth factor/c-Met pathway. *International journal of cancer. Journal internationale du cancer*. 119:2750-2759.
- Ijichi, H., A. Chytil, A.E. Gorska, M.E. Aakre, B. Bierie, M. Tada, D. Mohri, K. Miyabayashi, Y. Asaoka, S. Maeda, T. Ikenoue, K. Tateishi, C.V. Wright, K. Koike, M. Omata, and H.L. Moses. 2011. Inhibiting Cxcr2 disrupts tumor-stromal interactions and improves survival in a mouse model of pancreatic ductal adenocarcinoma. *J Clin Invest*. 121:4106-4117.
- Ikejiri, N. 1990. The vitamin A-storing cells in the human and rat pancreas. *The Kurume medical journal*. 37:67-81.
- Illina, O., and P. Friedl. 2009. Mechanisms of collective cell migration at a glance. *Journal of cell science*. 122:3203-3208.
- Itagaki, K., K.B. Kannan, B.B. Singh, and C.J. Hauser. 2004. Cytoskeletal reorganization internalizes multiple transient receptor potential channels and blocks calcium entry into human neutrophils. *J Immunol*. 172:601-607.
- Jacobsen, K.S., K. Zeeberg, D.R. Sauter, K.A. Poulsen, E.K. Hoffmann, and A. Schwab. 2013. The role of TMEM16A (ANO1) and TMEM16F (ANO6) in cell migration. *Pflugers Arch*. 465:1753-1762.
- Jang, H.S., S. Lal, and J.A. Greenwood. 2010. Calpain 2 is required for glioblastoma cell invasion: regulation of matrix metalloproteinase 2. *Neurochem Res*. 35:1796-1804.
- Jardin, I., L.J. Gomez, G.M. Salido, and J.A. Rosado. 2009. Dynamic interaction of hTRPC6 with the Orai1-STIM1 complex or hTRPC3 mediates its role in capacitative or non-capacitative Ca(2+) entry pathways. *Biochem J*. 420:267-276.
- Jardin, I., J.J. Lopez, G.M. Salido, and J.A. Rosado. 2008. Orai1 mediates the interaction between STIM1 and hTRPC1 and regulates the mode of activation of hTRPC1-forming Ca²⁺ channels. *J Biol Chem*. 283:25296-25304.
- Jaster, R. 2004. Molecular regulation of pancreatic stellate cell function. *Mol Cancer*. 3:26.
- Jaster, R., G. Sparmann, J. Emmrich, and S. Liebe. 2002. Extracellular signal regulated kinases are key mediators of mitogenic signals in rat pancreatic stellate cells. *Gut*. 51:579-584.
- Jemal, A., R. Siegel, E. Ward, Y. Hao, J. Xu, and M.J. Thun. 2009. Cancer statistics, 2009. *CA: a cancer journal for clinicians*. 59:225-249.
- Jesnowski, R., D. Furst, J. Ringel, Y. Chen, A. Schrodell, J. Kleeff, A. Kolb, W.D. Schareck, and M. Lohr. 2005. Immortalization of pancreatic stellate cells as an in vitro model of pancreatic fibrosis: deactivation is induced by matrigel and N-acetylcysteine. *Lab Invest*. 85:1276-1291.
- Jiang, Q., X. Fu, L. Tian, Y. Chen, K. Yang, X. Chen, J. Zhang, W. Lu, and J. Wang. 2014. NOX4 mediates BMP4-induced upregulation of TRPC1 and 6 protein expressions in distal pulmonary arterial smooth muscle cells. *PLoS one*. 9:e107135.
- Johnsen, I.K., M. Slawik, I. Shapiro, M.F. Hartmann, S.A. Wudy, B.D. Looyenga, G.D. Hammer, M. Reincke, and F. Beuschlein. 2006. Gonadectomy in mice of the inbred strain CE/J induces proliferation of sub-capsular adrenal cells expressing gonadal marker genes. *The Journal of endocrinology*. 190:47-57.
- Jones, O.P., J.D. Melling, and P. Ghaneh. 2014. Adjuvant therapy in pancreatic cancer. *World journal of gastroenterology : WJG*. 20:14733-14746.
- Jones, S., X. Zhang, D.W. Parsons, J.C. Lin, R.J. Leary, P. Angenendt, P. Mankoo, H. Carter, H. Kamiyama, A. Jimeno, S.M. Hong, B. Fu, M.T. Lin, E.S. Calhoun, M. Kamiyama, K. Walter, T. Nikolskaya, Y. Nikolsky, J. Hartigan, D.R. Smith, M. Hidalgo, S.D. Leach, A.P. Klein, E.M. Jaffee, M. Goggins, A. Maitra, C. Iacobuzio-Donahue, J.R. Eshleman, S.E. Kern, R.H. Hruban, R. Karchin, N. Papadopoulos, G. Parmigiani, B. Vogelstein, V.E. Velculescu, and K.W. Kinzler. 2008. Core signaling pathways in human pancreatic cancers revealed by global genomic analyses. *Science*. 321:1801-1806.
- Joyce, J.A., and J.W. Pollard. 2009. Microenvironmental regulation of metastasis. *Nature reviews. Cancer*. 9:239-252.
- Kalluri, R., and M. Zeisberg. 2006. Fibroblasts in cancer. *Nature reviews. Cancer*. 6:392-401.

- Katritch, V., G. Fenalti, E.E. Abola, B.L. Roth, V. Cherezov, and R.C. Stevens. 2014. Allosteric sodium in class A GPCR signaling. *Trends in biochemical sciences*. 39:233-244.
- Keren, K. 2011. Cell motility: the integrating role of the plasma membrane. *Eur Biophys J*. 40:1013-1027.
- Keren, K., Z. Pincus, G.M. Allen, E.L. Barnhart, G. Marriott, A. Mogilner, and J.A. Theriot. 2008. Mechanism of shape determination in motile cells. *Nature*. 453:475-480.
- Kessenbrock, K., V. Plaks, and Z. Werb. 2010. Matrix metalloproteinases: regulators of the tumor microenvironment. *Cell*. 141:52-67.
- Kharaishvili, G., D. Simkova, K. Bouchalova, M. Gachechiladze, N. Narsia, and J. Bouchal. 2014. The role of cancer-associated fibroblasts, solid stress and other microenvironmental factors in tumor progression and therapy resistance. *Cancer cell international*. 14:41.
- Kikuta, K., A. Masamune, M. Satoh, N. Suzuki, K. Satoh, and T. Shimosegawa. 2006. Hydrogen peroxide activates activator protein-1 and mitogen-activated protein kinases in pancreatic stellate cells. *Molecular and cellular biochemistry*. 291:11-20.
- Klimstra, D.S. 2007. Nonductal neoplasms of the pancreas. *Modern pathology : an official journal of the United States and Canadian Academy of Pathology, Inc*. 20 Suppl 1:S94-112.
- Klimstra, D.S., and D.S. Longnecker. 1994. K-ras mutations in pancreatic ductal proliferative lesions. *The American journal of pathology*. 145:1547-1550.
- Klonowski-Stumpe, H., R. Reinehr, R. Fischer, U. Warskulat, R. Luthen, and D. Haussinger. 2003. Production and effects of endothelin-1 in rat pancreatic stellate cells. *Pancreas*. 27:67-74.
- Knowles, H., J.W. Heizer, Y. Li, K. Chapman, C.A. Ogden, K. Andreasen, E. Shapland, G. Kucera, J. Mogan, J. Humann, L.L. Lenz, A.D. Morrison, and A.L. Perraud. 2011. Transient Receptor Potential Melastatin 2 (TRPM2) ion channel is required for innate immunity against *Listeria monocytogenes*. *Proc Natl Acad Sci U S A*. 108:11578-11583.
- Komuro, H., and T. Kumada. 2005. Ca²⁺ transients control CNS neuronal migration. *Cell Calcium*. 37:387-393.
- Komuro, H., and P. Rakic. 1998. Orchestration of neuronal migration by activity of ion channels, neurotransmitter receptors, and intracellular Ca²⁺ fluctuations. *J Neurobiol*. 37:110-130.
- Kondratska, K., A. Kondratskyi, M. Yassine, L. Lemonnier, G. Lepage, A. Morabito, R. Skryma, and N. Prevarskaya. 2014. Orai1 and STIM1 mediate SOCE and contribute to apoptotic resistance of pancreatic adenocarcinoma. *Biochimica et biophysica acta*. 1843:2263-2269.
- Kruse, M.L., P.B. Hildebrand, C. Timke, U.R. Folsch, and W.E. Schmidt. 2000. TGFbeta1 autocrine growth control in isolated pancreatic fibroblastoid cells/stellate cells in vitro. *Regulatory peptides*. 90:47-52.
- Kuehn, R., P.I. Lelkes, C. Bloechle, A. Niendorf, and J.R. Izbicki. 1999. Angiogenesis, angiogenic growth factors, and cell adhesion molecules are upregulated in chronic pancreatic diseases: angiogenesis in chronic pancreatitis and in pancreatic cancer. *Pancreas*. 18:96-103.
- Kuipers, A.J., J. Middelbeek, and F.N. van Leeuwen. 2012. Mechanoregulation of cytoskeletal dynamics by TRP channels. *Eur J Cell Biol*. 91:834-846.
- Kunert-Keil, C., F. Bisping, J. Kruger, and H. Brinkmeier. 2006. Tissue-specific expression of TRP channel genes in the mouse and its variation in three different mouse strains. *BMC Genomics*. 7:159.
- Kupffer, V.C. 1876. Ueber Sternzellen der Leber. Briefliche Mitteilung an Prof. Waldyer. *Arch mikr Anat*. 12:353-358.
- Kuras, Z., Y.H. Yun, A.A. Chimote, L. Neumeier, and L. Conforti. 2012. K_{Ca}3.1 and TRPM7 channels at the uropod regulate migration of activated human T cells. *PLoS One*. 7:e43859.
- Lammermann, T., B.L. Bader, S.J. Monkley, T. Worbs, R. Wedlich-Soldner, K. Hirsch, M. Keller, R. Forster, D.R. Critchley, R. Fassler, and M. Sixt. 2008. Rapid leukocyte migration by integrin-independent flowing and squeezing. *Nature*. 453:51-55.

- Landskron, G., M. De la Fuente, P. Thuwajit, C. Thuwajit, and M.A. Hermoso. 2014. Chronic inflammation and cytokines in the tumor microenvironment. *Journal of immunology research*. 2014:149185.
- Lauffenburger, D.A., and A.F. Horwitz. 1996. Cell migration: a physically integrated molecular process. *Cell*. 84:359-369.
- Launay, P., H. Cheng, S. Srivatsan, R. Penner, A. Fleig, and J.P. Kinet. 2004. TRPM4 regulates calcium oscillations after T cell activation. *Science*. 306:1374-1377.
- Lawson, M.A., and F.R. Maxfield. 1995. Ca^{2+} - and calcineurin-dependent recycling of an integrin to the front of migrating neutrophils. *Nature*. 377:75-79.
- Le Clainche, C., and M.F. Carlier. 2008. Regulation of actin assembly associated with protrusion and adhesion in cell migration. *Physiol Rev*. 88:489-513.
- Lee, M.G., E. Ohana, H.W. Park, D. Yang, and S. Muallem. 2012. Molecular mechanism of pancreatic and salivary gland fluid and HCO_3 secretion. *Physiol Rev*. 92:39-74.
- Li, C., D.G. Heidt, P. Dalerba, C.F. Burant, L. Zhang, V. Adsay, M. Wicha, M.F. Clarke, and D.M. Simeone. 2007a. Identification of pancreatic cancer stem cells. *Cancer Res*. 67:1030-1037.
- Li, H., X. Fan, and J. Houghton. 2007b. Tumor microenvironment: the role of the tumor stroma in cancer. *Journal of cellular biochemistry*. 101:805-815.
- Li, J., S. Zhang, X. Soto, S. Woolner, and E. Amaya. 2013. Erk and PI3K temporally coordinate different modes of actin-based motility during embryonic wound healing. *J Cell Sci*. 126(Pt 21):5005-5017.
- Li, S., Y. Ran, X. Zheng, X. Pang, Z. Wang, R. Zhang, and D. Zhu. 2010. 15-HETE mediates sub-acute hypoxia-induced TRPC1 expression and enhanced capacitative calcium entry in rat distal pulmonary arterial myocytes. *Prostaglandins & other lipid mediators*. 93:60-74.
- Liao, C., H. Yang, R. Zhang, H. Sun, B. Zhao, C. Gao, F. Zhu, and J. Jiao. 2012. The upregulation of TRPC6 contributes to Ca^{2+} signaling and actin assembly in human mesangial cells after chronic hypoxia. *Biochemical and biophysical research communications*. 421:750-756.
- Liedtke, W., Y. Choe, M.A. Marti-Renom, A.M. Bell, C.S. Denis, A. Sali, A.J. Hudspeth, J.M. Friedman, and S. Heller. 2000. Vanilloid receptor-related osmotically activated channel (VR-OAC), a candidate vertebrate osmoreceptor. *Cell*. 103:525-535.
- Lindemann, O., C. Strodthoff, M. Horstmann, N. Nielsen, F. Jung, S. Schimmelpfennig, M. Heitzmann, and A. Schwab. 2015. TRPC1 regulates fMLP-stimulated migration and chemotaxis of neutrophil granulocytes. *Biochimica et biophysica acta*.
- Lindemann, O., D. Umlauf, S. Frank, S. Schimmelpfennig, J. Bertrand, T. Pap, P.J. Hanley, A. Fabian, A. Dietrich, and A. Schwab. 2013. TRPC6 regulates CXCR2-mediated chemotaxis of murine neutrophils. *J Immunol*. 190:5496-5505.
- Liu, X., K.T. Cheng, B.C. Bandyopadhyay, B. Pani, A. Dietrich, B.C. Paria, W.D. Swaim, D. Beech, E. Yildirim, B.B. Singh, L. Birnbaumer, and I.S. Ambudkar. 2007. Attenuation of store-operated Ca^{2+} current impairs salivary gland fluid secretion in TRPC1(-/-) mice. *Proc Natl Acad Sci U S A*. 104:17542-17547.
- Livak, K.J., and T.D. Schmittgen. 2001. Analysis of relative gene expression data using real-time quantitative PCR and the $2^{-\Delta\Delta C(T)}$ Method. *Methods*. 25:402-408.
- Lodola, F., U. Laforenza, E. Bonetti, D. Lim, S. Dragoni, C. Bottino, H.L. Ong, G. Guerra, C. Ganini, M. Massa, M. Manzoni, I.S. Ambudkar, A.A. Genazzani, V. Rosti, P. Pedrazzoli, F. Tanzi, F. Moccia, and C. Porta. 2012. Store-operated Ca^{2+} entry is remodelled and controls in vitro angiogenesis in endothelial progenitor cells isolated from tumoral patients. *PLoS One*. 7:e42541.
- Lonardo, E., J. Frias-Aldeguer, P.C. Hermann, and C. Heeschen. 2012. Pancreatic stellate cells form a niche for cancer stem cells and promote their self-renewal and invasiveness. *Cell cycle*. 11:1282-1290.
- Lopez, J.J., G.M. Salido, J.A. Pariente, and J.A. Rosado. 2006. Interaction of STIM1 with endogenously expressed human canonical TRP1 upon depletion of intracellular Ca^{2+} stores. *J Biol Chem*. 281:28254-28264.

- Lowenfels, A.B., and P. Maisonneuve. 2006. Epidemiology and risk factors for pancreatic cancer. *Best practice & research. Clinical gastroenterology*. 20:197-209.
- Lu, W., J. Wang, L.A. Shimoda, and J.T. Sylvester. 2008. Differences in STIM1 and TRPC expression in proximal and distal pulmonary arterial smooth muscle are associated with differences in Ca²⁺ responses to hypoxia. *Am J Physiol Lung Cell Mol Physiol*. 295:L104-113.
- Lum, J.J., T. Bui, M. Gruber, J.D. Gordan, R.J. DeBerardinis, K.L. Covelto, M.C. Simon, and C.B. Thompson. 2007. The transcription factor HIF-1alpha plays a critical role in the growth factor-dependent regulation of both aerobic and anaerobic glycolysis. *Genes & development*. 21:1037-1049.
- Lunardi, S., N.B. Jamieson, S.Y. Lim, K.L. Griffiths, M. Carvalho-Gaspar, O. Al-Assar, S. Yameen, R.C. Carter, C.J. McKay, G. Spoletini, S. D'Ugo, M.A. Silva, O.J. Sansom, K.P. Janssen, R.J. Muschel, and T.B. Brunner. 2014. IP-10/CXCL10 induction in human pancreatic cancer stroma influences lymphocytes recruitment and correlates with poor survival. *Oncotarget*. 5:11064-11080.
- Luttenberger, T., A. Schmid-Kotsas, A. Menke, M. Siech, H. Beger, G. Adler, A. Grunert, and M.G. Bachem. 2000. Platelet-derived growth factors stimulate proliferation and extracellular matrix synthesis of pancreatic stellate cells: implications in pathogenesis of pancreas fibrosis. *Lab Invest*. 80:47-55.
- Mahadevan, D., and D.D. Von Hoff. 2007. Tumor-stroma interactions in pancreatic ductal adenocarcinoma. *Mol Cancer Ther*. 6:1186-1197.
- Maisonneuve, P., and A.B. Lowenfels. 2010. Epidemiology of pancreatic cancer: an update. *Digestive diseases*. 28:645-656.
- Maitra, A., N.V. Adsay, P. Argani, C. Iacobuzio-Donahue, A. De Marzo, J.L. Cameron, C.J. Yeo, and R.H. Hruban. 2003. Multicomponent analysis of the pancreatic adenocarcinoma progression model using a pancreatic intraepithelial neoplasia tissue microarray. *Modern pathology : an official journal of the United States and Canadian Academy of Pathology, Inc*. 16:902-912.
- Maitra, A., and R.H. Hruban. 2008. Pancreatic cancer. *Annu Rev Pathol*. 3:157-188.
- Maitra, A., S.E. Kern, and R.H. Hruban. 2006. Molecular pathogenesis of pancreatic cancer. *Best practice & research. Clinical gastroenterology*. 20:211-226.
- Malavasi, F., S. Deaglio, A. Funaro, E. Ferrero, A.L. Horenstein, E. Ortolan, T. Vaisitti, and S. Aydin. 2008. Evolution and function of the ADP ribosyl cyclase/CD38 gene family in physiology and pathology. *Physiol Rev*. 88:841-886.
- Malvezzi, M., P. Bertuccio, F. Levi, C. La Vecchia, and E. Negri. 2014. European cancer mortality predictions for the year 2014. *Annals of oncology : official journal of the European Society for Medical Oncology / ESMO*.
- Mantoni, T.S., S. Lunardi, O. Al-Assar, A. Masamune, and T.B. Brunner. 2011. Pancreatic stellate cells radioprotect pancreatic cancer cells through beta1-integrin signaling. *Cancer Res*. 71:3453-3458.
- Masamune, A., K. Kikuta, M. Satoh, K. Kume, and T. Shimosegawa. 2003a. Differential roles of signaling pathways for proliferation and migration of rat pancreatic stellate cells. *The Tohoku journal of experimental medicine*. 199:69-84.
- Masamune, A., K. Kikuta, M. Satoh, A. Satoh, and T. Shimosegawa. 2002. Alcohol activates activator protein-1 and mitogen-activated protein kinases in rat pancreatic stellate cells. *The Journal of pharmacology and experimental therapeutics*. 302:36-42.
- Masamune, A., K. Kikuta, M. Satoh, K. Satoh, and T. Shimosegawa. 2003b. Rho kinase inhibitors block activation of pancreatic stellate cells. *British journal of pharmacology*. 140:1292-1302.
- Masamune, A., K. Kikuta, T. Watanabe, K. Satoh, M. Hirota, S. Hamada, and T. Shimosegawa. 2009. Fibrinogen induces cytokine and collagen production in pancreatic stellate cells. *Gut*. 58:550-559.

- Masamune, A., K. Kikuta, T. Watanabe, K. Satoh, M. Hirota, and T. Shimosegawa. 2008a. Hypoxia stimulates pancreatic stellate cells to induce fibrosis and angiogenesis in pancreatic cancer. *Am J Physiol Gastrointest Liver Physiol.* 295:G709-717.
- Masamune, A., A. Satoh, T. Watanabe, K. Kikuta, M. Satoh, N. Suzuki, K. Satoh, and T. Shimosegawa. 2010. Effects of ethanol and its metabolites on human pancreatic stellate cells. *Digestive diseases and sciences.* 55:204-211.
- Masamune, A., and T. Shimosegawa. 2009. Signal transduction in pancreatic stellate cells. *J Gastroenterol.* 44:249-260.
- Masamune, A., T. Watanabe, K. Kikuta, K. Satoh, and T. Shimosegawa. 2008b. NADPH oxidase plays a crucial role in the activation of pancreatic stellate cells. *Am J Physiol Gastrointest Liver Physiol.* 294:G99-G108.
- Matthaios, D., P. Zarogoulidis, I. Balgouranidou, E. Chatzaki, and S. Kakolyris. 2011. Molecular pathogenesis of pancreatic cancer and clinical perspectives. *Oncology.* 81:259-272.
- Mazur, P.K., and J.T. Siveke. 2012. Genetically engineered mouse models of pancreatic cancer: unravelling tumour biology and progressing translational oncology. *Gut.* 61:1488-1500.
- Mazzochi, C., J.K. Bubien, P.R. Smith, and D.J. Benos. 2006. The carboxyl terminus of the alpha-subunit of the amiloride-sensitive epithelial sodium channel binds to F-actin. *J Biol Chem.* 281:6528-6538.
- McCarroll, J.A., P.A. Phillips, R.K. Kumar, S. Park, R.C. Pirola, J.S. Wilson, and M.V. Apte. 2004. Pancreatic stellate cell migration: role of the phosphatidylinositol 3-kinase(PI3-kinase) pathway. *Biochemical pharmacology.* 67:1215-1225.
- McMeekin, S.R., I. Dransfield, A.G. Rossi, C. Haslett, and T.R. Walker. 2006. E-selectin permits communication between PAF receptors and TRPC channels in human neutrophils. *Blood.* 107:4938-4945.
- Melzer, N., G. Hicking, K. Gobel, and H. Wiendl. 2012. TRPM2 cation channels modulate T cell effector functions and contribute to autoimmune CNS inflammation. *PLoS One.* 7:e47617.
- Merritt, J.E., R. Jacob, and T.J. Hallam. 1989. Use of manganese to discriminate between calcium influx and mobilization from internal stores in stimulated human neutrophils. *J Biol Chem.* 264:1522-1527.
- Mews, P., P. Phillips, R. Fahmy, M. Korsten, R. Pirola, J. Wilson, and M. Apte. 2002. Pancreatic stellate cells respond to inflammatory cytokines: potential role in chronic pancreatitis. *Gut.* 50:535-541.
- Middelbeek, J., A.J. Kuipers, L. Henneman, D. Visser, I. Eidhof, R. van Horssen, B. Wieringa, S.V. Canisius, W. Zwart, L.F. Wessels, F.C. Sweep, P. Bult, P.N. Span, F.N. van Leeuwen, and K. Jalink. 2012. TRPM7 is required for breast tumor cell metastasis. *Cancer Res.* 72:4250-4261.
- Mierke, C.T. 2012. Physical break-down of the classical view on cancer cell invasion and metastasis. *Eur J Cell Biol.* 92:89-104.
- Mihaljevic, A.L., C.W. Michalski, H. Friess, and J. Kleeff. 2010. Molecular mechanism of pancreatic cancer--understanding proliferation, invasion, and metastasis. *Langenbecks Arch Surg.* 395:295-308.
- Minke, B., and B. Cook. 2002. TRP channel proteins and signal transduction. *Physiol Rev.* 82:429-472.
- Monet, M., V. Lehen'kyi, F. Gackiere, V. Firllej, M. Vandenberghe, M. Roudbaraki, D. Gkika, A. Pourtier, G. Bidaux, C. Slomianny, P. Delcourt, F. Rassendren, J.P. Bergerat, J. Ceraline, F. Cabon, S. Humez, and N. Prevarskaya. 2010. Role of cationic channel TRPV2 in promoting prostate cancer migration and progression to androgen resistance. *Cancer Res.* 70:1225-1235.
- Montell, C., and G.M. Rubin. 1989. Molecular characterization of the *Drosophila* trp locus: a putative integral membrane protein required for phototransduction. *Neuron.* 2:1313-1323.

- Muller, C.E., A.C. Schiedel, and Y. Baqi. 2012. Allosteric modulators of rhodopsin-like G protein-coupled receptors: opportunities in drug development. *Pharmacology & therapeutics*. 135:292-315.
- Muraki, K., Y. Iwata, Y. Katanosaka, T. Ito, S. Ohya, M. Shigekawa, and Y. Imaizumi. 2003. TRPV2 is a component of osmotically sensitive cation channels in murine aortic myocytes. *Circ Res*. 93:829-838.
- Nabi, I.R. 1999. The polarization of the motile cell. *Journal of cell science*. 112 (Pt 12):1803-1811.
- Neesse, A., K.K. Frese, T.E. Bapiro, T. Nakagawa, M.D. Sternlicht, T.W. Seeley, C. Pilarsky, D.I. Jodrell, S.M. Spong, and D.A. Tuveson. 2013. CTGF antagonism with mAb FG-3019 enhances chemotherapy response without increasing drug delivery in murine ductal pancreas cancer. *Proc Natl Acad Sci U S A*. 110:12325-12330.
- Nesin, V., and L. Tsiokas. 2014. Trpc1. *Handbook of experimental pharmacology*. 222:15-51.
- Ng, L.C., K.G. O'Neill, D. French, J.A. Airey, C.A. Singer, H. Tian, X.M. Shen, and J.R. Hume. 2012. TRPC1 and Orai1 interact with STIM1 and mediate capacitative Ca²⁺ entry caused by acute hypoxia in mouse pulmonary arterial smooth muscle cells. *Am J Physiol Cell Physiol*. 303:C1156-1172.
- Nielsen, N., O. Lindemann, and A. Schwab. 2014. TRP channels and STIM/ORAI proteins: sensors and effectors of cancer and stroma cell migration. *British journal of pharmacology*. 171:5524-5540.
- Nilius, B., and G. Owsianik. 2011. The transient receptor potential family of ion channels. *Genome Biol*. 12:218.
- Nilius, B., and A. Szallasi. 2014. Transient receptor potential channels as drug targets: from the science of basic research to the art of medicine. *Pharmacological reviews*. 66:676-814.
- Nolz, J.C., T.S. Gomez, P. Zhu, S. Li, R.B. Medeiros, Y. Shimizu, J.K. Burkhardt, B.D. Freedman, and D.D. Billadeau. 2006. The WAVE2 complex regulates actin cytoskeletal reorganization and CRAC-mediated calcium entry during T cell activation. *Curr Biol*. 16:24-34.
- Novo, E., S. Cannito, E. Zamara, L. Valfre di Bonzo, A. Caligiuri, C. Cravanzola, A. Compagnone, S. Colombatto, F. Marra, M. Pinzani, and M. Parola. 2007. Proangiogenic cytokines as hypoxia-dependent factors stimulating migration of human hepatic stellate cells. *The American journal of pathology*. 170:1942-1953.
- Novo, E., D. Povero, C. Busletta, C. Paternostro, L.V. di Bonzo, S. Cannito, A. Compagnone, A. Bandino, F. Marra, S. Colombatto, E. David, M. Pinzani, and M. Parola. 2012. The biphasic nature of hypoxia-induced directional migration of activated human hepatic stellate cells. *The Journal of pathology*. 226:588-597.
- Numata, T., N. Ogawa, N. Takahashi, and Y. Mori. 2013. TRP channels as sensors of oxygen availability. *Pflugers Arch*. 465:1075-1085.
- Oettle, H. 2014. Progress in the knowledge and treatment of advanced pancreatic cancer: From benchside to bedside. *Cancer treatment reviews*.
- Ohnishi, N., T. Miyata, H. Ohnishi, H. Yasuda, K. Tamada, N. Ueda, H. Mashima, and K. Sugano. 2003. Activin A is an autocrine activator of rat pancreatic stellate cells: potential therapeutic role of follistatin for pancreatic fibrosis. *Gut*. 52:1487-1493.
- Olive, K.P., M.A. Jacobetz, C.J. Davidson, A. Gopinathan, D. McIntyre, D. Honess, B. Madhu, M.A. Goldgraben, M.E. Caldwell, D. Allard, K.K. Frese, G. Denicola, C. Feig, C. Combs, S.P. Winter, H. Ireland-Zecchini, S. Reichelt, W.J. Howat, A. Chang, M. Dhara, L. Wang, F. Ruckert, R. Grutzmann, C. Pilarsky, K. Izeradjene, S.R. Hingorani, P. Huang, S.E. Davies, W. Plunkett, M. Egorin, R.H. Hruban, N. Whitebread, K. McGovern, J. Adams, C. Iacobuzio-Donahue, J. Griffiths, and D.A. Tuveson. 2009. Inhibition of Hedgehog signaling enhances delivery of chemotherapy in a mouse model of pancreatic cancer. *Science*. 324:1457-1461.
- Omary, M.B., A. Lugea, A.W. Lowe, and S.J. Pandol. 2007. The pancreatic stellate cell: a star on the rise in pancreatic diseases. *J Clin Invest*. 117:50-59.

- Ong, H.L., K.T. Cheng, X. Liu, B.C. Bandyopadhyay, B.C. Paria, J. Soboloff, B. Pani, Y. Gwack, S. Srikanth, B.B. Singh, D.L. Gill, and I.S. Ambudkar. 2007. Dynamic assembly of TRPC1-STIM1-Orai1 ternary complex is involved in store-operated calcium influx. Evidence for similarities in store-operated and calcium release-activated calcium channel components. *J Biol Chem.* 282:9105-9116.
- Ottenhof, N.A., R.F. de Wilde, A. Maitra, R.H. Hruban, and G.J. Offerhaus. 2011. Molecular characteristics of pancreatic ductal adenocarcinoma. *Patholog Res Int.* 2011:620601.
- Ouadid-Ahidouch, H., I. Dhennin-Duthille, M. Gautier, H. Sevestre, and A. Ahidouch. 2013. TRP channels: diagnostic markers and therapeutic targets for breast cancer? *Trends Mol Med.* 19:117-124.
- Owsianik, G., K. Talavera, T. Voets, and B. Nilius. 2006. Permeation and selectivity of TRP channels. *Annu Rev Physiol.* 68:685-717.
- Ozdemir, B.C., T. Pentcheva-Hoang, J.L. Carstens, X. Zheng, C.C. Wu, T.R. Simpson, H. Laklai, H. Sugimoto, C. Kahlert, S.V. Novitskiy, A. De Jesus-Acosta, P. Sharma, P. Heidari, U. Mahmood, L. Chin, H.L. Moses, V.M. Weaver, A. Maitra, J.P. Allison, V.S. LeBleu, and R. Kalluri. 2014. Depletion of carcinoma-associated fibroblasts and fibrosis induces immunosuppression and accelerates pancreas cancer with reduced survival. *Cancer cell.* 25:719-734.
- Paget, S. 1889. The distribution of secondary growths in cancer of the breast. *The Lancet.* 133:571-573.
- Palecek, S.P., A. Huttenlocher, A.F. Horwitz, and D.A. Lauffenburger. 1998. Physical and biochemical regulation of integrin release during rear detachment of migrating cells. *Journal of cell science.* 111 (Pt 7):929-940.
- Parker, M.S., Y.Y. Wong, and S.L. Parker. 2008. An ion-responsive motif in the second transmembrane segment of rhodopsin-like receptors. *Amino acids.* 35:1-15.
- Partida-Sanchez, S., A. Gasser, R. Fliegert, C.C. Siebrands, W. Dammermann, G. Shi, B.J. Mousseau, A. Sumoza-Toledo, H. Bhagat, T.F. Walseth, A.H. Guse, and F.E. Lund. 2007. Chemotaxis of mouse bone marrow neutrophils and dendritic cells is controlled by adp-ribose, the major product generated by the CD38 enzyme reaction. *J Immunol.* 179:7827-7839.
- Pedersen, S.F., G. Owsianik, and B. Nilius. 2005. TRP channels: an overview. *Cell Calcium.* 38:233-252.
- Petrie, R.J., A.D. Doyle, and K.M. Yamada. 2009. Random versus directionally persistent cell migration. *Nat Rev Mol Cell Biol.* 10:538-549.
- Pettit, E.J., and F.S. Fay. 1998. Cytosolic free calcium and the cytoskeleton in the control of leukocyte chemotaxis. *Physiol Rev.* 78:949-967.
- Phillips, P.A., J.A. McCarroll, S. Park, M.J. Wu, R. Pirola, M. Korsten, J.S. Wilson, and M.V. Apte. 2003a. Rat pancreatic stellate cells secrete matrix metalloproteinases: implications for extracellular matrix turnover. *Gut.* 52:275-282.
- Phillips, P.A., M.J. Wu, R.K. Kumar, E. Doherty, J.A. McCarroll, S. Park, R.C. Pirola, J.S. Wilson, and M.V. Apte. 2003b. Cell migration: a novel aspect of pancreatic stellate cell biology. *Gut.* 52:677-682.
- Poburko, D., C.H. Liao, V.S. Lemos, E. Lin, Y. Maruyama, W.C. Cole, and C. van Breemen. 2007. Transient receptor potential channel 6-mediated, localized cytosolic [Na⁺] transients drive Na⁺/Ca²⁺ exchanger-mediated Ca²⁺ entry in purinergically stimulated aorta smooth muscle cells. *Circulation research.* 101:1030-1038.
- Pollard, T.D., and G.G. Borisy. 2003. Cellular motility driven by assembly and disassembly of actin filaments. *Cell.* 112:453-465.
- Prevarskaya, N., R. Skryma, and Y. Shuba. 2010. Ion channels and the hallmarks of cancer. *Trends Mol Med.* 16:107-121.
- Prevarskaya, N., L. Zhang, and G. Barritt. 2007. TRP channels in cancer. *Biochim Biophys Acta.* 1772:937-946.

- Qu, X., M.X. Yang, B.H. Kong, L. Qi, Q.L. Lam, S. Yan, P. Li, M. Zhang, and L. Lu. 2005. Hypoxia inhibits the migratory capacity of human monocyte-derived dendritic cells. *Immunology and cell biology*. 83:668-673.
- Rahib, L., B.D. Smith, R. Aizenberg, A.B. Rosenzweig, J.M. Fleshman, and L.M. Matrisian. 2014. Projecting cancer incidence and deaths to 2030: the unexpected burden of thyroid, liver, and pancreas cancers in the United States. *Cancer Res*. 74:2913-2921.
- Raimondi, S., P. Maisonneuve, and A.B. Lowenfels. 2009. Epidemiology of pancreatic cancer: an overview. *Nature reviews. Gastroenterology & hepatology*. 6:699-708.
- Rao, J.N., N. Rathor, T. Zou, L. Liu, L. Xiao, T.X. Yu, Y.H. Cui, and J.Y. Wang. 2010. STIM1 translocation to the plasma membrane enhances intestinal epithelial restitution by inducing TRPC1-mediated Ca^{2+} signaling after wounding. *Am J Physiol Cell Physiol*. 299:C579-588.
- Ray, P.D., B.W. Huang, and Y. Tsuji. 2012. Reactive oxygen species (ROS) homeostasis and redox regulation in cellular signaling. *Cell Signal*. 24:981-990.
- Rebours, V., M. Albuquerque, A. Sauvanet, P. Ruzsiewicz, P. Levy, V. Paradis, P. Bedossa, and A. Couvelard. 2013. Hypoxia pathways and cellular stress activate pancreatic stellate cells: development of an organotypic culture model of thick slices of normal human pancreas. *PloS one*. 8:e76229.
- Rhim, A.D., P.E. Oberstein, D.H. Thomas, E.T. Mirek, C.F. Palermo, S.A. Sastra, E.N. Dekleva, T. Saunders, C.P. Becerra, I.W. Tattersall, C.B. Westphalen, J. Kitajewski, M.G. Fernandez-Barrena, M.E. Fernandez-Zapico, C. Iacobuzio-Donahue, K.P. Olive, and B.Z. Stanger. 2014. Stromal elements act to restrain, rather than support, pancreatic ductal adenocarcinoma. *Cancer cell*. 25:735-747.
- Riches, K., M.E. Morley, N.A. Turner, D.J. O'Regan, S.G. Ball, C. Peers, and K.E. Porter. 2009. Chronic hypoxia inhibits MMP-2 activation and cellular invasion in human cardiac myofibroblasts. *Journal of molecular and cellular cardiology*. 47:391-399.
- Riopel, M.M., J. Li, S. Liu, A. Leask, and R. Wang. 2013. beta1 integrin-extracellular matrix interactions are essential for maintaining exocrine pancreas architecture and function. *Lab Invest*. 93:31-40.
- Roedding, A.S., A.F. Gao, W. Au-Yeung, T. Scarcelli, P.P. Li, and J.J. Warsh. 2012. Effect of oxidative stress on TRPM2 and TRPC3 channels in B lymphoblast cells in bipolar disorder. *Bipolar Disord*. 14:151-161.
- Rosser, B.G., S.P. Powers, and G.J. Gores. 1993. Calpain activity increases in hepatocytes following addition of ATP. Demonstration by a novel fluorescent approach. *J Biol Chem*. 268:23593-23600.
- Ryan, D.P., T.S. Hong, and N. Bardeesy. 2014. Pancreatic adenocarcinoma. *The New England journal of medicine*. 371:1039-1049.
- Saliba, Y., R. Karam, V. Smayra, G. Aftimos, J. Abramowitz, L. Birnbaumer, and N. Fares. 2014. Evidence of a Role for Fibroblast Transient Receptor Potential Canonical 3 Ca^{2+} Channel in Renal Fibrosis. *Journal of the American Society of Nephrology : JASN*.
- Santoni, G., and V. Farfariello. 2011. TRP channels and cancer: new targets for diagnosis and chemotherapy. *Endocr Metab Immune Disord Drug Targets*. 11:54-67.
- Saraiva, N., D.L. Prole, G. Carrara, B.F. Johnson, C.W. Taylor, M. Parsons, and G.L. Smith. 2013. hGAAP promotes cell adhesion and migration via the stimulation of store-operated Ca^{2+} entry and calpain 2. *J Cell Biol*. 202:699-713.
- Sasaki, S., N. Yui, and Y. Noda. 2014. Actin directly interacts with different membrane channel proteins and influences channel activities: AQP2 as a model. *Biochimica et biophysica acta*. 1838:514-520.
- Schafer, C., G. Rymarczyk, L. Ding, M.T. Kirber, and V.M. Bolotina. 2012. Role of molecular determinants of store-operated Ca^{2+} entry (Orai1, phospholipase A2 group 6, and STIM1) in focal adhesion formation and cell migration. *J Biol Chem*. 287:40745-40757.

- Schmidt, S., and P. Friedl. 2010. Interstitial cell migration: integrin-dependent and alternative adhesion mechanisms. *Cell Tissue Res.* 339:83-92.
- Schneider, E., A. Schmid-Kotsas, J. Zhao, H. Weidenbach, R.M. Schmid, A. Menke, G. Adler, J. Waltenberger, A. Grunert, and M.G. Bachem. 2001. Identification of mediators stimulating proliferation and matrix synthesis of rat pancreatic stellate cells. *Am J Physiol Cell Physiol.* 281:C532-543.
- Schneider, S.W., P. Pagel, C. Rotsch, T. Danker, H. Oberleithner, M. Radmacher, and A. Schwab. 2000. Volume dynamics in migrating epithelial cells measured with atomic force microscopy. *Pflugers Arch.* 439:297-303.
- Schneiderhan, W., F. Diaz, M. Fundel, S. Zhou, M. Siech, C. Hasel, P. Moller, J.E. Gschwend, T. Seufferlein, T. Gress, G. Adler, and M.G. Bachem. 2007. Pancreatic stellate cells are an important source of MMP-2 in human pancreatic cancer and accelerate tumor progression in a murine xenograft model and CAM assay. *Journal of cell science.* 120:512-519.
- Schober, M., R. Jesenofsky, R. Faissner, C. Weidenauer, W. Hagmann, P. Michl, R.L. Heuchel, S.L. Haas, and J.M. Lohr. 2014. Desmoplasia and chemoresistance in pancreatic cancer. *Cancers (Basel).* 6:2137-2154.
- Schofield, C.J., and P.J. Ratcliffe. 2004. Oxygen sensing by HIF hydroxylases. *Nat Rev Mol Cell Biol.* 5:343-354.
- Schwab, A., A. Fabian, P.J. Hanley, and C. Stock. 2012. Role of ion channels and transporters in cell migration. *Physiol Rev.* 92:1865-1913.
- Schwab, A., F. Finsterwalder, U. Kersting, T. Danker, and H. Oberleithner. 1997. Intracellular Ca²⁺ distribution in migrating transformed epithelial cells. *Pflugers Arch.* 434:70-76.
- Schwab, A., K. Gabriel, F. Finsterwalder, G. Folprecht, R. Greger, A. Kramer, and H. Oberleithner. 1995. Polarized ion transport during migration of transformed Madin-Darby canine kidney cells. *Pflugers Arch.* 430:802-807.
- Schwab, A., V. Nechyporuk-Zloy, A. Fabian, and C. Stock. 2007. Cells move when ions and water flow. *Pflugers Arch.* 453:421-432.
- Shek, F.W., R.C. Benyon, F.M. Walker, P.R. McCrudden, S.L. Pender, E.J. Williams, P.A. Johnson, C.D. Johnson, A.C. Bateman, D.R. Fine, and J.P. Iredale. 2002. Expression of transforming growth factor-beta 1 by pancreatic stellate cells and its implications for matrix secretion and turnover in chronic pancreatitis. *The American journal of pathology.* 160:1787-1798.
- Sherman, M.H., R.T. Yu, D.D. Engle, N. Ding, A.R. Atkins, H. Tiriach, E.A. Collisson, F. Connor, T. Van Dyke, S. Kozlov, P. Martin, T.W. Tseng, D.W. Dawson, T.R. Donahue, A. Masamune, T. Shimosegawa, M.V. Apte, J.S. Wilson, B. Ng, S.L. Lau, J.E. Gunton, G.M. Wahl, T. Hunter, J.A. Drebin, P.J. O'Dwyer, C. Liddle, D.A. Tuveson, M. Downes, and R.M. Evans. 2014. Vitamin d receptor-mediated stromal reprogramming suppresses pancreatitis and enhances pancreatic cancer therapy. *Cell.* 159:80-93.
- Shimizu, S., N. Takahashi, and Y. Mori. 2014. TRPs as chemosensors (ROS, RNS, RCS, gasotransmitters). *Handbook of experimental pharmacology.* 223:767-794.
- Shimoda, M., K.T. Mellody, and A. Orimo. 2010. Carcinoma-associated fibroblasts are a rate-limiting determinant for tumour progression. *Semin Cell Dev Biol.* 21:19-25.
- Shinozaki, S., H. Ohnishi, K. Hama, H. Kita, H. Yamamoto, H. Osawa, K. Sato, K. Tamada, H. Mashima, and K. Sugano. 2008. Indian hedgehog promotes the migration of rat activated pancreatic stellate cells by increasing membrane type-1 matrix metalloproteinase on the plasma membrane. *J Cell Physiol.* 216:38-46.
- Siddiqui, T.A., S. Lively, C. Vincent, and L.C. Schlichter. 2012. Regulation of podosome formation, microglial migration and invasion by Ca²⁺-signaling molecules expressed in podosomes. *J Neuroinflammation.* 9:250.
- Siegel, R.L., K.D. Miller, and A. Jemal. 2015. Cancer statistics, 2015. *CA: a cancer journal for clinicians.*

- Singh, I., N. Knezevic, G.U. Ahmmed, V. Kini, A.B. Malik, and D. Mehta. 2007. Galphaq-TRPC6-mediated Ca²⁺ entry induces RhoA activation and resultant endothelial cell shape change in response to thrombin. *J Biol Chem.* 282:7833-7843.
- Sleeman, J.P., G. Christofori, R. Fodde, J.G. Collard, G. Berx, C. Decraene, and C. Rugg. 2012. Concepts of metastasis in flux: the stromal progression model. *Semin Cancer Biol.* 22:174-186.
- Smani, T., N. Dionisio, J.J. Lopez, A. Berna-Erro, and J.A. Rosado. 2013. Cytoskeletal and scaffolding proteins as structural and functional determinants of TRP channels. *Biochim Biophys Acta.* 1838:658-664.
- Soboloff, J., B.S. Rothberg, M. Madesh, and D.L. Gill. 2012. STIM proteins: dynamic calcium signal transducers. *Nat Rev Mol Cell Biol.* 13:549-565.
- Soboloff, J., M.A. Spassova, X.D. Tang, T. Hewavitharana, W. Xu, and D.L. Gill. 2006. Orai1 and STIM reconstitute store-operated calcium channel function. *J Biol Chem.* 281:20661-20665.
- Song, Y., L. Zhan, M. Yu, C. Huang, X. Meng, T. Ma, L. Zhang, and J. Li. 2014. TRPV4 channel inhibits TGF-beta1-induced proliferation of hepatic stellate cells. *PLoS one.* 9:e101179.
- Sours-Brothers, S., M. Ding, S. Graham, and R. Ma. 2009. Interaction between TRPC1/TRPC4 assembly and STIM1 contributes to store-operated Ca²⁺ entry in mesangial cells. *Exp Biol Med (Maywood).* 234:673-682.
- Spassova, M.A., T. Hewavitharana, W. Xu, J. Soboloff, and D.L. Gill. 2006. A common mechanism underlies stretch activation and receptor activation of TRPC6 channels. *Proc Natl Acad Sci U S A.* 103:16586-16591.
- Stock, C., B. Gassner, C.R. Hauck, H. Arnold, S. Mally, J.A. Eble, P. Dieterich, and A. Schwab. 2005. Migration of human melanoma cells depends on extracellular pH and Na⁺/H⁺ exchange. *The Journal of physiology.* 567:225-238.
- Stock, C., F.T. Ludwig, P.J. Hanley, and A. Schwab. 2013. Roles of ion transport in control of cell motility. *Compr Physiol.* 3:59-119.
- Stock, C., and A. Schwab. 2014. Ion channels and transporters in metastasis. *Biochimica et biophysica acta.*
- Storch, U., A.L. Forst, M. Philipp, T. Gudermann, and M. Mederos y Schnitzler. 2012. Transient receptor potential channel 1 (TRPC1) reduces calcium permeability in heteromeric channel complexes. *J Biol Chem.* 287:3530-3540.
- Stromnes, I.M., K.E. DelGiorno, P.D. Greenberg, and S.R. Hingorani. 2014. Stromal reengineering to treat pancreas cancer. *Carcinogenesis.* 35:1451-1460.
- Su, L.T., W. Liu, H.C. Chen, O. Gonzalez-Pagan, R. Habas, and L.W. Runnels. 2011. TRPM7 regulates polarized cell movements. *Biochem J.* 434:513-521.
- Sukumaran, P., C. Lof, I. Pulli, K. Kemppainen, T. Viitanen, and K. Tornquist. 2013. Significance of the transient receptor potential canonical 2 (TRPC2) channel in the regulation of rat thyroid FRTL-5 cell proliferation, migration, adhesion and invasion. *Mol Cell Endocrinol.* 374:10-21.
- Svensson, L., A. McDowall, K.M. Giles, P. Stanley, S. Feske, and N. Hogg. 2010. Calpain 2 controls turnover of LFA-1 adhesions on migrating T lymphocytes. *PLoS one.* 5:e15090.
- Tahara, H., K. Sato, Y. Yamazaki, T. Ohyama, N. Horiguchi, H. Hashizume, S. Kakizaki, H. Takagi, I. Ozaki, H. Arai, J. Hirato, R. Jesenofsky, A. Masamune, and M. Mori. 2013. Transforming growth factor-alpha activates pancreatic stellate cells and may be involved in matrix metalloproteinase-1 upregulation. *Lab Invest.* 93:720-732.
- Tajeddine, N., and P. Gailly. 2012. TRPC1 protein channel is major regulator of epidermal growth factor receptor signaling. *J Biol Chem.* 287:16146-16157.
- Takahashi, K., K. Sakamoto, and J. Kimura. 2012a. Hypoxic stress induces transient receptor potential melastatin 2 (TRPM2) channel expression in adult rat cardiac fibroblasts. *J Pharmacol Sci.* 118:186-197.

- Takahashi, N., D. Kozai, and Y. Mori. 2012b. TRP channels: sensors and transducers of gasotransmitter signals. *Front Physiol.* 3:324.
- Takahashi, N., T. Kuwaki, S. Kiyonaka, T. Numata, D. Kozai, Y. Mizuno, S. Yamamoto, S. Naito, E. Knevels, P. Carmeliet, T. Oga, S. Kaneko, S. Suga, T. Nokami, J. Yoshida, and Y. Mori. 2011. TRPA1 underlies a sensing mechanism for O₂. *Nat Chem Biol.* 7:701-711.
- Takahashi, N., and Y. Mori. 2011. TRP Channels as Sensors and Signal Integrators of Redox Status Changes. *Frontiers in pharmacology.* 2:58.
- Tang, C., W.K. To, F. Meng, Y. Wang, and Y. Gu. 2010. A role for receptor-operated Ca²⁺ entry in human pulmonary artery smooth muscle cells in response to hypoxia. *Physiological research / Academia Scientiarum Bohemoslovaca.* 59:909-918.
- Tang, D., D. Wang, Z. Yuan, X. Xue, Y. Zhang, Y. An, J. Chen, M. Tu, Z. Lu, J. Wei, K. Jiang, and Y. Miao. 2012. Persistent activation of pancreatic stellate cells creates a microenvironment favorable for the malignant behavior of pancreatic ductal adenocarcinoma. *International journal of cancer. Journal international du cancer.* 132:993-1003.
- Tang, Y., J. Tang, Z. Chen, C. Trost, V. Flockerzi, M. Li, V. Ramesh, and M.X. Zhu. 2000. Association of mammalian trp4 and phospholipase C isozymes with a PDZ domain-containing protein, NHERF. *J Biol Chem.* 275:37559-37564.
- Tatum, J.L., G.J. Kelloff, R.J. Gillies, J.M. Arbeit, J.M. Brown, K.S. Chao, J.D. Chapman, W.C. Eckelman, A.W. Fyles, A.J. Giaccia, R.P. Hill, C.J. Koch, M.C. Krishna, K.A. Krohn, J.S. Lewis, R.P. Mason, G. Melillo, A.R. Padhani, G. Powis, J.G. Rajendran, R. Reba, S.P. Robinson, G.L. Semenza, H.M. Swartz, P. Vaupel, D. Yang, B. Croft, J. Hoffman, G. Liu, H. Stone, and D. Sullivan. 2006. Hypoxia: importance in tumor biology, noninvasive measurement by imaging, and value of its measurement in the management of cancer therapy. *Int J Radiat Biol.* 82:699-757.
- Tian, D., S.M. Jacobo, D. Billing, A. Rozkalne, S.D. Gage, T. Anagnostou, H. Pavenstadt, H.H. Hsu, J. Schlondorff, A. Ramos, and A. Greka. 2010. Antagonistic regulation of actin dynamics and cell motility by TRPC5 and TRPC6 channels. *Sci Signal.* 3:ra77.
- Tochhawng, L., S. Deng, S. Pervaiz, and C.T. Yap. 2013. Redox regulation of cancer cell migration and invasion. *Mitochondrion.* 13:246-253.
- Tsai, F.C., and T. Meyer. 2012. Ca²⁺ pulses control local cycles of lamellipodia retraction and adhesion along the front of migrating cells. *Curr Biol.* 22:837-842.
- Turner, K.L., and H. Sontheimer. 2013. K_{Ca}3.1 Modulates Neuroblast Migration Along the Rostral Migratory Stream (RMS) In Vivo. *Cereb Cortex.*
- Turner, L., C. Scotton, R. Negus, and F. Balkwill. 1999. Hypoxia inhibits macrophage migration. *European journal of immunology.* 29:2280-2287.
- Upadhyay, M., J. Samal, M. Kandpal, O.V. Singh, and P. Vivekanandan. 2013. The Warburg effect: insights from the past decade. *Pharmacology & therapeutics.* 137:318-330.
- Vaisitti, T., V. Audrito, S. Serra, C. Bologna, D. Brusa, F. Malavasi, and S. Deaglio. 2011. NAD⁺-metabolizing ecto-enzymes shape tumor-host interactions: the chronic lymphocytic leukemia model. *FEBS Lett.* 585:1514-1520.
- Van Haute, C., D. De Ridder, and B. Nilius. 2010. TRP channels in human prostate. *ScientificWorldJournal.* 10:1597-1611.
- van Heek, N.T., A.K. Meeker, S.E. Kern, C.J. Yeo, K.D. Lillemoe, J.L. Cameron, G.J. Offerhaus, J.L. Hicks, R.E. Wilentz, M.G. Goggins, A.M. De Marzo, R.H. Hruban, and A. Maitra. 2002. Telomere shortening is nearly universal in pancreatic intraepithelial neoplasia. *The American journal of pathology.* 161:1541-1547.
- Vandebrouck, A., J. Sabourin, J. Rivet, H. Balghi, S. Sebillé, A. Kitzis, G. Raymond, C. Cognard, N. Bourmeyster, and B. Constantin. 2007. Regulation of capacitative calcium entries by alpha1-syntrophin: association of TRPC1 with dystrophin complex and the PDZ domain of alpha1-syntrophin. *Faseb J.* 21:608-617.

- Vaquero, E.C., M. Edderkaoui, K.J. Nam, I. Gukovsky, S.J. Pandol, and A.S. Gukovskaya. 2003. Extracellular matrix proteins protect pancreatic cancer cells from death via mitochondrial and nonmitochondrial pathways. *Gastroenterology*. 125:1188-1202.
- Varga-Szabo, D., K.S. Authi, A. Braun, M. Bender, A. Ambily, S.R. Hassock, T. Gudermann, A. Dietrich, and B. Nieswandt. 2008. Store-operated Ca(2+) entry in platelets occurs independently of transient receptor potential (TRP) C1. *Pflugers Arch*. 457:377-387.
- Visser, B.C., V.R. Muthusamy, B.M. Yeh, F.V. Coakley, and L.W. Way. 2008. Diagnostic evaluation of cystic pancreatic lesions. *HPB : the official journal of the International Hepato Pancreato Biliary Association*. 10:63-69.
- Vogler, M., S. Vogel, S. Krull, K. Farhat, P. Leisering, S. Lutz, C.M. Wuertz, D.M. Katschinski, and A. Zieseniss. 2013. Hypoxia modulates fibroblastic architecture, adhesion and migration: a role for HIF-1alpha in cofilin regulation and cytoplasmic actin distribution. *PLoS one*. 8:e69128.
- Von Hoff, D.D., T. Ervin, F.P. Arena, E.G. Chiorean, J. Infante, M. Moore, T. Seay, S.A. Tjulandin, W.W. Ma, M.N. Saleh, M. Harris, M. Reni, S. Dowden, D. Laheru, N. Bahary, R.K. Ramanathan, J. Tabernero, M. Hidalgo, D. Goldstein, E. Van Cutsem, X. Wei, J. Iglesias, and M.F. Renschler. 2013. Increased survival in pancreatic cancer with nab-paclitaxel plus gemcitabine. *The New England journal of medicine*. 369:1691-1703.
- Von Hoff, D.D., R.K. Ramanathan, M.J. Borad, D.A. Laheru, L.S. Smith, T.E. Wood, R.L. Korn, N. Desai, V. Trieu, J.L. Iglesias, H. Zhang, P. Soon-Shiong, T. Shi, N.V. Rajeshkumar, A. Maitra, and M. Hidalgo. 2011. Gemcitabine plus nab-paclitaxel is an active regimen in patients with advanced pancreatic cancer: a phase I/II trial. *Journal of clinical oncology : official journal of the American Society of Clinical Oncology*. 29:4548-4554.
- Vonlaufen, A., S. Joshi, C. Qu, P.A. Phillips, Z. Xu, N.R. Parker, C.S. Toi, R.C. Pirola, J.S. Wilson, D. Goldstein, and M.V. Apte. 2008a. Pancreatic stellate cells: partners in crime with pancreatic cancer cells. *Cancer Res*. 68:2085-2093.
- Vonlaufen, A., P.A. Phillips, Z. Xu, D. Goldstein, R.C. Pirola, J.S. Wilson, and M.V. Apte. 2008b. Pancreatic stellate cells and pancreatic cancer cells: an unholy alliance. *Cancer Res*. 68:7707-7710.
- Vonlaufen, A., P.A. Phillips, L. Yang, Z. Xu, E. Fiala-Beer, X. Zhang, R.C. Pirola, J.S. Wilson, and M.V. Apte. 2010. Isolation of quiescent human pancreatic stellate cells: a promising in vitro tool for studies of human pancreatic stellate cell biology. *Pancreatology*. 10:434-443.
- Wake, K. 1971. "Sternzellen" in the liver: perisinusoidal cells with special reference to storage of vitamin A. *The American journal of anatomy*. 132:429-462.
- Wang, J., L. Weigand, W. Lu, J.T. Sylvester, G.L. Semenza, and L.A. Shimoda. 2006. Hypoxia inducible factor 1 mediates hypoxia-induced TRPC expression and elevated intracellular Ca2+ in pulmonary arterial smooth muscle cells. *Circulation research*. 98:1528-1537.
- Wang, Y., Y. Huang, F. Guan, Y. Xiao, J. Deng, H. Chen, X. Chen, J. Li, H. Huang, and C. Shi. 2013. Hypoxia-inducible factor-1alpha and MAPK co-regulate activation of hepatic stellate cells upon hypoxia stimulation. *PLoS one*. 8:e74051.
- Wang, Z., X. Wei, Y. Zhang, X. Ma, B. Li, S. Zhang, P. Du, X. Zhang, and F. Yi. 2009. NADPH oxidase-derived ROS contributes to upregulation of TRPC6 expression in puromycin aminonucleoside-induced podocyte injury. *Cell Physiol Biochem*. 24:619-626.
- Wanitchakool, P., L. Wolf, G.E. Koehl, L. Sirianant, R. Schreiber, S. Kulkarni, U. Duvvuri, and K. Kunzelmann. 2014. Role of anoctamins in cancer and apoptosis. *Philosophical transactions of the Royal Society of London. Series B, Biological sciences*. 369:20130096.
- Watanabe, S., Y. Nagashio, H. Asaumi, Y. Nomiya, M. Taguchi, M. Tashiro, Y. Kihara, H. Nakamura, and M. Otsuki. 2004. Pressure activates rat pancreatic stellate cells. *Am J Physiol Gastrointest Liver Physiol*. 287:G1175-1181.
- Watari, N., Y. Hotta, and Y. Mabuchi. 1982. Morphological studies on a vitamin A-storing cell and its complex with macrophage observed in mouse pancreatic tissues following excess vitamin A administration. *Okajimas folia anatomica Japonica*. 58:837-858.

- Watkins, S., and H. Sontheimer. 2011. Hydrodynamic cellular volume changes enable glioma cell invasion. *J Neurosci.* 31:17250-17259.
- Webb, J.D., M.L. Coleman, and C.W. Pugh. 2009. Hypoxia, hypoxia-inducible factors (HIF), HIF hydroxylases and oxygen sensing. *Cellular and molecular life sciences : CMLS.* 66:3539-3554.
- Weber, K.S., K. Hildner, K.M. Murphy, and P.M. Allen. 2010. Trpm4 differentially regulates Th1 and Th2 function by altering calcium signaling and NFAT localization. *J Immunol.* 185:2836-2846.
- Wehr, A.Y., E.E. Furth, V. Sangar, I.A. Blair, and K.H. Yu. 2011. Analysis of the human pancreatic stellate cell secreted proteome. *Pancreas.* 40:557-566.
- Wehrhahn, J., R. Kraft, C. Harteneck, and S. Hauschildt. 2010. Transient receptor potential melastatin 2 is required for lipopolysaccharide-induced cytokine production in human monocytes. *J Immunol.* 184:2386-2393.
- Wei, C., X. Wang, M. Chen, K. Ouyang, L.S. Song, and H. Cheng. 2009. Calcium flickers steer cell migration. *Nature.* 457:901-905.
- Weihuang, Y., S.J. Chang, H.I. Harn, H.T. Huang, H.H. Lin, M.R. Shen, M.J. Tang, and W.T. Chiu. 2015. MechanosensitiveStore-Operated Calcium Entry Regulatesthe Formation of Cell Polarity. *J Cell Physiol.*
- Weissmann, N., A. Dietrich, B. Fuchs, H. Kalwa, M. Ay, R. Dumitrascu, A. Olschewski, U. Storch, M. Mederos y Schnitzler, H.A. Ghofrani, R.T. Schermuly, O. Pinkenburg, W. Seeger, F. Grimminger, and T. Gudermann. 2006. Classical transient receptor potential channel 6 (TRPC6) is essential for hypoxic pulmonary vasoconstriction and alveolar gas exchange. *Proc Natl Acad Sci U S A.* 103:19093-19098.
- Weissmann, N., A. Sydykov, H. Kalwa, U. Storch, B. Fuchs, M. Mederos y Schnitzler, R.P. Brandes, F. Grimminger, M. Meissner, M. Freichel, S. Offermanns, F. Veit, O. Pak, K.H. Krause, R.T. Schermuly, A.C. Brewer, H.H. Schmidt, W. Seeger, A.M. Shah, T. Gudermann, H.A. Ghofrani, and A. Dietrich. 2011. Activation of TRPC6 channels is essential for lung ischaemia-reperfusion induced oedema in mice. *Nat Commun.* 3:649.
- Wells, A., A. Huttenlocher, and D.A. Lauffenburger. 2005. Calpain proteases in cell adhesion and motility. *Int Rev Cytol.* 245:1-16.
- Werfel, J., S. Krause, A.G. Bischof, R.J. Mannix, H. Tobin, Y. Bar-Yam, R.M. Bellin, and D.E. Ingber. 2013. How changes in extracellular matrix mechanics and gene expression variability might combine to drive cancer progression. *PLoS one.* 8:e76122.
- Wes, P.D., J. Chevesich, A. Jeromin, C. Rosenberg, G. Stetten, and C. Montell. 1995. TRPC1, a human homolog of a Drosophila store-operated channel. *Proc Natl Acad Sci U S A.* 92:9652-9656.
- Williams, B.R., R.A. Gelman, D.C. Poppke, and K.A. Piez. 1978. Collagen fibril formation. Optimal in vitro conditions and preliminary kinetic results. *J Biol Chem.* 253:6578-6585.
- Wolf, K., and P. Friedl. 2011. Extracellular matrix determinants of proteolytic and non-proteolytic cell migration. *Trends Cell Biol.* 21:736-744.
- Won, J.H., Y. Zhang, B. Ji, C.D. Logsdon, and D.I. Yule. 2010. Phenotypic changes in mouse pancreatic stellate cell Ca²⁺ signaling events following activation in culture and in a disease model of pancreatitis. *Mol Biol Cell.* 22:421-436.
- Wormann, S.M., K.N. Diakopoulos, M. Lesina, and H. Algul. 2014. The immune network in pancreatic cancer development and progression. *Oncogene.* 33:2956-2967.
- Wuensch, T., F. Thilo, K. Krueger, A. Scholze, M. Ristow, and M. Tepel. 2010. High glucose-induced oxidative stress increases transient receptor potential channel expression in human monocytes. *Diabetes.* 59:844-849.
- Xu, L., Y. Chen, K. Yang, Y. Wang, L. Tian, J. Zhang, E.W. Wang, D. Sun, W. Lu, and J. Wang. 2014. Chronic hypoxia increases TRPC6 expression and basal intracellular Ca²⁺ concentration in rat distal pulmonary venous smooth muscle. *PLoS One.* 9:e112007.

-
- Xu, Z., A. Vonlaufen, P.A. Phillips, E. Fiala-Beer, X. Zhang, L. Yang, A.V. Biankin, D. Goldstein, R.C. Pirola, J.S. Wilson, and M.V. Apte. 2010. Role of pancreatic stellate cells in pancreatic cancer metastasis. *The American journal of pathology*. 177:2585-2596.
- Yamamoto, S., S. Shimizu, S. Kiyonaka, N. Takahashi, T. Wajima, Y. Hara, T. Negoro, T. Hiroi, Y. Kiuchi, T. Okada, S. Kaneko, I. Lange, A. Fleig, R. Penner, M. Nishi, H. Takeshima, and Y. Mori. 2008. TRPM2-mediated Ca²⁺ influx induces chemokine production in monocytes that aggravates inflammatory neutrophil infiltration. *Nat Med*. 14:738-747.
- Yamashiro, K., T. Sasano, K. Tojo, I. Namekata, J. Kurokawa, N. Sawada, T. Suganami, Y. Kamei, H. Tanaka, N. Tajima, K. Utsunomiya, Y. Ogawa, and T. Furukawa. 2010. Role of transient receptor potential vanilloid 2 in LPS-induced cytokine production in macrophages. *Biochemical and biophysical research communications*. 398:284-289.
- Yang, K., J. Jia, J. Zhang, M. Zhao, S. Wang, H. Jiang, L. Xu, W. Lu, and J. Wang. 2015. Noggin Inhibits Hypoxia-induced Proliferation by Targeting Store-operated Calcium Entry and Transient Receptor Potential Cation Channels. *Am J Physiol Cell Physiol*:ajpcell 00349 02014.
- Yang, S., and X.Y. Huang. 2005. Ca²⁺ influx through L-type Ca²⁺ channels controls the trailing tail contraction in growth factor-induced fibroblast cell migration. *J Biol Chem*. 280:27130-27137.
- Yang, Y., S. Karakhanova, J. Werner, and A.V. Bazhin. 2013. Reactive oxygen species in cancer biology and anticancer therapy. *Current medicinal chemistry*. 20:3677-3692.
- Yao, H., M. Duan, L. Yang, and S. Buch. 2012. Platelet-derived growth factor-BB restores human immunodeficiency virus Tat-cocaine-mediated impairment of neurogenesis: role of TRPC1 channels. *J Neurosci*. 32:9835-9847.
- Yoshida, S., M. Ujiki, X.Z. Ding, C. Pelham, M.S. Talamonti, R.H. Bell, Jr., W. Denham, and T.E. Adrian. 2005. Pancreatic stellate cells (PSCs) express cyclooxygenase-2 (COX-2) and pancreatic cancer stimulates COX-2 in PSCs. *Mol Cancer*. 4:27.
- Yoshida, S., T. Yokota, M. Ujiki, X.Z. Ding, C. Pelham, T.E. Adrian, M.S. Talamonti, R.H. Bell, Jr., and W. Denham. 2004. Pancreatic cancer stimulates pancreatic stellate cell proliferation and TIMP-1 production through the MAP kinase pathway. *Biochemical and biophysical research communications*. 323:1241-1245.
- Yoshida, T., R. Inoue, T. Morii, N. Takahashi, S. Yamamoto, Y. Hara, M. Tominaga, S. Shimizu, Y. Sato, and Y. Mori. 2006. Nitric oxide activates TRP channels by cysteine S-nitrosylation. *Nat Chem Biol*. 2:596-607.
- Yu, J.H., and H. Kim. 2014. Oxidative stress and cytokines in the pathogenesis of pancreatic cancer. *Journal of cancer prevention*. 19:97-102.
- Yuan, J.P., W. Zeng, G.N. Huang, P.F. Worley, and S. Muallem. 2007. STIM1 heteromultimerizes TRPC channels to determine their function as store-operated channels. *Nat Cell Biol*. 9:636-645.
- Zhang, L.P., F. Ma, S.M. Abshire, and K.N. Westlund. 2013. Prolonged high fat/alcohol exposure increases TRPV4 and its functional responses in pancreatic stellate cells. *American journal of physiology. Regulatory, integrative and comparative physiology*. 304:R702-711.
- Zhu, X., P.B. Chu, M. Peyton, and L. Birnbaumer. 1995. Molecular cloning of a widely expressed human homologue for the *Drosophila* trp gene. *FEBS Lett*. 373:193-198.